

REPORT DOCUMENTATION PAGE			Form Approved OMB No. 0704-0188	
Public reporting burden for this collection of information is estimated to average 1 hour per response, including the time for reviewing instructions, searching existing data sources, gathering and maintaining the data needed, and completing and reviewing the collection of information. Send comments regarding this burden estimate or any other aspect of this collection of information, including suggestions for reducing this burden, to Washington Headquarters Services, Directorate for Information Operations and Reports, 1215 Jefferson Davis Highway, Suite 1204, Arlington, VA 22202-4302, and to the Office of Management and Budget, Paperwork Reduction Project (0704-0188) Washington, DC 20503.				
1. AGENCY USE ONLY (Leave Blank)	2. REPORT DATE 1995	3. REPORT TYPE AND DATES COVERED Final		
4. TITLE AND SUBTITLE The Mechanism of Catalytic Hydrocarbon Oxidation by Molecular Oxygen and Halogenated Ruthenium and Iron Porphyrins		5. FUNDING NUMBERS AFRL-SR-BL-TR-98- 0020		
6. AUTHORS Eva Rachel Birnbaum				
7. PERFORMING ORGANIZATION NAME(S) AND ADDRESS(ES) California Institute of Technology				
9. SPONSORING/MONITORING AGENCY NAME(S) AND ADDRESS(ES) AFOSR/NI 110 Duncan Avenue, Room B-115 Bolling Air Force Base, DC 20332-8080		SPONSORING/MONITORING AGENCY REPORT NUMBER		
11. SUPPLEMENTARY NOTES				
12a. DISTRIBUTION AVAILABILITY STATEMENT Approved for Public Release		12b. DISTRIBUTION CODE		
13. ABSTRACT (Maximum 200 words) See attached. <div data-bbox="399 1092 867 1226" data-label="Text"> <p>DISTRIBUTION STATEMENT A Approved for public release Distribution Unlimited</p> </div>				
14. SUBJECT TERMS DTIC QUALITY INSPECTED 2		15. NUMBER OF PAGES		
		16. PRICE CODE		
17. SECURITY CLASSIFICATION OF REPORT Unclassified	18. SECURITY CLASSIFICATION OF THIS PAGE Unclassified	19. SECURITY CLASSIFICATION OF ABSTRACT Unclassified	20. LIMITATION OF ABSTRACT UL	

P176

Abstract

Highly halogenated ruthenium and iron porphyrins are shown to be active catalysts for alkene oxidation with dioxygen or iodosobenzene. The synthesis and characterization of β -octachloro-tetrakis(pentafluorophenyl)porphyrinato-ruthenium(II) carbonyl $[\text{RuTFPPCl}_8(\text{CO})]$ and β -octabromo-tetrakis(pentafluorophenyl)porphyrinato-iron(III) chloride $[\text{Fe}(\text{TFPPBr}_8)\text{Cl}]$ are reported. Crystal structures of $\text{RuTFPPCl}_8(\text{CO})$ and the zinc and free ligand precursor complexes show extensive distortion of the halogenated porphyrin macrocycles due to steric interactions between the β -chlorine atoms and the pentafluorophenyl rings. ^{19}F NMR is developed as a method to characterize both paramagnetic and diamagnetic fluorinated porphyrins in solution. The anodically shifted reduction potentials and red shifted absorptions in the UV-Vis spectroscopy of the halogenated porphyrins are discussed in terms of steric and electronic effects on porphyrin frontier orbitals.

Both $\text{Fe}(\text{TFPPBr}_8)\text{Cl}$ and $\text{RuTFPPCl}_8(\text{CO})$ catalyze the oxidation of cyclohexene with dioxygen and without added coreductant, with 73 and 296 turnovers, respectively, in 24 hours. Although both porphyrins will catalyze reactions with iodosobenzene, showing selectivity consistent with high-valent metal-oxo formation, overall activity with dioxygen is much higher. In accord with earlier work, cyclohexene oxidation by $\text{Fe}(\text{TFPPBr}_8)\text{Cl}$ is consistent with a mechanism involving porphyrin-mediated decomposition of alkyl peroxides, which generates free radicals in solution. $\text{RuTFPPCl}_8(\text{CO})$ is shown to have a photochemical reaction mechanism involving olefin binding to the excited ruthenium porphyrin, resulting in a dramatic increase in the reaction rate upon irradiation with low energy light. This catalyst represents the first stable, effective metalloporphyrin catalyst for olefin oxidation with dioxygen and light.

THE MECHANISM OF CATALYTIC HYDROCARBON OXIDATION
BY MOLECULAR OXYGEN AND
HALOGENATED RUTHENIUM AND IRON PORPHYRINS

Thesis by

Eva Rachel Birnbaum

In Partial Fulfillment of the Requirements
for the degree of
Doctor of Philosophy

California Institute of Technology

Pasadena, California

1995

(Submitted May 8th, 1995)

Approved for release,
distribution and sale

MAY 30 1995
Oam

Acknowledgment

B176

Abstract

Highly halogenated ruthenium and iron porphyrins are shown to be active catalysts for alkene oxidation with dioxygen or iodosobenzene. The synthesis and characterization of β -octachloro-tetrakis(pentafluorophenyl)porphyrinato-ruthenium(II) carbonyl $[\text{RuTFPPCl}_8(\text{CO})]$ and β -octabromo-tetrakis(pentafluorophenyl)porphyrinato-iron(III) chloride $[\text{Fe}(\text{TFPPBr}_8)\text{Cl}]$ are reported. Crystal structures of $\text{RuTFPPCl}_8(\text{CO})$ and the zinc and free ligand precursor complexes show extensive distortion of the halogenated porphyrin macrocycles due to steric interactions between the β -chlorine atoms and the pentafluorophenyl rings. ^{19}F NMR is developed as a method to characterize both paramagnetic and diamagnetic fluorinated porphyrins in solution. The anodically shifted reduction potentials and red shifted absorptions in the UV-Vis spectroscopy of the halogenated porphyrins are discussed in terms of steric and electronic effects on porphyrin frontier orbitals.

Both $\text{Fe}(\text{TFPPBr}_8)\text{Cl}$ and $\text{RuTFPPCl}_8(\text{CO})$ catalyze the oxidation of cyclohexene with dioxygen and without added coreductant, with 73 and 296 turnovers, respectively, in 24 hours. Although both porphyrins will catalyze reactions with iodosobenzene, showing selectivity consistent with high-valent metal-oxo formation, overall activity with dioxygen is much higher. In accord with earlier work, cyclohexene oxidation by $\text{Fe}(\text{TFPPBr}_8)\text{Cl}$ is consistent with a mechanism involving porphyrin-mediated decomposition of alkyl peroxides, which generates free radicals in solution. $\text{RuTFPPCl}_8(\text{CO})$ is shown to have a photochemical reaction mechanism involving olefin binding to the excited ruthenium porphyrin, resulting in a dramatic increase in the reaction rate upon irradiation with low energy light. This catalyst represents the first stable, effective metalloporphyrin catalyst for olefin oxidation with dioxygen and light.

19980116 093

Table of Contents

List of Figures	v
List of Tables	viii
Abbreviations Used	ix
Introduction	1
Synthesis, Molecular Structures, and Nuclear Magnetic Resonance Spectroscopy of Halogenated Porphyrins	18
Spectroscopy and Electronic Structures of Halogenated Porphyrins	67
Oxidation of Olefins with Halogenated Iron Porphyrins	104
Mechanism of Oxidation of Hydrocarbons with Perhalogenated Ruthenium Porphyrins	133
Oxidation Chemistry in Supercritical Carbon Dioxide	206
Appendix (Chapter 2)	247
Appendix (Chapter 5)	349

List of Figures

Figure 1.1	Catalytic Cycle of Cytochrome P-450	10
Figure 1.2	Structure of Protoporphyrin IX and Octaethylporphyrin	12
Figure 1.3	Sterically Hindered Porphyrins	14
Figure 1.4	Second and Third Generation Porphyrin Structures	16
Figure 2.1	Structure and Standard Labeling of Porphyrins	38
Figure 2.2	HPLC Trace of Separation of $\text{RuTFPPCl}_x(\text{CO})$ Compounds	40
Figure 2.3	ORTEP Diagram of $\text{H}_2\text{TFPPCl}_8$	42
Figure 2.4	ORTEP Diagram of ZnTFPPCl_8	44
Figure 2.5	ORTEP Diagram of $\text{RuTFPPCl}_8(\text{CO})$	46
Figure 2.6	Projection of Free Ligand Series: H_2TPP , H_2TFPP , and $\text{H}_2\text{TFPPCl}_8$	48
Figure 2.7	Side-on View of $\text{RuTFPPCl}_8(\text{CO})$	50
Figure 2.8	^{19}F NMR Spectra of a) H_2TFPP and b) ZnTFPP in CDCl_3	52
Figure 2.9	^{19}F NMR Spectrum of $\text{Fe}(\text{TFPP})\text{Cl}$	54
Figure 2.10	Curie Plot of the Temperature Dependence of $\text{Fe}(\text{TFPP})\text{Cl}$	56
Figure 2.11	^{19}F NMR Spectrum of $(\text{FeTFPP})_2\text{O}$	58
Figure 2.12	^{19}F NMR Spectrum of $\text{Fe}(\text{TFPPBr}_8)\text{Cl}$	60
Figure 2.13	^{19}F NMR Spectra of Reduced $\text{Fe}(\text{TFPPBr}_8)\text{Cl}$ Produced by a) Bulk Electrolysis and b) Chemical Reduction	62
Figure 3.1	Normal Porphyrin UV-Visible Spectrum	77
Figure 3.2	Gouterman Four Orbital Model of Porphyrin Frontier Orbitals and Modification upon Halogenation	79
Figure 3.3	UV-Vis Spectra of ZnTPP , ZnTFPP , ZnTFPPCl_8 , and ZnTFPPBr_8	81
Figure 3.4	UV-Vis Spectra of $\text{Fe}(\text{TFPP})\text{Cl}$ and $\text{Fe}(\text{TFPPBr}_8)\text{Cl}$	83
Figure 3.5	UV-Vis Spectra of Reduced $\text{Fe}(\text{TFPPBr}_8)\text{Cl}$	85
Figure 3.6	Frontier Orbital Diagram of $\text{RuTFPPCl}_8(\text{CO})$	87
Figure 3.7	UV-Vis Spectra of $\text{RuTPP}(\text{CO})$ and $\text{RuTFPPCl}_8(\text{CO})$	89
Figure 3.8	UV-Vis Spectra of $\text{RuTPP}(\text{py})_2$ and $\text{RuTFPPCl}_8(\text{py})_2$	91
Figure 3.9	UV-Vis Spectra of $\text{RuTFPPX}_n(\text{CO})$ Series	93
Figure 3.10	Charge Transfer Bands in Halogenated Ruthenium Porphyrins	95
Figure 3.11	Spectroelectrochemical Reduction of $\text{RuTFPPCl}_8(\text{py})_2$	97

Figure 3.12	Spectroelectrochemical Reduction of RuTFPPCl ₈ (CO)	99
Figure 4.1	Proposed Intermediates in Epoxidation by a High-Valent Metal-Oxo	115
Figure 4.2	Competing Mechanisms for Epoxidation by a High-Valent Metal-Oxo	117
Figure 4.3	Mechanism of Cyclohexene Epoxidation and Hydroxylation	119
Figure 4.4	Turnovers of Cyclohexene Oxidation by Iron Porphyrins with Iodosobenzene or Dioxygen	121
Figure 4.5	Cyclohexene Oxidation by Fe(TFPPBr ₈)Cl with Dioxygen versus Time	123
Figure 4.6	Activity of Iron Porphyrins versus Iron Reduction Potential	125
Figure 4.7	Dioxygenase Activity by Halogenated Iron Porphyrins	127
Figure 4.8	Alkyl Peroxide Decomposition by Fe(TFPPBr ₈)Cl	129
Figure 4.9	Diagram of Reaction Vessel Used for Oxidation Reactions	131
Figure 5.1	Groves Mechanism for Aerobic Olefin Epoxidation with Ruthenium Porphyrins	161
Figure 5.2	Cyclohexene Oxidation by RuTFPPCl ₈ (CO) with PhIO	163
Figure 5.3	Cyclohexene Oxidation by RuTFPPCl ₈ (CO) with Oxygen	165
Figure 5.4	Hydrogen Peroxide Decomposition by RuTFPPCl ₈ (CO) and Fe(TFPPBr ₈)Cl	167
Figure 5.5	Titration of RuTFPPCl ₈ (CO) with mCPBA	169
Figure 5.6	Oxidation of Cyclohexene by Ru ^{VI} TFPPCl ₈ (O) ₂	171
Figure 5.7	Oxidation of Triphenylphosphine by Ru ^{VI} TFPPCl ₈ (O) ₂	173
Figure 5.8	Mechanism for Dioxygen Activation via Loss of CO	175
Figure 5.9	Effect of CO Removal from RuTFPPCl ₈ (CO)	177
Figure 5.10	Effect of <i>t</i> -Butyl Hydroperoxide Addition	179
Figure 5.11	Effect of Stir Rate	181
Figure 5.12	Mixed Atmosphere Reaction	183
Figure 5.13	UV-Vis of RuTFPPCl ₈ (CO) after Exposure to 1100 psi CO	185
Figure 5.14	Isotope Effect	187
Figure 5.15	Cyclohexene Oxidation by RuTFPPCl ₈ (CO) with Dioxygen in the Absence of Light	189
Figure 5.16	Effect of Photolysis on an Oxidation Reaction	191
Figure 5.17	Transient Absorption Spectrum of RuTFPPCl ₈ (CO)	193
Figure 5.18	5 μs Transient Spectrum of RuTFPPCl ₈ (CO) at 415 nm	195

Figure 5.19	50 μ s Transient Spectrum of RuTFPPCl ₈ (CO) at 415 nm	197
Figure 5.20	50 μ s Transient Absorption Spectrum of RuTFPPCl ₈ (CO) under CO, Ar, Ethylene, and Dioxygen Atmospheres	199
Figure 5.21	UV-Vis Spectra of RuTFPPCl ₈ (CO) after Photolysis	201
Figure 5.22	Proposed Photochemical Mechanism for Olefin Oxidation by RuTFPPCl ₈ (CO) with Dioxygen	203
Figure 6.1	Phase Diagram of Carbon Dioxide	220
Figure 6.2	Apparatus for UV-Vis Spectroscopy in Supercritical Carbon Dioxide	222
Figure 6.3	UV-Vis Spectrum of Fe(TFPP)Cl in Supercritical Carbon Dioxide	224
Figure 6.4	UV-Vis Spectrum of Fe(TFPPBr ₈)Cl in Supercritical Carbon Dioxide	226
Figure 6.5	UV-Vis Spectrum of RuTFPPCl ₈ (CO) in Supercritical Carbon Dioxide	228
Figure 6.6	Solubility of Halogenated Porphyrins versus Pressure CO ₂	230
Figure 6.7	Corrected UV-Vis Spectrum of RuTFPPCl ₈ (CO)	232
Figure 6.8	UV-Vis Spectrum of RuTFPPCl ₈ (CO) in the Presence of Cyclohexene	234
Figure 6.9	Apparatus for Oxidation Reactions in Supercritical Carbon Dioxide	236
Figure 6.10	Cyclohexene Oxidation by Fe(TFPP)Cl in SC CO ₂	238
Figure 6.11	Cyclohexene Oxidation by Fe(TFPPBr ₈)Cl in SC CO ₂	240
Figure 6.12	Cyclohexene Oxidation by RuTFPPCl ₈ (CO) in SC CO ₂	242
Figure 6.13	Partitioning to Multiple Oxidation Products	242

List of Tables

Table 2.1	X-ray Experimental Parameters	64
Table 2.2	Average Bond Lengths in Halogenated Porphyrins	65
Table 2.3	Average Angles in Halogenated Porphyrins	65
Table 2.4	Atom Displacements from the Mean Porphyrin Plane	65
Table 2.5	^{19}F and ^1H NMR Chemical Shifts of Halogenated Porphyrins	66
Table 3.1	Electronic Absorptions of Halogenated Zinc, Free Base, and Ruthenium Porphyrins	101
Table 3.2	Reduction Potentials of Halogenated Porphyrins	102
Table 3.3	Electronic Absorptions of Iron Porphyrins	103
Table 5.1	Oxidation of Olefins by $\text{RuTFPPCl}_8(\text{CO})$	205

Abbreviations Used

mCPBA	<i>m</i> -chloroperoxybenzoic acid
OEP	octaethylporphyrin
SCF	supercritical fluid
SC CO ₂	supercritical carbon dioxide
TBHP	<i>tert</i> -butyl hydroperoxide
TDBPP	tetrakis-(2,6-dibromophenyl)porphyrin
TDCPP	tetrakis-(2,6-dichlorophenyl)porphyrin
TDFPP	tetrakis-(2,6-difluorophenyl)porphyrin
TFPP	tetrakis(pentafluorophenyl)porphyrin
TFPPBr ₈	β-octabromo-tetrakis(pentafluorophenyl)porphyrin
TFPPCl ₈	β-octachloro-tetrakis(pentafluorophenyl)porphyrin
TMP	tetramesitylporphyrin
TPP	tetraphenylporphyrin

Chapter 1

Introduction to Catalysis with Metalloporphyrins

Science has "explained" nothing; the more we know the more fantastic the world becomes and the profounder the surrounding darkness.

-- Aldous Huxley, *Along the Road*, pt. 2 (1925).¹

The whole of science is nothing more than a refinement of everyday thinking.

-- Albert Einstein, *Out of My Later Years*, ch. 12 (1950).²

Oxidation chemistry is one of many arenas in which chemists are attempting to devise catalysts that achieve the remarkable efficiency, selectivity, and specificity of enzymes. Cytochrome P-450, a heme-based enzyme involved in respiration, has long been a target for the generation of a biomimetic catalyst.^{3,4} Found in a wide variety of tissues, this membrane-bound enzyme catalyzes the oxidation of a wide variety of organic substrates with reductively activated dioxygen.⁴ In particular, the ability of P-450 to selectively activate the more inert C-H bonds is quite desirable for industrial applications. Although many catalysts have been investigated, this selectivity has yet to be duplicated by a synthetic system.

The catalytic cycle of cytochrome P-450 is shown in Figure 1.1. From the resting state as the ferric porphyrin, two reducing equivalents from NADH are required to fully activate the enzyme. The first reduces the porphyrin to the ferrous state, enabling it to bind dioxygen. A second electron reduces the bound oxygen complex, and subsequent addition of two protons induces heterolytic cleavage of the dioxygen bond and release of a water molecule to form a high-valent metal-oxo iron porphyrin. The iron oxo

intermediate, which has never been isolated from P-450 due to its high reactivity, is generally believed to be an iron(IV)oxo porphyrin radical cation. Although early steps in the cycle are well documented, assignment of the active species is largely by analogy to Compound I of the enzyme horseradish peroxidase (HRP), which has been definitively characterized as an iron(IV)oxo porphyrin π radical cation.^{4,5} The active intermediate can also be directly generated with an O-atom donor such as iodosobenzene or peroxide; this "peroxide shunt" pathway is a convenient test for P-450 monooxygenase-like activity in model complexes.

A general technique in catalyst design is to model the active site of an enzyme, in the hope that one small section of the protein will exhibit the same activity as the whole. The porphyrin core of P-450 lends itself to this type of study for several reasons: reliable syntheses for porphyrins have been developed, the periphery of the porphyrin ligand is easily modified to alter the properties of the porphyrin, and the ligand has distinctive spectroscopy which facilitates investigation. Indeed, the past two decades have produced a plethora of work on metalloporphyrin derivatives.^{4,6,7}

Initial investigations on a derivative of the naturally occurring protoporphyrin IX (Figure 1.2) demonstrated that a species spectroscopically similar to compound I could be generated with an O-atom donor.⁸ However, rather than oxidizing substrate, this intermediate hydroxylated its own β -side chain. A synthetic analog, octaethylporphyrin, was even less stable outside of the protective protein environment. Although a high-valent iron-oxo was believed to be generated in the presence of iodosobenzene, the planar porphyrin degraded by hydroxylation at the meso position, followed by complete destruction of the porphyrin chromophore. Oxidation of a second porphyrin molecule was clearly more favorable than oxidizing substrate.⁸ The protein fold, which protects the porphyrin against autooxidation, prohibits unproductive μ -oxo dimer formation, and enhances substrate-porphyrin interactions, is clearly vital for these simple planar hemes to act as catalysts. A more stable porphyrin molecule would be necessary to mimic

monooxygenase behavior in solution. And so the quest to design a better porphyrin ligand began.

A simple iron tetraphenylporphyrin, Fe(TPP)Cl, was found to oxidize hydrocarbons in the presence of PhIO.⁹ Substitution at the meso position with a bulky phenyl moiety was found to reduce aggregation in solution and protect the reactive meso position from reactions leading to porphyrin degradation. Oxidation of tetramesitylporphyrinato-iron(III) chloride (Fe(TMP)Cl) with *m*-chloroperoxybenzoic acid at low temperatures produced a species that both shares spectral features with Compound I and is capable of epoxidizing alkenes.¹⁰ Although more promising than OEP, these ligands still showed substantial degradation in solution.

The second generation of metalloporphyrin catalysts were designed to increase the lifetime of porphyrins in solution by reducing their susceptibility to oxidative degradation. Halogenation of the meso phenyl rings would raise the reduction potential as well as increase steric bulk along the porphyrin periphery, decreasing the likelihood of dimerization or hydrogen abstraction by other porphyrin molecules. Tetrakis-(pentafluorophenyl)porphyrin (TFPP) was indeed found to be more stable than TPP, and iron complexes were found to show high selectivity for epoxidation of olefins.¹¹ Similarly, tetrakis(2,6-dichlorophenyl)porphyrinato-iron(III) chloride [Fe(TDCPP)Cl] was found to show high activity with pentafluoriodosobenzene.¹² Iron(III), manganese(III) and chromium(III) complexes of TDCPP all exhibited higher activity for cyclohexene oxidation with iodobenzene than their TPP analogs, as well as higher selectivity for epoxide formation. Furthermore, the 2,6-dichlorophenylporphyrin complexes remained intact after an oxidation reaction, while the tetraphenylporphyrin complexes were completely degraded.¹³

In addition to halogenation, other elegant methods have been developed for generating steric barriers against the close approach of two porphyrin molecules. Tailed porphyrins (Figure 1.3) have an imidazole or other nitrogen containing function linked to

the porphyrin ring by a flexible hydrocarbon chain, allowing it to swing around and axially bind to the metal center in simulation of histidine coordination.¹⁴ Picket fence,¹⁵ strapped,¹⁶ basket handle,¹⁷ and capped¹⁸ porphyrins have large organic groups that project perpendicular to the plane of the porphyrin as pickets, or, in the latter cases, actually bridge across from one side of the porphyrin ring to the other. All of the above methods provide some steric protection as well as a pocket in which the substrate may bind. Although these types of porphyrins have led to some extremely interesting work in the area of enantioselective and regioselective oxidation chemistry,¹⁹ they have not been further pursued as general oxidation catalysts. The hydrocarbon side chains that drive the selectivity found with these metalloporphyrins, while stable enough under mild conditions, are susceptible to degradation in a highly oxidizing environment.

Instead of building a pocket around the porphyrin, the third generation catalysts have completely protected the porphyrin periphery by full substitution at both the meso and beta positions (Figure 1.4). Steric bulk from mesityl,^{20,21} pentafluorophenyl,²¹⁻²⁸ or 2,6-dihalophenyl^{22,29-32} groups at the meso carbons is paired with electron-withdrawing substituents at the β -carbons. The electronic and steric crowding created by the full periphery imparts unusual structural and spectroscopic features to the porphyrin ligand, while the steric bulk of these complexes causes severe distortion of the porphyrin macrocycle, preventing dimerization (Chapter 2 and 3). The electronic demands of the substituents have been shown to decrease oxidative degradation of the porphyrin, thereby increasing net activity.^{22,28,29,33,34}

Indeed, these highly halogenated porphyrins are found to be active catalysts. Iron and manganese complexes of β -octachloro, β -octabromo,^{20,22,26,28-30,34-40} and β -octanitro³² tetraphenylporphyrin derivatives are reported to catalyze the oxidation of both alkanes and alkenes with a variety of O-atom donors, with tremendous increases in both activity and catalyst lifetime over the second generation porphyrins. For example, β -octabromo-tetramesitylporphyrinato-manganese(III) chloride catalyzes the epoxidation

of cyclooctene with hydrogen peroxide in 96% yield,³⁴ and the hydroxylation of adamantane with KHSO_5 in 62% yield.²⁰ Iron(III) chloride complexes of β -octachloro-tetrakis(2,6-dichlorophenyl)porphyrin catalyze the hydroxylation of heptane with iodosobenzene in 80% yield.²² These reactions show increases in rate, total activity, selectivity, and porphyrin lifetime relative to the unhalogenated derivatives.

An even more unique finding is the activity of the third generation porphyrins with dioxygen. At 80 °C and 75 atm O_2 , β -octabromo-tetrakis(pentafluorophenyl)-porphyrinato-iron(III) chloride ($\text{Fe}(\text{TFPPBr}_8)\text{Cl}$) catalyzes 17,150 turnovers of isobutane to *tert*-butyl alcohol in three hours. At slightly lower temperatures, the selectivity of the reaction for the desired alcohol can be increased to 92%.²⁶

The unprecedented activity of a metalloporphyrin with dioxygen and without a coreductant gave rise to new ideas for mechanisms for O_2 activation. Most recent porphyrin literature examines catalysis with O-atom donors that attempt to directly mimic enzymatic P-450 reactions. The reports of $\text{Fe}(\text{TFPPBr}_8)\text{Cl}$ activity imply that alternate mechanisms may exist in addition to traditional high-valent metal-oxo chemistry, and prompted a more thorough investigation of this and similar third generation compounds in our lab.

This brief review of recent metalloporphyrin catalysis literature is not meant to be comprehensive, but rather to explain some of the history behind the development of the unusual perhalogenated porphyrin ligand. The more contemporary metalloporphyrin catalysts are now only distant cousins to the natural hemes they were initially designed to model. The following chapters are a more thorough investigation of the spectroscopy and catalytic properties of several fluorinated metalloporphyrins.

Chapter 2 describes the synthesis of halogenated iron and ruthenium porphyrins and their precursors. Molecular structures of β -octachloro-tetrakis(pentafluorophenyl)-porphyrinato-ruthenium(II) carbonyl, $[\text{RuTFPPCl}_8(\text{CO})]$ and the zinc and free ligand precursor complexes, are shown to be extremely distorted, in line with other halogenated

porphyrin structures. ^{19}F NMR is developed as a method for characterizing the solution structure of both paramagnetic and diamagnetic fluorinated porphyrin structures.

The unusual spectroscopy and electrochemistry of halogenated porphyrins is discussed in Chapter 3. The changes in the frontier orbital energies upon phenyl and pyrrole halogenation are described. A full molecular orbital diagram is shown for $\text{RuTFPPCl}_8(\text{CO})$ and discussed in terms of the distortion and electron-withdrawing effects of halogenation.

Enhanced catalytic activity is observed with the highly halogenated complexes. Alkene oxidation by halogenated iron porphyrins is described in Chapter 4. $\text{Fe}(\text{TFPPBr}_8)\text{Cl}$ is an active catalyst with both iodosobenzene and dioxygen, and shows a significant increase in activity and catalyst lifetime relative to $\text{Fe}(\text{TFPP})\text{Cl}$. Observations support a mechanism involving porphyrin-mediated decomposition of alkyl peroxide, as proposed earlier in our group.^{37,41}

Chapter 5 is a discussion of catalysis with $\text{RuTFPPCl}_8(\text{CO})$. Similar to the iron complex, this porphyrin is an extremely active catalyst for the oxidation of olefins under very mild conditions: 1 atm dioxygen, room temperature, and without addition of co-reductant. Alkene oxidation is also observed with iodosobenzene. Observations of oxidation reactions catalyzed by $\text{RuTFPPCl}_8(\text{CO})$ with dioxygen are not consistent with mechanisms proposed for the activity of either the iron analog, $\text{Fe}(\text{TFPPBr}_8)\text{Cl}$, or other ruthenium porphyrins. Instead, olefin oxidation is dependent on light, possibly initiated by an interaction of the alkene with a $\text{RuTFPPCl}_8(\text{CO})$ excited state. As oxidation mechanisms in metalloporphyrins involving electronic excited states are rare, a photochemical reaction mechanism would be an interesting result, suggesting intermediates and ideas completely distinct from traditional high-valent metal-oxo chemistry.

The final chapter investigates the use of halogenated porphyrin catalysts in supercritical carbon dioxide. An apparatus was set up to measure the solubility of three

halogenated porphyrins in supercritical carbon dioxide by optical spectroscopy. Each porphyrin was tested with both iodosobenzene and dioxygen as a catalyst for the oxidation of cyclohexene in a supercritical medium. Although the results are extremely preliminary, they suggest that selectivity was more affected than net activity by the change in solvent. More multiple oxidations of the same substrate molecule were observed relative to reactions run in methylene chloride. Supercritical carbon dioxide was shown for the first time to be a good medium for oxidation catalysis.

References

- (1) Huxley, A. In *Along the Road*; George Doran: New York, 1925; pp 266.
- (2) Einstein, A. *Out of my Later Years*; Greenwood Press: Westport, CT, 1950, pp 282.
- (3) McMurray, T. J.; Groves, J. T. In *Cytochrome P-450*; P. K. Ortiz de Montellano, Ed.; Plenum Press: New York, 1986; pp 1-28.
- (4) Gunter, M. J.; Turner, P. *Coord. Chem. Rev.* **1991**, *108*, 115-161.
- (5) *Cytochrome P-450*; Ortiz de Montellano, P. K., Ed.; Plenum Press: New York, 1986.
- (6) Meunier, B. *Chem. Rev.* **1992**, *92*, 1411-1456.
- (7) Mansuy, D. *Coord. Chem. Rev.* **1993**, *125*, 129-142.
- (8) Chang, C. K.; Kuo, M.-S. *J. Am. Chem. Soc.* **1979**, *101*, 3413-3415.
- (9) Groves, J. T.; Nemo, T. E.; Myers, R. S. *J. Am. Chem. Soc.* **1979**, *101*, 1032-1033.
- (10) Groves, J. T.; Haushalter, R. C.; Nakamura, M.; Nemo, T. E.; Evans, B. J. *J. Am. Chem. Soc.* **1981**, *103*, 2884-2886.
- (11) Chang, C. K.; Ebina, F. *J. Chem. Soc., Chem. Commun.* **1981**, 778-779.
- (12) Traylor, P. S.; Dolphin, D.; Traylor, T. G. *J. Chem. Soc., Chem. Commun.* **1984**, 279-280.
- (13) Traylor, T. G.; Miksztal, A. R. *J. Am. Chem. Soc.* **1989**, *111*, 7443-7448.
- (14) Collman, J. P.; Groh, S. E. *J. Am. Chem. Soc.* **1982**, *104*, 1391-1403.
- (15) Gunter, M. J.; McLaughlin, G. M.; Berry, K. J.; Murray, K. S.; Irving, M.; Clark, P. E. *Inorg. Chem.* **1984**, *23*, 283-300.
- (16) Battersby, A. R.; Howson, W.; Hamilton, A. D. *J. Chem. Soc., Chem. Commun.* **1982**, 1266-1268.
- (17) Lexa, D.; Mamenteau, M.; Saveant, J. M.; Xu, F. *Inorg. Chem.* **1986**, *25*, 4857-4865.
- (18) Kim, K.; Ibers, J. A. *J. Am. Chem. Soc.* **1991**, *113*, 6077-6081.
- (19) Collman, J. P.; Zhang, X.; Lee, V. J.; Uffelman, E. S.; Brauman, J. I. *Science* **1993**, *261*, 1404-1411.
- (20) Hoffmann, P.; Robert, A.; Meunier, B. *Bull. Chem. Soc. Fr.* **1992**, *129*, 85-97.
- (21) Mandon, D.; Ochsenbein, P.; Fischer, J.; Weiss, R.; Jayaraj, K.; Austin, R. N.; Gold, A.; White, P. S.; Brigaud, O.; Battioni, P.; Mansuy, D. *Inorg. Chem.* **1992**, *31*, 2044-2049.

- (22) Bartoli, J. F.; Brigaud, O.; Battioni, P.; Mansuy, D. *J. Chem. Soc., Chem. Commun.* **1991**, 440-442.
- (23) Marsh, R. E.; Schaefer, W. P.; Hodge, J. A.; Hughes, M. E.; Gray, H. B.; Lyons, J. E.; Ellis, P. E., Jr. *Acta Crystallogr.* **1993**, C49, 1339-1342.
- (24) Schaefer, W. P.; Hodge, J. A.; Hughes, M. E.; Gray, H. B.; Lyons, J. E.; Ellis, P. E., Jr.; Wagner, R. W. *Acta Crystallogr.* **1993**, C49, 1342-1345.
- (25) Henling, L. M.; Schaefer, W. P.; Hodge, J. A.; Hughes, M. E.; Gray, H. B.; Lyons, J. E.; Ellis, P. E., Jr. *Acta Crystallogr.* **1993**, C49, 1745-1747.
- (26) Lyons, J. E.; Ellis, P. E., Jr.; Durante, V. A. In *Structure-Activity and Selectivity Relationships in Heterogeneous Catalysis*; R. K. Grasselli and A. W. Sleight, Eds.; Elsevier Science Publishers B.V.: Amsterdam, 1991; pp 99-116.
- (27) D'Souza, F.; Villard, A.; Caemelbecke, E. V.; Franzen, M.; Boschi, T.; Tagliatesta, P.; Kadish, K. M. *Inorg. Chem.* **1993**, 32, 4042-4048.
- (28) d'A. Rocha Gonsalves, A. M.; Johnstone, R. A. W.; Pereira, M. M.; Shaw, J.; Sobral, D. N.; Abilio, J. F. *Tetrahedron Lett.* **1991**, 32, 1355-1358.
- (29) Traylor, T. G.; Tsuchiya, S. *Inorg. Chem.* **1987**, 26, 1338-1339.
- (30) Hoffmann, P.; Meunier, B. *New J. Chem.* **1992**, 16, 559-561.
- (31) Lu, W. Y.; Bartoli, J. F.; Battioni, P.; Mansuy, D. *New J. Chem.* **1992**, 16, 621-628.
- (32) Bartoli, J. F.; Battioni, P.; Foor, W. R. D.; Mansuy, D. *J. Chem. Soc., Chem. Commun.* **1994**, 23-24.
- (33) Ellis, P. E., Jr.; Lyons, J. E. *Catal. Lett.* **1989**, 3, 389-398.
- (34) Banfi, S.; Mandelli, R.; Montanari, F.; Quici, S. *Gazz. Chim. Ital.* **1993**, 123, 409-415.
- (35) d'A. Rocha Gonsalves, A. M.; Pereira, M. M.; Serra, A. C.; Johnstone, R. A. W.; Nunes, M. L. P. G. *J. Chem. Soc., Perkin Trans. 1* **1994**, 2053-2057.
- (36) Ellis, P. E., Jr.; Lyons, J. E. *Coord. Chem. Rev.* **1990**, 105, 181-193.
- (37) Grinstaff, M. W.; Hill, M. G.; Labinger, J. A.; Gray, H. B. *Science* **1994**, 264, 1311-1313.
- (38) Lyons, J. E.; Ellis, P. E., Jr. *Catal. Lett.* **1991**, 8, 45-52.
- (39) Traylor, T. G.; Hill, K. W.; Fann, W.; Tsuchiya, S.; Dunlap, B. E. *J. Am. Chem. Soc.* **1992**, 114, 1308-1312.
- (40) Wijesekera, T.; Matsumoto, A.; Dolphin, D.; Lexa, D. *Angew. Chem., Int. Ed. Eng.* **1990**, 29, 1028-1030.
- (41) Labinger, J. A. *Catal. Lett.* **1994**, 26, 95-99.

Figure 1.1 -- The proposed catalytic cycle for oxidation reactions by cytochrome P-450.

All steps before the generation of the high-valent metal-oxo are well documented, but the actual active intermediate has not been isolated.

Addition of an O-atom donor such as iodosobenzene to the ferric porphyrin (peroxide shunt) will directly form the oxidizing species, generally believed to be $\text{Fe}^{\text{IV}}(\text{P})(\text{O})^{\bullet+}$ (diagram modified from reference 1).

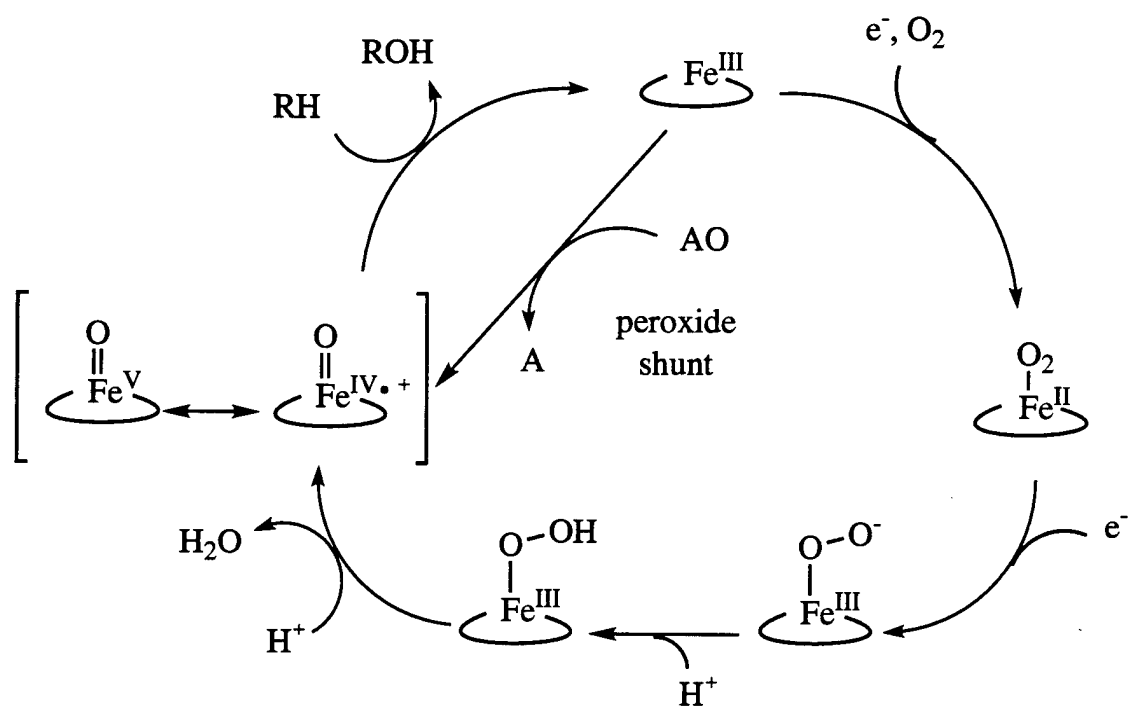
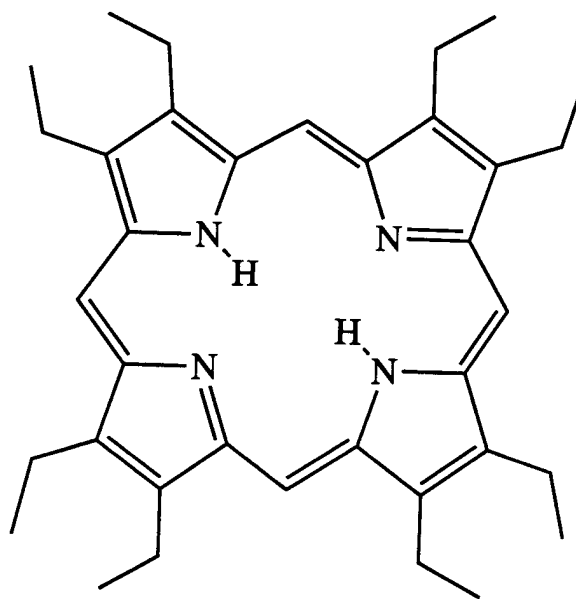
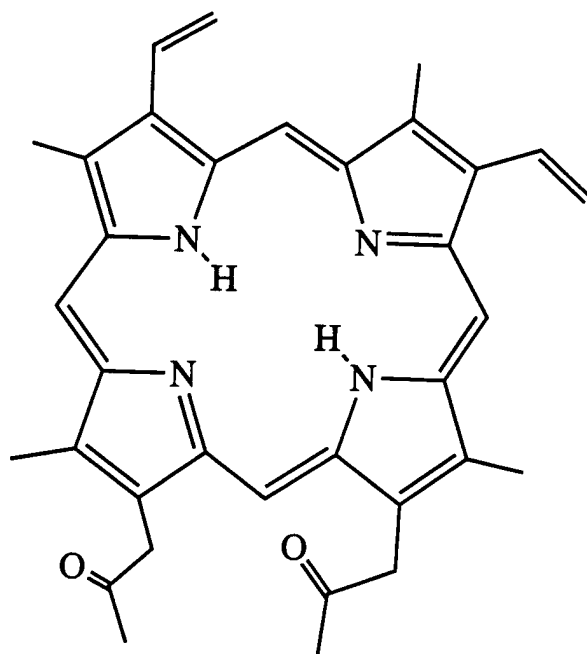
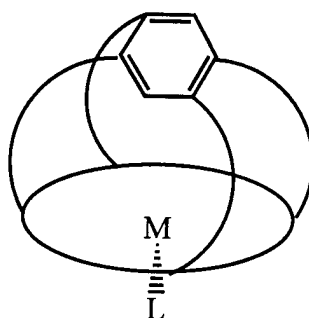
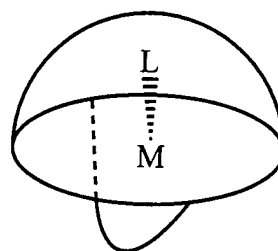
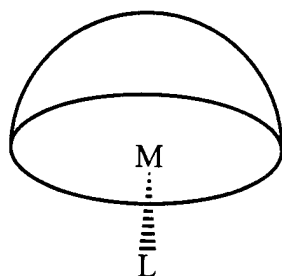
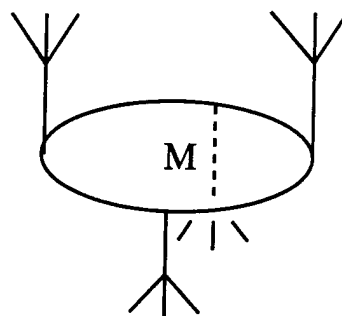
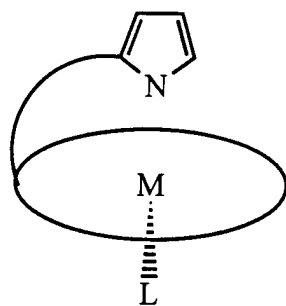


Figure 1.2 -- Diagram of the heme center from cytochrome P-450, protoporphyrin IX, and a synthetic equivalent, octaethylporphyrin (OEP). Naturally occurring hemes commonly bear alkyl or vinyl substituents at the pyrrole carbons.



Protoporphyrin IX (above) and Octaethylporphyrin (OEP)

Figure 1.3 -- Representations of tailed, picket fence, basket handle, and capped porphyrins. The bulky ligands create a steric barrier in the plane perpendicular to the porphyrin to prevent μ -oxo dimerization.




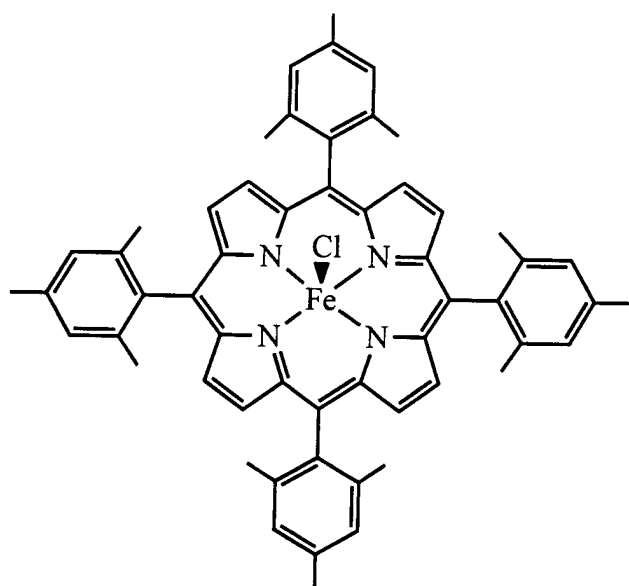
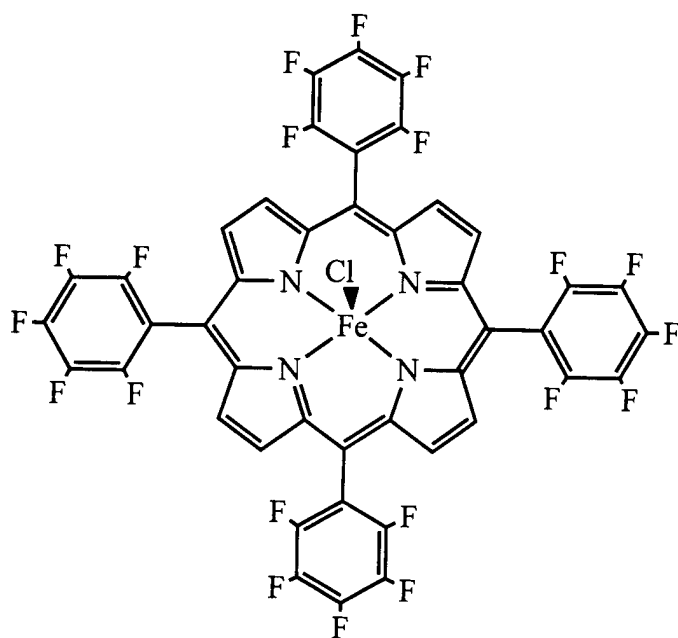
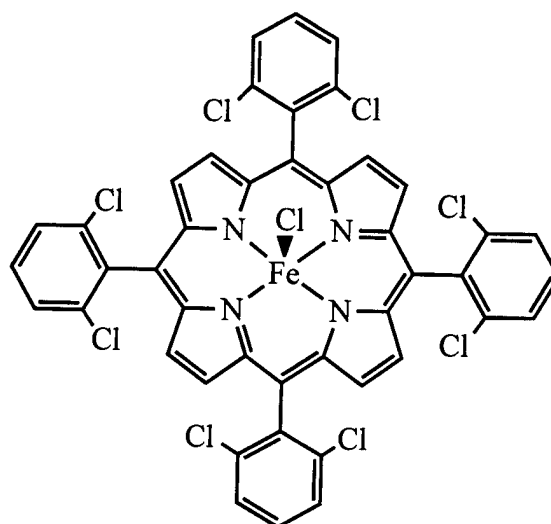
 = porphyrin
ring

Figure 1.4 -- Drawings of three iron complexes of second generation porphyrins showing the groups commonly substituted at the meso positions: mesityl, 2,6-dichlorophenyl, and pentafluorophenyl groups. Halogenation of the pyrrole carbons would form third generation catalysts.



Fe(TMP)Cl

Fe(TDCPP)Cl



Fe(TFPP)Cl

Chapter 2

Synthesis, Molecular Structures, and Nuclear Magnetic Resonance Spectroscopy of Halogenated Porphyrins

Introduction

Biomimetic metalloporphyrin oxidation catalysts are often based on a tetraphenylporphyrin template because these complexes are not as susceptible to aggregation and are protected from degradation to oxophlorins (oxo substitution at the meso position) by meso-phenyl substitution. Mesityl (TMP) or 2,6-dichlorophenyl (TDCPP) groups at the meso positions are more successful than unsubstituted phenyl rings, since the additional steric bulk of a substituted phenyl moiety decreases the tendency to form μ -oxo dimers in solution. The next generation of metalloporphyrins further enhanced the tetraphenylporphyrin ligands with electron-withdrawing substituents at the beta positions, removing reactive C-H bonds from the porphyrin periphery and increasing the steric bulk of the molecules. Many β -substituted TDCPP and TMP metalloporphyrins have been synthesized and investigated as oxidation catalysts (see Chapter 4). In addition to these ligands, another option is to begin with a tetrakis(pentafluorophenyl)porphyrin (TFPP) template, and then halogenate the β -positions to give a perhalogenated macrocycle. These "Teflon" porphyrins are designed to be extremely resistant to normal porphyrin decomposition in oxidizing environments.

Although extremely efficient porphyrin condensation reactions have been developed,¹ allowing porphyrins to be made in high yield from the appropriate benzaldehyde and pyrrole, this methodology has not been reported to be successful for β -halo derivatives. Recent advances have developed a the synthesis for the required

3,4-halogenated pyrroles,^{2,3} but these compounds readily polymerize and are difficult to purify. Instead, halogenation of the β -positions is accomplished on an intact porphyrin macrocycle.⁴⁻¹⁴ The fluorinated porphyrin, 5,10,15,20-tetrakis(pentafluorophenyl)-porphyrinato-zinc(II) (ZnTFPP), is commercially available or can be synthesized from pyrrole and pentafluorobenzaldehyde. The zinc, rather than the unmetallated porphyrin, is used because the metallated porphyrins are found to better withstand the halogenation reactions.¹⁴

Synthesis

Halogenation to form β -octachloro- or β -octabromo-tetrakis(pentafluorophenyl)-porphyrinato-zinc(II) (ZnTFPPCl₈ and ZnTFPPBr₈; Figure 1.1) was initially accomplished with direct addition of Cl_{2(g)} or Br_{2(l)}. However, a less hazardous synthesis with N-halosuccinamide was developed¹⁰ and found to proceed in good yield. Addition of excess N-halosuccinamide to a refluxing solution of ZnTFPP in methanol gave the desired product in 1-3 hours. Synthesis of the octabromo porphyrin was easier to drive to completion than that of the octachloro. The relative size of chlorine (atomic radii = 0.99) versus bromine (1.14 Å)¹⁵ would have predicted a more difficult synthesis for ZnTFPPBr₈ based on the greater steric demands of eight bromines on the porphyrin periphery. However, the relative ease of synthesis of the two ligands suggests that the electronic effect, which leads to a decrease in reactivity for further substitution on the ligand, (electronegativity = 3.617 Cl, 3.365 Br)¹⁶ is more significant. If the trend follows to fluorine, the lack of success in our lab¹⁴ in synthesizing the β -octafluoro porphyrin is not surprising.

Although ZnTFPPBr₈ was readily purified by column chromatography, the large amount of partially halogenated porphyrins in the ZnTFPPCl₈ reaction mixture necessitated high performance liquid chromatography (HPLC). Once the β -octahalo porphyrins were isolated, they were demetallated with HCl_(g) and purified from the zinc salts by alumina

chromatography. The yields for $\text{H}_2\text{TFPPCl}_8$ and $\text{H}_2\text{TFPPBr}_8$ were 40 and 82%, respectively, based on ZnTFPP .

Iron was inserted into the porphyrins by the standard methods: iron(II) acetate in refluxing glacial acetic acid or iron(II) chloride in DMF.^{17,18} With the TFPPBr_8 ligand, the metal is oxidized to iron(III) during the aqueous workup, and the porphyrin isolated as the chloride salt, $\text{Fe}(\text{TFPPBr}_8)\text{Cl}$. The iron porphyrins were found to demetallate during standard column chromatography, and could only be purified by washing or recrystallization. Therefore, high quality free ligand was a prerequisite for generation of pure iron porphyrin.

Addition of pyridine to a solution of $\text{Fe}(\text{TFPPBr}_8)\text{Cl}$ reduced the metal and formed the bis-pyridine adduct. Both $\text{Fe}^{\text{III}}(\text{TFPPBr}_8)\text{Cl}$ ¹⁹ and $\text{Fe}^{\text{II}}(\text{TFPPBr}_8)\text{py}_2$ ²⁰ have been crystallographically characterized. The absorption spectrum of $[\text{Fe}(\text{TFPPCl}_8)]$ in the presence of pyridine indicates formation of $\text{Fe}(\text{TFPPCl}_8)\text{py}_2$, but this species was not isolated. Attempts to synthesize $[\text{Fe}(\text{TFPPCl}_8)]$ were made using air-free, high vacuum techniques, in hopes of isolating a clean, oxygen-free sample for the anticipated investigation of O_2 activation. In retrospect, the removal of oxygen is believed to have complicated its synthesis. Allowing oxygen into the synthesis of $\text{Fe}(\text{TFPPBr}_8)\text{Cl}$ did not lead to oxygen coordination, but clean oxidation of the Fe^{II} porphyrins to $\text{Fe}^{\text{III}}(\text{TFPPBr}_8)\text{Cl}$. In the absence of oxygen, the β -octachloro porphyrin appeared to form an iron(II) complex, based on the red shifted Soret band (see Chapter 3), but with mixed axial ligands. Due to the difficulty in isolating any pure $\text{Fe}(\text{TFPPCl}_8)$ species, further work concentrated on the β -octabromo species.

Insertion of Ru from $\text{Ru}_3(\text{CO})_{12}$ into H_2TFPPX_8 in perfluorobenzene yields a bright red ($\text{X} = \text{Cl}$) or green ($\text{X} = \text{Br}$) $\text{RuTFPPX}_8(\text{CO})$ compound.²¹ In perprotiobenzene, the extended time at reflux necessary to insert the ruthenium atom results in partial porphyrin dehalogenation and decomposition. In these reactions, ruthenium also inserts into the partially chlorinated derivatives $\text{H}_2\text{TFPPCl}_7$ and $\text{H}_2\text{TFPPCl}_6$ to form

$\text{RuTFPPCl}_7(\text{CO})$ and $\text{RuTFPPCl}_6(\text{CO})$, which can be isolated by sequential column chromatography and HPLC (Figure 2.2).

A single band attributable to CO stretching ($1990, \text{Cl}_8$; 1973 cm^{-1} , Br $_8$) is observed in the IR spectrum of $\text{RuTFPPX}_8(\text{CO})$, confirming a single carbonyl ligand.²² Identification of the other axial ligand is problematic; this ligand is labile in $\text{Ru}(\text{CO})$ porphyrins due to the strong trans effect of the CO.²³ Photolysis of $\text{RuTFPPCl}_8(\text{CO})$ in pyridine results in the formation of $\text{RuTFPPCl}_8(\text{py})_2$. After photolysis, a single symmetrically coordinated species is observed by ^{19}F NMR spectroscopy, indicating that the multiple signals in the spectrum of the carbonyl complex are due to variations in trans ligation and not dehalogenation of the porphyrin ring (*vide infra*).

Ruthenium insertion from $\text{Ru}_3(\text{CO})_{12}$ was found to proceed in very low yield: approximately 10-20 % for TFPPCl_8 , and less than 5 % for TFPPBr_8 . Attempts to modify the reaction were unsuccessful. Solvent choice is limited, since any proton bearing solvent will exchange protons with the β -halogens of the porphyrin. Other ruthenium starting materials were tried, including $\text{Ru}(\text{DMSO})_4\text{Cl}_2$, $[\text{Ru}(\text{DMSO})_6]\text{Cl}_2$, RuCl_3 , and $[\text{Ru}_5\text{Cl}_{12}]^{2-}$ (generated in situ). None showed significant reactivity with the TFPPCl_8 ligand.

Surprisingly, attempts to insert ruthenium into TFPP were also unsuccessful. Similar reaction conditions as above showed no reaction with H_2TFPP before substantial decomposition of the ligand occurred. No reports of RuTFPP have been found in the literature, although many metallated derivatives of TFPP have been synthesized.

Molecular Structures

ORTEP diagrams for $\text{H}_2\text{TFPPCl}_8$, ZnTFPPCl_8 ,¹⁰ and $\text{RuTFPPCl}_8(\text{CO})\text{H}_2\text{O}$ ²⁴ complexes are shown in Figure 2.3 - 2.5, with the atom numbering shown. Complete crystallographic reports are included in Appendix 2.

$\text{H}_2\text{TFPPCl}_8$ crystallized from an acetone/water solution in space group $P\bar{1}$, with two porphyrins in the unit cell. The two parallel porphyrin molecules are 4.74 Å apart, with the porphyrin centers slightly offset (center to center distance 6.1 Å). The zinc derivative, ZnTFPPCl_8 , crystallized from a saturated *o*-dichlorobenzene solution with a solvent molecule in a parallel plane both above and below the porphyrin molecule. The solvent molecules are located 3.4 Å from the mean plane of the porphyrin (defined as the average plane of the four nitrogen atoms), a distance suggestive of a π -stacking interaction between the π systems of the porphyrin and the *o*-dichlorobenzene molecules. Aromatic solvent molecules were found to stack in a similar fashion in the crystal structure of tetraphenylporphyrinato-zinc(II) bis-toluene, $\text{ZnTPP}(\text{C}_6\text{H}_5\text{CH}_3)_2$, where two toluene molecules occupy these positions.²⁵ The π donor ability of the aromatic solvent may help stabilize the zinc ion in the electron deficient macrocycle. Similarly, $\text{H}_2\text{TFPPBr}_8$ was found to crystallize with an *o*-dichlorobenzene molecule stacked above each porphyrin molecule.¹⁰

Recrystallization of $\text{RuTFPPCl}_8(\text{CO})$ in air from ethyl acetate and hexane gave $\text{RuTFPPCl}_8(\text{CO})\text{H}_2\text{O}$ (Figure 2.5). An ethyl acetate molecule is hydrogen bonded to the water ligand ($\text{O} \cdots \text{O}$ 2.668 Å), and the stability provided by this hydrogen bond network may explain why no crystals were obtained with other solvents. Trans coordination of CO and H_2O to Ru is unusual, but is preceded in $\text{RuOEP}(\text{CO})\text{H}_2\text{O}$ and the non-porphyrin compound *trans*- $\text{RuCl}_2(\text{PEt}_3)_2(\text{CO})\text{H}_2\text{O}$.^{26,27}

Chlorination of the β -pyrrole carbons induces severe tetrahedral distortions (Figures 2.6 and 2.7) reducing the molecular symmetry of the porphyrin from D_{4h} to D_2 . The pairs of β -halogen atoms are located alternately above and below the average plane determined by the four central nitrogen atoms, and the phenyl rings are rotated slightly towards the mean porphyrin plane to minimize steric contact between the halogen atoms at the pyrrole positions and the ortho carbons of the pentafluorophenyl rings. The distortion of the macrocycle is quantified as the distances of the *meso* and β -carbons from the mean

plane of the porphyrin (Table 2.2). A view of the free ligand porphyrins H_2TFPP , $\text{H}_2\text{TFPPCl}_8$, and $\text{H}_2\text{TFPPBr}_8$ (Figure 2.6), generated from crystal structure coordinates, shows the increasing distortion along the series.

The three β -octachloro porphyrins described above exhibit severe distortions common to perhalogenated and other highly substituted porphyrins:^{7,10,13,20,28-32} 'ruffling' or twist (distortion manifested at the *meso*-carbons) and 'saddling' (distortion manifested at the β -carbons).³³ As expected, saddling increases with halogenation (Figure 2.6), as manifested by increasing average C_β displacements from the plane from 0.051 to 0.62 to 0.90 Å in the free ligand series.¹⁰ The free ligand, $\text{H}_2\text{TFPPCl}_8$, is the least distorted of the structurally characterized chlorinated porphyrins [ZnTFPPCl_8 , $\text{H}_2\text{TFPPCl}_8$, $\text{RuTFPPCl}_8(\text{CO})\text{H}_2\text{O}$, CuTFPPCl_8 ²⁹], as reflected by the smaller perpendicular displacements of atoms from the mean porphyrin plane and a lack of the twisting or ruffling observed in the metallated derivatives. The saddle distortion in the free ligand (average C_β displacement = 0.62 Å) is smaller than in the metallated derivatives ZnTFPPCl_8 (0.75), and CuTFPPCl_8 (0.70),²⁹ but greater than in the octahedrally coordinated $\text{RuTFPPCl}_8(\text{CO})\text{H}_2\text{O}$ (0.48 Å).²⁴

Though saddled, the unmetallated $\text{H}_2\text{TFPPCl}_8$ has essentially no twist distortion (average C_m displacement = 0.023 Å). When the metal atom sits inside the core, a large twist distortion is observed: ZnTFPPCl_8 (0.13), $\text{RuTFPPCl}_8(\text{CO})\text{H}_2\text{O}$ (0.20),²⁴ and CuTFPPBr_8 (0.16 Å).²⁸ Extended to the porphyrin periphery, this results in one halogen atom of each pyrrole being significantly farther out of the mean plane than the other. In ZnTFPPCl_8 the displacements differ by 0.31 Å,¹⁰ and in $\text{RuTFPPCl}_8(\text{CO})\text{H}_2\text{O}$ by 0.43 Å.²⁴ The twist distortion is apparent in the side-on view of $\text{RuTFPPCl}_8(\text{CO})\text{H}_2\text{O}$ (Figure 2.7).

A final measure of distortion is one based on the phenyl dihedral angles; to minimize steric contact with the β -substituents, the phenyl rings rotate towards the mean porphyrin plane (Figure 2.6). The dihedral angles decrease with halogenation from 79° in

H₂TFPP to 73° in H₂TFPPCl₈ to 54° in H₂TFPPBr₈. Metallation also affects the dihedral angle. In the TFPPCl₈ complexes, octahedral RuTFPPCl₈(CO) has a much larger dihedral angle (81°) than the free ligand (73°) or the zinc complex (59°) (Table 2.3).

Remarkably, bond lengths (Table 2.4) in the porphyrin skeleton are essentially preserved throughout the series of metalloderivatives of TPP,^{25,34,35} TFPP, and TFPPX₈ (X= Cl, Br).^{10,36} Bond lengths and angles in the porphyrin skeleton are very similar for all three TFPPCl₈ species, indicating that metallation does not greatly affect porphyrin bond lengths.

The Ru-C bond is slightly longer in RuTFPPCl₈(CO)H₂O (Table 2.2) than in RuOEP(CO)H₂O (1.785)²⁶ or RuTPP(CO)EtOH (1.77 Å),³⁷ consistent with the relatively high value of ν_{CO} .²² The Ru-C-O bond is nearly linear in the three porphyrins, at 178.9, 178.5, and 175.8°, respectively. The Ru-O bond length (2.172 Å) is shorter for the perhalogenated porphyrin than for RuOEP(CO)H₂O (2.253 Å), and closer to the distance found for *trans*-RuCl₂(PEt₃)₂(CO)H₂O (2.189 Å).^{26,27} Interestingly, although the Ru-N bond lengths in RuTFPPCl₈(CO)H₂O and RuTPP(CO)EtOH are the same (~2.05 Å), the TPP derivative is planar, whereas the metal in the halogenated derivative is 0.11 Å out of the mean plane towards the carbonyl ligand. The distorted structure decreases the core size, and may explain why ruthenium insertion is so difficult for TFPPCl₈ and has almost no yield for TFPPBr₈.

NMR Spectra

Fluorine-19 NMR has been extremely helpful in ascertaining both the identity and purity of halogenated compounds. The 100% natural abundance of spin 1/2 ¹⁹F and its high gyromagnetic ratio allow ¹⁹F NMR spectra to be obtained readily.³⁸ As observed in ¹H NMR of tetraphenylporphyrins, the corresponding fluorine atoms from all four phenyl rings appear equivalent in ¹⁹F NMR. The four phenyl rings on the porphyrin are related in the high degree of symmetry of the approximate *D*_{4h} or *D*_{2d} point groups of these

compounds. The chemical shifts of the fluorine atoms on the meso-phenyl rings are extremely sensitive to the metal center, its axial ligands, and the pyrrole carbon substituents, however, such that each porphyrin has a unique spectrum. Correlations in ^{19}F shifts and splitting patterns may be related to various TFPP structures.

The ^{19}F NMR for the unmetallated and zinc TFPP and TFPPCl_8 complexes (Figure 2.8; Table 2.5) display one set of signals each for the ortho, meta, and para fluorines. The para signal, identified by its intensity of 1/2 relative to the ortho and meta signals, is most sensitive to metallation, and shifts 1.7 ppm upfield from $\text{H}_2\text{TFPPCl}_8$ to ZnTFPPCl_8 . The signal appears as a triplet due to coupling to the meta-Fs ($^3J_{\text{F-F}} = -21$ Hz). The ortho signal, farthest downfield, is split into a doublet of doublets, and the meta is a triplet of doublets. The additional splitting is attributed to coupling of fluorines positioned para to one another, as only the para signal does not show any additional structure, with $^5J_{\text{F-F}} = 6.7$ Hz. Computer simulation of the observed spectrum with only these parameters was not satisfactory. Additional coupling between meta fluorines of $^4J \approx -2$ Hz was needed to increase linewidth and generate the proper intensities in the model spectrum. The signs of the coupling constants are consistent with literature values, as are the magnitudes of the various Js (ortho > para > meta).³⁹

Substitution with a paramagnetic or an axially unsymmetric metal center results in significantly different NMR spectra. As with proton NMR, fluorine resonances of the paramagnetic species exhibit a large isotropic shift from those of the diamagnetic derivatives. High spin five-coordinate $\text{Fe}^{\text{III}}\text{TFPP}(\text{Cl})$ (Figure 2.9) or $\text{Fe}^{\text{III}}\text{TFPP}(\text{OH})$ samples, identified by their characteristic UV-Vis and EPR spectra,⁴⁰ show *five* separate ^{19}F NMR signals that fall over a much larger window than those of the diamagnetic porphyrins. The ortho and ortho' (and meta and meta') fluorines, no longer related by an S_4 axis, now have chemical shifts separated by several ppm, and previously observed fine structure is lost due to paramagnetic line broadening. The resonances do not coalesce at temperatures up to 298 K, indicating that rotation of the phenyl rings is slow on the NMR

time scale at room temperature. A Curie plot (Figure 2.10) shows a linear relationship between the isotropic shift and inverse temperature. The isotropic shift is the sum of a contact shift (dependent on $1/T$) and a dipolar shift (dependent on $1/T^2$)⁴¹; the linear dependence on $1/T$ suggests that the dipolar contribution is small. However, the lines do not intersect the origin, which may indicate some dipolar contribution is present.⁴²

The axial ligand is known to affect the ^1H NMR shifts of paramagnetic Fe^{III} porphyrins. In general terms, the porphyrin and the axial ligand compete for bonding interactions with the metal, and the strength of these interactions affects the ring current and π electron density on the protons and therefore their chemical shift.⁴³ A substantial downfield shift of all five resonances (Table 5) is observed upon substitution of an ^-OH for a Cl^- ligand on FeTFPP , consistent with axial ligand effects observed with $p\text{-CH}_3\text{-TPPMnX}$ complexes. Increased π bonding between the metal and the stronger field axial ligand reduces π electron density in the porphyrin, resulting in smaller contact shifts in the ^1H NMR spectrum.⁴⁴ Although the direction of the shift is similar in the fluorine spectrum, the different magnitudes for the contact shift at the ortho and para positions relative to the meta are not observed. Therefore, contact shift alone is not sufficient to explain the ^{19}F NMR spectrum. This is consistent with theory that expects a large temperature independent paramagnetic contribution to fluorine chemical shifts (relative to proton). Further study involving additional compounds would be needed to fully explore this effect.

The five-coordinate $(\text{FeTFPP})_2\text{O}$ dimer also shows 5 peaks in its NMR spectrum (Figure 2.11); however, the signals show significantly less broadening and appear in a much narrower window than the other Fe^{III} porphyrins. Strong antiferromagnetic coupling between the two metal centers⁴⁰ reduces the paramagnetic shift in the ^{19}F NMR of the μ -oxo dimer. Similarly, the resonance for the β -hydrogens in the ^1H NMR spectrum is shifted less in the dimer relative to the monomeric iron(III) complexes. The pyrrole protons of $(\text{FeTFPP})_2\text{O}$ and $(\text{FeTPP})_2\text{O}$ ⁴² show similar isotropic shifts of 5.1 and 5.02 ppm,

respectively, from the diamagnetic Zn complexes, whereas the pyrrole protons are shifted over 70 ppm downfield in the spectrum of $\text{Fe}(\text{TFPP})\text{Cl}$.

The distinctive patterns observed in ^{19}F NMR play important roles in the structural assignment of other perhalogenated compounds. The ^{19}F NMR spectrum of $\text{Fe}^{\text{III}}\text{TFPPBr}_8(\text{Cl})$ (Figure 2.12) shows a broadened five-signal pattern similar to that of $\text{Fe}^{\text{III}}\text{TFPP}(\text{Cl})$. The ortho fluorine resonances exhibit a smaller paramagnetic shift in the perhalogenated compound, consistent with the mixed spin character of the $\text{Fe}^{\text{III}}\text{TFPPBr}_8(\text{Cl})$ ground state.²⁰ The addition of pyridine to $\text{Fe}^{\text{III}}\text{TFPPBr}_8(\text{Cl})$ results in reduction of the iron and formation of the symmetric bis-pyridine compound, $\text{Fe}^{\text{II}}\text{TFPPBr}_8(\text{py})_2$. The assignment of this compound was confirmed as low-spin iron(II) due to the sharp signals and splitting pattern consistent with an axially symmetric, diamagnetic species. Most unusual is the NMR of $[\text{Fe}^{\text{II}}\text{TFPPBr}_8(\text{Cl})]^-$, produced by electrochemical reduction of $\text{Fe}^{\text{III}}\text{TFPPBr}_8(\text{Cl})$ (Figure 2.13a). The relatively sharp signals support the reduction of the metal center, but the splitting of the ortho and meta signals suggests an axially unsymmetric porphyrin; the Fe(II) porphyrin appears to retain an association with the chloride ligand even in the reduced state.¹⁹ Chemical reduction in methanol with ascorbic acid, however, gives a very different spectrum. Only three resonances appear instead of five, indicating a symmetric porphyrin, most likely the bis-methanol derivative $[\text{Fe}^{\text{II}}\text{TFPPBr}_8(\text{OMe})_2]$.

NMR also revealed interesting properties of $\text{RuTFPPCl}_8(\text{CO})\text{H}_2\text{O}$.²⁴ Although an X-ray structure for this compound was obtained, ^{19}F NMR on crystalline material fails to yield a simple spectrum. Instead, several 5-signal patterns are observed, suggesting that the strong trans effect of the carbonyl ligand results in lability of the sixth ligand. The unsymmetric trans coordination around the Ru again leads to dual ortho and meta signals (as in $\text{FeTFPP}(\text{Cl})$), but with the diamagnetic metal center, the fine structure is retained. Upon photolysis in pyridine, a single species, $\text{RuTFPPCl}_8(\text{py})_2$, is obtained. The simple pattern now seen in the ^{19}F NMR shows that previous overlapping signals were due to

multiple species with varying ligands trans to the CO rather than to partial decomposition or dehalogenation of the porphyrin macrocycle.

Conclusions

A series of tetrakis(pentafluorophenyl)- and β -octahalo-tetrakis(pentafluorophenyl)-porphyrins have been synthesized. TFPP derivatives have been studied to provide a comparison for understanding the spectroscopy and catalytic properties of the perhalogenated iron and ruthenium complexes (Chapters 3 - 6).

Crystal structures of unmetallated, zinc, and ruthenium octachloro-tetrakis(pentafluorophenyl) porphyrins are consistent with other structures that demonstrate that halogenation of the β -pyrrole carbons causes a severe saddling of the porphyrin macrocycle. The free base porphyrin, however, does not show the twisting distortion seen in the metallated octahalo derivatives, suggesting that the metal plays a significant role in determining the type and degree of distortion.

The distortions and metal effects observed in the structures of the halogenated metalloporphyrins are analogous to those reported for the octamethyl and octaethyl derivatives of TPP; 2,3,7,8,12,13,17,18- β -octaalkyl-5,10,15,20-tetraphenylporphyrin (TPPX₈, X = methyl, and ethyl).^{32,45} ZnTPPMe₈ and ZnTPPEt₈ are essentially the steric analogs of ZnTFPPCl₈ and ZnTFPPBr₈, respectively. The implication is that the observed distortion is a result of the steric interactions involving the β -halo substituents, and is not electronic in origin.

Fluorine-19 NMR has been shown to be a useful tool for characterization of perhalogenated porphyrin compounds. The identification of various FeTFPPX species will allow another mechanism to study catalysis reactions, for example, by monitoring deactivation of the catalyst via formation of a μ -oxo dimer. Trends in linewidths, shift dispersions, and multiplicities all provide information on the oxidation state and coordination sphere of the metal center. As a supplement to crystallographic data, NMR

allows a more direct examination of the behavior of these highly halogenated porphyrins in solution.

Experimental

Materials Omnisolv grade methanol, acetone, dichloromethane, benzene, pyridine, dimethylformamide, and hexane were purchased from EM Science. N-chloro- and N-bromosuccinimide, glacial acetic acid, iron(II) chloride, triruthenium dodecacarbonyl, and tetraphenylporphyrinato ruthenium(II) carbonyl were purchased from Aldrich and used as received. ZnTFPP and H₂TFPP were purchased from Porphyrin Products and used as received. UV-Vis (CH₂Cl₂): ZnTFPP λ_{max} nm (ϵ 10⁵ M⁻¹ cm⁻¹); 414 (5.0), 544 (0.24); H₂TFPP λ_{max} nm 412, 506, 584. Fe^{III}TFPPCl was purchased from Aldrich and purified by chromatography on alumina before use. UV-Vis (acetone): λ_{max} nm (ϵ 10⁵ M⁻¹ cm⁻¹) 350 (0.7), 410 (1.0), 50 (0.11), 629 (0.06). RuTPP(py)₂ was prepared by a literature method.⁴⁶

Methods UV-Vis spectra were recorded on a Hewlett Packard HP8452 diode array interfaced to an IBM or a Cary-14 spectrophotometer with an Olis 3820 conversion system. Infrared spectra were recorded as solutions in carbon tetrachloride or benzene on a Perkin-Elmer Model 1600 FT-IR spectrophotometer. Separation of the ruthenium porphyrins was accomplished with a Beckman Model 126 dual pump and 166 single channel detector on a Vydac C-18 reverse phase column. A 1000 W tungsten lamp was used for photolysis experiments. ¹H and ¹⁹F NMR spectra were recorded on a Brüker AM-500 (tuned down to 470.56 MHz for fluorine detection) instrument in CDCl₃ or deuterated acetone and referenced internally to C₆H₅F at -113.6 ppm (vs. CFCl₃ at 0 ppm). Porphyrin purification was accomplished with alumina (Fluka or Baker 40 μ alumina) or silica (Analtech 150 Å pore, 75-100 particle size silica) column chromatography. Further purification of the zinc and ruthenium perhalogenated porphyrins was accomplished with a Beckman Model HPLC system (126 dual pump and 166 single channel detector) on a

Vydac C-18 reverse phase column with isocratic acetone:water elution. Mass spectroscopy was performed at Caltech with a cesium ion fast atom bombardment spectrometer.

Elemental analysis on the perhalogenated compounds was obtained, and varied greatly by compound. Results were not satisfactory, even on crystalline samples that were pure by other criteria.

Fe^{III}TFPP(OH) and (Fe^{III}TFPP)₂O: Fe^{III}TFPP(OH) and (Fe^{III}TFPP)₂O were synthesized from the chloride by published methods.⁴⁰ Fe^{III}TFPP(Cl) was dissolved in benzene, and a small amount of NaOH solution was added. After stirring for several hours, the water was removed using a separatory funnel, and the benzene solution was chromatographed on neutral alumina with a benzene/acetone solution. The μ -oxo elutes first, and the hydroxide elutes with a higher percent acetone. Fe^{III}TFPP(OH): UV-Vis (acetone): λ_{max} 406, 563 nm. (Fe^{III}TFPP)₂O: UV-Vis; CH₂Cl₂; λ_{max} 398, 415(shoulder), 560 nm.

H₂TFPPCl₈: Chlorination of ZnTFPP was accomplished by a modification of earlier methods.^{8,47,48} Approximately 500 mg ZnTFPP was dissolved in 50 mL dry methanol with forty equivalents of N-chlorosuccinimide, and the mixture refluxed for an hour. When chlorination of the pyrrole positions was complete, as determined by the red shift of the Soret band in the UV-Vis and thin layer chromatography on silica plates (1:1 hexane: dichloromethane) the solution was allowed to cool. The product was precipitated with water, filtered, and washed with cold hexane to remove decomposed porphyrin by-products. Further purification by HPLC was necessary to separate partially chlorinated species. Yield ZnTFPPCl₈ 60 to 80%. UV-Vis (CH₂Cl₂): λ_{max} nm (ϵ 10⁵ M⁻¹ cm⁻¹); 364, 440 (1.6), 572 (0.13). Mass spectrum m/z = 1314 (calc. 1313). The chlorinated zinc porphyrin was demetallated as previously by Lyons, et al.⁴⁷ ZnTFPPCl₈ was redissolved in approximately 50 mL chloroform, and HCl gas was passed through a gas dispersion tube into the solution for 1-2 minutes. The volume of the reaction mixture was reduced, and the solution was chromatographed on alumina, eluting with 95% chloroform - 5%

methanol. The product, $\text{H}_2\text{TFPPCl}_8$, was collected and rotary evaporated to dryness, with a yield of approximately 95%. UV-Vis (CH_2Cl_2): λ_{max} nm ($\epsilon \times 10^5 \text{ M}^{-1} \text{ cm}^{-1}$); 436 (16), 536 (1.3), 622 (0.46).

$\text{H}_2\text{TFPPBr}_8$: The bromo analog was similarly synthesized via bromination of ZnTFPP with N-bromosuccinimide. ZnTFPPBr_8 : UV-Vis (CH_2Cl_2): λ_{max} nm ($\epsilon \times 10^5 \text{ M}^{-1} \text{ cm}^{-1}$); 460 (1.9), 594 (0.17). The free ligand was obtained by demetallation with HCl gas, and the product chromatographed on alumina. UV-Vis (CH_2Cl_2): λ_{max} 454, 552, 636 nm.

$\text{FeTFPPBr}_8(\text{Cl})$ and $[\text{FeTFPPCl}_8]$: Iron was inserted into H_2TFPPX_8 with freshly prepared iron(II) acetate in glacial acetic acid,¹⁷ or with $\text{Fe}^{\text{II}}\text{Cl}_2$ in DMF.¹⁸ Insertion was evident by the red color of the solution. The iron porphyrin was precipitated with brine, dried, and washed with hexane to remove impurities. UV-Vis (CH_2Cl_2) Br_8 : λ_{max} nm($\epsilon \times 10^5 \text{ M}^{-1} \text{ cm}^{-1}$) 402 (8.1), 442 (8.5), 560 (1.4). With $\text{H}_2\text{TFPPCl}_8$, reactions were conducted on a high vacuum line and precipitated with deoxygenated water. UV-Vis (CH_2Cl_2): λ_{max} 404, 582 nm. Addition of pyridine to a solution of $\text{FeTFPPX}_8(\text{Cl})$ led to formation of $\text{Fe}^{\text{II}}\text{TFPPX}_8(\text{py})_2$. UV-Vis (CH_2Cl_2) Br_8 : λ_{max} 450, 556, 588 nm; Cl : λ_{max} 438, 542, 574 nm.

$\text{RuTFPPCl}_8(\text{CO})$: The preparation of $\text{RuTFPPCl}_8(\text{CO})$ was based on the methods of Tsutsui⁴⁹ and Chow.⁵⁰ 300 mg $\text{H}_2\text{TFPPCl}_8$ ¹⁰ reacts with 300 mg $\text{Ru}_3(\text{CO})_{12}$ (48 h, refluxing benzene) to form $\text{RuTFPPCl}_8(\text{CO})$. $\text{RuTFPPCl}_7(\text{CO})$ and $\text{RuTFPPCl}_6(\text{CO})$ also were isolated from the reaction mixture. $\text{RuTFPPCl}_n(\text{CO})$ ($n = 6, 7, 8$) complexes were separated from unreacted free ligand by column chromatography on silica gel eluting with hexane and increasing percentages of methylene chloride. The partially chlorinated isomers were purified by HPLC, and the identity of each fraction was confirmed by mass spectroscopy. The parent peak in each mass spectrum appears at the mass for RuTFPPCl_n ($n = 6, 7, 8$), with a smaller peak appearing at the mass for the monocarbonyl complex. Parent peaks appeared at $m/z = 1351.2$ (RuTFPPCl_8), 1315.8

(RuTFPPCl₇), and 1280.1 (RuTFPPCl₆). UV-Vis (CH₂Cl₂): λ_{\max} nm (ϵ 10⁵ M⁻¹ cm⁻¹) 416 (1.7), 542 (0.14). RuTFPPBr₈(CO) (mass spectrum; m/z = 1703) was synthesized from Ru₃(CO)₁₂ and H₂TFPPBr₈ (50 h refluxing benzene). UV-Vis (CH₂Cl₂): λ_{\max} 424, 560 nm.

RuTFPPCl₈(py)₂: Photolysis of the carbonyl was accomplished by modification of Chow's methods.⁵⁰ Pyridine solutions of RuTFPPCl_n(CO) exposed to a 1000W mercury lamp for several hours lose a carbonyl ligand to form RuTFPPCl_n(py)₂. Loss of the carbonyl was confirmed by the disappearance of the CO stretch (IR, CCl₄ solution) and by ¹⁹F-NMR spectroscopy (CDCl₃ solution): δ (RuTFPPCl₈(py)₂) = -138.7 (2F, q, ortho); -152.3 (1F, t, para); -163.2 ppm (2F, m, meta). UV-Vis (CH₂Cl₂): λ_{\max} 415, 510, 536 nm. ¹⁹F-NMR: -138.7 (2F, q, ortho), -152.3 (1F, t, para), -163.2 ppm (2F, m, meta).

Crystal Structure Analysis: Since the halogenated porphyrin crystals lost solvent easily, a single crystal was removed directly from the crystallization solution and mounted in a capillary with silicon grease. Data were collected on an Enraf-Nonius CAD-4 diffractometer using Mo K α radiation. Atomic scattering factors and values for f' were taken from Cromer and Waber⁵¹ and Cromer,⁵² and CRYM,⁵³ MULTAN,⁵⁴ and ORTEP⁵⁵ computer programs were used for calculations. The weights were taken as $1/\sigma^2(F_o^2)$; variances ($\sigma^2(F_o^2)$) were derived from counting statistics plus an additional term, $(0.014I)^2$; variances of the merged data were obtained by propagation of error plus another additional term, $(0.014 \bar{I})^2$.

Purple crystals of ZnTFPPCl₈ were grown from a saturated solution of *o*-dichlorobenzene at 0 °C. Crystals of this compound lost solvent quickly, so one was covered with epoxy glue before being cooled to -44 °C on the diffractometer. The zinc crystal was found to be tetragonal, belonging to space group P $\bar{4}$ 2₁c. The structure was solved by location of the zinc atom from a Patterson map. Structure factors and Fourier calculations showed Cl1 and Cl2, and subsequent structure factor Fourier calculations gave the rest of the porphyrin. Solvent molecules were found in difference Fourier maps

calculated in their planes. The solvent molecules occupy two separate regions in the cell, each region holding one dichlorobenzene molecule. The molecules are disordered in these regions, and were initially modeled with idealized $C_6H_4Cl_2$ groups. Eventually, some of the chlorine atoms of the solvent were refined, as well as the population parameters for alternate orientations, but the carbon atoms were always positioned based on Fourier maps. For one region (C31-36 and C41-46) anisotropic displacement parameters were assigned by hand based on the maps and the refined parameters of the Cl atoms of the solvent; the other carbon atoms of the solvent were left isotropic. The disordered solvent regions are the cause, in all probability, of the somewhat larger than usual values for R and goodness of fit.

Brown crystals of $H_2TFPPCl_8$ were grown by slow evaporation from an acetone/water solution. The crystals were found to be triclinic, belonging to space group $P\bar{1}$. Porphyrin molecules were located from a Patterson map, and the two inner hydrogen atoms were located in a difference map as disordered among the four nitrogen atoms. Their positional parameters were refined, with B values fixed at 1.2 times the isotropic equivalent U_{ij} value of the bonded nitrogen atoms and the population factors assigned at one-half.

Deep red crystals of $RuTFPPCl_8(CO)(H_2O)$ were grown by slow evaporation from an ethyl acetate/hexane solution. Ruthenium atom coordinates were obtained from a Patterson map, and the remaining atoms located with structure factor-Fourier calculations. Hydrogen atoms on the solvent molecules were positioned by calculation in idealized locations with staggered geometry and a C-H bond length of 0.95 Å. Of the solvent molecules, only one ethyl acetate site is fully populated (C71, C72, O2, O3, C73, and C74). The second (C81, C82, O4, O5, C83, and C84) is half-populated, near a center of symmetry. The region occupied by hexane is not easily interpreted. There are five peaks in a difference map in an area of broadly diffuse electron density. These five were co-planar within 0.15 Å, so we fitted idealized hexane molecules to the difference density in this plane. Our model has three orientations of the hexane; there may be twice that many. We

kept the positional and thermal parameters of these idealized molecules fixed but refined their population parameters independently. The sum of the three was 0.84; we believe this represents some loss of hexane from the crystal during data collection. We kept the populations fixed in the final refinement. The final difference map has peaks of 0.88, 0.82 and 0.79 Å⁻³ and valleys of -1.24 and -0.84 Å⁻³ in this region.

Appendix 2 contains unit cell diagrams, final heavy atom parameters, anisotropic displacement parameters, complete distances and angles, and structure factors for H₂TFPPCl₈, ZnTFPPCl₈, and RuTFPPCl₈(CO)H₂O, H atom parameters for H₂TFPPCl₈, and intermolecular distances less than 3.5 Å for ZnTFPPCl₈ and RuTFPPCl₈(CO)H₂O.

References and Notes

- (1) Lindsey, J. S.; Wagner, R. W. *J. Org. Chem.* **1989**, *54*, 828-836.
- (2) Bray, B. L.; Mathies, P. H.; Naef, R.; Solas, D. R.; Tidwell, T. T.; Artis, D. R.; Muchowski, J. M. *J. Org. Chem.* **1990**, *55*, 6317-6328.
- (3) Qui, Z.-M.; Burton, D. J. *Tetrahedron Lett.* **1994**, *35*, 4319-4322.
- (4) Traylor, T. G.; Tsuchiya, S. *Inorg. Chem.* **1987**, *26*, 1338-1339.
- (5) Wijesekera, T.; Matsumoto, A.; Dolphin, D.; Lexa, D. *Angew. Chem., Int. Ed. Eng.* **1990**, *29*, 1028-1030.
- (6) Bartoli, J. F.; Brigaud, O.; Battioni, P.; Mansuy, D. *J. Chem. Soc., Chem. Commun.* **1991**, 440-442.
- (7) Mandon, D.; Ochsenbein, P.; Fischer, J.; Weiss, R.; Jayaraj, K.; Austin, R. N.; Gold, A.; White, P. S.; Brigaud, O.; Battioni, P.; Mansuy, D. *Inorg. Chem.* **1992**, *31*, 2044-2049.
- (8) Hoffmann, P.; Robert, A.; Meunier, B. *Bull. Chem. Soc. Fr.* **1992**, *129*, 85-97.
- (9) D'Souza, F.; Villard, A.; Caemelbecke, E. V.; Franzen, M.; Boschi, T.; Tagliatesta, P.; Kadish, K. M. *Inorg. Chem.* **1993**, *32*, 4042-4048.
- (10) Birnbaum, E. R.; Hodge, J. A.; Grinstaff, M. G.; Schaefer, W. P.; Marsh, R. E.; Henling, L. M.; Labinger, J. A.; Bercaw, J. E.; Gray, H. B. *Inorg. Chem.* **in press**.
- (11) d'A. Rocha Gonsalves, A. M.; Johnstone, R. A. W.; Pereira, M. M.; Shaw, J.; Sobral, D. N.; Abilio, J. F. *Tetrahedron Lett.* **1991**, *32*, 1355-1358.
- (12) Banfi, S.; Mandelli, R.; Montanari, F.; Quici, S. *Gazz. Chim. Ital.* **1993**, *123*, 409-415.
- (13) Ochsenbein, P.; Ayougou, K.; Mondon, D.; Fischer, J.; Weiss, R.; Austin, R. N.; Jayaraj, K.; Gold, A.; Turner, J.; Fajer, J. *Angew. Chem., Int. Ed. Eng.* **1994**, *33*, 348-350.
- (14) Bartoli, J. F.; Battioni, P.; Foor, W. R. D.; Mansuy, D. *J. Chem. Soc., Chem. Commun.* **1994**, 23-24.
- (15) *Tables of Interatomic Distances and Configurations in Molecules and Ions*; Sutton, L. E., Ed.; The Chemical Society: London, 1965; Vol. Special Publication 18.
- (16) Allred, A. L. *J. Inorg. Nucl. Chem.* **1961**, *17*, 215-221.
- (17) Warburg, O.; Negelein, E. *Z. Biochem* **1932**, 14-32.
- (18) Adler, A. D.; Longo, F. R.; Kampas, F.; Kim, J. J. *Inorg. Nucl. Chem.* **1970**, *32*, 2443-2445.

- (19) Grinstaff, M. W.; Hill, M. G.; Labinger, J. A.; Gray, H. B. *Science* **1994**, *264*, 1311-1313.
- (20) Grinstaff, M. W.; Hill, M. G.; Birnbaum, E. R.; Schaefer, W. P.; Labinger, J. A.; Gray, H. B. *Inorg. Chem.* **in press**.
- (21) The axial ligand trans to the carbonyl ligand in ruthenium porphyrins is usually assumed to be solvent, and is not specifically mentioned. Unless otherwise indicated, the oxidation state of ruthenium is 2+.
- (22) For reference, the CO stretch in the IR spectrum of RuTPP(CO) is at 1945 cm⁻¹: Chow, B. C.; Cohen, I. A. *Bioinorg. Chem.* **1971**, *1*, 57. Since the probable trans ligands (water, ethanol, acetone) are all O-atom donors, we would not expect any splitting of ν_{CO} .
- (23) Buchler, J. W.; Kokisch, W.; Smith, P. D. *Struct. Bonding* **1978**, *34*, 79-134.
- (24) Birnbaum, E. R.; Schaefer, W. P.; Labinger, J. A.; Bercaw, J. E.; Gray, H. B. *Inorg. Chem.* **1995**, *34*, 1751-1755.
- (25) Scheidt, W. R.; Kastner, M. E.; Hatano, K. *Inorg. Chem.* **1978**, *17*, 706-710.
- (26) Kadish, K. M.; Hu, Y.; Mu, X. H. *J. Heterocycl. Chem.* **1991**, *28*, 1821-1824.
- (27) Sun, Y.; Taylor, N. J.; Carty, A. J. *Inorg. Chem.* **1993**, *32*, 4457-4459.
- (28) Henling, L. M.; Schaefer, W. P.; Hodge, J. A.; Hughes, M. E.; Gray, H. B.; Lyons, J. E.; Ellis, P. E., Jr. *Acta Crystallogr.* **1993**, *C49*, 1745-1747.
- (29) Schaefer, W. P.; Hodge, J. A.; Hughes, M. E.; Gray, H. B.; Lyons, J. E.; Ellis, P. E., Jr.; Wagner, R. W. *Acta Crystallogr.* **1993**, *C49*, 1342-1345.
- (30) Marsh, R. E.; Schaefer, W. P.; Hodge, J. A.; Hughes, M. E.; Gray, H. B.; Lyons, J. E.; Ellis, P. E., Jr. *Acta Crystallogr.* **1993**, *C49*, 1339-1342.
- (31) Bhyrappa, P.; Krishnan, V. *Inorg. Chem.* **1991**, *30*, 239-245.
- (32) Barkigia, K. M.; Berber, M. D.; Fajer, J.; Medforth, C. J.; Renner, M. W.; Smith, K. M. *J. Am. Chem. Soc.* **1990**, *112*, 8851-8857.
- (33) Scheidt, W. R.; Lee, Y. J. In *Metal Complexes with Tetrapyrrole Ligands I*; J. W. Buchler, Ed.; Springer-Verlag: New York, 1987; Vol. 64; pp 2-70.
- (34) Hoard, J. L. *Ann. N.Y. Acad. Sci.* **1973**, *206*, 18-31.
- (35) Fleischer, E. B.; Miller, C. K.; Webb, L. E. *J. Am. Chem. Soc.* **1964**, *86*, 2342-2347.
- (36) Hodge, J. A. Thesis, California Institute of Technology, 1995.
- (37) Bonnet, J. J.; Eaton, S. S.; Eaton, G. R.; Holm, R. H.; Ibers, J. A. *J. Am. Chem. Soc.* **1973**, *95*, 2141-2149.
- (38) Harris, R. K. *Nuclear Magnetic Resonance Spectroscopy*; Pitman Publishing, Inc.: Marshfield, MA, 1983.

- (39) Bovey, F. A.; Jelinski, L. *Nuclear Magnetic Resonance Spectroscopy*; 2nd ed.; Academic Press, Inc: San Diego, CA, 1988, pp 437-488.
- (40) Jayaraj, K.; Gold, A.; Toney, G. E.; Helms, J. H.; Hatfield, W. E. *Inorg. Chem.* **1986**, 25, 3516-3518.
- (41) La Mar, G. N.; Eaton, G. R.; Holm, R. H.; Walker, F. A. *J. Am. Chem. Soc.* **1971**, 95, 63-75.
- (42) La Mar, G. N.; Walker, F. A. *J. Am. Chem. Soc.* **1973**, 95, 1782-1790.
- (43) Caughey, W. S.; Johson, L. F. *J. Chem. Soc., Chem. Commun.* **1969**, 1362-1363.
- (44) La Mar, G. N.; Walker, F. A. *J. Am. Chem. Soc.* **1975**, 97, 5013-5106.
- (45) Sparks, L. D.; Medforth, C. J.; Park, M.-S.; Chamberlain, J. R.; Ondrias, M. R.; Senge, M. O.; Smith, K. M.; Shelnutt, J. A. *J. Am. Chem. Soc.* **1993**, 115, 581-592.
- (46) Brown, G. M.; Hopf, F. R.; Ferguson, J. A.; Meyer, T. J.; Whitten, D. G. *J. Am. Chem. Soc.* **1973**, 95, 5939-5942.
- (47) Lyons, J. E.; Ellis, P. E., Jr.; Myers, H. K., Jr.; Wagner, R. W. *J. Catal.* **1993**, 141, 311-315.
- (48) Ellis, P. E., Jr.; Lyons, J. E. *Coord. Chem. Rev.* **1990**, 105, 181-193.
- (49) Tsutsui, M.; Ostfeld, D.; Hoffman, L. M. *J. Am. Chem. Soc.* **1971**, 93, 1820-1823.
- (50) Chow, B. C.; Cohen, I. A. *Bioinorg. Chem.* **1971**, 1, 57-63.
- (51) Cromer, D. T.; Waber, J. T. *International Tables For X-ray Crystallography*; Kynoch Press: Birmingham, 1974; Vol. IV, pp 99-101.
- (52) Cromer, D. T. *International Tables For X-ray Crystallography*; Kluwer Academic Publishers: Dordrecht, 1974; Vol. IV, pp 149-151.
- (53) Duchamp, D. J. In Am. Crystallogr. Assoc. Meet., Paper B14: Bozeman, Montana, 1964; pp 29-30.
- (54) Debaerdemaeker, T.; Germain, G.; Main, P.; Refaat, L. S.; Tate, C.; Woolfson, M. M. *MULTAN 88. Computer Programs for the Automatic Solution of Crystal Structures from X-ray Diffraction Data*, University of York, England and Louvain, Belgium, 1988.
- (55) Johnson, C. K. *ORTEP II*, Report ORNL-3794: Oak Ridge National Laboratory, Oak Ridge, Tennessee, 1976.

Figure 2.1 -- The general structure of third generation pentafluorophenyl metalloporphyrins discussed in this chapter. The α , β , and meso carbons are marked.

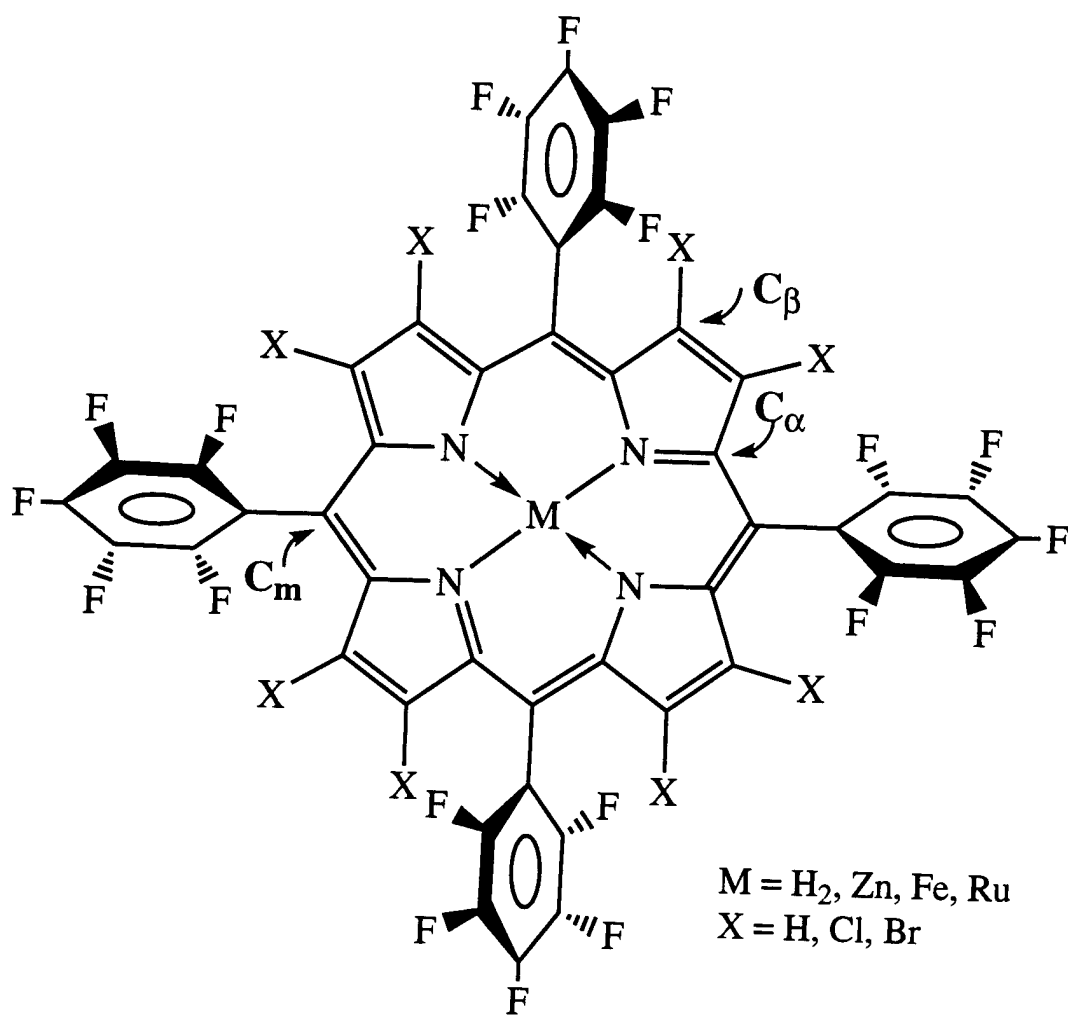


Figure 2.2 -- HPLC trace showing separation of partially halogenated ruthenium porphyrins on a reverse phase C₁₈ column with isocratic elution of 88% ethanol in water. Excess free ligand comes off the column earliest, followed by ruthenium porphyrins bearing increasing numbers of β -chlorines. Zinc porphyrin is likely produced from metallation of the free ligand in the stainless steel HPLC tubing.

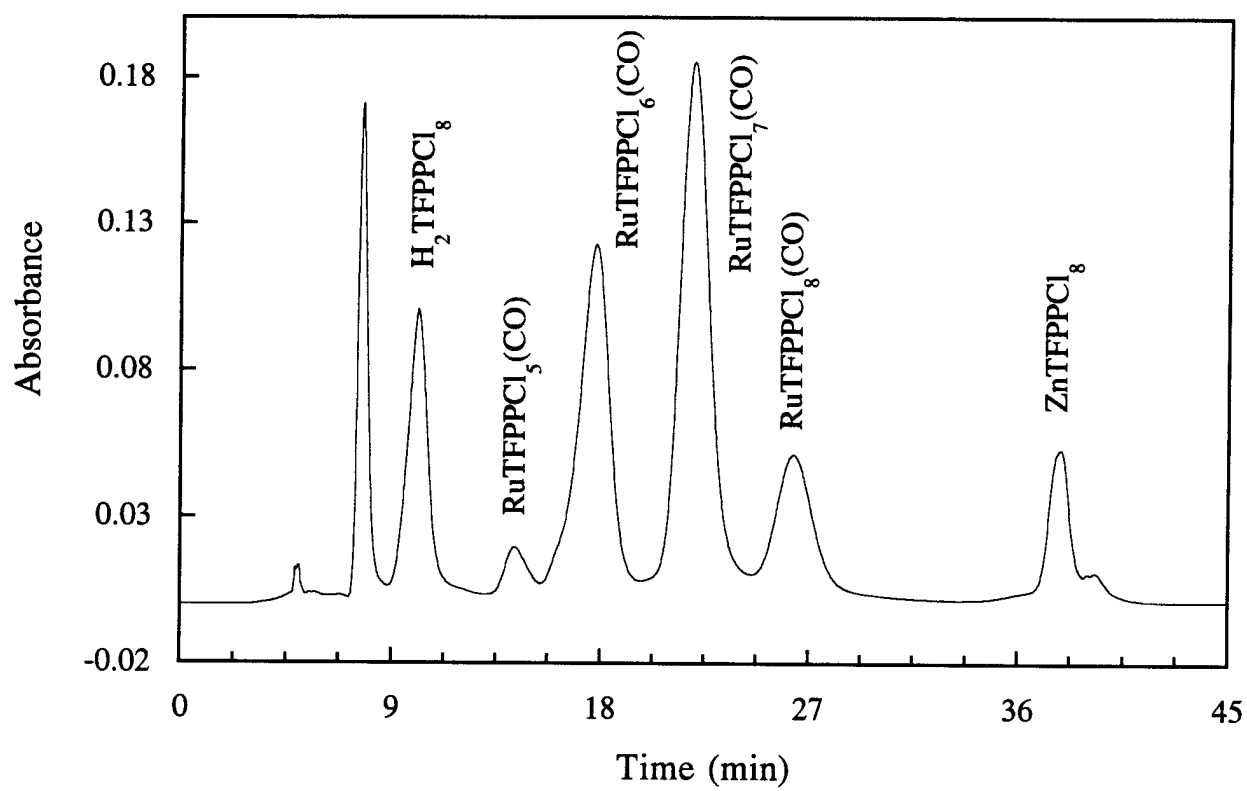


Figure 2.3 -- ORTEP diagram of $\text{H}_2\text{TFPPCl}_8$ with 50% probability ellipsoids of the molecule showing the numbering used. Only two hydrogen atom sites are shown.

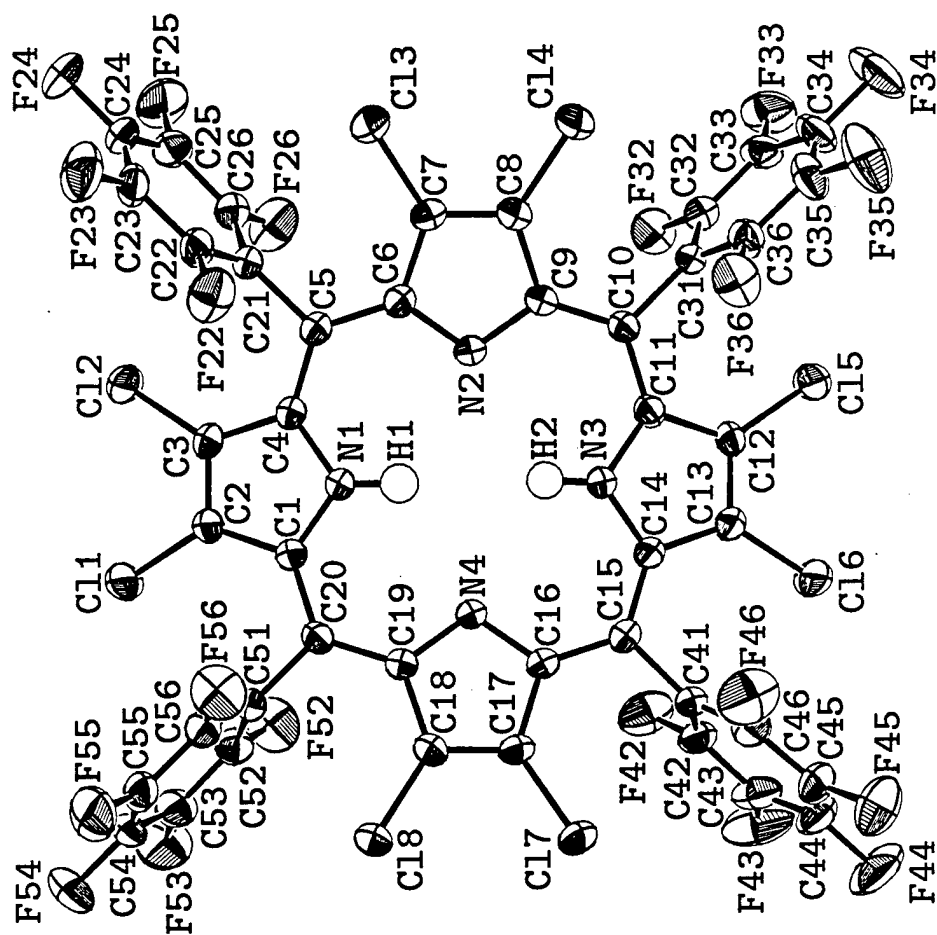


Figure 2.4 -- ORTEP diagram of ZnTFPPCl_8 with 50% probability ellipsoids of the molecule showing the numbering system used.

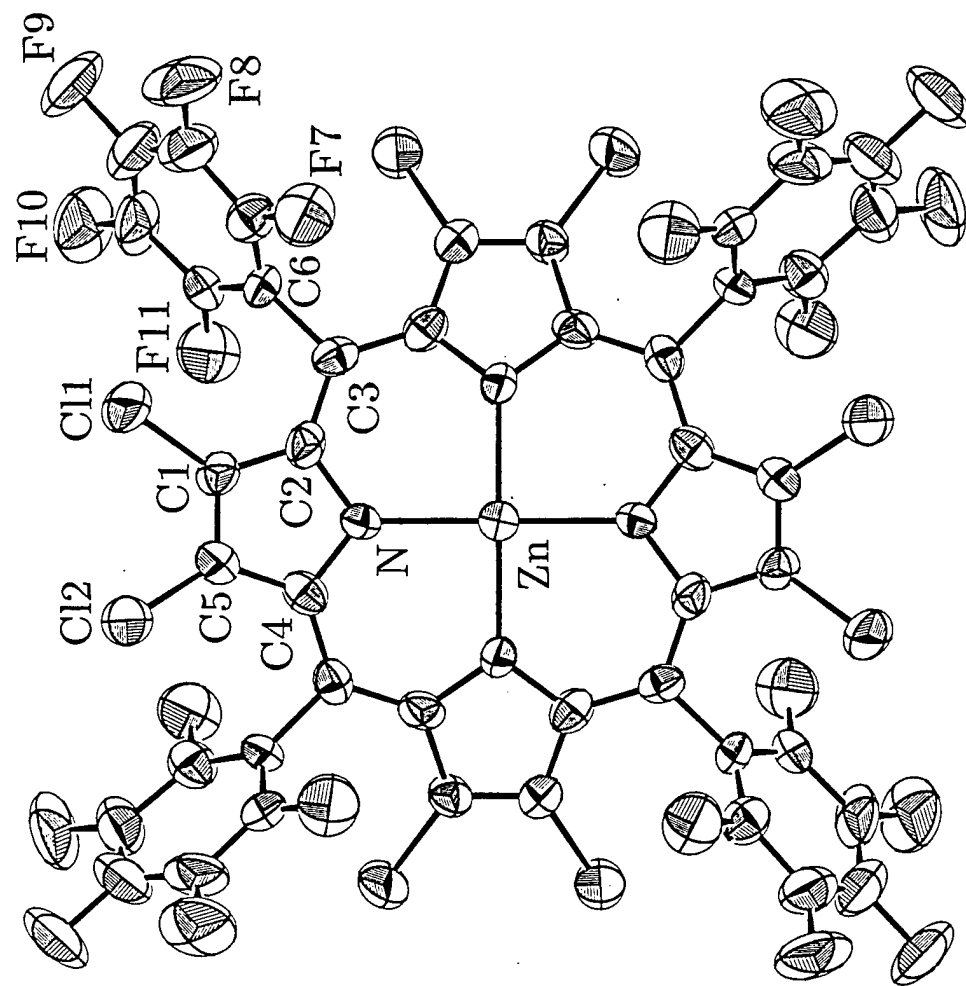


Figure 2.5 -- ORTEP diagram of $\text{RuTFPPCl}_8(\text{CO})\text{H}_2\text{O}$ with 50% probability ellipsoids showing the numbering system used. Atoms C21, C31, C41, and C51 (not numbered) are bonded to C3, C8, C13, and C18, respectively; carbon atoms in the pentafluorophenyl groups have the same numbers as the attached fluorine atoms.

Figure 2.6 -- Molecular representations of the series H_2TFPP , $\text{H}_2\text{TFPPCl}_8$, and $\text{H}_2\text{TFPPBr}_8$ using the actual crystal structure coordinates. From the planar H_2TFPP , the saddle distortion clearly increases upon further halogenation.

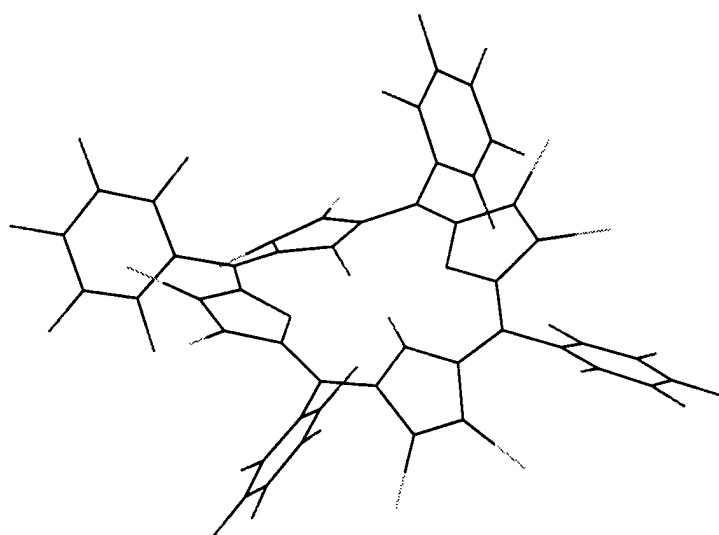
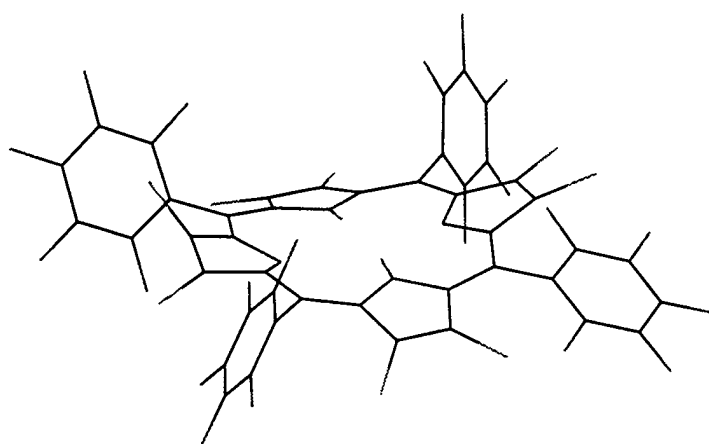
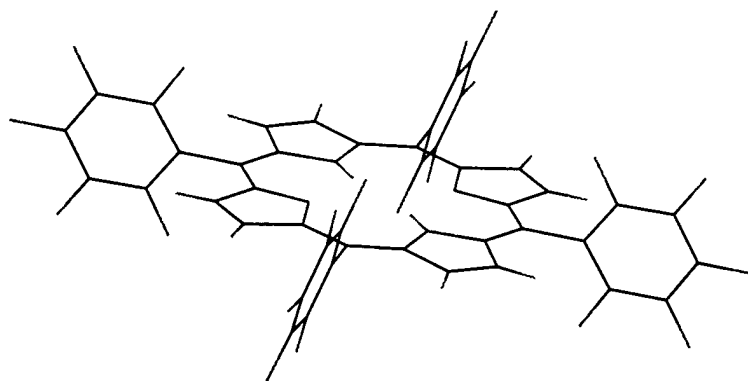


Figure 2.7 -- Edge-on view of a Chem 3D drawing of $\text{RuTFPPCl}_8(\text{CO})\text{H}_2\text{O}$ using crystal structure coordinates. The ruffle in the porphyrin macrocycle is apparent in the different displacements of the chlorine atoms (striped) from the mean porphyrin plane.

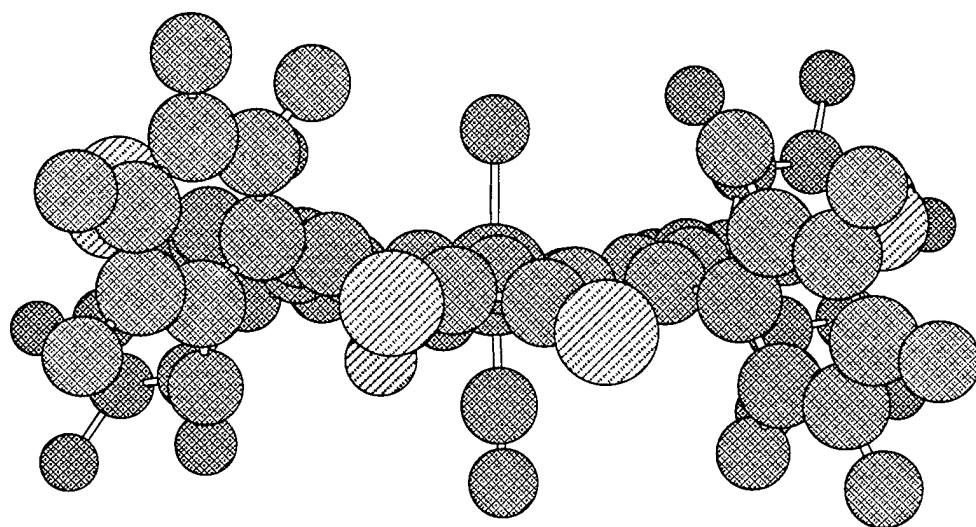


Figure 2.8 -- ^{19}F -NMR spectra of a) $\text{H}_2\text{TFPPCl}_8$ and b) ZnTFPPCl_8 in CDCl_3 . The signals are assigned ortho, para, meta, from left to right. The signals for the free ligand have been enlarged to show the fine structure observed in the spectra of free ligand, zinc, and other diamagnetic metal porphyrins.

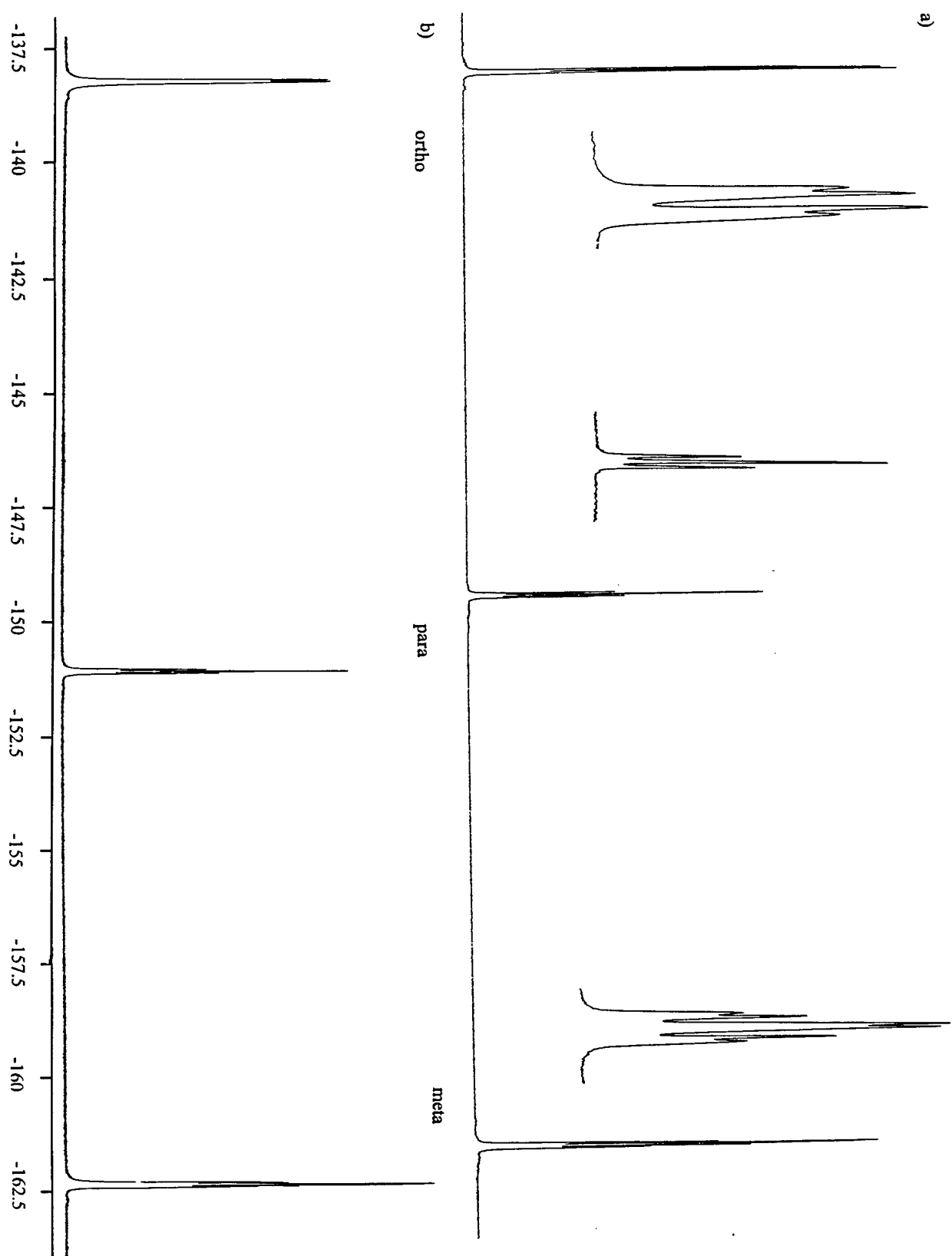


Figure 2.9 -- ^{19}F -NMR spectrum of $\text{Fe}^{\text{III}}\text{TFPP}(\text{Cl})$. The ortho resonances are shifted over 20 ppm downfield from those of H_2TFPP .

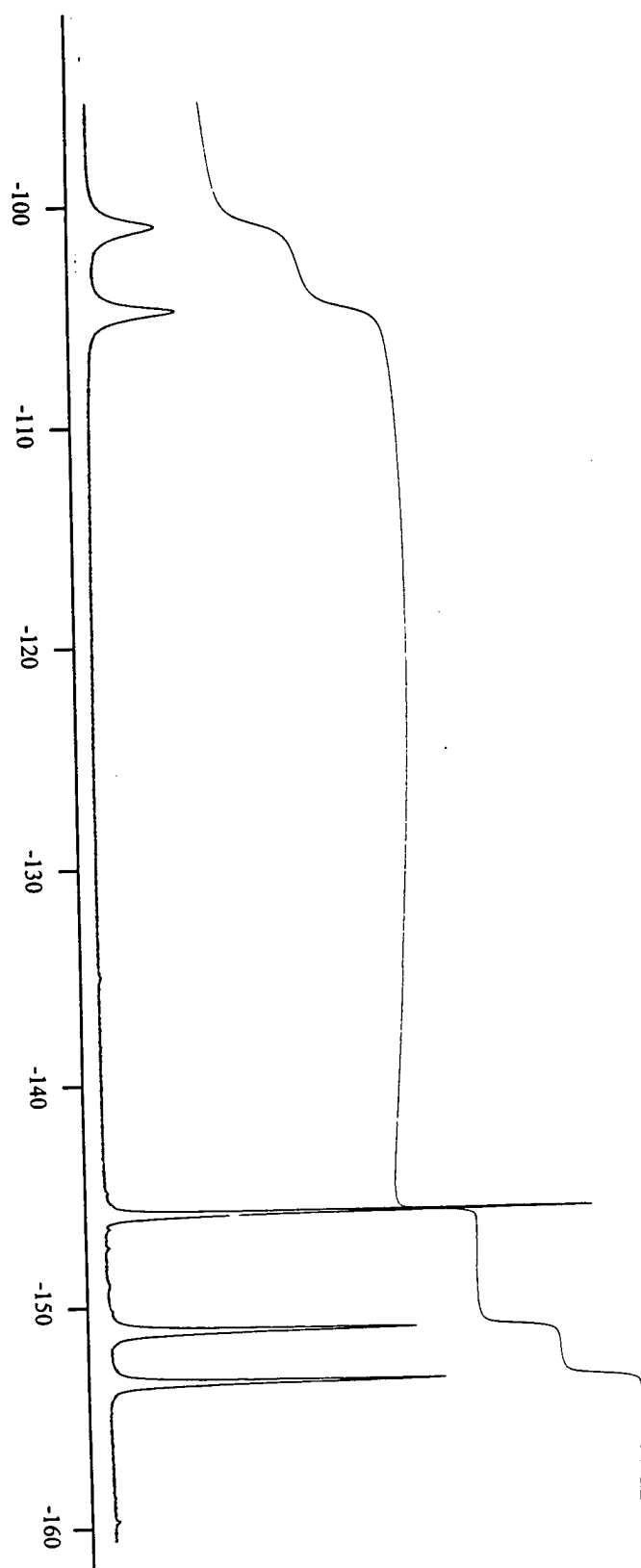


Figure 2.10 -- Curie plot showing the temperature dependence of the chemical shift of $\text{Fe}^{\text{III}}\text{TFPP}(\text{Cl})$ resonances. The isotropic shift is calculated relative to the diamagnetic $\text{Zn}^{\text{II}}\text{TFPP}$ complex.

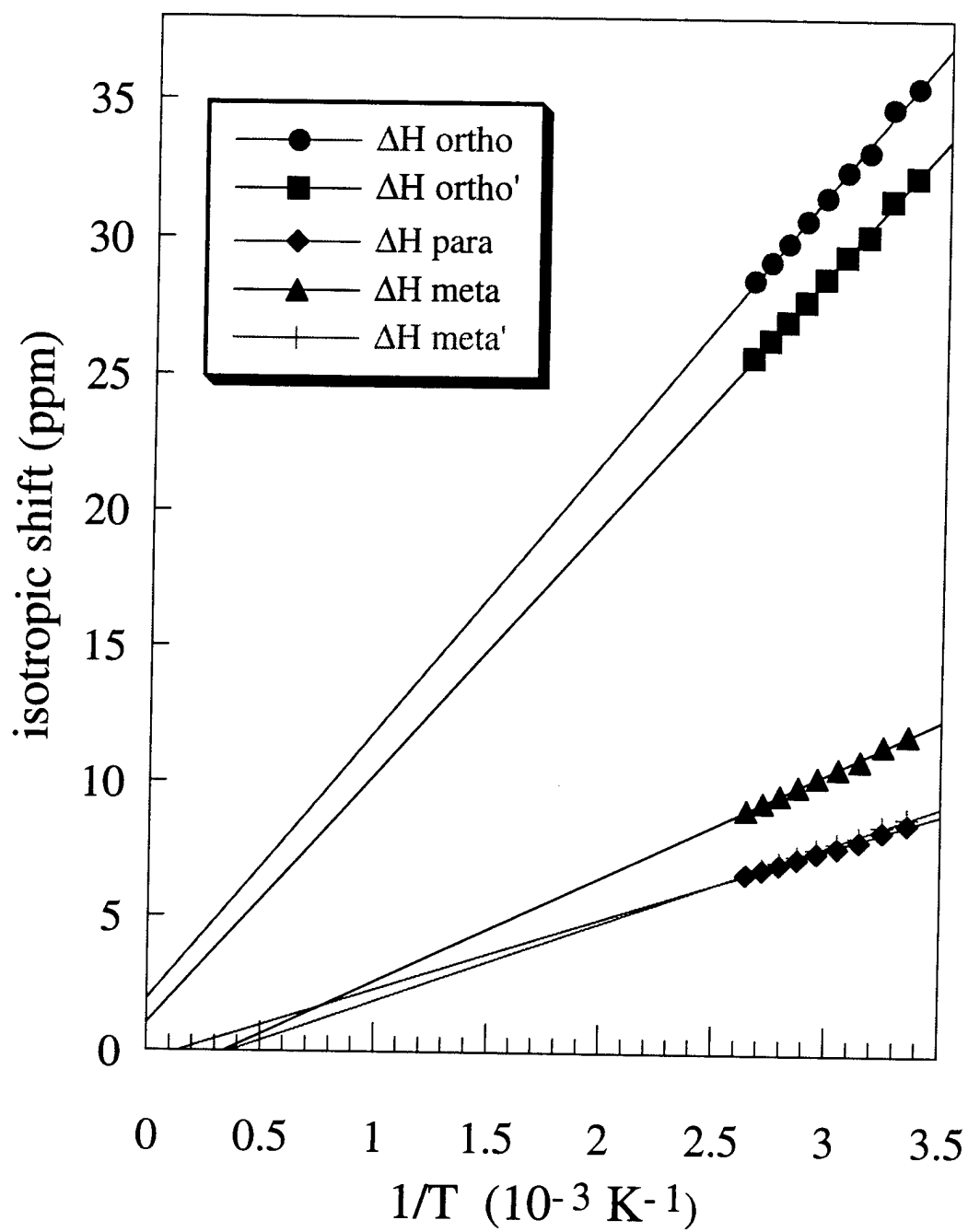


Figure 2.11 -- ^{19}F -NMR spectrum of $(\text{Fe}^{\text{III}}\text{TFPP})_2\text{O}$ in acetone- d_6 . The window is much smaller than that of the paramagnetic $\text{FeTFPP}(\text{Cl})$ monomer due to antiferromagnetic coupling between the two iron atoms.

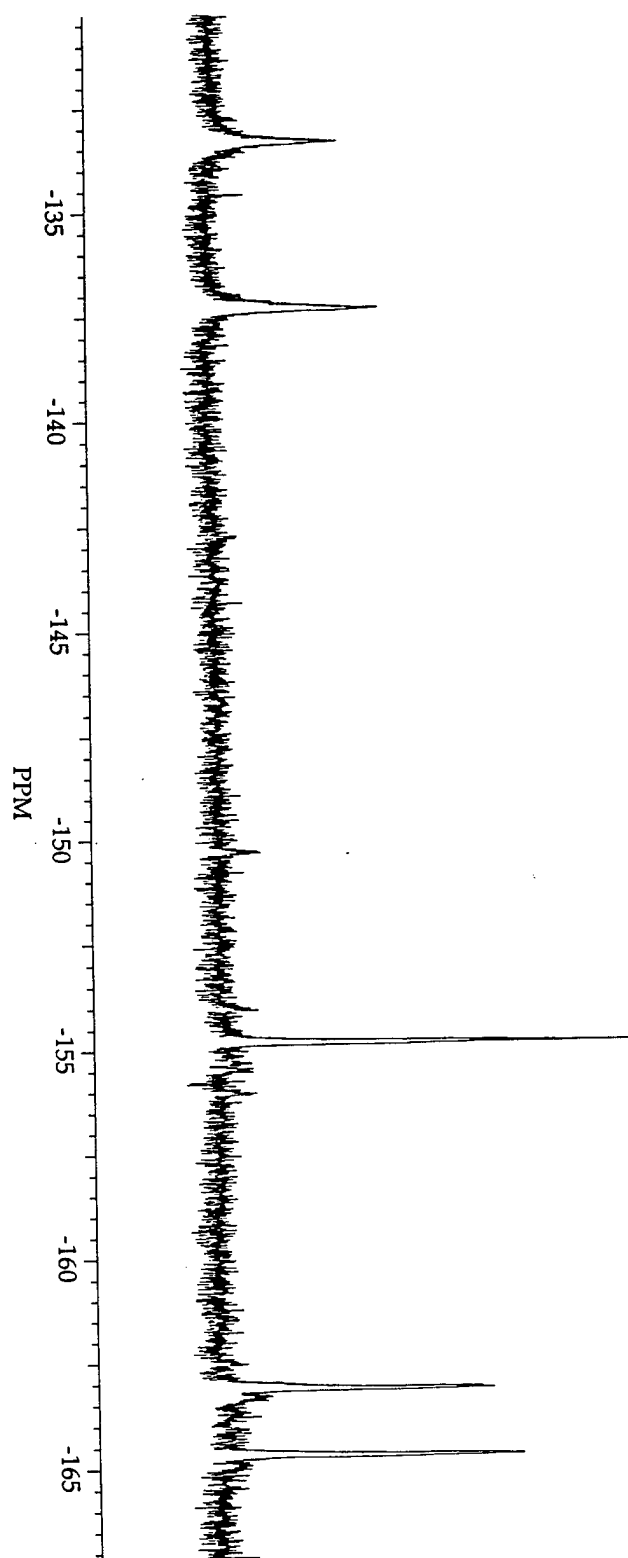


Figure 2.12 -- ^{19}F -NMR spectrum of $\text{Fe}^{\text{III}}\text{TFPPBr}_8\text{Cl}$ in acetone- d_6 . The paramagnetic shift is less than in the partially halogenated $\text{FeTFPP}(\text{Cl})$.

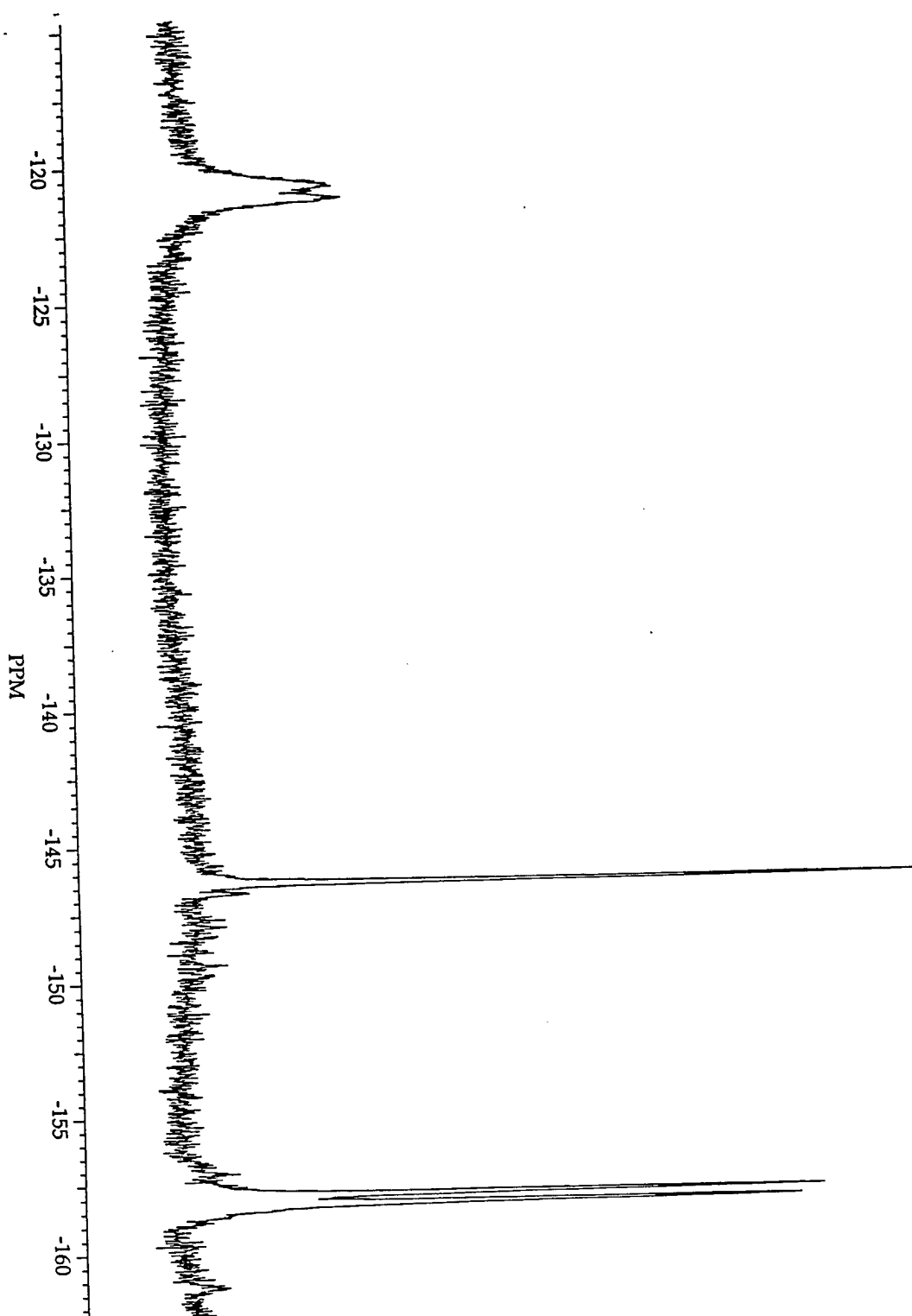


Figure 2.13 -- ^{19}F -NMR spectra of electrochemically (bottom) and chemically (top) generated $[\text{Fe}^{\text{II}}\text{TFPPBr}_8]$. The five line pattern in the electrochemically generated spectrum indicates an axially unsymmetric species, $[\text{Fe}^{\text{II}}(\text{TFPPBr}_8)\text{Cl}]^-$, while the lack of splitting in the ortho and meta resonances in the top spectrum is suggestive of a symmetric coordination sphere, i.e. $\text{Fe}^{\text{II}}(\text{TFPPBr}_8)(\text{OMe})_2$. The five spikes in the bottom spectrum are instrument noise.

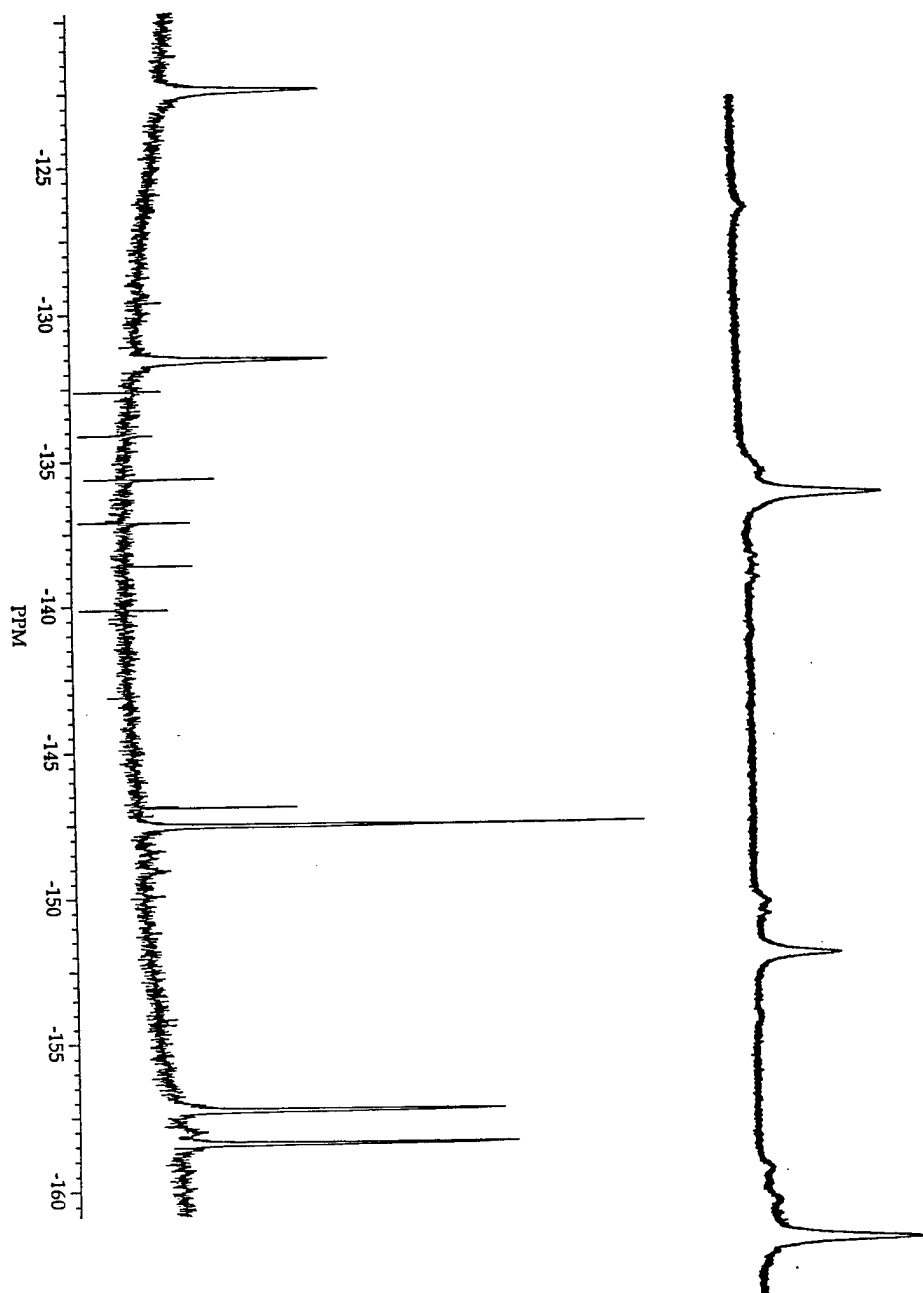


Table 2.1. X-ray Experimental Parameters.

	H ₂ TFPPCl ₈	ZnTFPPCl ₈	RuTFPPCl ₈ (CO)H ₂ O
formula	C ₄₄ H ₂ Cl ₈ F ₂₀ N ₄	C ₄₄ Cl ₈ F ₂₀ N ₄ Zn · 6(C ₆ H ₄ Cl ₂)	C ₅₇ H ₂₈ Cl ₈ F ₂₀ N ₄ O ₅ Ru
molecular weight	1250.12	2139.48	1613.53
color	brown	dull red	dark red
shape	plate	thick needles	rectangular tablet
crystal system	triclinic	tetragonal	monoclinic
space group	P $\bar{1}$	P $\bar{4}2_1c$	P2 ₁ /c
a, Å	11.066(1)	19.502(20)	14.364(3)
b, Å	14.641(3)		16.012(4)
c, Å	14.678(2)	10.916(8)	26.679(8)
α , °	88.97(1)		
β , °	76.05(1)		90.29(2)
γ , °	71.29(1)		
V, Å ³	2181.4(6)	4152(6)	6136(3)
Z	2	2	4
D _x , g cm ⁻³	1.90	1.71	1.75
radiation	MoK α		
μ , cm ⁻¹	6.4	10.41	7.11
temperature, K	293	229	295
crystal size, mm	0.11 X 0.35 X 0.42	0.19 X 0.19 X 0.59	0.16 x 0.29 x 0.44
diffractometer	Enraf-Nonius Cad-4		
collection method	omega scans		
h _{min} /max	± 12	0/23	-15/+15
k _{min} /max	± 16	0/23	-17/+17
l _{min} /max	± 16	± 13	0/28
reflections measured	12455	8027	16,813
indep. reflections	6054	2050	8006
reflections used	6054	2050	8005
R _{int} (F)	0.019	0.033	0.043
R(F)	0.042	0.0949	0.089
R _w (F ²)	0.0061	0.0286	0.028
(Δ/σ) _{max}	0.01	0.07	0.00 (for porphyrin)
goodness of fit	2.05	3.29	2.14

Table 2.2. Selected Average Bond Lengths (Å).

Bond	H ₂ TFPPCl ₈	ZnTFPPCl ₈	RuTFPPCl ₈ (CO)H ₂ O
N - C _α	1.372	1.380	1.378
C _α - C _β	1.448	1.427	1.448
C _β - C _β	1.347	1.337	1.339
C _α - C _m	1.402	1.403	1.399
N - M (or H)	0.94	2.032	2.059
N - Ct	2.075	2.029	not determined
Ru - C	—	—	1.828
Ru - O	—	—	2.172

Table 2.3. Selected Average Angles (°).

Angle	H ₂ TFPPCl ₈	ZnTFPPCl ₈	RuTFPPCl ₈ (CO)H ₂ O
N - M - N	—	90.2	175.5
C _α - N - C _α	109.5	106.9	177.6
N - C _α - C _m	125.4	124.2	125.1
N - C _α - C _β	107.2	107.4	107.8
C _α - C _β - C _β	107.9	108.8	108.0
C _α - C _m - C _α	125.8	126.5	126.0
C _m - C _α - C _β	127.2	128.4	127.0
Dihedral (C ₆ F ₅ groups)	72.6	59.1	80.7
C - Ru - O	—	—	177.6

Table 2.4. Average Deviations of Atoms from the Least-Squares Plane (Å).

Atom	H ₂ TFPPCl ₈	ZnTFPPCl ₈	RuTFPPCl ₈ (CO)H ₂ O
N	0.088	0.10	0.06
C _m	0.023	0.13	0.20
C _β	0.625	0.79, 0.68	0.48
Cl _{odd}	1.06	1.17	1.11
Cl _{even}	1.06	1.48	0.68
M	—	0.0	0.11 (towards CO)

Table 2.5: NMR Shifts for Halogenated Porphyrins.

Compound	NMR values in acetone- d_6^a				^1H N-H	$\beta\text{-H}$
	ortho	^{19}F para	meta			
ZnTFPP	-138.5 (d)	-154.8 (t)	-163.7 (m)	—	—	9.17
H ₂ TFPP	-136.9 (d)	-151.7 (t)	-161.8 (m)	-2.91	—	9.40
FeTFPP(Cl)	-105.8, -107.7	-150.2	-153.9, -156.0	—	—	83
FeTFPP(OH)	-108.0, -114.5	-152.0	-156.6, -158.0	—	—	83
(FeTFPP) ₂ O	-133.3, -137.1	-154.8	-163.1, -164.7	—	—	14.3
ZnTFPPCl ₈	-138.9 (d)	-151.5 (t)	-163.4 (m)	—	—	—
H ₂ TFPPCl ₈	-140.0 (d)	-149.8 (t)	-162.4 (m)	-1.0 ^b	—	—
RuTFPPCl ₈ (CO) ^c	-138.8, -139.3	-151.3 (t)	-163.2, -163.6	—	—	—
RuTFPPCl ₈ (py) ₂	-136.9 (d)	-149.7 (t)	-161.1 (m)	—	—	—
ZnTFPPBr ₈	-138.4 (d)	-151.7 (t)	-163.4 (m)	—	—	—
H ₂ TFPPBr ₈	-139.7 (d)	-150.1 (t)	-162.7 (m)	-0.5 ^b	—	—
FeTFPPBr ₈ (Cl)	-121.4, -122.3	-146.5	-158.1, -158.5	—	—	—
[FeTFPPBr ₈ (Cl)] ^{-d}	-124, -133	-148	-158, -160	—	—	—
[FeTFPPBr ₈] ^e	-136	-152	-163	—	—	—
FeTFPPBr ₈ (py) ₂ ^f	-138.6	-152.0	-163.1	—	—	—

- a. ^{19}F -NMR values are versus CFCl_3 at 0 ppm. ^1H -NMR values are versus TMS at 0 ppm. Fine structure given as follows: (d) doublet of doublets, (t) triplet, (m) multiplet.
- b. Very broad; the inner nitrogen protons are much more distinct in chlorocarbon solvents such as CDCl_3 .
- c. Major set of resonances, each with fine structure as observed in diamagnetic species; other resonances are also observed, as discussed in text.
- d. Produced by bulk electrolysis.
- e. Produced by reduction with ascorbic acid in methanol. Presumably the bis-methanol complex (see text).
- f. Values in CDCl_3 .

Spectroscopy and Electronic Structures of Halogenated Porphyrins

Introduction

Metalloporphyrins have distinctive UV-visible spectroscopy due to the aromatic porphyrin chromophore. Two strong $\pi \rightarrow \pi^*$ absorptions in the near UV ($\log \epsilon \approx 5 \text{ M}^{-1} \text{ cm}^{-1}$) and visible regions ($\log \epsilon \approx 4 \text{ M}^{-1} \text{ cm}^{-1}$) dominate the spectrum. The higher energy transition is known as the Soret (or B) band, and the less intense, lower energy transition as the Q band. Other higher energy bands of moderate intensity often appear, designated N, L, and M with increasing energy. A typical porphyrin spectrum is pictured in Figure 3.1, with the various transitions labeled with standard porphyrin nomenclature.¹

A satisfactory theoretical basis for these bands was developed by extension of work on polyarenes,^{2,3} which developed a new method for calculating frontier molecular orbital energies for extended π systems. LCAO calculations were based on a postulate assuming free electron movement along the perimeter of the π system. Essentially, this allowed the porphyrin macrocycle to be treated as an 18-electron polyarene; after several iterations, the now-standard Gouterman four orbital model for porphyrin spectroscopy evolved from these calculations.^{4,5} The frontier orbital picture is as follows (Figure 3.2); in D_{4h} symmetry, the two lowest occupied molecular orbitals consist of a nearly degenerate a_{1u} and a_{2u} pair, and the highest unoccupied molecular orbitals are a degenerate e_g set, both of π symmetry. Generally, the a_{1u} orbital is found at slightly lower energy than the a_{2u} , resulting in the two observed electronic transitions. Strong configurational interactions between the lowest energy states give rise to the different intensities in the Soret and Q bands.⁵

Although $\pi \rightarrow \pi^*$ in origin, the two intense transitions observed in porphyrin spectra are remarkably sensitive to the metal coordination sphere and oxidation state. In

combination with NMR data, UV-visible spectroscopy is a valuable tool for porphyrin characterization, and in some situations, is the sole method of characterization for some intermediates in metalloporphyrin oxidation reactions.

The substituents on the porphyrin periphery are found to effect the relative energies of the porphyrin frontier molecular orbitals. Substitution at the β -positions of the porphyrin ring with electron withdrawing groups such as halogens or cyano groups has been found to substantially red-shift the Soret band.⁶⁻⁸ A combination of theoretical and experimental work has separated the effects of halogenation into electronic⁹⁻¹³ and steric¹⁴⁻¹⁷ factors. Electrochemical data and semi-empirical calculations have both suggested that electron withdrawing substituents on the porphyrin periphery stabilize both the HOMO and the LUMO. This effect is offset by the distortion of the porphyrin macrocycle, which results in a large destabilization of the HOMO, and a smaller destabilization of the LUMO (Figure 3.2). The different magnitude of these shifts results in a red shifted electronic transition.^{14,15,18,19} Characterization of non-planar β -alkyl porphyrins supports this separation of electronic and steric effects.¹⁵ Similar to β -halo-porphyrins, these complexes have red-shifted Soret bands from the distortion-induced destabilization of frontier orbitals; however, the reduction potentials for these compounds are substantially more negative than in halogenated derivatives.

Results and Discussion

The electronic spectroscopy of the perhalogenated porphyrins described in Chapter 2 is consistent with this electronic model. The UV-Vis spectra for the zinc(II) tetraphenylporphyrin series are in Figure 3.3. Fluorination of the phenyl moiety has little effect on the Soret or Q band positions, consistent with the planar structures for both these compounds.^{20,21} In fact, rather than the red shift observed with pyrrole halogenation, a slight blue shift in the Soret band is observed for both the zinc and free base porphyrins. The direction of the change may be explained by the effect of meso substitution on the

relative energy of the porphyrin HOMOs. The a_{2u} orbital, which has greater electron density at meso position,⁵ is stabilized by the pentafluorophenyl groups such that it falls at lower energy than the a_{1u} orbital.²² The a_{1u} orbital, with no density at the meso position, remains relatively unchanged in energy, resulting in a larger HOMO-LUMO gap for the TFPP compounds. Electrochemical experiments also show that the HOMO shifts more than the LUMO, as ZnTFPP is 0.57 V more difficult to oxidize, but only 0.38 V harder to reduce than ZnTPP.

The effect of pyrrole substitution is more substantial. Chlorination induces a 1405 cm^{-1} red shift in the Soret energy of ZnTFPPCl₈ relative to ZnTFPP; as expected, the larger bromine atom induces a greater shift (2405 cm^{-1}) in ZnTFPPBr₈. The magnitude of the shift is consistent with other halogenated porphyrins, i.e., H₂TMP exhibits a 2210 cm^{-1} red shift upon bromination.²³ The decrease in Soret intensity is offset by increasing strength of the Q bands (Table 3.1), consistent with a decrease in the configurational interaction upon β -halogenation.¹⁸ However, the oscillator strength throughout the zinc porphyrin series remains fairly constant: 2.58, 3.40, 2.5, and $2.8\text{ M}^{-1}\text{ cm}^{-2}$ (from ZnTPP to ZnTFPPBr₈).²⁴

The anodic shift in the reduction potentials of ZnTFPPX₈²⁵ and H₂TFPPX₈ relative to the TFPP complexes (Table 3.2) also indicate that electron-withdrawing groups at the β positions stabilize both the highest occupied and lowest unoccupied molecular orbitals of tetraphenylporphyrins. Furthermore, the reduction potentials reflect the contraction of the HOMO-LUMO gap observed in the spectroscopy. Relative to H₂TFPP, H₂TFPPCl₈ is 0.46 V easier to reduce, but only 0.13 V harder to oxidize.

Addition of a redox active metal does not alter the observed trends. The Soret transition red shifts 1808 cm^{-1} from Fe^{III}(TFPP)Cl to Fe^{III}(TFPPBr₈)Cl (Figure 3.4), and the Soret bands of the bis-pyridine derivatives, Fe^{II}(TFPPBr₈)py₂ and Fe^{II}(TFPPCl₈)py₂, are also found at lower energy than those of Fe^{II}(TFPP)py₂ (Table 3.3). Although Fe^{III}(TFPPBr₈)Cl may appear to have a split Soret at 404 and 440 nm, the higher energy

absorbance may be a chloride to iron charge transfer, as is the 351 nm band in the spectrum of $\text{Fe}^{\text{III}}(\text{TFPP})\text{Cl}$. As the LMCT falls at closer energy to the Soret, it steals intensity from it, resulting in the unusually large extinction coefficient for this absorption. The reduction potential of the metal ($\text{Fe}^{\text{III/II}}$) follows the same trend as the ligand upon halogenation, increasing from -0.29, to -0.08, to 0.31 V vs. AgCl/Ag along the series $\text{Fe}(\text{TPP})\text{Cl}$, $\text{Fe}(\text{TFPP})\text{Cl}$, and $\text{Fe}(\text{TFPPBr}_8)\text{Cl}$.²⁶

Electrochemical reduction of $\text{Fe}(\text{TFPPBr}_8)\text{Cl}$ is found to red shift the Soret from 440 nm to 478 nm, similar to the 25 nm shift observed in the reduction of $\text{Fe}(\text{TPP})\text{Cl}$. Chemical reduction with ascorbic acid in methanol results in a similar but less shifted spectrum (Figure 3.5). NMR (Chapter 2) of both species suggests that the first is a five-coordinate anion, $[\text{Fe}^{\text{II}}(\text{TFPPBr}_8)\text{Cl}]^-$, and the second a low spin six-coordinate species, likely $\text{Fe}^{\text{II}}(\text{TFPPBr}_8)(\text{OMe})_2$. The spectrum obtained during the attempted synthesis of $\text{Fe}(\text{TFPPCl}_8)$ was also at very low energy, 440 nm, suggesting that an Fe^{II} species was transiently formed. Addition of pyridine resulted in an optical spectrum very similar to that of $\text{Fe}(\text{TFPPBr}_8)\text{py}_2$, but no single species was isolated.

Following the same trends, the $\text{RuTFPPX}_8(\text{CO})$ complexes are harder to oxidize and easier to reduce than $\text{RuTPP}(\text{CO})$.²⁷ Notably, the $\text{RuTFPPX}_8(\text{CO})^{+/0}$ potentials are within 0.07 V of those of the unmetallated H_2TFPPX_8 molecules, indicating that the first electron is removed from a ligand-based orbital. Oxidation of $\text{RuTFPPCl}_8(\text{py})_2$ occurs 0.63 V lower than $\text{RuTFPPCl}_8(\text{CO})$, suggesting that the HOMO is a $d\pi$ level in the pyridine derivative. The magnitude of this shift is similar to the 0.64 V shift between the metal-centered oxidation of $\text{RuTPP}(\text{py})_2$ ²⁸ and the ligand-centered oxidation of $\text{RuTPP}(\text{CO})$.²⁹

This sterically induced contraction of the HOMO-LUMO gap is surprisingly small for $\text{RuTFPPCl}_8(\text{CO})$ (0.11 V relative to $\text{RuTPP}(\text{CO})$)²⁷ as extracted from the values of the $+/-0$ and $0/-$ potentials). Enhanced backbonding from Ru^{II} to TFPPCl_8 is the likely explanation of this finding, as discussed below.

The electronic properties of perhalogenated Ru^{II} porphyrins can be interpreted in terms of a Gouterman four-orbital model^{4,9} modified by the inclusion of the Ru d π orbitals (Figure 3.6).³⁰ Increased backbonding in the TFPPX₈ complexes promotes mixing of $\pi \rightarrow e\pi^*$ and Ru^{II} $\rightarrow e\pi^*$ excited states, with the result that the Soret (mainly $\pi \rightarrow e\pi^*$) transition falls at higher energies than would be predicted by a simple one-electron (HOMO-LUMO) model.^{1,31,32} The Soret band of RuTFPPCl₈(CO) (418 nm) is substantially blue-shifted from that of H₂TFPPCl₈ (440 nm). A blue shift upon metalation with a 2nd or 3rd row metal is often observed; i.e., the Soret band of PdTFPPCl₈ is 705 cm⁻¹ shifted from the free ligand. The magnitude of the shift in RuTFPPCl₈(CO), ~ 1300 cm⁻¹, is surprisingly high, indicating that the electronic coupling of Ru^{II} to the porphyrin is unusually strong. The offsetting effect of extensive backbonding in the distorted porphyrins is the reason that the Soret bands for both RuTFPPCl₈(CO) and RuTFPPCl₈(py)₂ (414 nm) are only slightly red-shifted from those of RuTPP(CO) (412 nm) and RuTPP(py)₂ (413 nm) (Figure 3.7 and 3.8).

IR data also indicate that halogenated porphyrins are π acceptors. The peak attributable to the CO stretch appears at much higher energy in the halogenated porphyrins relative to the 1945 cm⁻¹ band observed for RuTPP(CO).³³ The transition energy decreases according to RuTFPPCl₈(CO) (1990) > RuTFPPCl₇(CO) (1987) > RuTFPPCl₆(CO) (1984) > RuTFPPBr₈(CO) (1973 cm⁻¹), further reflecting the increased competition between the porphyrin and the carbonyl ligand for π electron density upon halogenation.

The distortion-induced contraction of the HOMO-LUMO gap^{9,10,12,14,17,18} is evidenced by a decrease of the Soret transition energy according to RuTFPPCl₆(CO) (410) > RuTFPPCl₇(CO) (413.5) > RuTFPPCl₈(CO) (418 nm) (Figure 3.9). The Soret band of RuTFPPBr₈(CO) is further red-shifted to 424 nm; as predicted,⁹ the larger halogen atoms generate a greater distortion of the porphyrin, thereby producing a smaller HOMO-LUMO

gap. Porphyrin saddling also is responsible for the red shifts of the Q(0,1) bands of RuTFPPX₈ complexes from those of the corresponding TPP derivatives (Figure 3.7 and 3.8).

Relatively weak bands at 670 ($\epsilon \approx 800$) and 792 nm ($\epsilon \approx 300 \text{ M}^{-1}\text{cm}^{-1}$) are observed in the spectrum of RuTFPPCl₈(py)₂ (Figure 3.10). Low-lying Ru^{II} \rightarrow $e\pi^*$ (TFPPCl₈) transitions are expected, since the electrochemical data show that both Ru^{II} oxidation and TFPPCl₈ reduction are accessible. Extensive backbonding to $e\pi^*$ (TFPPCl₈) orbitals would stabilize d_{xz} , d_{yz} relative to d_{xy} (Figure 3.6); it is likely, then, that a d_{xy} electron is involved in both electrochemical and the 792-nm spectroscopic oxidation of Ru^{II} to Ru^{III}. No bands above 650 nm were observed in the spectrum of RuTFPPCl₈(CO), consistent with the absence of any Ru^{II} oxidations in the electrochemical experiments. The $d\pi$ orbitals for RuTFPPCl₈(CO) are anticipated to fall at a similar energy as the porphyrin $b_2 \pi$ orbital. Any charge transfer band in this region would be obscured by the intense porphyrin $\pi \rightarrow \pi^*$ transition. However, a $b_2 d\pi \rightarrow e\pi^*$ transition may be contributing to the slight tailing on the low energy side of the Soret band of RuTFPPCl₈(CO).

Spectroelectrochemistry was performed to confirm the assignment of the LUMO as metal or ligand based in the ruthenium porphyrins. Reduction of RuOEP(CO)³⁴ and RuTPP(CO)³⁵ has demonstrated distinct differences in the UV-Vis depending on the site of reduction. Formation of a radical porphyrin anion is accompanied by a broadening of the Soret, with a concomitant decrease in intensity. The Q bands disappear, and a new band around 600 - 700 nm grows into the spectrum. RuOEP(CO)(THF)³⁴ and RuTPP(CO)³⁵ in THF both show these type of spectral features upon reduction. Reduction of RuTFPPCl₈(py)₂ (Figure 3.11) is accompanied by a decrease in the Soret intensity, with a red shift to 420 nm, as well as a decrease in the Q band intensity. A new band appears at 580 nm, consistent with formation of a porphyrin based radical anion. Spectroelectrochemistry in a different solvent has been shown to have completely different

characteristics, indicating that the axial ligand can alter the site of reduction. Upon reduction in benzonitrile, the Soret band of RuOEP(CO) is still sharp, and shows a slight red shift. No new features are observed in the lower wavelength regions.³⁴ Reduction of RuTFPPCl₈(CO) is shown in Figure 3.12. The Soret band decreases in intensity, and shows a similar red shift as in RuTFPPCl₈(py)₂, but the broadening generally associated with radical anion formation is not observed. In addition, there is no major change in the Q-band region. Isosbestic points at 270, 376, 420, and 440 nm indicate that clean reduction is occurring, but the decrease in Soret intensity suggests that this reduction may have both metal and ligand character.

Conclusion

The distortion of the porphyrin macrocycle, as observed in the crystal structures of the halogenated free ligand, zinc, and ruthenium porphyrins (Chapter 2), gives rise to the expected red shifted optical spectra and anodically shifted electrochemistry common to porphyrins substituted with electron withdrawing ligands. Only the RuTFPPX₈ complexes show Soret transitions at higher energy, which has been demonstrated to stem from strong coupling between the ruthenium and porphyrin orbitals. Attempts to photolyze the carbonyl ligand further support strong interactions between these orbitals; despite a relatively high ν_{CO} (indicating a correspondingly weak Ru-C bond), it is difficult to remove the carbonyl ligand with light energy. Rather than leading to dissociation, the excited state appears to decay by non-radiative pathways. No emission is observed for either the RuTFPPCl₈(CO) or Ru(TFPPCl₈)py₂ complexes.

The highly positive reduction potentials of the perhalogenated ruthenium and iron complexes indicate that these compounds will be quite stable in a highly oxidizing environment. Further experiments will test to see if they display the high activity as oxidation catalysts for which they were designed.

Methods

Infrared spectra were recorded as solutions in carbon tetrachloride or benzene on a Perkin-Elmer Model 1600 FT-IR spectrophotometer. Electronic absorption spectra were recorded on an Olis-modified Cary-14 spectrophotometer. Electrochemistry was performed under Ar in three compartment cell consisting of a highly polished glassy carbon working electrode, a Ag/AgCl reference electrode in 1M KCl, and a platinum auxiliary electrode. The working electrode and reference electrode are connected by a modified Luggin capillary. Spectroelectrochemical experiments were performed in an optically transparent platinum working electrode.³⁶ Spectral changes were monitored with a Hewlett Packard 8452A diode array spectrophotometer. A 1000 W tungsten lamp was used for photolysis experiments.

Materials

Porphyrins were obtained as described in Chapter 2. Solvents were Omnisolv grade from EM Science, and used as received.

References and Notes

- (1) Gouterman, M. In *The Porphyrins*; D. Dolphin, Ed.; Academic Press, Inc.: New York, NY, 1978; Vol. III; pp 1-156.
- (2) Platt, J. R. *J. Chem. Phys.* **1949**, *17*, 484.
- (3) Simpson, W. T. *J. Chem. Phys.* **1949**, *17*, 1218.
- (4) Gouterman, M. *J. Mol. Spectrosc.* **1961**, *6*, 138-163.
- (5) Gouterman, M. *J. Chem. Phys.* **1959**, *30*, 1139-1161.
- (6) Callot, H. J. *Bull. Chem. Soc. Fr.* **1974**, *7*, 1492-1496.
- (7) Callot, H. J.; Giraudeau, A.; Gross, M. *J. Chem. Soc., Perkin Trans. 2* **1975**, 1321-1324.
- (8) Wijesekera, T.; Matsumoto, A.; Dolphin, D.; Lexa, D. *Angew. Chem., Int. Ed. Eng.* **1990**, *29*, 1028-1030.
- (9) Takeuchi, T.; Gray, H. B.; Goddard, W. A., III *J. Am. Chem. Soc.* **1994**, *116*, 9730-9732.
- (10) Barkigia, K. M.; Chantranupong, L.; Smith, K. M.; Fajer, J. *J. Am. Chem. Soc.* **1988**, *110*, 7566-7567.
- (11) Binstead, R. A.; Crossley, M. J.; Hush, N. S. *Inorg. Chem.* **1991**, *30*, 1259-1264.
- (12) Giraudeau, A.; Callot, J. H.; Gross, M. *Inorg. Chem.* **1979**, *18*, 201-206.
- (13) Hodge, J. A.; Hill, M. G.; Gray, H. B. *Inorg. Chem.* **1995**, *34*, 802-812.
- (14) Ochsenbein, P.; Ayougou, K.; Mondon, D.; Fischer, J.; Weiss, R.; Austin, R. N.; Jayaraj, K.; Gold, A.; Turner, J.; Fajer, J. *Angew. Chem., Int. Ed. Eng.* **1994**, *33*, 348-350.
- (15) Barkigia, K. M.; Berber, M. D.; Fajer, J.; Medforth, C. J.; Renner, M. W.; Smith, K. M. *J. Am. Chem. Soc.* **1990**, *112*, 8851-8857.
- (16) Mandon, D.; Ochsenbein, P.; Fischer, J.; Weiss, R.; Jayaraj, K.; Austin, R. N.; Gold, A.; White, P. S.; Brigaud, O.; Battioni, P.; Mansuy, D. *Inorg. Chem.* **1992**, *31*, 2044-2049.
- (17) Senge, M. O.; Medforth, C. J.; Sparks, L. D.; Shelnutt, J. A.; Smith, K. M. *Inorg. Chem.* **1993**, *32*, 1716-1723.
- (18) Bhyrappa, P.; Krishnan, V. *Inorg. Chem.* **1991**, *30*, 239-245.
- (19) D'Souza, F.; Villard, A.; Caemelbecke, E. V.; Franzen, M.; Boschi, T.; Tagliatesta, P.; Kadish, K. M. *Inorg. Chem.* **1993**, *32*, 4042-4048.
- (20) Scheidt, W. R.; Kastner, M. E.; Hatano, K. *Inorg. Chem.* **1978**, *17*, 706-710.

- (21) Birnbaum, E. R.; Hodge, J. A.; Grinstaff, M. G.; Schaefer, W. P.; Marsh, R. E.; Henling, L. M.; Labinger, J. A.; Bercaw, J. E.; Gray, H. B. *Inorg. Chem.* **in press**.
- (22) Gross, Z.; Barzilay, C. *Angew. Chem., Int. Ed. Eng.* **1992**, 1615-1617.
- (23) Hoffmann, P.; Robert, A.; Meunier, B. *Bull. Chem. Soc. Fr.* **1992**, 129, 85-97.
- (24) Oscillator strength is calculated as $4.6 \times 10^{-9} \epsilon \nu_{1/2}$.
- (25) The ZnTFPPX₈ compounds also show anoidcally shifted electrochemistry, but are complicated by two-electron waves. See reference 13.
- (26) Grinstaff, M. W.; Hill, M. G.; Birnbaum, E. R.; Schaefer, W. P.; Labinger, J. A.; Gray, H. B. *Inorg. Chem.* **in press**.
- (27) The potentials of RuTPP(CO) are 0.87 (+/0) and -1.59 (0/-) V vs. SCE (CH₂Cl₂, 0.1M TBAP): Mu, X. H.; Kadish, K. M. *Langmuir* **1990**, 6, 51-56.
- (28) Brown, G. M.; Hopf, F. R.; Ferguson, J. A.; Meyer, T. J.; Whitten, D. G. *J. Am. Chem. Soc.* **1973**, 95, 5939-5942.
- (29) Kadish, K. M.; Chang, D. *Inorg. Chem.* **1982**, 21, 3614-3619.
- (30) Since pyridine is a much weaker π acceptor than CO, we would expect Ru^{II} to backbond more strongly to TFPPCl₈ in the bis(pyridine) than in the carbonyl derivative. For discussions of M^{II} (M = Fe, Ru, Os) backbonding to CO and py in porphyrin complexes, see: Gentemann, S.; Albaneze, J.; Garcia-Ferrer, R.; Knapp, S.; Potenza, J. A.; Schugar, H. J.; Holten, D. *J. Am. Chem. Soc.* **1994**, 116, 281-289; Kim, D.; Su, Y. O.; Spiro, T. G. *Inorg. Chem.* **1986**, 25, 3993-3997; Schick, G. A.; Bocian, D. F. *J. Am. Chem. Soc.* **1984**, 106, 1682-1694.
- (31) Buchler, J. W.; Kokisch, W.; Smith, P. D. *Struct. Bonding* **1978**, 34, 79-134.
- (32) Antipas, A.; Buchler, J. W.; Gouterman, M.; Smith, P. D. *J. Am. Chem. Soc.* **1978**, 100, 3015-3024.
- (33) Chow, B. C.; Cohen, I. A. *Bioinorg. Chem.* **1971**, 1, 57-63.
- (34) Kadish, K. M.; Tagliatesta, P.; Hu, Y.; Deng, Y. J.; Mu, X. H.; Bao, L. Y. *Inorg. Chem.* **1991**, 30, 3737-3743.
- (35) Mu, X. H.; Kadish, K. M. *Langmuir* **1990**, 6, 51-56.
- (36) Hill, M. G.; Mann, K. R. *Inorg. Chem.* **1991**, 30, 1429-1431.

Figure 3.1 -- An absorption spectrum of ZnTPP, a normal porphyrin. The Soret (or B) absorption usually lies around 410 nm, and the Q bands are at lower energy. The shoulder on the Soret has been assigned as a $\pi \rightarrow \pi^*$ transition (N band).

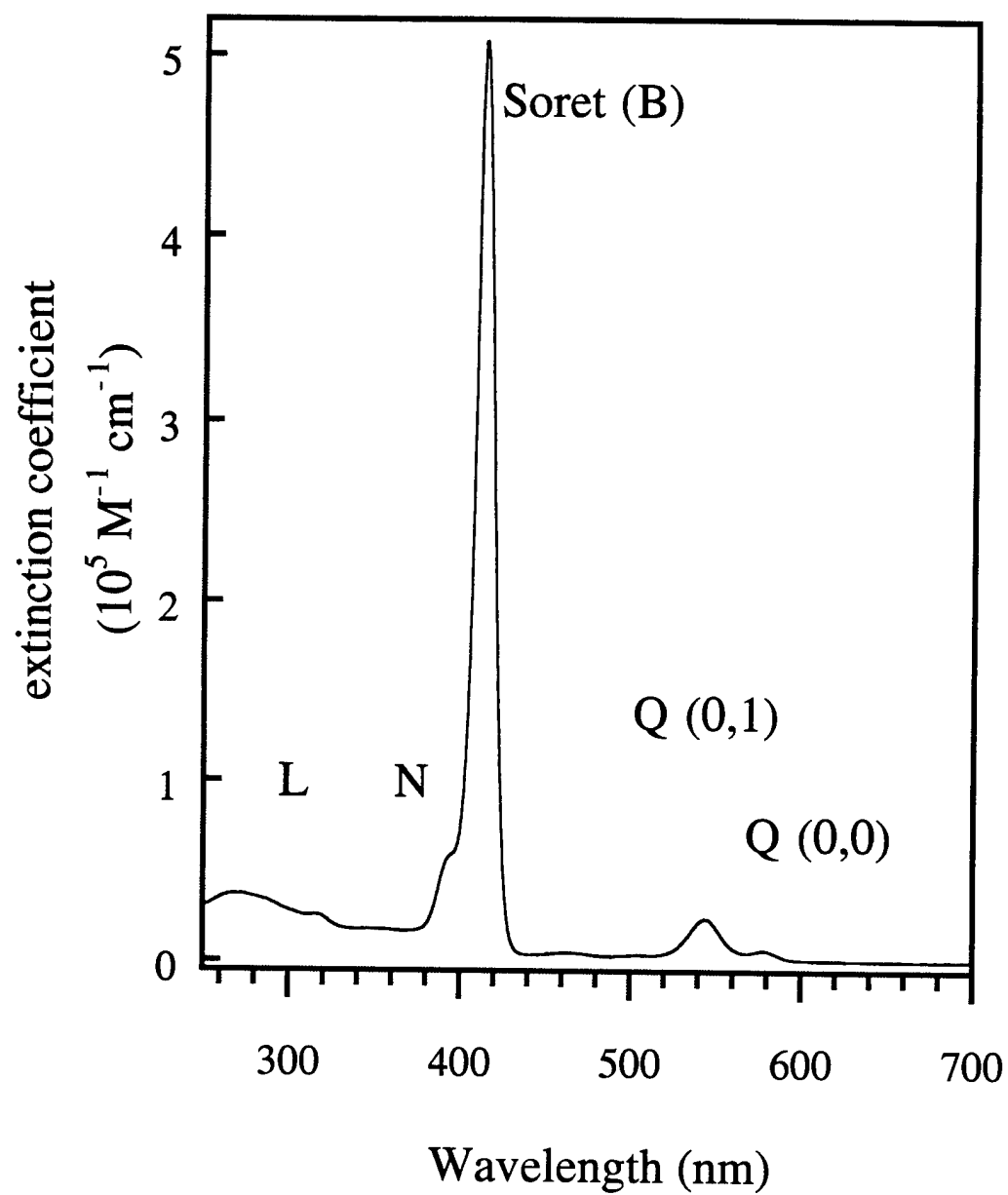


Figure 3.2 -- The Gouterman four orbital model for normal porphyrins is shown on the left (with D_{4h} symmetry labels). Upon fluorination of the phenyl rings, both the HOMO and the LUMO are stabilized, and the relative energy of the a_{1u} and a_{2u} HOMOs are reversed. Halogenation of the pyrrole carbons results in a further stabilization of all of the orbitals (pictured on the right). The distortion of the molecule drops the symmetry to approximately D_{2d} . The Soret transition is marked on each molecular orbital diagram with an arrow of equal length, showing the increase in the HOMO-LUMO gap in TFPP and the decrease in TFPPCl₈.

Gouterman Four Orbital Model

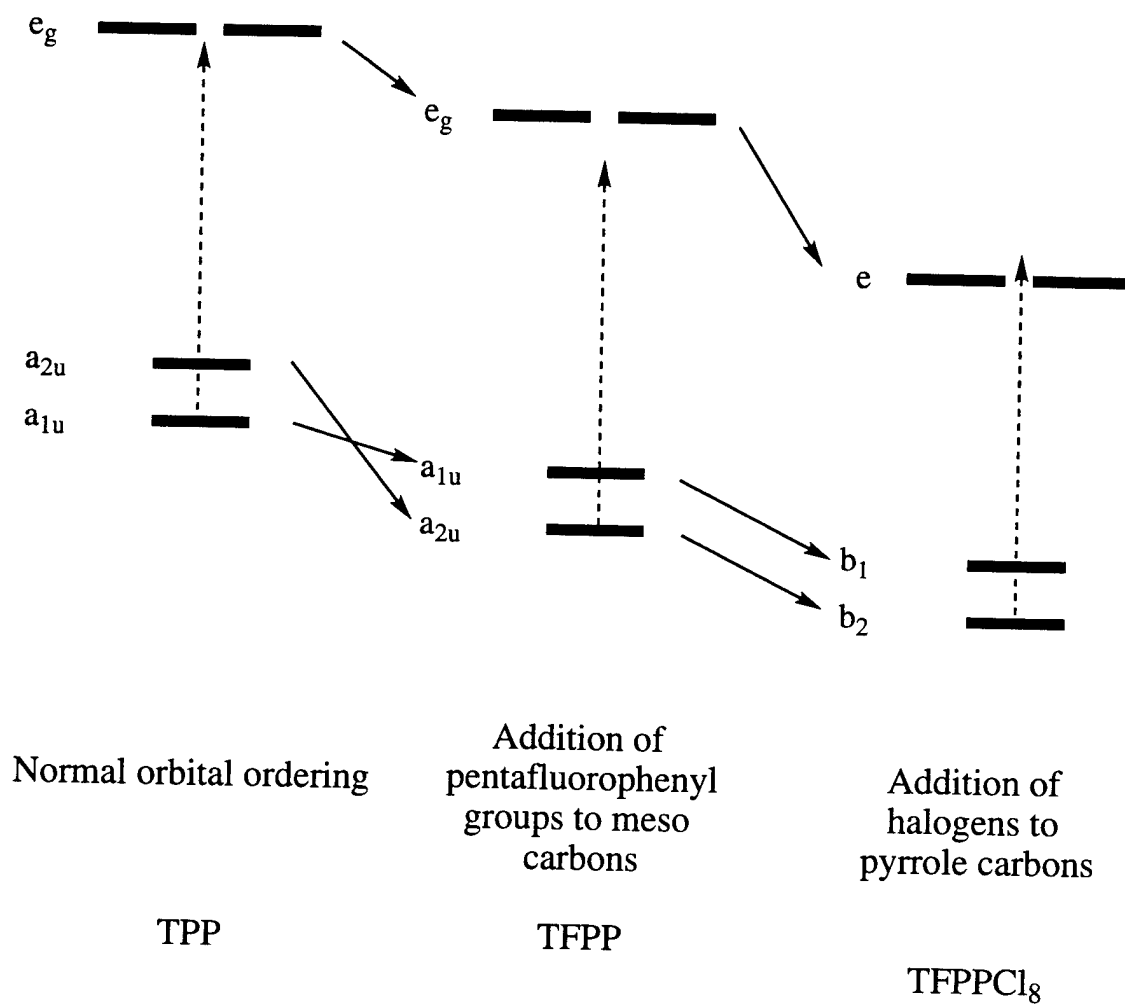


Figure 3.3 -- The UV-Vis spectra of the ZnTPP series of porphyrins in methylene chloride. As shown in the molecular orbital diagrams in Figure 3.2, the energy of the Soret transition decreases as $\text{ZnTFPP} > \text{ZnTPP} > \text{ZnTFPPCl}_8 > \text{ZnTFPPBr}_8$.

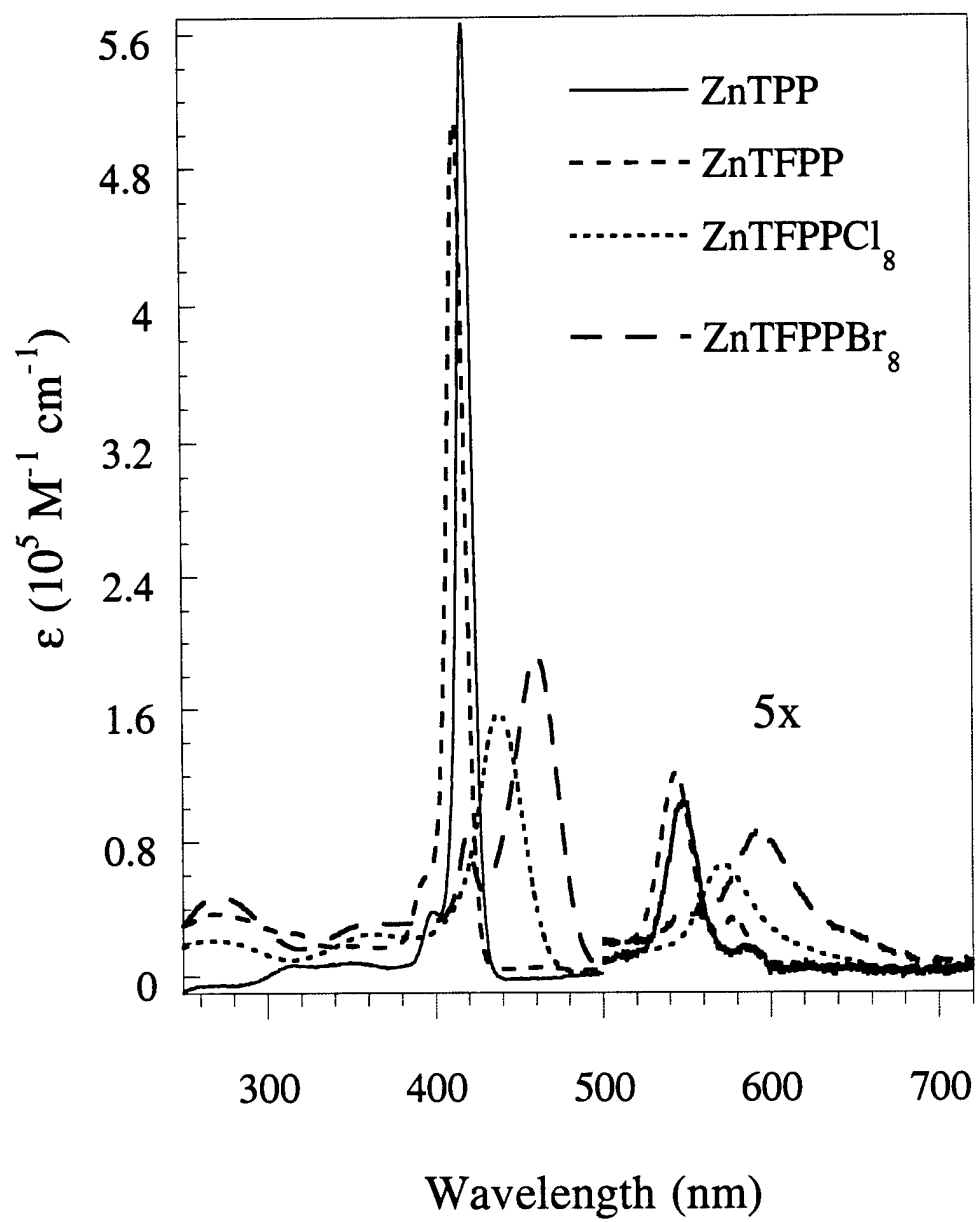


Figure 3.4 -- The UV-Vis spectra of $\text{Fe}(\text{TFPP})\text{Cl}$ and $\text{Fe}(\text{TFPPBr}_8)\text{Cl}$ in methylene chloride. The LMCT of $\text{Fe}(\text{TFPPBr}_8)\text{Cl}$ mixes with the Soret band, increasing the extinction coefficient of this transition relative to the 350 nm band in $\text{Fe}(\text{TFPP})\text{Cl}$.

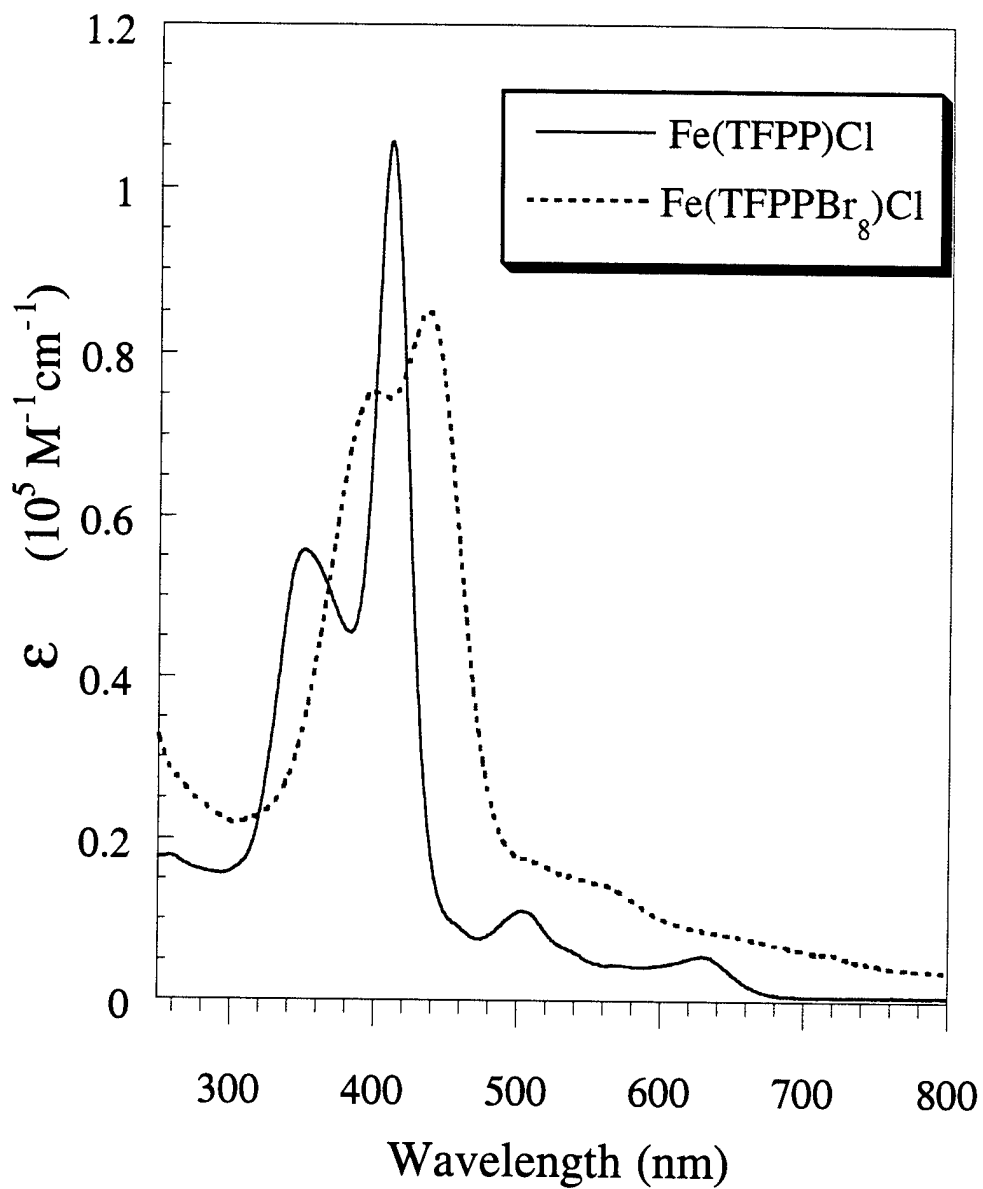


Figure 3.5 -- The UV-Vis spectra of $[\text{Fe}^{\text{II}}(\text{TFPPBr}_8)\text{Cl}]^-$ and $[\text{Fe}^{\text{II}}(\text{TFPPBr}_8)(\text{OCH}_3)_2]$ produced by bulk electrolysis or chemical reduction in methylene chloride. The red shifted Soret band and the single Q band are consistent with formation of an iron(II) porphyrin. The axial ligands for the two complexes are determined from a combination of electrochemical data and ^{19}F NMR.

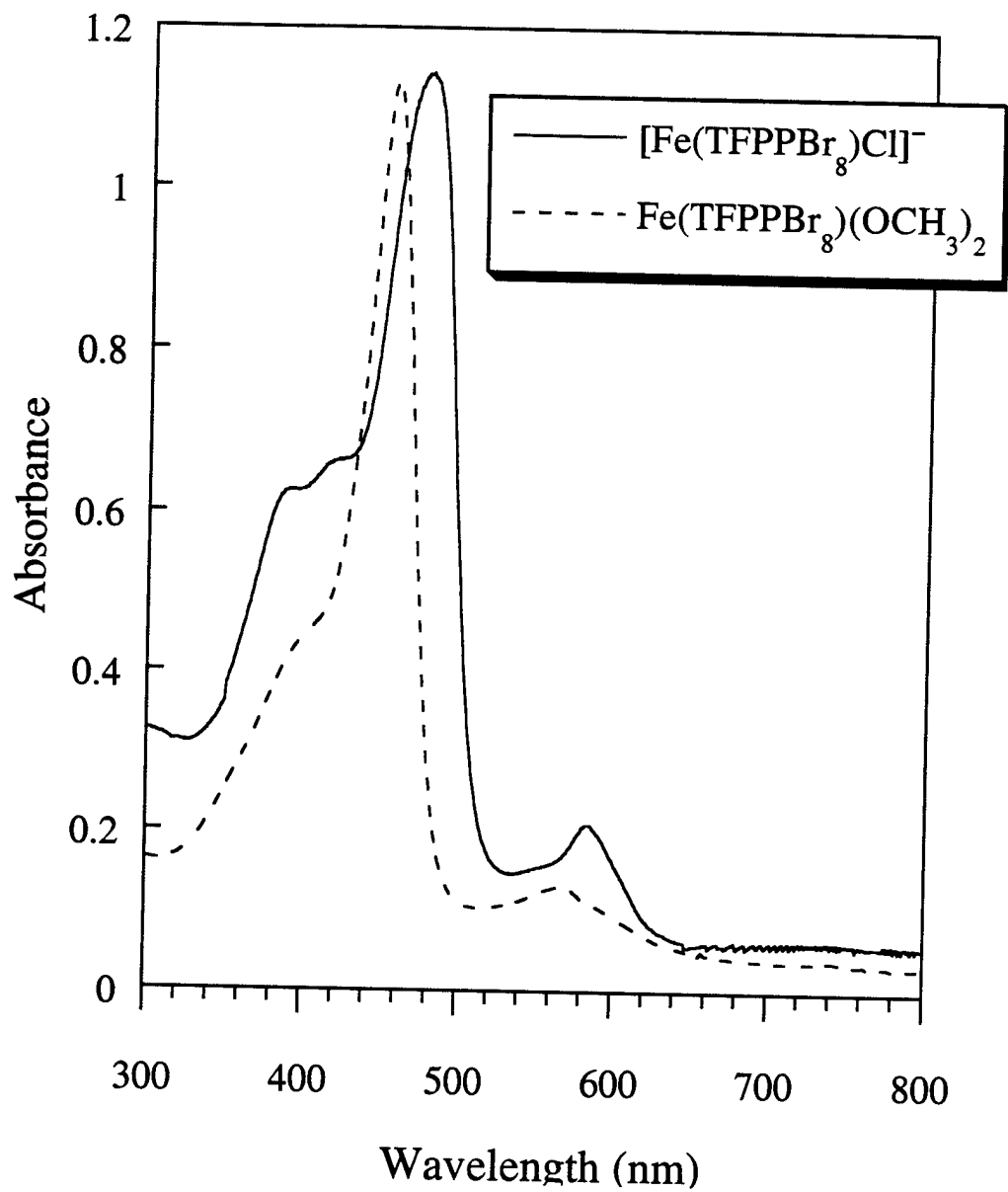
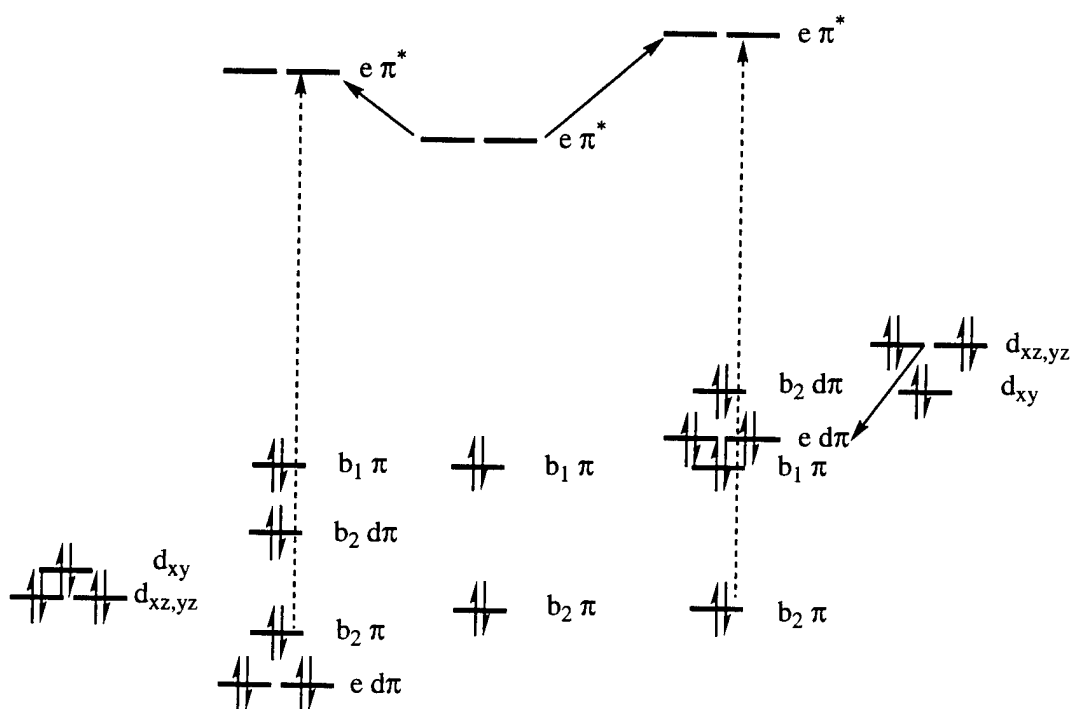


Figure 3.6 -- The Gouterman four orbital model for RuTFPPX₈ complexes. The porphyrin TFPPX₈ orbitals are allowed to interact with the d π orbitals of carbonyl or bis-pyridine ruthenium fragments (D_{2d} symmetry). Extensive π -backbonding to the carbonyl ligand strongly stabilizes the d_{xz}, d_{yz} orbitals, resulting in a ligand based HOMO for RuTFPPX₈(CO). Weaker interactions in the bis-pyridine complex leaves the d π orbitals at higher energies, consistent with a Ru-based HOMO and low energy charge transfer transitions in RuTFPPX₈(py)₂. The Soret transition is shown with an arrow for both complexes.



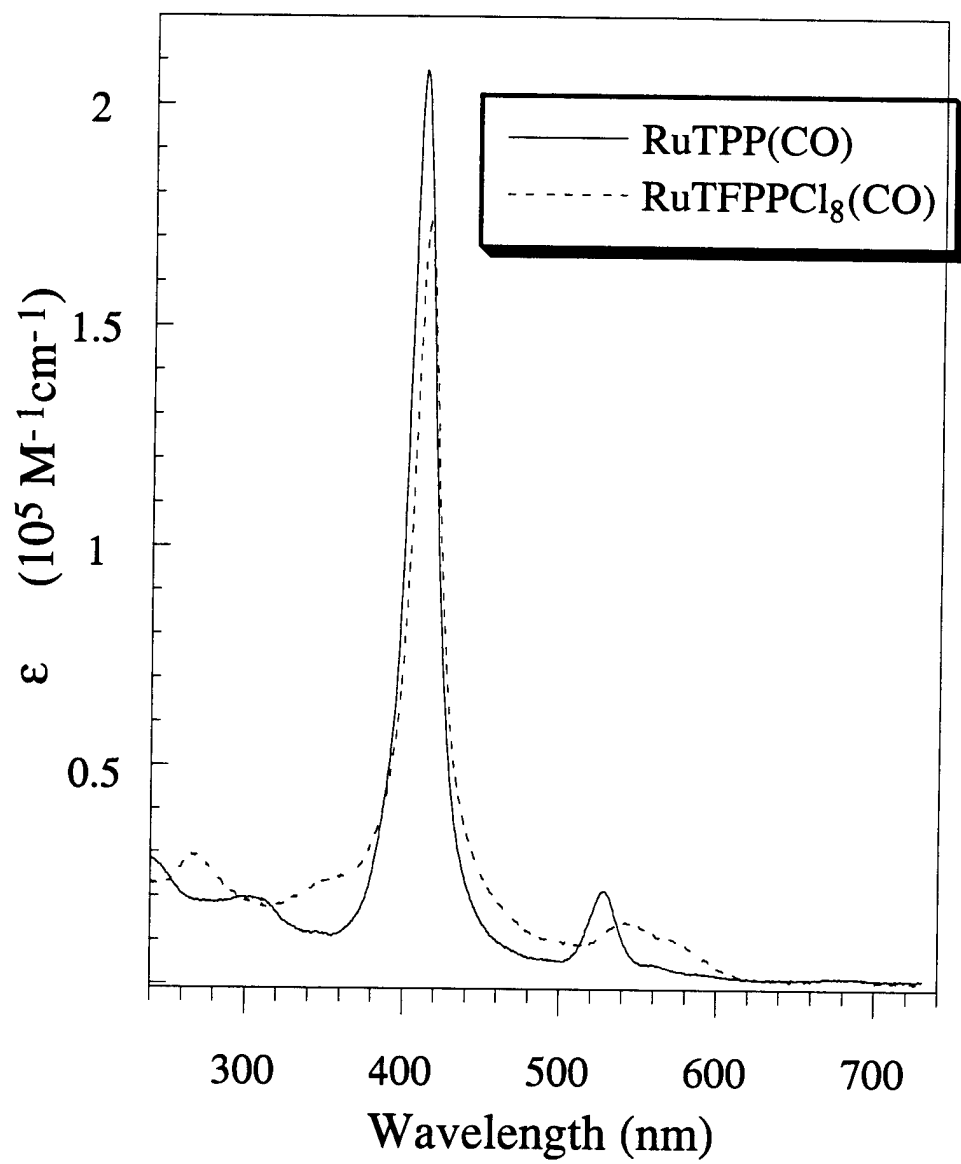


Figure 3.7 -- The UV-Vis spectra of RuTPP(CO) and RuTFPPCl₈(CO) in methylene chloride. Although the Soret energy is similar for the two complexes, the Q(1,0) transition is red shifted for the perhalogenated complex.

Figure 3.8 -- The UV-Vis spectra of $\text{RuTPP}(\text{py})_2$ and $\text{RuTFPPCl}_8(\text{py})_2$ in methylene chloride.

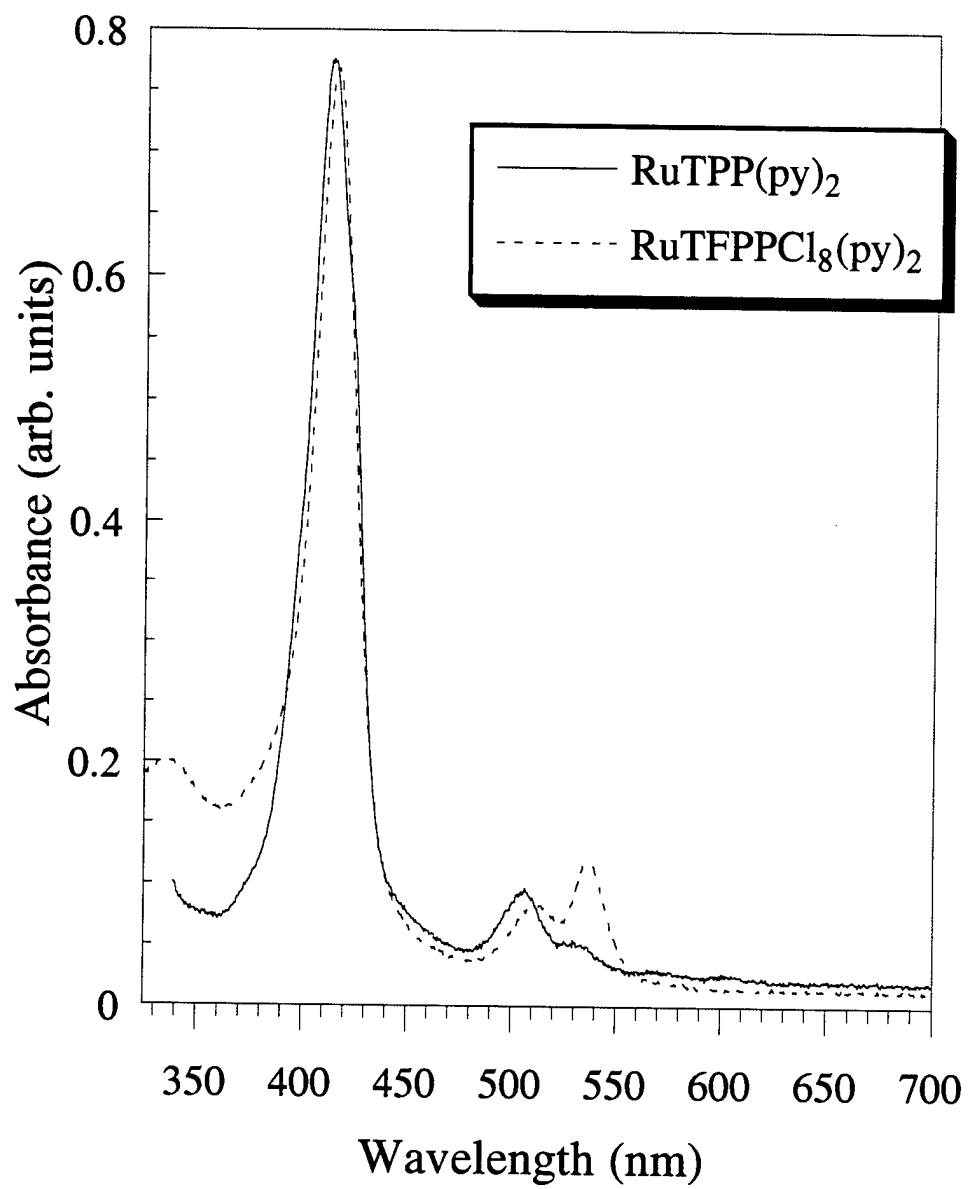


Figure 3.9 -- The UV-Vis spectra of the $\text{RuTFPPX}_n(\text{CO})$ complexes in methylene chloride. The Soret energy decreases with halogenation: $\text{RuTFPPCl}_6(\text{CO}) > \text{RuTFPPCl}_7(\text{CO}) > \text{RuTFPPCl}_8(\text{CO}) > \text{RuTFPPBr}_8(\text{CO})$, with the larger bromine atoms inducing a larger red shift than chlorine. The Q bands (not shown) show a similar change in energy.

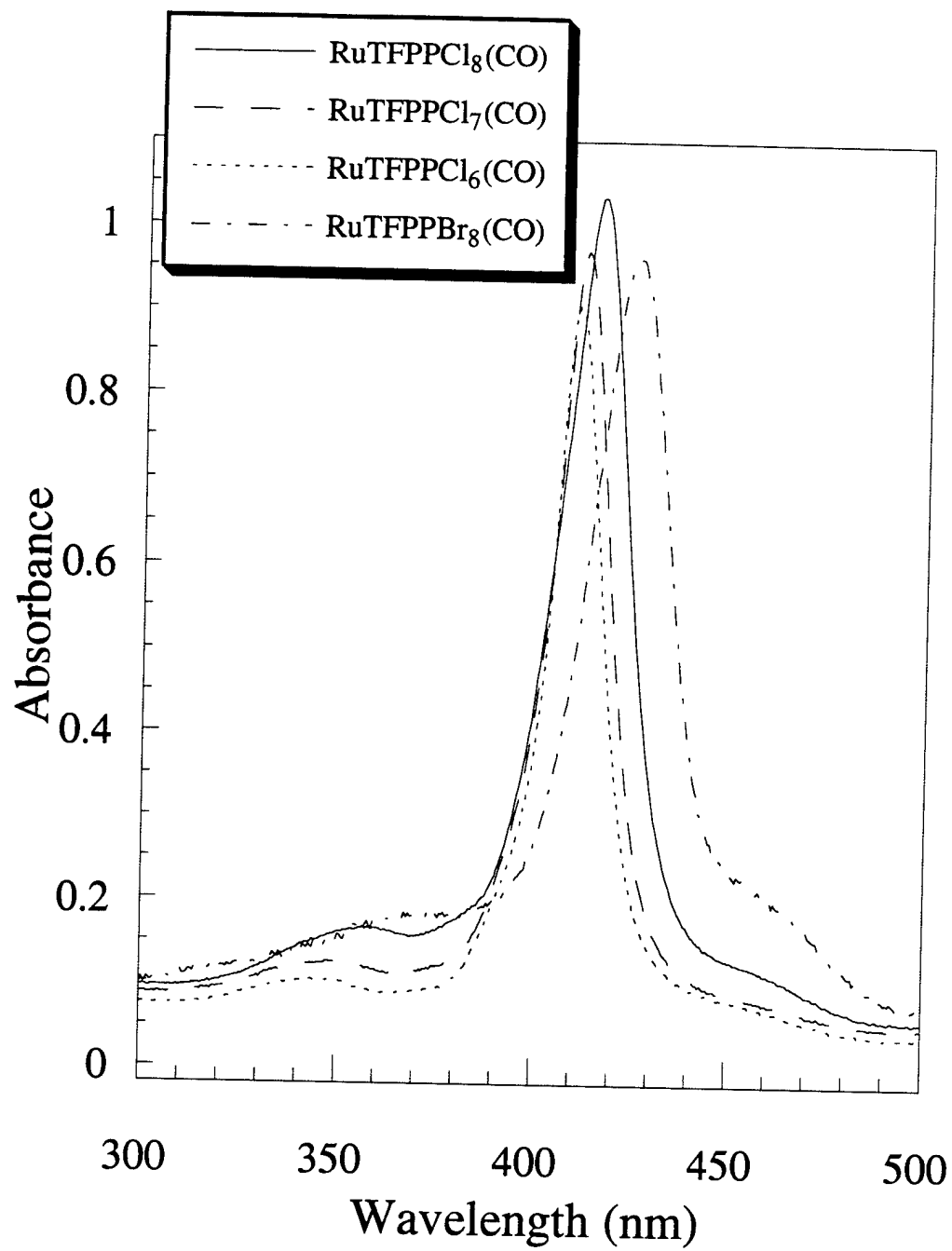


Figure 3.10 -- The low energy visible spectrum of $\text{RuTFPPCl}_8(\text{CO})$ and $\text{RuTFPPCl}_8(\text{py})_2$. The two absorptions at 670 and 792 nm in the bis-pyridine spectrum are assigned to $\text{Ru}^{\text{II}} \rightarrow \epsilon\pi^*$ (TFPPCl_8) transitions. MLCT transitions in the carbonyl complex are anticipated to lie at higher energy and are obscured by porphyrin $\pi \rightarrow \epsilon\pi^*$ transitions.

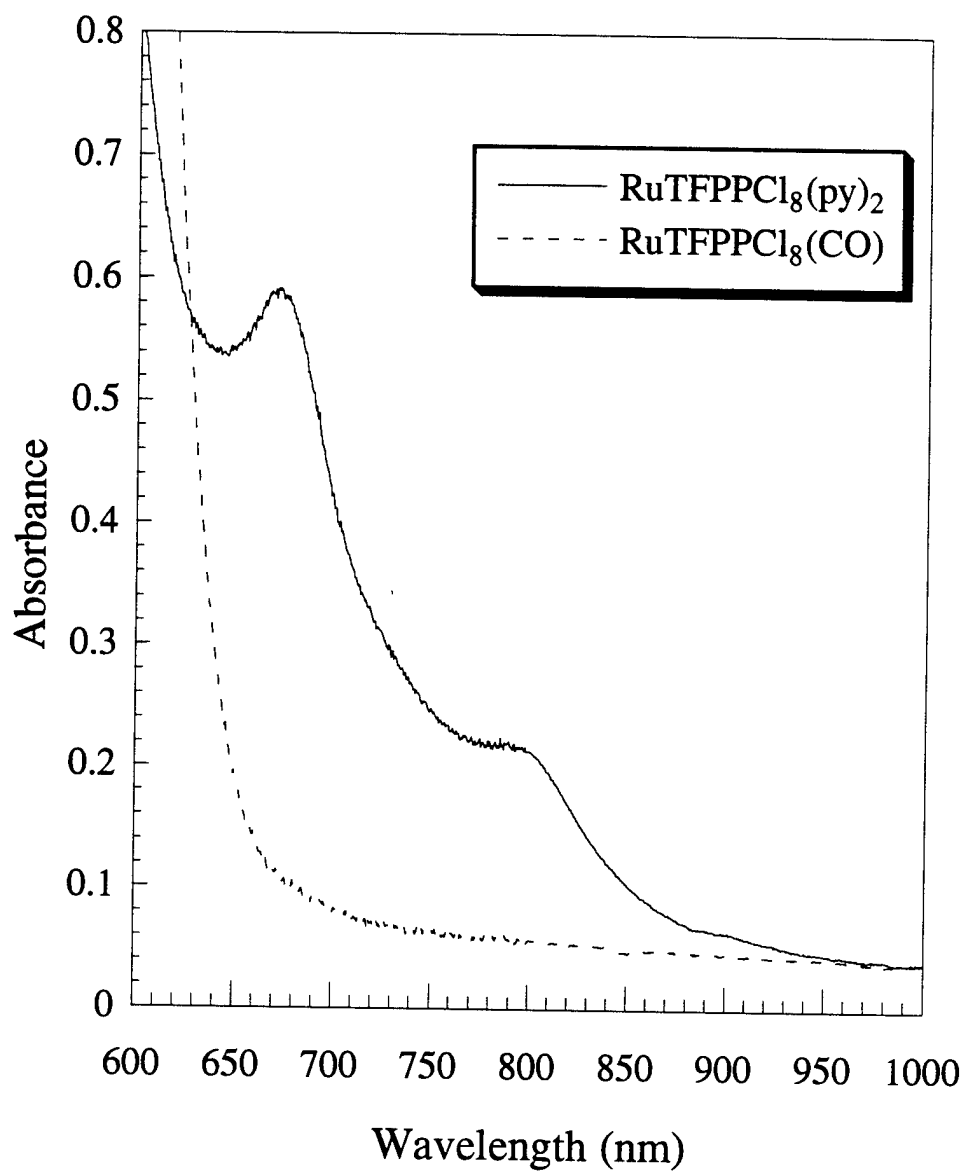


Figure 3.11 -- Spectroelectrochemical reduction of $\text{RuTFPPCl}_8(\text{py})_2$ in methylene chloride. The reduced species shows clear porphyrin radical character.

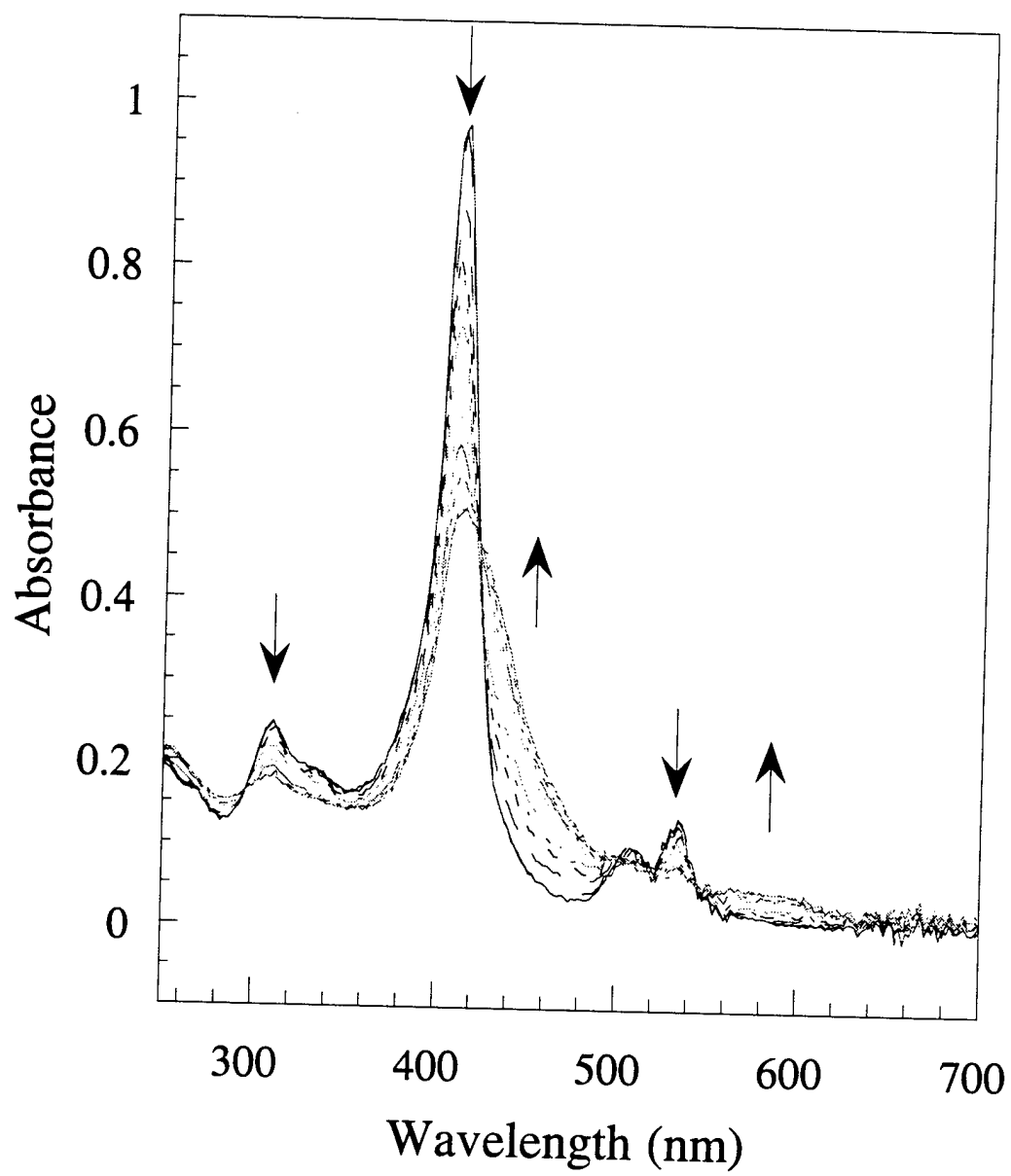


Figure 3.12 -- Spectroelectrochemical reduction of RuTFPPCl₈(CO) in methylene chloride. While the reduced species shows a decrease in the Soret intensity, consistent with formation of a porphyrin radical anion, no change in the Q band region is observed.

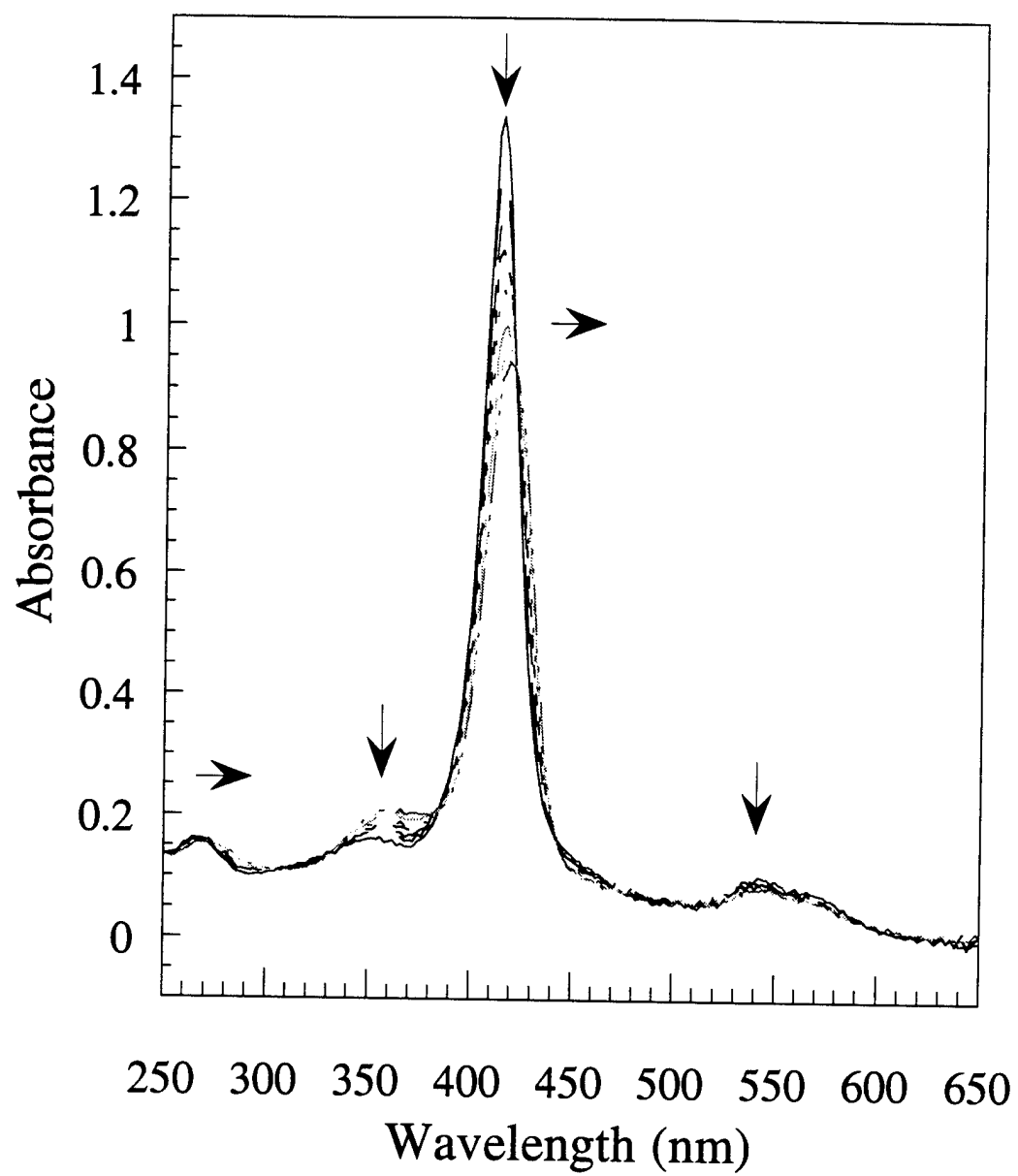


Table 3.1. Electronic Absorptions of Halogenated Porphyrins.

Porphyrin	L, M bands (ϵ , $10^3 \text{ M}^{-1} \text{ cm}^{-1}$)	Soret, nm (ϵ , $10^5 \text{ M}^{-1} \text{ cm}^{-1}$)	Q bands, nm (ϵ , $10^4 \text{ M}^{-1} \text{ cm}^{-1}$)			
ZnTPP	315 (1.0) 350 (1.5)	418 (5.6)	548 (2.1)			
ZnTFPP	318 (4)	413.5 (5.0)	544 (2.4)			
ZnTFPPCl ₈	360 (3.0)	439 (1.6)	572 (1.3)			
ZnTFPPBr ₈	364 (3.3)	460 (1.9)	594 (1.7)			
H ₂ TPP ^a		419 (4.7)	514 (1.9)	549 (0.77)	591 (0.54)	647 (0.34)
H ₂ TFPP ^a		412 (2.4)	506 (1.9)	584 (0.58)	659 (0.36)	
H ₂ TFPPCl ₈		438 (1.6)	538 (1.3)	626 (0.46)		
H ₂ TFPPBr ₈		454	532	636		
RuTPP(CO)	300 (20)	412 (2.0)	528 (2.1)			
RuTFPPCl ₈ (CO)	355 (25)	416 (1.7)	548 (1.4)	580 (1.0)		
RuTFPPCl ₇ (CO)	345	413	541	576		
RuTFPPCl ₆ (CO)	340	411	539	572		
RuTFPPBr ₈ (CO)	370	426	595			
RuTPP(py) ₂		413	507	534		
RuTFPPCl ₈ (py) ₂	355	414 (1.6)	512 (2.0)	536 (2.5)	670 ^b (0.08)	790 ^b (0.03)
RuTFPPCl ₇ (py) ₂		414	510	536	672 ^b	790 ^b
RuTFPPCl ₆ (py) ₂		412	508	534	674 ^b	790 ^b
RuTFPPBr ₈ (py) ₂		424	518	572		

- a. Extinction coefficients in benzene, from Longo, F. R.; Finarelli, M. G.; Kim, J. B. *J. Hetero. Chem.*, **1969**, 6, 927-931.
 b. Assigned as MCLT absorptions.

Table 3.2. Reduction Potentials of Halogenated Porphyrins.

Porphyrin ^a	$E''_{+/0}$	$E''_{M(III)/M(II)}$	$E''_{0/-}$
ZnTPP ^b	0.80	—	-1.33
ZnTFPP ^b	1.37	—	-0.95
ZnTFPPCl ₈ ^b	1.60 ^c	—	-0.76
ZnTFPPBr ₈ ^b	1.55 ^c	—	-0.75
H ₂ TPP ^d	1.08	—	-1.21
H ₂ TFPP	1.53	—	-0.78
H ₂ TFPPCl ₈	1.66 ^e	—	-0.32
H ₂ TFPPBr ₈	1.56 ^e	—	-0.31
RuTPP(CO) ^f	0.86	—	-1.46
RuTFPPCl ₆ (CO)	1.64	—	-0.76
RuTFPPCl ₇ (CO)	1.69	—	-0.69
RuTFPPCl ₈ (CO)	1.71	—	-0.64
RuTFPPBr ₈ (CO)	1.63	—	-0.84
RuTPP(py) ₂ ^d	—	0.21	—
RuTFPPCl ₆ (py) ₂	—	0.89	-1.12
RuTFPPCl ₇ (py) ₂	—	1.04	-0.98
RuTFPPCl ₈ (py) ₂	—	1.08	-0.94
Fe(TPP)Cl ₈ ^g	1.14	-0.29	-1.07
Fe(TFPP)Cl	1.65	-0.08	-1.10
Fe(TFPPBr ₈)Cl	—	0.31	-0.63

a. Potentials in CH₂Cl₂ solution at room temperature (V vs. AgCl/Ag, 0.1M TBAPF₆).

b. The zinc potentials are from reference 13.

c. $E''_{2+/0}$.

d. V. vs SCE in 0.05M THAP. From reference 12.

e. E_{pa} .

f. V. vs. SCE in 0.1 M TBAP in CH₃CN. From reference 29.

g. From reference 26.

Table 3.3. Electronic Absorptions of Halogenated Iron Porphyrins.

Porphyrin	L, M bands	Soret, nm ($\epsilon, 10^5 \text{ M}^{-1} \text{ cm}^{-1}$)	Q bands, nm ($\epsilon, 10^4 \text{ M}^{-1} \text{ cm}^{-1}$)		
$\text{Fe}^{\text{III}}(\text{TPP})\text{Cl}^{\text{a}}$		419 (1.7)	510 (1.2)	573 (0.037)	656, 692 (0.028, 0.32)
$\text{Fe}^{\text{II}}(\text{TPP})\text{Cl}^{\text{a}}$		444 (1.7)	530 (0.32)	571 (0.75)	612 (0.65)
$\text{Fe}^{\text{III}}(\text{TFPP})\text{Cl}$		411 (1.0)	351 (0.70)	504 (1.1)	621 (0.56)
" $\text{Fe}^{\text{II}}(\text{TFPPCl}_8)$ " ^b	398	440	566		
$\text{Fe}^{\text{III}}(\text{TFPPBr}_8)\text{Cl}$	404 (0.81)	440 (0.85)	560 (2.0)		
$[\text{Fe}^{\text{II}}(\text{TFPPBr}_8)\text{Cl}]^-$	388, 420	478	585		
$\text{Fe}^{\text{II}}(\text{TFPPBr}_8)(\text{OMe})_2$		454	568		
$\text{Fe}(\text{TPP})\text{py}_2$					
$\text{Fe}(\text{TFPP})\text{py}_2$		418	525	552	
$\text{Fe}(\text{TFPPCl}_8)\text{py}_2$		438	542	574	
$\text{Fe}(\text{TFPPBr}_8)\text{py}_2$		452	556	588	
$(\text{FeTFPP})_2\text{O}^{\text{c}}$		398 (0.62)	577 (0.7)	590 (sh)	
$\text{Fe}(\text{TFPP})\text{OH}^{\text{c}}$		406 (7.6)	563 (1.2)		

a. Spectra taken in PhCN; from reference 8.

b. Appears to be iron (II) based on the red color. See text.

c. Extinction coefficients from reference 40, Chapter 2.

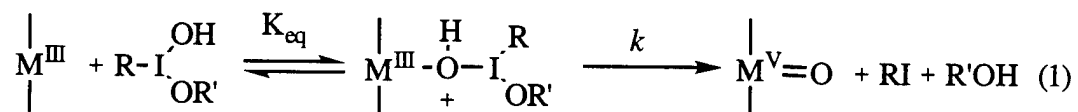
Chapter 4

Mechanism of Catalytic Alkene Oxidation with Molecular Oxygen or Iodosobenzene and Halogenated Iron Porphyrins

Introduction

Since the discovery that tetraphenylporphyrinato-iron(III) chloride [Fe(TPP)Cl] catalyzes olefin epoxidation with iodosobenzene,¹ a variety of porphyrins have been tested for the ability to mediate hydrocarbon oxidation reactions utilizing assorted oxygen sources.² These studies have generally striven to generate high-valent metal-oxo intermediates to mimic the putative active species in cytochrome P-450. Most experiments take advantage of the peroxide shunt pathway to directly form the desired metal-oxo species, while reactions with dioxygen are usually carried out in the presence of a reductant to follow the complete P-450 oxygen activation mechanism.

The reaction of iodosobenzene (PhIO) with metalloporphyrins has been well documented.^{1,3-8} The iodosobenzene polymer oxidizes $M^{III}(P)X$ complexes to $M^V(P)(O)$ species as shown in Eq. 1, where P = porphyrin, X = halide, ^-OH , etc., R = phenyl, and R' is the continuing iodosobenzene polymer.⁹ Some evidence also exists for the transient



formation of a μ -oxo dimer intermediate, $(P)M^{IV} - O - M^{IV}(P)^{++}$, formed from a reaction of $M^V(P)(O)$ with another porphyrin molecule.^{10,11}

Whether the last oxidizing equivalent is more appropriately characterized as a M^V or as a $M^{IV}(P^{++})$ depends on the metal and porphyrin involved. Spectroscopic evidence indicates that most iron porphyrins are oxidized to form porphyrin radical cations,¹²⁻¹⁴ as does the heme center in the enzyme horseradish peroxidase (HRP). The high-valent metal-oxo of HRP (compound I) is well characterized as $Fe^{IV}(P^{++})(O)$ and is often used as a standard for comparisons with model complexes.¹⁵ Oxidation of $Fe^{III}(TMP)Cl$ with

m-chloroperbenzoic acid (mCPBA) at -77 °C is reported to give UV-Vis and ¹H NMR spectra consistent with formation of an iron(IV) porphyrin π -radical cation.¹⁴ EXAFS and Mössbauer spectra are similar to those of HRP compound I, further supporting this assignment.¹⁶ With other metals, such as chromium, the last electron is removed from a metal based orbital.¹⁷ For Cr^{III}TPPCL, UV-Vis and IR spectroscopy, in combination with magnetic susceptibility measurements, indicate formation of Cr^VTPP(O) upon oxidation with mCPBA or PhIO.¹⁸

Once the high-valent metal-oxo is generated, there are a number of mechanisms for interaction with an olefin. Possible intermediates include a metallaoxetane (I), a π -radical cation (II), a carbocation (III), a carbon radical (IV), or a process of concerted oxene insertion (V) (Figure 4.1).¹⁹ The metallocyclo intermediate has been excluded, especially for sterically encumbered porphyrins, since modeling demonstrates that the reaction coordination sphere is not large enough to accommodate formation of the four-membered ring.^{20,21} Although many elegant experiments have been conducted to further probe the transition state, there is no consensus indicating a general metalloporphyrin oxidation mechanism. The academically unsatisfying conclusion seems to be that the mechanism is dependent on the metal ion and the electron density of the porphyrin and alkene substrate.¹⁹

Nevertheless, a few general concepts concerning the mechanism have been proposed (Figure 4.2).^{17,21-23} The first step has been proposed to be association of the metal-oxo and the olefin, in some cases called a charge transfer (CT) complex. With Cr^V(TDBPP)(O) (TDBPP = tetrakis-(2,6-dibromophenyl)porphyrin), the formation of this complex is rate limiting,¹⁷ and other evidence suggests this is also true for the iron derivative. The reaction of Fe(TMP)Cl with mCPBA and cyclooctene at -43 °C resulted in an observable intermediate prior to epoxide formation, again suggested to be an olefin π -complex.¹³ The charge transfer complex may then react through various pathways, including concerted oxene transfer (V), electrophilic addition (III), or electron

transfer (IV).¹⁹⁻²¹ The relative rates for each pathway are determined in each case by the electron density on the olefin and the electrochemical potential of the metal center. Unfortunately, the actual oxo transfer step is after the rate limiting formation of the CT complex, precluding its direct observation.

For the specific case of cyclohexene oxidation, different pathways are implicated for hydroxylation and epoxidation (Figure 4.3). Oxidation of deuterated cyclohexene with Fe(TPP)Cl and Cr(TPP)Cl has shown that allylic oxidation occurs via allylic hydrogen atom abstraction followed by geminate radical recombination.²⁴ Further experiments with partially halogenated porphyrins supported this mechanism for hydroxylation²⁵ and suggested that formation of cyclohexene epoxide occurs by direct electron transfer to form a carbocation intermediate (Figure 4.3). Competition between direct hydrogen abstraction and electron transfer depends on the electron density at the metal, allowing for different selectivity as observed with different metals.²⁵ The higher selectivity for epoxidation observed with electron-withdrawing iron porphyrins suggests that the higher reduction potential favors the electron transfer mechanism.²⁵ Correlations of epoxidation rates with the reduction potential or the Hammett parameter of the olefin have also been argued to support an electron transfer mechanism for Fe(TDCPP)Cl.²⁶

The perhalogenated porphyrin, 2,3,7,8,12,13,17,18-octabromo-5,10,15,20-tetrakis(pentafluorophenyl)porphyrinato-iron(III) chloride, [Fe(TFPPBr₈)Cl], is an active catalyst for the selective oxidation of light alkanes at elevated temperatures (80 °C) and under high dioxygen pressure (80 atm).^{27,28} Recently, we reported that at room temperature and one atmosphere of molecular oxygen, Fe(TFPPBr₈)Cl will oxidize 3-methylpentane to 3-methylpentan-3-ol.²⁹ We have now found that this metalloporphyrin is also an efficient catalyst for the oxidation of cyclohexene with either dioxygen or single O-atom donors such as iodosobenzene.

Results

In the presence of $\text{Fe}(\text{TFPPBr}_8)\text{Cl}$, cyclohexene oxidation to a mixture of cyclohexene oxide, 2-cyclohexen-1-ol, and 2-cyclohexen-1-one, was observed (Figures 4.4 and 4.5). The product distribution and activity varied greatly with the oxidant. With PhIO, the majority of product (77%) consisted of the epoxide. With dioxygen, mainly allylic oxidation products were generated (49 and 44% of alcohol and ketone, respectively). Reactions with styrene exhibited similar differences in product distribution with oxidant. With PhIO, the majority of the product (67%) was styrene oxide, while with dioxygen, only the cleavage product, benzaldehyde (> 95%), was observed.

Catalytic activity also varied with oxidant. Iodosobenzene reactions deactivated in 1 to 5 hours, accompanied by a shift in the Soret band from 442 to 418 nm. However, 18 ± 4 turnovers (TO) were completed during this time period, and the product distribution (Figure 4.4) was consistent between runs. Although the initial activity with PhIO was greater, overall activity was higher with dioxygen, suggesting an induction period for the latter reaction. Furthermore, in reactions with dioxygen, the perhalogenated porphyrin showed much higher activity at 24 hours (73 TO) as compared to the related porphyrins tetrakis(pentafluorophenyl)porphyrinato-iron(III) chloride ($\text{Fe}(\text{TFPP})\text{Cl}$) (31 TO) and tetraphenylporphyrinato-iron(III) chloride ($\text{Fe}(\text{TPP})\text{Cl}$) (< 1 TO) (Figure 4.6).

The variations in selectivity with $\text{Fe}(\text{TFPPBr}_8)\text{Cl}$ can be explained by invoking different mechanisms for the two oxidants. Iodosobenzene is believed to react with metalloporphyrins to generate a high-valent metal-oxo intermediate, as described above.³⁰ Indeed, the large percentage of epoxide formed with PhIO and $\text{Fe}(\text{TFPPBr}_8)\text{Cl}$ is consistent with a ferryl as the oxidizing species. The increase in activity from $\text{Fe}(\text{TFPPBr}_8)\text{Cl}$ relative to $\text{Fe}(\text{TFPP})\text{Cl}$, however, is not as great as one might predict: the positive $E^\circ \text{Fe}^{3+/2+}$ (0.31 V vs. AgCl/Ag)²⁹ of the perhalogenated porphyrin would make an " $\text{Fe}^{\text{V}}=\text{O}$ " of this porphyrin high in energy and difficulty to attain.²³ In line with

this prediction, reductive generation of a ferryl (O_2 , Zn , H^+) has been shown to be inefficient for highly halogenated porphyrins.^{31,32} The lower potentials of $\text{Fe}(\text{TFPP})\text{Cl}$ (-0.08 V)²⁹ and $\text{Fe}(\text{TPP})\text{Cl}$ (-0.29 V vs. SCE)³³ suggest that a ferryl complex can be generated more readily in these complexes. However, once formed, the ferryl can attack the C-H bonds on other porphyrins, leading to catalyst decomposition and lower net activity with these two complexes.

With dioxygen, the formation of a metal-oxo is not observed. Previously in the literature,³⁴ the active species was proposed to be $(\text{P})\text{Fe}^{\text{IV}}=\text{O}$, formed by reaction of dioxygen with $(\text{P})\text{Fe}^{\text{II}}$ to form a μ -peroxy bridged dimer (Figure 4.7). Homolytic cleavage of the dimer to $(\text{P})\text{Fe}^{\text{IV}}=\text{O}$ would result in dioxygenase-type oxygen activation.^{27,34,35} With electron-withdrawing porphyrins, it was proposed that an iron(IV)-oxo would have as much oxidizing power as a typical iron(V)-oxo porphyrin. Although the positive reduction potential of $\text{Fe}(\text{TFPPBr}_8)\text{Cl}$ is consistent with this mechanism, the increased stability of the ferrous state causes both the iron(II) and iron(III) oxidation states to be stable to oxygen. A solution of electrochemically generated $[\text{Fe}^{\text{II}}(\text{TFPPBr}_8)\text{Cl}]^-$ only shows minimal oxidation after several weeks under an O_2 atmosphere,³⁶ indicating that this pathway is not operative.²⁹ Attempts to generate an iron(IV)-oxo directly, by addition of iodosobenzene to electrochemically produced $[\text{Fe}^{\text{II}}(\text{TFPPBr}_8)\text{Cl}]^-$ in methylene chloride, resulted only in immediate conversion to $\text{Fe}^{\text{III}}(\text{TFPPBr}_8)\text{Cl}$.

The possibility of reductive ferryl generation with $\text{Fe}(\text{TFPPBr}_8)\text{Cl}$ is eliminated for several reasons. First, the lack of an added co-reductant allows no mechanism for the reduction of the ferric porphyrin to the ferrous state. Furthermore, $[\text{Fe}^{\text{II}}(\text{TFPPBr}_8)\text{Cl}]^-$ is stable to dioxygen, meaning that the oxygen binding step from the P-450 cycle does not occur. As mentioned above, reductive ferryl generation has been shown to be inefficient for halogenated iron porphyrins,^{31,32} suggesting that a high-valent metal-oxo is not

implicated in reactions of $\text{Fe}(\text{TFPPBr}_8)\text{Cl}$ with dioxygen. A mechanism less common to metalloporphyrins must be investigated.

Indeed, the reaction has been shown to involve formation and porphyrin-catalyzed decomposition of alkyl peroxides (Figure 4.8).^{29,37} Free radicals present in solution react with oxygen to form alkyl peroxides. The alkyl peroxides, unlike dioxygen, react more readily with highly electron-deficient porphyrins such as $\text{Fe}(\text{TFPPBr}_8)\text{Cl}$ (*vide infra*). The radicals generated by the $\text{Fe}(\text{TFPPBr}_8)\text{Cl}$ -catalyzed peroxide decomposition react with additional molecules of substrate to form the observed products, propagating a radical chain reaction. A plot of moles product produced versus time (Figure 4.5) indicates that the reaction is autocatalytic. Competitive experiments with cyclohexene and cyclohexene-*d*₁₀ show an isotope effect of 8.2, consistent with a mechanism involving hydrogen abstraction in the rate-determining step. Addition of a radical trap, BHT, completely inhibits the reaction. The radical chain mechanism is also consistent with the high percentage of allylic oxidation products observed in the reaction of cyclohexene with dioxygen.

Moreover, this mechanism explains the greater reactivity observed with dioxygen and $\text{Fe}(\text{TFPPBr}_8)\text{Cl}$ compared to tetraphenylporphyrinato-iron(III) chloride or tetrakis(pentafluorophenyl)porphyrinato-iron(III) chloride. The electron-withdrawing TFPPBr₈ ligand stabilizes the ferrous state, thereby enhancing the rate of alkyl peroxide oxidation.³⁶ In contrast, the lower reduction potentials of $\text{Fe}(\text{TFPP})\text{Cl}$ and $\text{Fe}(\text{TPP})\text{Cl}$ make these species poor oxidants, greatly slowing the ferric \rightarrow ferrous step in the catalytic cycle. Furthermore, as with ferryl complexes, any radicals generated in the presence of $\text{Fe}(\text{TFPP})\text{Cl}$ or $\text{Fe}(\text{TPP})\text{Cl}$ may decompose the porphyrin by attacking C-H bonds. Halogenation of the β positions of the porphyrin is also believed to prevent formation of a μ -oxo dimer,^{29,35} which is a mode of deactivation for both $\text{Fe}(\text{TPP})\text{Cl}$ and $\text{Fe}(\text{TFPP})\text{Cl}$ in reactions with dioxygen.³⁸ Thus the perhalogenated porphyrin has a faster rate of catalysis but a lower rate of catalyst degradation in solution

In order to further explore the possibility of an active iron(IV) or iron(V) oxo species, the synthesis of $\text{Fe}^{\text{III}}(\text{TFPPBr}_8)\text{OH}$ was attempted. Either chemical oxidants or bulk electrolysis could be used to generate a high-valent metal-oxo from an iron(III) hydroxide porphyrin. The pentafluorophenyl derivative, $\text{Fe}(\text{TFPP})\text{OH}$, has been produced by washing $\text{Fe}(\text{TFPP})\text{Cl}$ with NaOH in benzene.³⁹ Instead, we attempted to isolate the hydroxide salt directly from the iron insertion reaction. As described in Chapter 2, $\text{Fe}^{\text{II}}(\text{OAc})_2$ in glacial acetic acid inserts into $\text{H}_2\text{TFPPBr}_8$. The red color and red shifted Soret band of this species (in situ, $\lambda_{\text{max}} = 448$ and 578 nm) are consistent with formation of $\text{Fe}^{\text{II}}(\text{TFPPBr}_8)(\text{OAc})_2$. Instead of brine, a weak sodium hydroxide solution was used to quench the metal insertion reaction, which would provide a hydroxide ligand for the iron ion. The porphyrin that precipitated from the reaction was filtered and washed with water; the absorption spectrum of resulting solid has a maximum at 434 nm and a Q band at 584 nm. The blue shift from $\text{Fe}(\text{TFPPBr}_8)\text{Cl}$, as well as the shape of the spectrum, is analogous to the change from $\text{Fe}(\text{TFPP})\text{Cl}$ to $\text{Fe}(\text{TFPP})\text{OH}$, suggesting formation of $\text{Fe}(\text{TFPPBr}_8)\text{OH}$. Purification by column chromatography resulted in a new species, with a Soret at 418 , a strong shoulder at 486 , and a Q band at 600 nm. This species had the same spectrum as $\text{Fe}(\text{TFPPBr}_8)\text{Cl}$ after 48 hours in a methylene chloride/ PhIO solution, and may be the μ -oxo dimer. The blue shift of the Soret band and red shift in the Q bands is again the same as observed in the TFPP complexes. Although modeling has suggested that formation of $[\text{Fe}(\text{TFPPBr}_8)]_2\text{O}$ is unfavorable due to poor steric interactions, a weak complex may form. Rather than becoming a permanently unreactive species, however, this dimer may be able to break apart and undergo further reactions, as has been suggested for $(\text{FeTFPP})_2\text{O}$.⁴⁰ An alternative explanation of catalysis with a μ -oxo dimer is that dimerization *protects* one side of the porphyrin ligand, allowing oxidation to occur on the opposite side.⁴¹ Attempts to obtain a ^{19}F NMR of this material were unsuccessful, and due to the small amounts of compound obtained, this chemistry was not further pursued.

Conclusion

$\text{Fe}(\text{TFPPBr}_8)\text{Cl}$ is a remarkably active catalyst for the oxidation of cyclohexene with dioxygen, without added coreductant or light. The mechanism does not involve traditional high-valent metal-oxo intermediates, but interacts through the lower oxidation states of the porphyrin. Catalytic oxidation and reduction of alkyl peroxides by $\text{Fe}(\text{TFPPBr}_8)\text{Cl}$ generates radicals that continue free-radical chemistry in solution.

Other than halogenated porphyrins, only the highly activated porphyrin $\text{RuTMP}(\text{O})_2$ [dioxo(tetramesitylporphyrinato)-ruthenium(VI)] is known to catalyze the aerobic epoxidation of alkenes at ambient temperatures and pressures. Although able to catalyze 26 turnovers of cyclooctene in 24 hours (versus 73 TO of cyclohexene by $\text{Fe}(\text{TFPPBr}_8)\text{Cl}$), the Ru catalyst decomposes within this time period.⁴² Another electron-deficient porphyrin, β -hexanitro-tetrakis(2,6-dichlorophenyl)porphyrinato iron (III) chloride, has been shown to activate alkanes at higher temperatures and high pressures of O_2 .⁴³ Considering the similarity of the two porphyrins, it is likely that they operate by the same peroxide decomposition mechanism. Unfortunately, the exceptional reactivity of $\text{Fe}(\text{TFPPBr}_8)\text{Cl}$ with dioxygen appears to come at the expense of the selectivity found with high-valent metal-oxo species.

Methods

Oxidation reactions were run as follows. 3-4 mg of porphyrin (approximately 2-3 μmol) were added to a clean, oven-dried reaction vessel with a stir bar. For iodosobenzene experiments, 20-30 mg of PhIO were also weighed out into the flask (~ 50 eq PhIO/Fe). The reaction vessel was then fully assembled (Figure 4.9) and flushed from the top with Ar (for PhIO reactions) or O_2 , allowing gas to escape through the open stopcock. 15 mL freshly distilled methylene chloride (under Ar or saturated with dioxygen) was added by syringe into the reaction vessel, followed by 1 mL of freshly

distilled substrate. From the solubility of oxygen in methylene chloride and the volume of the flask, the dioxygen reactions were calculated to have approximately 1240 μmol of O_2 , or ~ 450 equivalents based on iron. The Kontes valve and stopcock were then closed, isolating the flask from the external atmosphere. The reactions were stirred for the next 24 - 48 hours, and aliquots taken by syringe every few hours for analysis of oxidation products.

The reactions were carried out in special flasks designed to minimize evaporation from the vessel during a reaction. A stopcock was attached to the side of a 25 mL Kjeldahl flask as shown in Figure 4.9. A hose could be attached to one of the two tubes on the stopcock, such that sample aliquots were not exposed to oxygen, and additional air did not leak into the flasks when an aliquot was removed. Unfortunately, this method prohibited clean kinetic measurements, since the concentration of oxygen in the flask at any given time was unknown. However, the rather excessive caution in sealing the flask was found to be necessary, since experiments run in round bottom flasks sealed only with a rubber septum had evidence of significant evaporation and/or leakage. Even with these precautions, the reaction volume decreased due to evaporation of the volatile solvent, and measurement reliability decreased significantly after 24 hours.

Gas chromatography was performed on a Hewlett Packard with a SD 1 column. Samples were identified by retention times relative to authentic samples. An internal standard (toluene) was added to each aliquot before injection in the GC and used to determine the concentration of each product.

Materials

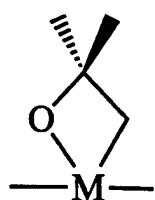
Porphyrins were obtained as described in Chapter 2. Iodosobenzene was purchased from TCI. Some batches were rather yellow in color, and were washed with benzene to remove impurities, with only some success. Methylene chloride, styrene, cyclohexene, *tert*-butyl hydroperoxide, and GC standards were purchased from Aldrich.

- (23) Traylor, T. G.; Nakano, T.; Dunlap, B. E.; Traylor, P. S.; Dolphin, D. *J. Am. Chem. Soc.* **1986**, *108*, 2782-2784.
- (24) Groves, J. T.; Subramanian, D. V. *J. Am. Chem. Soc.* **1984**, *106*, 2177-2181.
- (25) Traylor, T. G.; Miksztal, A. R. *J. Am. Chem. Soc.* **1989**, *111*, 7443-7448.
- (26) Traylor, T. G.; Xu, F. *J. Am. Chem. Soc.* **1988**, *110*, 1953-1958.
- (27) Ellis, P. E., Jr.; Lyons, J. E. *Coord. Chem. Rev.* **1990**, *105*, 181-193.
- (28) Lyons, J. E.; Ellis, P. E., Jr. *Catal. Lett.* **1991**, *8*, 45-52.
- (29) Grinstaff, M. W.; Hill, M. G.; Labinger, J. A.; Gray, H. B. *Science* **1994**, *264*, 1311-1313.
- (30) Smegal, J. A.; Schardt, B. C.; Hill, C. L. *J. Am. Chem. Soc.* **1983**, *105*, 3510-3515.
- (31) Ji, L.-N.; Liu, M.; Hsieh, A.-K.; Hor, T. S. A. *J. Mol. Catal.* **1991**, *70*, 247-257.
- (32) Lu, W. Y.; Bartoli, J. F.; Battioni, P.; Mansuy, D. *New J. Chem.* **1992**, *16*, 621-628.
- (33) Bottomley, L. A.; Kadish, K. M. *Inorg. Chem.* **1981**, *20*, 1348-1357.
- (34) Lyons, J. E.; Ellis, P. E., Jr.; Durante, V. A. In *Structure-Activity and Selectivity Relationships in Heterogeneous Catalysis*; R. K. Grasselli and A. W. Sleight, Eds.; Elsevier Science Publishers B.V.: Amsterdam, 1991; pp 99-116.
- (35) Ellis, P. E., Jr.; Lyons, J. E. *J. Chem. Soc., Chem. Commun.* **1989**, 1315-1316.
- (36) Grinstaff, M. W.; Hill, M. G.; Birnbaum, E. R.; Schaefer, W. P.; Labinger, J. A.; Gray, H. B. submitted to *Inorg. Chem.*
- (37) Labinger, J. A. *Catal. Lett.* **1994**, *26*, 95-99.
- (38) Gunter, M. J.; Turner, P. *Coord. Chem. Rev.* **1991**, *108*, 115-161.
- (39) Jayaraj, K.; Gold, A.; Toney, G. E.; Helms, J. H.; Hatfield, W. E. *Inorg. Chem.* **1986**, *25*, 3516-3518.
- (40) Ellis, P. E., Jr.; Lyons, J. E. *Catal. Lett.* **1989**, *3*, 389-398.
- (41) Chang, C. K.; Kuo, M.-S. *J. Am. Chem. Soc.* **1979**, *101*, 3413-3415.
- (42) Groves, J. T.; Quinn, R. *J. Am. Chem. Soc.* **1985**, *107*, 5790-5792.
- (43) Bartoli, J. F.; Battioni, P.; Foor, W. R. D.; Mansuy, D. *J. Chem. Soc., Chem. Commun.* **1994**, 23-24.

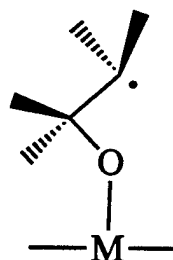
References

- (1) Groves, J. T.; Nemo, T. E.; Myers, R. S. *J. Am. Chem. Soc.* **1979**, *101*, 1032-1033.
- (2) Meunier, B. *Chem. Rev.* **1992**, *92*, 1411-1456.
- (3) Smith, J. L.; Sleath, P. J. *Chem. Soc., Perkin Trans. 2* **1982**, 1009-1014.
- (4) Traylor, T. G.; Tsuchiya, S. *Inorg. Chem.* **1987**, *26*, 1338-1339.
- (5) Traylor, P. S.; Dolphin, D.; Traylor, T. G. *J. Chem. Soc., Chem. Commun.* **1984**, 279-280.
- (6) Groves, J. T.; Quinn, R. *Inorg. Chem.* **1984**, *23*, 3844-3846.
- (7) Chang, C. K.; Ebina, F. *J. Chem. Soc., Chem. Commun.* **1981**, 778-779.
- (8) Bartoli, J. F.; Brigaud, O.; Battioni, P.; Mansuy, D. *J. Chem. Soc., Chem. Commun.* **1991**, 440-442.
- (9) Traylor, T. G.; Hill, K. W.; Fann, W.; Tsuchiya, S.; Dunlap, B. E. *J. Am. Chem. Soc.* **1992**, *114*, 1308-1312.
- (10) Assis, M. d. D.; Serra, O. A.; Iamamoto, Y.; Nascimento, O. R. *Inorg. Chim. Acta* **1987**, *187*, 107-114.
- (11) Iamamoto, Y.; Assis, M. d. D.; Baffa, O.; Nakagaki, S.; Nascimento, O. R. *J. Inorg. Biochem.* **1993**, *52*, 191-200.
- (12) Fujii, H. *J. Am. Chem. Soc.* **1993**, *115*, 4641-4648.
- (13) Groves, J. T.; Watanabe, Y. *J. Am. Chem. Soc.* **1986**, *108*, 507-508.
- (14) Groves, J. T.; Haushalter, R. C.; Nakamura, M.; Nemo, T. E.; Evans, B. J. *J. Am. Chem. Soc.* **1981**, *103*, 2884-2886.
- (15) Hewson, W. D.; Hager, L. P. *Porphyrins* **1979**, *7*, 295-315.
- (16) Penner-Hahn, J. E.; Eble, K. S.; McMurry, T. J.; Renner, M.; Balch, A. L.; Groves, J. T.; Dawson, J. H.; Hodgson, K. O. *J. Am. Chem. Soc.* **1986**, *108*, 7819-7825.
- (17) He, G.-X.; Arasasingham, R. D.; Zhang, G.-H.; Bruce, T. C. *J. Am. Chem. Soc.* **1991**, *113*, 9828-9833.
- (18) Groves, J. T.; W. J. Kruper, J. *J. Am. Chem. Soc.* **1979**, *101*, 7613-7615.
- (19) Ostovic, D.; Bruce, T. C. *Acc. Chem. Res.* **1992**, *25*, 314-320.
- (20) Ostovic, D.; Bruce, T. C. *J. Am. Chem. Soc.* **1988**, *110*, 6906-6908.
- (21) Ostovic, D.; Bruce, T. C. *J. Am. Chem. Soc.* **1989**, *111*, 6511-6517.
- (22) Naruta, Y.; Tani, F.; Ishihara, B.; Maruyama, K. *J. Am. Chem. Soc.* **1991**, *113*, 6865-6872.

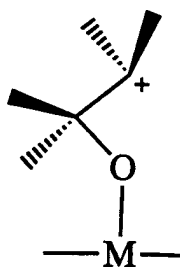
Figure 4.1 -- Intermediates that have been proposed in the literature for epoxidation by a high-valent metal-oxo. The metallaoxetane (I) and carbon radical (II) have been ruled out by recent experiments (see text), although this is not universally accepted. The carbocation (III) and carbocation radical (IV) are still considered viable intermediates, as is concerted oxygen insertion (V).



I



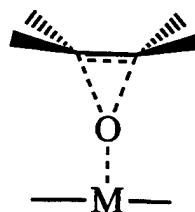
II



III



IV



V

Figure 4.2 -- A proposed mechanism for epoxidation where the rate limiting step involves association of the olefin with the metal-oxo to form a charge transfer complex (CT). The CT can form an epoxide by concerted oxygen insertion, electrophilic addition, or electron transfer (shown from left to right). The carbocation radical (IV) can either recombine and form an epoxide, or continue on a radical pathway leading to hydroxylation or other rearrangement products. Mechanism modified from reference 19.

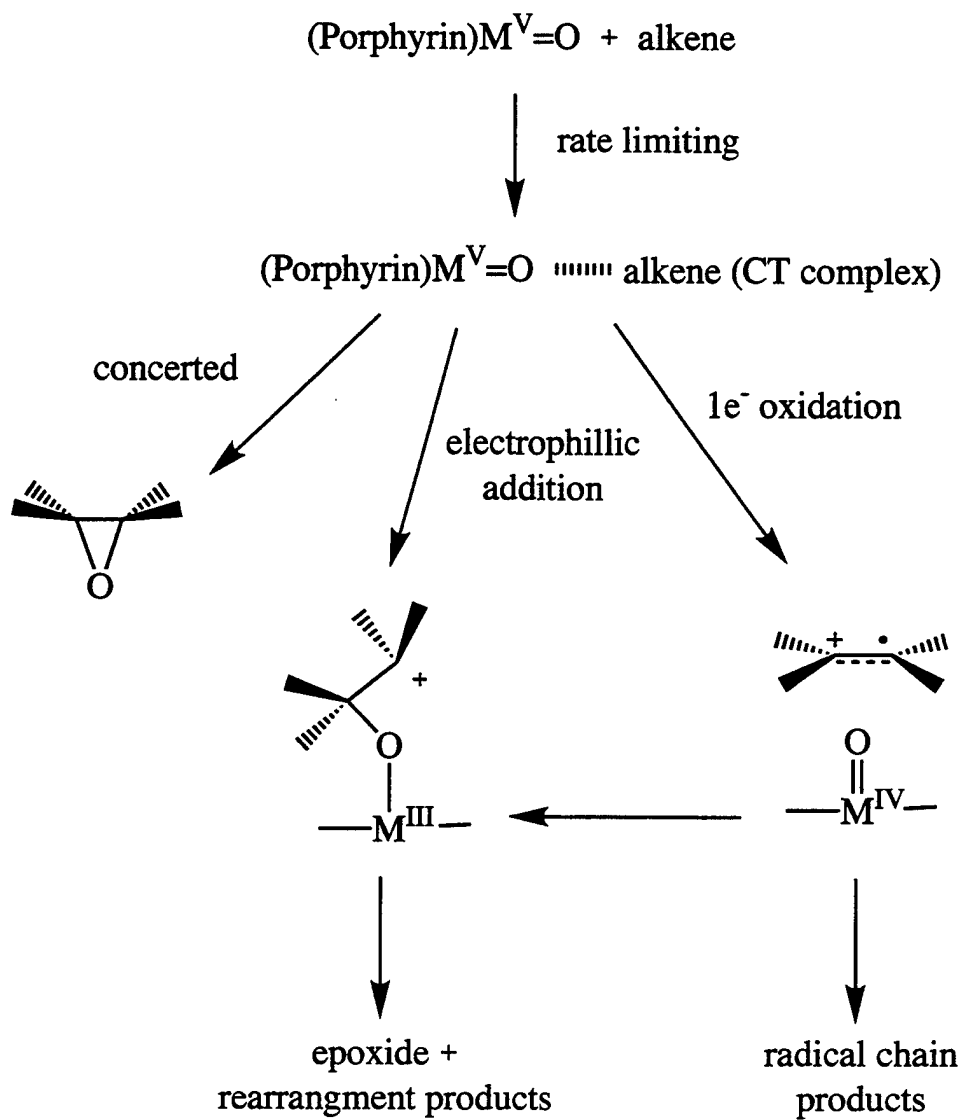


Figure 4.3 -- Multiple pathways are believed to be responsible for epoxidation and hydroxylation of cyclohexene. Hydroxylation is generally believed to occur via hydrogen abstraction. In addition to the electron-transfer epoxidation mechanism shown, direct oxygen insertion may also occur. The branching ratio is dependent on the nature of the olefin, the porphyrin, and the solvent.

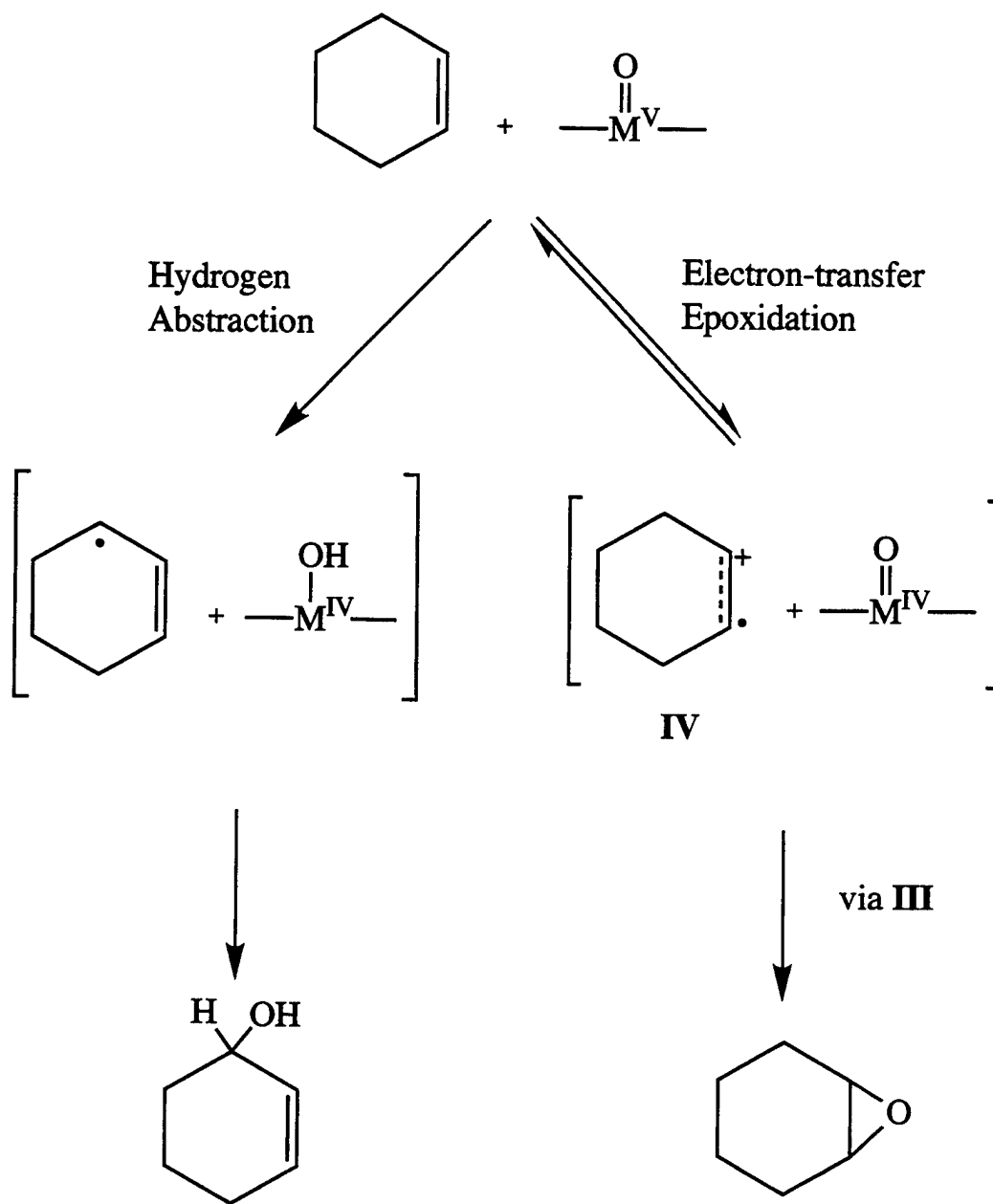


Figure 4.4 -- Turnovers and product distributions with cyclohexene and iron(III) porphyrins with dioxygen (at 3 hours) and PhIO (at 4 hours).

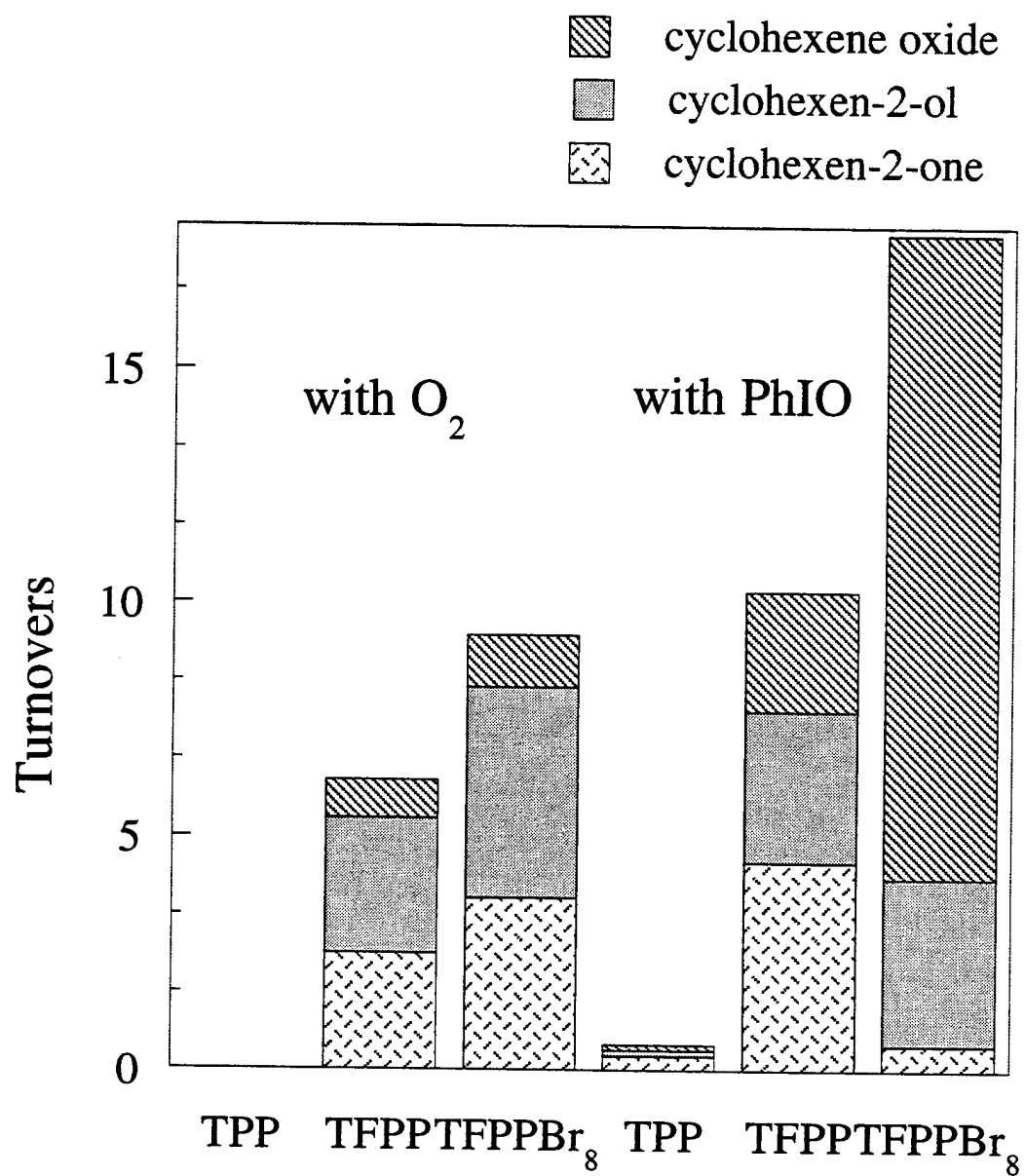


Figure 4.5 -- Product formation during cyclohexene oxidation with $\text{Fe}(\text{TFPPBr}_8)\text{Cl}$ and dioxygen. The curvature of the plot indicates the autocatalytic nature of the reaction.

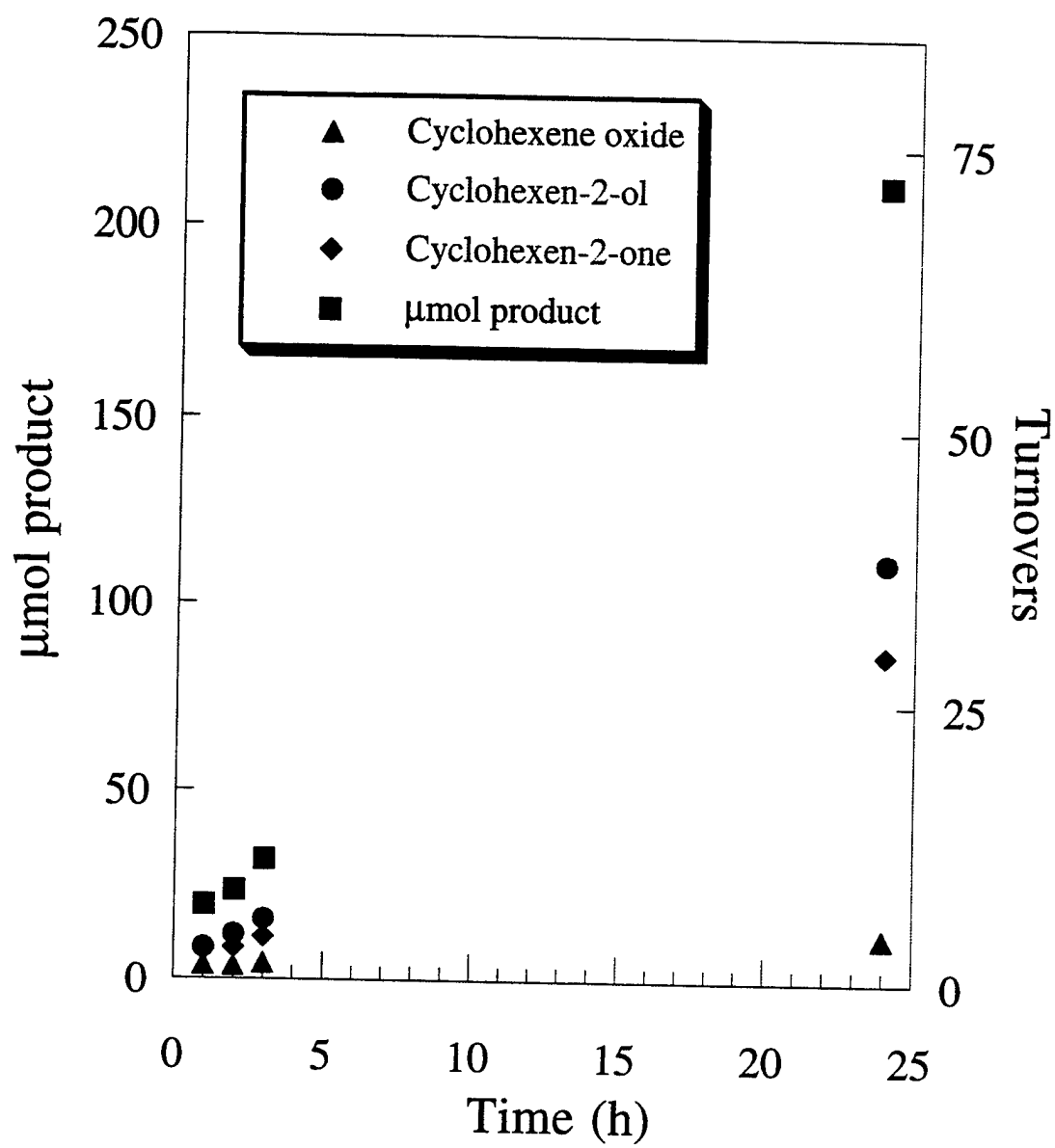


Figure 4.6 -- A plot of the catalytic activity (turnovers at 24 hours) observed for cyclohexene oxidation with dioxygen versus the reduction potential of the iron(III)-porphyrin catalyst (E° values: $\text{Fe(TPP)Cl} < \text{Fe(TFPP)Cl} < \text{Fe(TFPPBr}_8\text{)Cl}$).

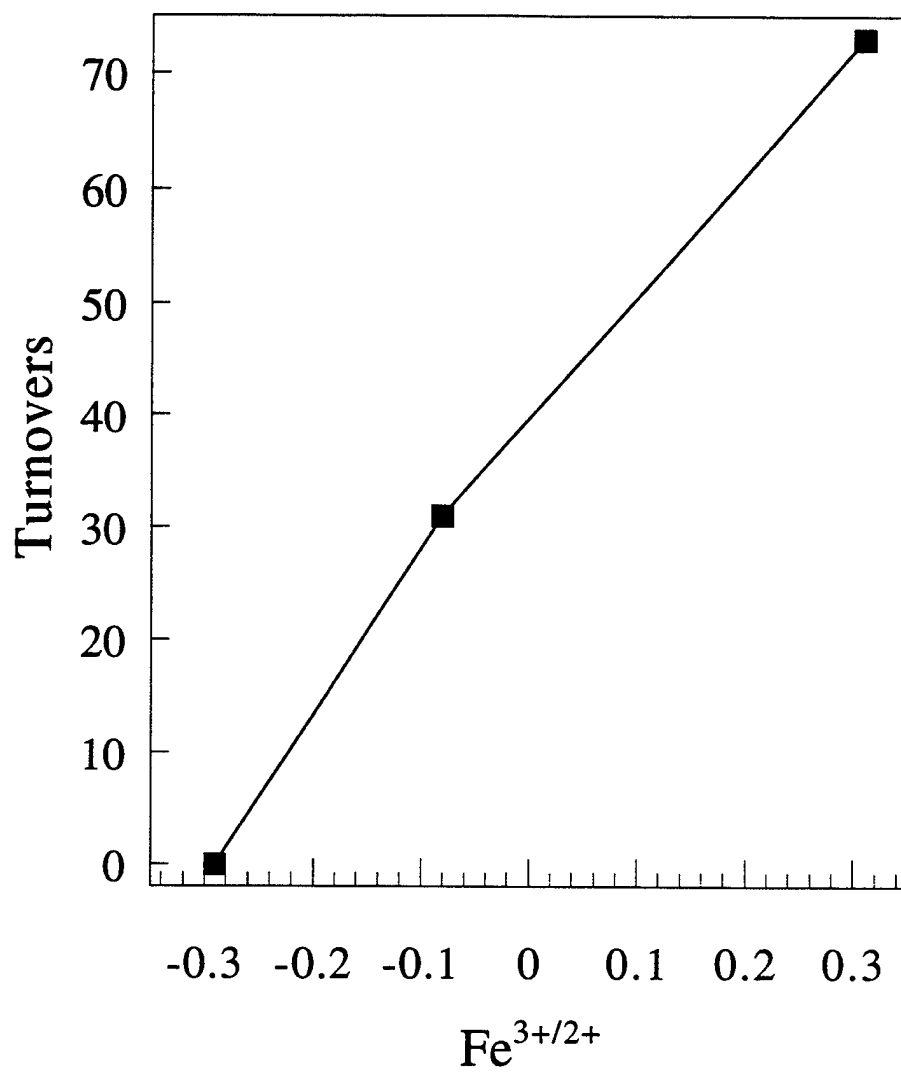


Figure 4.7 -- A proposed mechanism for direct activation of dioxygen initiated by oxygen binding to a ferrous porphyrin (modified from reference 34). The positive electrochemical potential ($\text{Fe}^{2+/3+}$) of the halogenated iron porphyrins were proposed to generate an iron(IV) oxo of comparable activity to that of a biological iron(V) oxo.

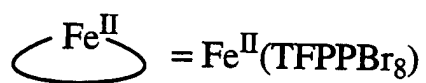
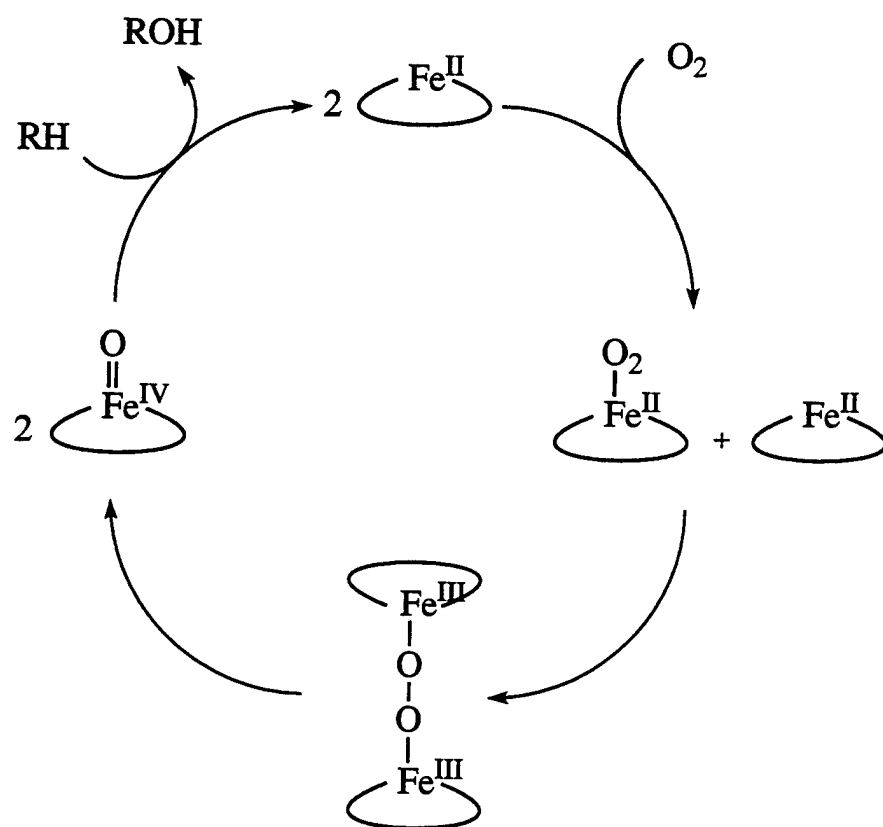


Figure 4.8 -- The alkyl peroxide decomposition mechanism for dioxygen reactions with Fe(TFPPBr₈)Cl. Initiated by radicals in solution, the peroxides thereby generated are catalytically decomposed by the iron porphyrin. These radicals can further propagate the reaction.

Initiation by radicals
present in solution.

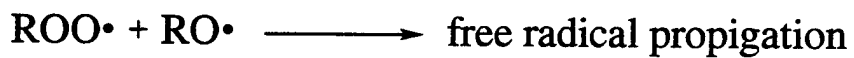
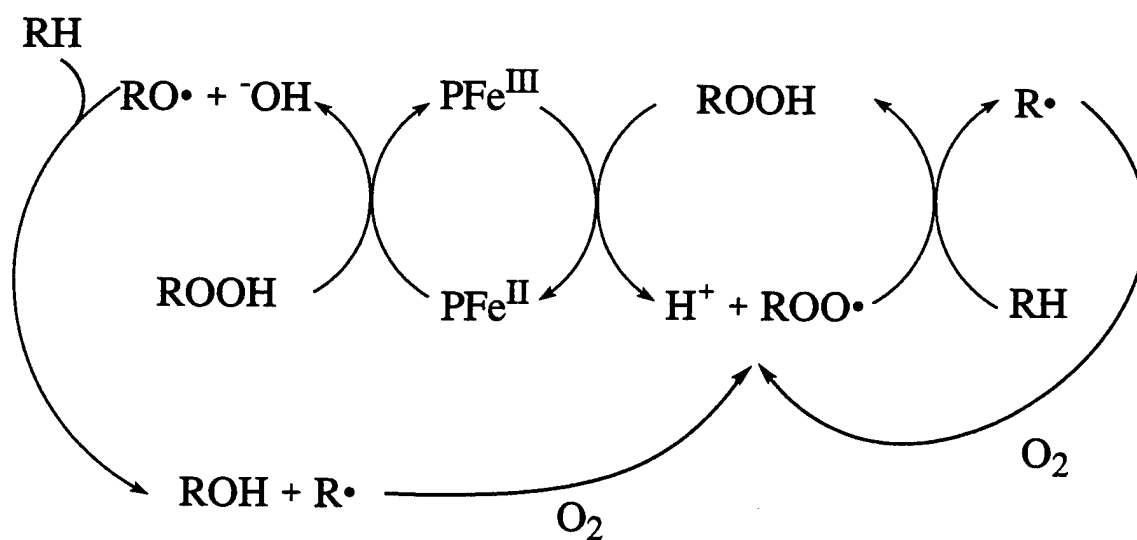
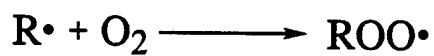
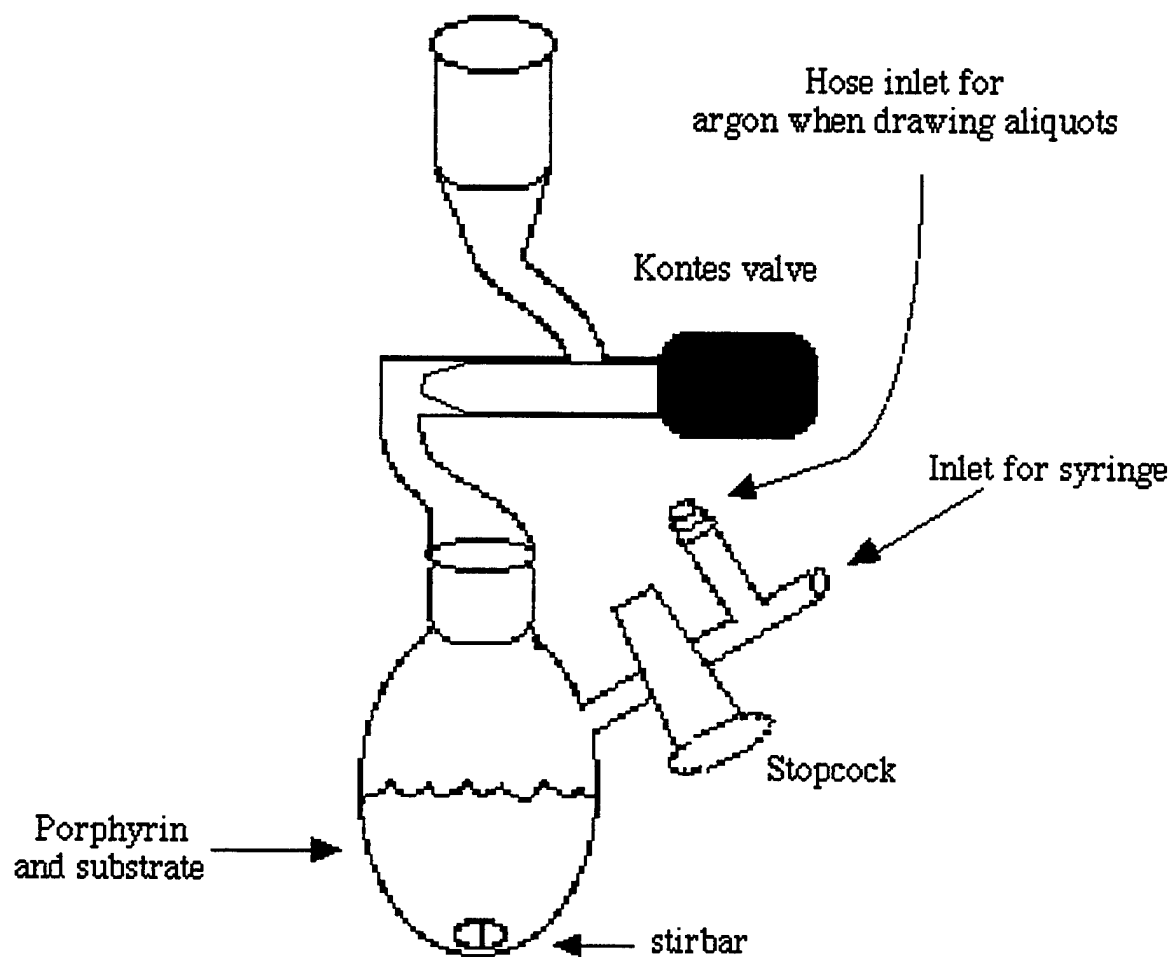


Figure 4.9 -- The modified Kjeldahl flask used for oxidation reactions. The porphyrin and iodosobenzene are added dry, then solvent and substrate are added. Aliquots can be removed without exposing the sample to air.

\$24/40 Joint,
Could evacuate on a vacuum line
or flush with argon or dioxygen.



Chapter 5

On the Mechanism of Alkene Oxidation by Ruthenium Porphyrins and Molecular Oxygen

Introduction

As described in the preceding chapter, iron tetraphenylporphyrin derivatives are catalysts for the oxidation of alkenes and alkanes with oxygen donors. A smaller number of ruthenium porphyrins have also been synthesized to further explore biomimetic metalloporphyrin oxidation chemistry. Although a few have been investigated as oxidation catalysts, a greater portion of work has focused on using ruthenium porphyrins as model complexes for iron porphyrins or as systems for dihydrogen or dinitrogen activation. For example, cofacial ruthenium porphyrin dimers have been shown to bind dihydrogen in the core between the two porphyrin molecules.¹

Ruthenium porphyrins are commonly isolated as six-coordinate $\text{Ru}^{\text{II}}(\text{porphyrin})\text{L}_2$ species with $2e^-$ donor ligands such as pyridine or CO as compared to five-coordinate $\text{Fe}^{\text{III}}(\text{porphyrin})\text{X}$ complexes. Greater ligand field stabilization energy for the second row metal and π bonding from π acid ligands give ruthenium(II) porphyrins greater stability relative to iron hemes.² This increase in stability is exploited for mechanistic investigations, as intermediates in ruthenium oxidation reactions, such as $(\text{P})\text{Ru}^{\text{IV}}=\text{O}$, can be isolated and better characterized than the corresponding iron porphyrin species. Furthermore, comparisons of iron, ruthenium, and osmium porphyrin spectroscopy have been useful in determining orbital energies in iron porphyrin compounds.³⁻⁹

Ruthenium tetramesitylporphyrins have been investigated as catalysts for the oxidation of hydrocarbons. Groves¹⁰ found that $\text{RuTMP}(\text{CO})$ is oxidized to $\text{Ru}^{\text{VI}}\text{TMP}(\text{O})_2$ with two equivalents of *m*-chloroperoxybenzoic acid (mCPBA). This species is moderately stable, and has been characterized by NMR, elemental analysis, and

UV-Vis spectroscopy. The ruthenium dioxo porphyrin complex is a competent stoichiometric oxidant of norbornene, resulting in 1.6 equivalents (eq) norbornene oxide per mole of porphyrin and a solvated $\text{Ru}^{\text{II}}\text{TMP}$ complex.¹¹ Transfer of the first oxygen occurs more readily than the second, indicating that the monooxo complex is not as effective an oxo transfer agent as the dioxo complex.¹² However, various N-oxides have been used as O-atom donors with $\text{Ru}^{\text{VI}}\text{TMP}(\text{O})_2$ to catalytically oxidize alkenes^{13,14} and alkanes¹⁵ in good yields (30-90% based on N-oxide).

The carbonyl complexes $\text{RuTMP}(\text{CO})$, $\text{RuTPP}(\text{CO})$, $\text{RuOEP}(\text{CO})$ and $\text{RuTDFPP}(\text{CO})$ (TDFPP = 2,6-difluorophenylporphyrin) are also observed to catalyze hydrocarbon oxidation.^{15,16} With *tert*-butyl hydroperoxide (TBHP) or sodium hypochlorite as the oxidant, over 100 turnovers of styrene in 24 hours are reported for $\text{RuTDFPP}(\text{CO})$, and even higher activity was reported with $\text{RuOEP}(\text{CO})$.¹⁶ $\text{RuTMP}(\text{CO})$ and $\text{RuTPP}(\text{CO})$ do not show activity until addition of strong acid to the solution; once activated, both porphyrins catalyze the oxidation of adamantane with 2,6-dichloropyridine N-oxide. Activity is higher when the dioxo complex is used.¹⁵ No mechanism was proposed to explain either the high activity with planar, unhalogenated OEP, or the "activation" of the carbonyl porphyrins by acid.

In addition to catalysis observed with N-oxides and peroxides, the dioxo ruthenium porphyrins are a unique example of porphyrin catalysis with dioxygen but without addition of a coreductant. $\text{Ru}^{\text{VI}}\text{TMP}(\text{O})_2$ catalyzes the aerobic oxidation of olefins under mild conditions.¹¹ The proposed mechanism (Figure 5.1) suggests that $\text{Ru}^{\text{IV}}\text{TMP}(\text{O})$, formed upon a single oxidation of substrate, disproportionates to reform the active Ru^{VI} species and a solvated ruthenium(II) porphyrin, $\text{Ru}^{\text{II}}\text{TMP}(\text{S})_2$.¹² The weakly coordinated ruthenium(II) reacts with O_2 to complete the cycle. While other porphyrins such as $\text{Ru}^{\text{VI}}\text{OEP}(\text{O})_2$ and $\text{Ru}^{\text{VI}}\text{TPP}(\text{O})_2$ share the ability to stoichiometrically oxidize alkenes, the less sterically bulky compounds dimerize to $(\text{Ru}^{\text{IV}}\text{P}(\text{OH}))_2\text{O}$ rather than reform $\text{Ru}^{\text{VI}}\text{P}(\text{O})_2$ in the presence of dioxygen.^{17,18}

$\text{RuTMP}(\text{O})_2$ has been utilized as a catalyst for the aerobic oxidation of thioethers, steroids, and esters.¹⁹⁻²² Although these papers describe catalysis by $\text{RuTMP}(\text{O})_2$ in good yield, few experiments have been conducted to probe the validity of the initially proposed Groves mechanism (Figure 5.1). Furthermore, there has been little comment on the unusual ability to activate dioxygen in combination with the inability of this species to oxidize alkanes. The mechanism of $\text{RuP}(\text{CO})$ activation by strong acid, or the possibility of a different mechanism with N-oxides (versus dioxygen) have also not been adequately addressed. In summary, although some of the extremely interesting and unique chemistry displayed by ruthenium porphyrins has been noted, little of it is well understood.

Our investigations into oxidation catalysis with perhalogenated iron porphyrins (Chapter 4) led to the synthesis and characterization of a perhalogenated ruthenium porphyrin complex, β -octachloro-tetrakis(pentafluorophenyl)porphyrinato-ruthenium(II) carbonyl ($\text{RuTFPPCl}_8(\text{CO})$) (Chapters 2 and 3). Initially, the ruthenium porphyrin was to be used to generate stable ruthenium analogs to iron peroxy intermediates proposed in the decomposition of alkyl peroxides by $\text{Fe}(\text{TFPPBr}_8)\text{Cl}$, allowing a better understanding of the iron oxidation mechanism. Alternatively, the halogenated porphyrin could share the unusual reactivity of $\text{Ru}^{\text{II}}\text{TMP}$ with dioxygen. Catalytic activity in iron porphyrins has been shown to increase with the anodic shift in the iron reduction potential, suggesting that a halogenated ruthenium porphyrin may show higher activity than RuTMP . Indeed, $\text{RuTFPPCl}_8(\text{CO})$ is an extremely active catalyst for olefin oxidation with dioxygen. The mechanism does not appear to be related to either the other halogenated metalloporphyrins or the unhalogenated ruthenium porphyrins, but is unique to $\text{RuTFPPCl}_8(\text{CO})$.

Results

$\text{RuTFPPCl}_8(\text{CO})$ is an efficient catalyst for the oxidation of alkenes with PhIO or molecular oxygen. The oxidation reactions were run under comparable conditions to those with $\text{Fe}(\text{TFPPBr}_8)\text{Cl}$ described in Chapter 4. Each reaction was initiated by addition of 1 mL substrate to 15 mL of a 0.1 mM solution of $\text{RuTFPPCl}_8(\text{CO})$ in methylene chloride. The reaction vessel (Figure 4.9) also contained 40 equivalents iodobenzene under argon, or if O_2 was the oxygen source, the solution and head space in the reaction vessel were saturated with dioxygen. Aliquots were taken every 2 hours and products detected by GC.

Iodobenzene is not a very efficient oxygen source for cyclohexene oxidation with $\text{RuTFPPCl}_8(\text{CO})$ (Figure 5.2, Table 5.1). Only 10 turnovers are observed in 24 hours, with formation of 42% epoxide. The selectivity for epoxide is less than with $\text{Fe}(\text{TFPPBr}_8)\text{Cl}$, but a notable lack of ketone is produced ($< 2\%$). The reaction rate is highest initially, tapering off after the first 6 hours. The UV-Vis spectrum remains unchanged at the end of 24 hours, indicating that the decrease in rate is not due to porphyrin decomposition. Styrene is better oxidized by iodobenzene and $\text{RuTFPPCl}_8(\text{CO})$, with 26 turnovers in only 3 hours, 81% of which are styrene oxide.

The high selectivity for epoxidation observed with PhIO and $\text{RuTFPPCl}_8(\text{CO})$ is consistent with formation of $\text{Ru}^{\text{IV}}\text{TFPPCl}_8(\text{O})$. As described in Chapter 4, iodobenzene reacts with metalloporphyrins to form a metal-oxo intermediate. In the presence of olefin, the oxo species forms a charge transfer complex that may lead to epoxidation via concerted oxene transfer or electrophilic addition to the carbon-carbon double bond (Figure 4.3). The decreased activity for cyclohexene oxidation by $\text{Ru}^{\text{IV}}\text{TFPPCl}_8(\text{O})$ relative to " $\text{Fe}^{\text{V}}(\text{TFPPBr}_8)\text{Cl}(\text{O})$ " is not surprising, since the ruthenium porphyrin is one oxidation state lower than the iron analog.

Activity with dioxygen is quite substantial (Table 5.1). In 24 hours, 42 equivalents of cyclooctene are epoxidized to cyclooctene oxide. Benzaldehyde is the

sole product of styrene oxidation, producing only 2.5 turnovers in 3 hours. The greatest activity is seen in the oxidation of cyclohexene; 296 turnovers consisting of cyclohexene oxide (15%), 2-cyclohexen-1-ol (58%) and 2-cyclohexen-1-one (27%) are observed in 24 hours (Figure 5.3).

The mechanism with dioxygen is not as obvious. The different product selectivity observed in oxidation of both styrene and cyclohexene with dioxygen versus iodosobenzene suggests there is a different mechanism for the two O-atom sources. The increased amount of allylic and carbon-carbon bond cleavage oxidation products suggests that the mechanism with O_2 has a substantial radical contribution. Since reactions with PhIO are believed to go through a Ru^{IV} oxo intermediate, a different oxidizing species must be generated upon reaction with O_2 . Unfortunately, the difficulty in obtaining large quantities of porphyrin has precluded the direct observation of intermediates in the dioxygen reactions. Instead, indirect methods have been used to probe the reaction mechanism. As many modes of interaction between oxygen and the porphyrin are possible, we have tried to test the viability of the most likely candidates.

A simple, direct method of dioxygen activation mimics dioxygenase rather than monooxygenase activity (Figure 4.7). Such a mechanism, initially proposed to explain oxidations with highly halogenated iron porphyrins,²³ is even more attractive for the ruthenium analogs, since no addition of coreductant would be required to initiate the cycle. Oxygen binds to $RuTFPPCl_8(CO)$, which reacts with another porphyrin molecule to form a μ -peroxo dimer, $(TFPPCl_8)Ru^{III}-O-O-Ru^{III}(TFPPCl_8)$. Homolytic O-O bond cleavage forms the active oxidant, Ru^{IV} monooxo, which returns to the catalyst resting state after oxidizing substrate. This mechanism is unlikely for two reasons. First, cleavage of the μ -peroxo bond to form $(P)Ru^{IV}=O$ would produce the same oxidizing species as PhIO, and would therefore be expected to yield the same product distribution. This mechanism does not allow for the different selectivity observed with different oxidants. Furthermore, $Ru^{II}TFPPCl_8(CO)$ is air stable and shows no reaction with

dioxygen, even upon recrystallization from an air saturated solution. Thus the first step in the cycle does not occur.

A second possibility is that $\text{RuTFPPCl}_8(\text{CO})$ and $\text{Fe}(\text{TFPPBr}_8)\text{Cl}$ operate by the same mechanism with oxygen (Figure 4.8). A plot of moles of cyclohexene product versus time for catalysis by $\text{RuTFPPCl}_8(\text{CO})$ (Figure 5.3) shows a slight curvature, suggesting some initiation for this catalyst, although not as significant as observed for the iron analog. More importantly, no metal couple is accessible in the ruthenium porphyrin electrochemistry (Chapter 3), so no orbital of reasonable energy is available to transfer electrons to or from an alkyl peroxide.

The best evidence that $\text{RuTFPPCl}_8(\text{CO})$ does not operate by an alkyl peroxide decomposition mechanism, however, is that it does not decompose peroxides at an appreciable rate. $\text{Fe}(\text{TFPPBr}_8)\text{Cl}$ has been shown to rapidly decompose *tert*-butyl hydroperoxide^{24,25}; when TBHP is added to a solution of $\text{Fe}(\text{TFPPBr}_8)\text{Cl}$, oxygen is vigorously evolved. A similar concentration of $\text{RuTFPPCl}_8(\text{CO})$ does not exhibit a visible reaction. A more sensitive analysis of hydrogen peroxide decomposition shows that the ruthenium porphyrin only decomposes 4.5 equivalents of peroxide in four hours, as measured by oxygen evolution. The iron porphyrin is much more efficient, with 68 turnovers in the same time period (Figure 5.4). The opposite relative activity is observed for cyclohexene oxidation with dioxygen, where $\text{RuTFPPCl}_8(\text{CO})$ catalyzes 296 turnovers compared to only 73 by $\text{Fe}(\text{TFPPBr}_8)\text{Cl}$ in 24 hours. A purely radical peroxide decomposition mechanism is not consistent with these observations.

A third possibility is that this catalyst mimics the behavior of $\text{RuTMP}(\text{CO})$ with oxygen. A Ru^{VI} dioxo complex would be expected to exhibit different reactivity than a monooxo, thus resolving the problem of dissimilarity with the iodosobenzene results. Therefore an attempt was made to reproduce the Groves cycle with $\text{RuTFPPCl}_8(\text{CO})$. As in the conversion of $\text{RuTMP}(\text{CO})$ to $\text{Ru}^{\text{VI}}\text{TMP}(\text{O})_2$,¹⁰ careful titration of a solution of $\text{RuTFPPCl}_8(\text{CO})$ with mCPBA resulted in complete formation of a new species

($\lambda_{\text{max}} = 420, 514, 552 \text{ nm}$) after addition of two equivalents peroxide (Figure 5.5). Isosbestic points at 390, 417, 525, and 585 nm indicate that only a single species is formed. The slight red shift in the Soret band and the blue shift in the Q bands are consistent with spectral changes observed in the oxidation of RuOEP(CO) to RuOEP(O)₂,¹⁸ suggesting that Ru^{VI}TFPPCl₈(O)₂ is formed. The disappearance of the carbonyl stretch in the IR indicates removal of the CO ligand, but no strong stretch is observable in the 700 to 900 cm⁻¹ region, as would be expected for a ruthenium oxo.^{12,18} However, this region contains strong solvent stretches, making detection of $\nu_{\text{Ru=O}}$ difficult by solution infrared spectroscopy.

The anodically shifted reduction potentials of RuTFPPCl₈(CO) would destabilize the higher oxidation states relative to those of RuTPP complexes, making Ru^{VI}TFPPCl₈(O)₂ extremely reactive. In line with this expectation, any attempt to concentrate or isolate this species led to decomposition to a variety of porphyrin products. However, at low concentrations, such as in a range where UV-Visible spectroscopy of the porphyrin ligand is feasible (1 - 10 μM), the steps of the catalytic cycle can be observed (Figure 5.6). Addition of mCPBA to form Ru^{VI}TFPPCl₈(O)₂, followed by addition of a small amount of cyclohexene, results in a large decrease in the intensity of both the Soret and Q band absorptions. The bleach is not due to porphyrin decomposition, because addition of carbon monoxide gas regenerates the original spectrum with over 85% of the original intensity. The new spectrum is similar to that of Ru^{IV}OEP(O)₂²⁶ or Ru^{IV}TPP(O),¹⁷ with a slight blue shift in the Soret band and broad absorptions in the Q band region relative to the dioxo complex, suggesting formation of Ru^{IV}TFPPCl₈(O). Increased recovery of the Soret band after 24 hours in the presence of substrate could indicate transfer of the second oxo ligand from Ru^{IV}TFPPCl₈(O) to form another molecule of oxidized substrate and Ru^{II}TFPPCl₈(S)₂. Unfortunately, the amount of product generated was too small to be detected by the GC method used for the general catalysis experiments, and oxo-transfer to the olefin could not be confirmed.²⁷

Oxidation of triphenylphosphine to triphenylphosphine oxide can be confirmed by ^{31}P NMR. Addition of two equivalents PPh_3 to a solution of $\text{Ru}^{\text{VI}}\text{TFPPCl}_8(\text{O})_2$ led to a decrease in the 514 nm band and the 600 nm tailing associated with dioxo formation, and new Q bands at 542 and 553 nm (Figure 5.7a). Continued addition of PPh_3 resulted in a blue shift of the Q bands to 517 and 540 nm, which may correspond to the coordination of triphenylphosphine to $\text{Ru}^{\text{II}}\text{TFPPCl}_8$ (Figure 5.7b). These two steps are believed to correspond to oxidation of 2 eq PPh_3 by the dioxo porphyrin followed by coordination of PPh_3 to the solvated ruthenium(II) porphyrin.

The ^{31}P NMR of this sample after the reaction is complete does show a resonance for Ph_3PO at 29.9 ppm. A second signal, consistent with PPh_3 coordination to Ru^{II} , appears at 40 ppm in the ^{31}P NMR (no signal is observed at -6 ppm for free triphenylphosphine). For example, $\text{Ru}(\text{COOMe})_2(\text{CO})_2\text{PPh}_3$ has a chemical shift of 30.5 ppm.²⁸ Although the UV-Vis showed isosbestic conversion to " $\text{RuTFPPCl}_8(\text{PPh}_3)_2$ ", the ^{19}F NMR was not clean, indicating that coordination of triphenylphosphine is not quantitative. Additional peaks in the ^{19}F NMR may be due to partial degradation of the porphyrin ligand after treatment with a harsh oxidant such as mCPBA.

Addition of styrene to a solution of $\text{Ru}^{\text{VI}}\text{TFPPCl}_8(\text{O})_2$ led to similar spectroscopic changes, indicating that the decrease in Soret intensity ("oxo transfer") is not dependent on the substrate. In the absence of a potential ligand, the Soret bleach was even more pronounced. Addition of a small amount of pyridine to this solution led to the formation of $\text{RuTFPPCl}_8(\text{py})_2$ (confirmed by UV-Vis). The ease of formation of the bis-pyridine adduct is consistent with oxidation of substrate by $\text{Ru}^{\text{VI}}\text{TFPPCl}_8(\text{O})_2$ to form $\text{Ru}^{\text{II}}\text{TFPPCl}_8(\text{S})_2$ that is able to coordinate an available ligand.

These experiments suggest that $\text{RuTFPPCl}_8(\text{CO})$ can undergo Groves type chemistry. The catalytic oxidation reactions with O_2 , however, were conducted without any additional oxidant, allowing no mechanism for the initial formation of $\text{Ru}^{\text{VI}}\text{TFPPCl}_8(\text{O})_2$ from the carbonyl species. In addition, oxo transfer is generally

accepted to be more selective than the catalysis observed in the dioxygen reactions.

Although Groves chemistry is possible, it does not seem probable for the main mechanism for catalysis by $\text{RuTFPPCl}_8(\text{CO})$ with dioxygen.

Therefore a modified mechanism is proposed, which reacts through the lower oxidation states, involving both a monooxo and a peroxo intermediate. As mentioned above, $\text{Ru}^{\text{IV}}\text{TMP}(\text{O})$ is a weak oxo transfer agent; the more electron-withdrawing TFPPCl_8 ligand would be expected to result in a much more reactive monooxo complex. The reaction is initiated by a slow loss of CO (Figure 5.8). The solvated ruthenium(II) porphyrin, without the strong π acid effect of the carbonyl, would have a much lower $\text{Ru}^{\text{III/II}}$ couple, increasing the possibility of a reaction with dioxygen. Instead of forming $\text{Ru}^{\text{IV}}\text{TFPPCl}_8(\text{O})$, as in the direct oxygen activation mechanism (Figure 4.7), the ruthenium(II) dioxygen complex could rearrange to a ruthenium peroxo species that can react with substrate. The peroxide intermediate can either abstract a hydrogen atom from substrate to form $\text{Ru}^{\text{III}}\text{TFPPCl}_8(\text{OOH})$ or attack olefin to epoxidize one substrate molecule and form $\text{Ru}^{\text{IV}}\text{TFPPCl}_8(\text{O})$. The branching at this point in the mechanism would accommodate the observation of allylic oxidation products from escape of R^\bullet which could initiate a free radical reaction. Decomposition of the alkyl peroxide radical to product and $\text{RuTFPPCl}_8(\text{O})$ would result in a larger amount of epoxide formation relative to the purely radical alkyl peroxide mechanism of $\text{Fe}(\text{TFPPBr}_8)\text{Cl}$. This mechanism is similar to one proposed for stoichiometric oxidation by vanadium(V) peroxo complexes where a mixture of epoxidation and hydroxylation was observed.²⁹

The modified peroxo intermediate mechanism does implicate an initiation period for the catalyst, as loss of the carbonyl ligand is required before interaction with dioxygen can occur. Chemical removal of the carbonyl ligand should abolish the initiation period and increase the amount of active catalyst, resulting in higher overall product formation. However, addition of a small amount of triethylamine-N-oxide (10 eq) or mCPBA (5-10 eq) to remove the carbonyl ligand did not increase the rate of reaction. The oxidation

reactions were initiated by addition of oxygen and cyclohexene to a solution of $\text{RuTFPPCl}_8(\text{CO})$ and $(\text{Et})_3\text{NO}$ or mCPBA. No change in the rate of catalysis was observed with triethylamine-N-oxide (Figure 5.9), though the product distribution was much more similar to that of $\text{Fe}(\text{TFPPBr}_8)\text{Cl}$ with dioxygen, with only 6% epoxide and 59% 2-cyclohexen-1-ol. The porphyrin spectrum was also affected by addition of $(\text{Et})_3\text{NO}$. The Q band absorptions grew in intensity and moved to 510 and 535 nm, similar to the spectrum of $\text{RuTFPPCl}_8(\text{py})_2$, suggesting that triethylamine may bind to ruthenium.

Reactions with mCPBA were substantially different; only 20 turnovers were observed, all within the first 2 hours. More epoxide was produced: 35% versus 15% with dioxygen alone. The lack of products suggests that the catalyst deactivated, although the spectrum was unchanged. It is possible that $\text{Ru}^{\text{II}}\text{TFPPCl}_8(\text{L})_2$ remaining after the reaction with mCPBA dimerizes or forms another porphyrin product with a Soret at similar energy to $\text{RuTFPPCl}_8(\text{CO})$. Although titrations with mCPBA suggest relatively stable formation of $\text{Ru}^{\text{VI}}\text{TFPPCl}_8(\text{O})_2$, the catalysis experiments are run at significantly higher concentration of porphyrin ($> 25 \text{ X}$). The lack of activity suggests that the carbonyl free porphyrin is not stable at higher concentrations, and perhaps dimerizes to a catalytically inactive species. In a normal cyclohexene oxidation reaction, only a small amount of ruthenium porphyrin is an active catalyst (has lost CO) at any given time. Therefore the concentration of $\text{Ru}^{\text{IV}}\text{TFPPCl}_8(\text{O})$ is quite low, and reacts with substrate before deactivation (via dimerization) can occur. Alternatively, the mechanism proposed in Figure 5.9 may be incorrect; the carbonyl ligand may remain on the ruthenium for the duration of the reaction, and activation of the catalyst occurs by some other means.

Addition of TBHP could also serve to initiate the reaction. Unlike mCPBA, TBHP is not a strong enough oxidant to remove the carbonyl ligand. However, it is capable of generating free radicals, and could initiate a radical based reaction in solution.

Addition of 10 equivalents TBHP to a solution of $\text{RuTFPPCl}_8(\text{CO})$ in the presence of cyclohexene and O_2 results in no increase in the number of moles of products produced (Figure 5.10a). The product distribution in these reactions is the same as with dioxygen alone.

If a larger amount of TBHP is added, the reaction is much faster, with 200 turnovers in the first hour. The product distribution is also significantly different, with 10% epoxide and 50% 2-cyclohexen-1-ol throughout the run. It is not clear if the porphyrin is involved in this chemistry, or if the TBHP has simply initiated a free radical reaction. If the data is replotted in terms of turnovers, then a significant increase in rate is observed with either 10 or 300 equivalents of TBHP (Figure 5.10b). Interpretation of this result is complicated by the fact that only 50% as much porphyrin catalyst was used in the peroxide experiment.

Phase transfer of dioxygen into the solution is not rate limiting. Although solubility of dioxygen in methylene chloride is only 10 mM, this does not limit the reaction rate. A decrease in the stir rate (Figure 5.11) or even a complete lack of stirring does not curtail the rate of product formation. In fact, as seen in Figure 5.11, the slower stirred reaction showed more turnovers in an equal time period. A completely unstirred reaction also showed slightly higher activity, suggesting that a lower concentration of oxygen in solution may enhance reactivity.

A further test of the peroxo mechanism used the presence of additional carbon monoxide to inhibit the reaction. If catalyst activation involves spontaneous loss of CO, exposure to a carbon monoxide atmosphere should shut down catalysis by pushing the equilibrium towards the inactive CO bound form. As mentioned above, both UV-Vis and IR spectroscopy indicate that the carbonyl ligand remains bound both during and after a catalytic run. However, the presence of a small amount of ruthenium porphyrin without CO would be difficult to detect by these methods. To further explore the role of the carbonyl ligand, oxidation of cyclohexene by $\text{RuTFPPCl}_8(\text{CO})$ was conducted under a

mixture of oxygen and carbon monoxide. Rather than preventing oxidation, identical rates of product formation were observed under a 50/50 O₂/CO atmosphere. The mixed atmosphere reaction only produced less product at the 24 hour time point, since only half as much total oxygen was in the reaction vessel (Figure 5.12).

The lack of inhibition by CO, while not encouraging, does not completely rule out the loss of CO as the first step in the reaction mechanism. As described above, if the carbonyl ligand is never lost, the subsequent reaction with dioxygen would never occur. However, if the reaction with dioxygen is much faster than recombination with carbon monoxide, some ruthenium porphyrin would remain active, allowing oxidation chemistry to take place in the presence of CO. However, it is surprising that absolutely no decrease in rate is observed.

A more interesting result from the mixed atmosphere experiments is the decrease in epoxide formation. At 24 hours, epoxide comprises only 7% of the total products, compared to 15% in a pure dioxygen environment. The decrease in epoxidation is offset by an increase in the amount of 2-cyclohexen-1-one to 36%. A possible explanation for the change in product distribution is that multiple oxidation pathways with dioxygen are available, and one that favors epoxidation is inhibited by carbon monoxide, while the other is not.

To insure that a small amount of uncarbonylated porphyrin is not present, a sample was exposed to a high pressure of CO. A small amount of RuTFPPCl₈(CO) in CCl₄ or CH₂Cl₂ was placed into a Parr reactor and sealed under 1100 psi of carbon monoxide for 2 or 4 days. The pressure was released from the Parr bomb, and a measured amount of the porphyrin solution (containing ~ 2 μmol porphyrin) was injected directly into a solution of methylene chloride and cyclohexene to initiate a dioxygen catalysis reaction. Some carbon monoxide remained in the porphyrin solution, but as the mixed atmosphere experiments demonstrated, the presence of a small amount of CO does not inhibit the oxidation reaction.

Catalysis with the CO treated $\text{RuTFPPCl}_8(\text{CO})$, however, had an extremely long initiation period. In 24 hours, only ten turnovers are observed, composed entirely of allylic oxidation products. By 48 hours, the reaction has fully initiated, with 238 turnovers comprised of 7% epoxide, 53% 2-cyclohexen-1-ol, and 40% 2-cyclohexen-one, similar to the product distribution observed in the mixed atmosphere reactions.

Spectroscopy of the CO treated porphyrin showed that the porphyrin had been modified during the long exposure to CO. The infrared spectrum of the porphyrin shows a new peak at 2112 cm^{-1} in addition to the peak assigned to the CO stretch of mono-carbonyl complex at 1981 cm^{-1} . The shift of ν_{CO} to higher energy is consistent with formation of $\text{RuTFPPCl}_8(\text{CO})_2$; calculations indicate that a single CO stretch is expected for the bis-carbonyl porphyrin (approximating the porphyrin as D_{2d} symmetry). An intense peak also appeared in the IR spectrum at 1730 cm^{-1} , as discussed below.

The UV-Vis spectrum in either methylene chloride or carbon tetrachloride showed a slight red shift of the Soret to 420 nm and a slight blue shift and broadening of the Q bands (Figure 5.13). A strong absorption was also observed at 280 nm, but is not believed to be related to the porphyrin, since it appeared at different intensity relative to the porphyrin bands in the two runs. The high energy electronic transition and the 1730 cm^{-1} IR band are consistent with signals from a ketone. It is possible that some reaction between the reactive halogenated solvent and carbon monoxide could have occurred, resulting in formation of an acyl chloride or halogenated ketone. Low molecular weight acyl chlorides have a strong absorption around 1800 cm^{-1} , while halogenated ketones are at slightly lower energy. ^1H NMR of the carbon tetrachloride solution after removal from the Parr reactor showed a weak resonance at 4.3 ppm; chloroacetyl chloride has a chemical shift of 4.6 ppm. Unfortunately, it is impossible to do more than speculate on the source of these organic-type absorptions. However, repurification of the porphyrin by column chromatography does remove the 280 nm band from the UV-Vis and the 2112 cm^{-1} band from the IR. The purified porphyrin regains

catalytic activity, suggesting that chromatography removes the second CO from the ruthenium. In the absence of another axial ligand to displace the second carbonyl, such as water or acetone available in the usual post-synthesis workup, the second carbonyl ligand remains bound. The bis-carbonyl complex has no coordination sites available for chemistry, and no catalysis is observed. The pressure experiments suggest some interesting activation of CO under high pressures, but do not elucidate the role of the carbonyl ligand in catalysis.

Oxidation reactions with cyclohexene- d_{10} show a large isotope effect in reactions with dioxygen (Figure 5.14). In competitive experiments with equal amounts of deuterated and non-deuterated cyclohexene, the ratio of products at 24 hours gives an isotope effect of 7.0. The product distribution indicates a significant difference between epoxidation and allylic oxidation. Epoxide formation has no isotope effect (ratio = 1.0), 2-cyclohexen-1-ol has an isotope effect of 14.1, and the isotope effect for 2-cyclohexen-1-one formation is twice that number (29.5), suggesting that different processes are responsible for epoxidation and hydroxylation. Both the total isotope effect (8.2) and the individual isotope effects (1.15 for epoxidation, 9.2 and 19.3 for allylic oxidation) are of similar magnitude to those of $\text{Fe}(\text{TFPPBr}_8)\text{Cl}$, suggesting that hydrogen abstraction is involved in the rate determining step.

Non-competitive experiments reveal that the two cases are not the same. With $\text{Fe}(\text{TFPPBr}_8)\text{Cl}$, no reaction was seen with cyclohexene- d_{10} alone. Presumably, spontaneous radical formation from deuterated cyclohexene is slow due to the stronger C-D bond, and the reaction is never initiated. With $\text{RuTFPPCl}_8(\text{CO})$, however, some reaction with cyclohexene- d_{10} was observed, indicating that the ruthenium porphyrin does not initiate solely by the same mechanism as the iron porphyrin. The non-competitive isotope effect is extremely large, $(\text{mol cyclohexene products})/(\text{mol cyclohexene-}d_{10} \text{ products}) = 85$. A large non-competitive isotope effect (50) has been reported for the oxidation of alcohols by $[(\text{bpy})_2(\text{py})\text{Ru}^{\text{IV}}(\text{O})]^{2+}$.³⁰ The mechanism

involves hydride transfer followed by rapid proton equilibration from the aqueous medium, which is not applicable to the organic solvent reaction of $\text{RuTFPPCl}_8(\text{CO})$.

Further experiments probed the possibility of a photochemical reaction. Since the reaction vessel is made of glass, ambient light enters the reaction, allowing the possibility of a light activated mechanism. Porphyrins are known to sensitize singlet oxygen,³¹ and the actual oxygen transfer step could be completely unrelated to the ruthenium center. To test the possibility of singlet oxygen production, ZnTFPPCl_8 was used in place of $\text{RuTFPPCl}_8(\text{CO})$. Visible light has enough energy to cause a $\pi \rightarrow \pi^*$ transition in either the zinc or ruthenium porphyrin to form a triplet excited state. The triplet can act as a sensitizer to generate singlet oxygen, which could then react with cyclohexene. Under similar conditions to catalysis with $\text{RuTFPPCl}_8(\text{CO})$, ZnTFPPCl_8 produced only 3 turnovers of cyclohexene in 24 hours, all of which were allylic oxidation products. This is within the range of products observed without any catalyst (between zero and 20 μmol product, approximately equal to up to 10 turnovers), suggesting that ZnTFPPCl_8 does not catalyze the oxidation of cyclohexene by any mechanism. The lack of activity from the porphyrin suggests that the TFPPCl_8 ligand is not an efficient oxygen sensitizer. Furthermore, the products are not consistent with an organic singlet oxygen reaction. $^1\text{O}_2$ generates ketones and carbon - carbon bond cleavage products rather than epoxides and alcohols.³²

A second control was performed by excluding light from a catalysis reaction of $\text{RuTFPPCl}_8(\text{CO})$ with dioxygen and cyclohexene. The initiation period increased dramatically, with almost no reaction in the first 10 hours. The initiation period for one reaction was longer than the second trial, resulting in very different turnover numbers at 24 hours (Figure 5.15). Once started, however, the reaction rate does increase; at 24 hours, Run 1 has 75% of the products of an average reaction in ambient light. The second reaction, which was slower to initiate, has only 16% as much activity in 24 hours. Product distributions are similar to a reaction in the light, suggesting that the same

mechanism is operating in both cases. Although singlet oxygen is not implicated, ambient light does play a role in initiating the reaction with $\text{RuTFPPCl}_8(\text{CO})$ and O_2 . The catalyst appears to be both thermally and photochemically activated.

Photolysis with visible light dramatically increases the rate of reaction (Figure 5.16). Two identical reactions were set up, one in the presence of normal room light (one light bulb from a hood lamp), and one continuously irradiated with a tungsten lamp (150W). The visible photolysis reaction shows 3.5 times as many turnovers in 8 hours (270 vs. 77), a tremendous enhancement by relatively low energy light. No porphyrin decomposition was observed. Product distributions are similar in the two reactions, indicating that a similar reaction is occurring in both cases.

To further explore the effect of light, the photophysics of $\text{RuTFPPCl}_8(\text{CO})$ were investigated. Samples of $\text{RuTFPPCl}_8(\text{CO})$ in methylene chloride were irradiated with pulses from a Nd-YAG or dye laser. Laser photolysis is known to photodissociate carbonyl ligands,⁸ allowing an investigation of the reactivity of the bare ruthenium porphyrin. Excitation with 355 or 480 nm light produced a transient difference spectrum consistent with promotion of an electron into the $\pi^* e_g$ orbital. A positive absorbance at 620 nm (Figure 5.17) and a negative change in optical density (ΔOD) in the Soret region indicate formation of a porphyrin triplet.

The kinetics describing decay of the excited state were dependent on the atmosphere over the solution. Both the 5 μs and 50 μs transient absorption spectra from 390 to 440 nm were obtained under carbon monoxide, ethylene, oxygen, and argon atmospheres; the transient spectra at 415 nm are shown in Figures 5.18 and 5.19 (additional traces are in Appendix 5). Under CO, biexponential decay of the excited state is observed. The faster rate,³³ $k_1 = 3.9 \times 10^6 \text{ s}^{-1}$, most likely corresponds to the decay of the porphyrin triplet excited state. The lifetime, 286 ns, is much shorter than the 36 μs porphyrin-based triplet excited state of $\text{RuTPP}(\text{CO})$,³⁴ but longer than the 15 ns charge transfer excited state of $\text{RuTPP}(\text{py})_2$.³⁵ Generally, ruthenium porphyrin complexes have

$^3(\pi - \pi^*)$ lifetimes of tens of microseconds, while $(d - \pi^*)$ lifetimes are only a few nanoseconds.³¹ Although the transient spectrum (at $t = 0$; Figure 5.17) shows porphyrin triplet characteristics, the short lifetime suggests that substantial mixing of the triplet and charge transfer states is occurring. The molecular orbital diagram of $\text{RuTFPPCl}_8(\text{CO})$ (Figure 3.6) indicates that these two transitions are expected to be very close in energy. No emission was detected either at room temperature or from 2-methyl-tetrahydrofuran glass (77 K) at any wavelength out to 1100 nm.

The second kinetic term, $k_2 = 1.3 \times 10^5 \text{ s}^{-1}$, is believed to be due to recombination of CO. The concentration of CO in chloroform is 8.5 mM; assuming pseudo first order kinetics (and a similar concentration in CH_2Cl_2), the CO recombination rate is calculated as $1.5 \times 10^7 \text{ M}^{-1} \text{ s}^{-1}$.

As observed in the laser traces at 415 nm on a 50 μs time base (Figure 5.19), the signal does not completely return to zero. The transient at 50 μs is after the excited state has decayed, and should correspond to the spectrum of the photoproduct from loss of the carbonyl ligand. The magnitude of the ΔOD indicates that the quantum yield for loss of CO is quite small, consistent with quantum yields observed for other ruthenium porphyrins.⁸ Comparisons of the transient spectra under different atmospheres at 50 μs may give some indication of the reactivity of the carbonyl free ruthenium.

Oxygen efficiently quenches the triplet at a rate of $1.25 \times 10^7 \text{ s}^{-1}$. However, comparison of the transient absorption spectra at 50 μs under CO and O_2 does not suggest that oxygen binds to ruthenium (Figure 5.20). In fact, none of the spectra from the four samples have a distinct photoproduct at 50 μs , not supporting a mechanism involving oxygen binding to RuTFPPCl_8 after loss of CO. Furthermore, a spectrum taken of each sample after laser photolysis (Figure 5.21) indicates that significant amounts of porphyrin decomposition occur under an oxygen atmosphere.

An ethylene atmosphere results in decay rates of $k_1 = 8.9 \times 10^6 \text{ s}^{-1}$ and $k_2 = 4.2 \times 10^5 \text{ s}^{-1}$, indicating substantial quenching of the porphyrin excited state. Since ethylene is

unable to quench an excited state by energy transfer, it must be interacting more directly with the porphyrin to protect it from decomposition. The 50 μ s transient under ethylene shows the greatest bleach in the Soret region, suggesting some interaction between ruthenium and olefin on this time scale. The ethylene sample shows no decomposition after photolysis, and even shows a slight increase in the Soret intensity. One explanation for these results is that ethylene binds to the excited state of RuTFPPCl₈(CO) (k_1), and also to the photodissociated ruthenium porphyrin (k_2). Approximating the concentration of ethylene in solution as 5 mM gives an ethylene recombination rate with the photodissociated RuTFPPCl₈ of $8.4 \times 10^7 \text{ M}^{-1} \text{ s}^{-1}$. However, olefin complexation after loss of CO is not likely to be relevant to the catalytic mechanism since the quantum yield is very small. Photolysis of CO is only observed with high energy light (355 nm), and the oxidation reactions are only irradiated with visible wavelengths.

Under an atmosphere of argon, the excited state again shows biexponential decay kinetics with $k_1 = 7.1 \times 10^6 \text{ s}^{-1}$ and $k_2 = 7.6 \times 10^5 \text{ s}^{-1}$. These results are not consistent with the description of the ethylene and dioxygen chemistry above. It is difficult to find an explanation for the increase in the decay rates under an inert atmosphere. One possibility is that in the absence of another ligand, the excited state interacts with methylene chloride, which is not a completely inert solvent. However, the decay rate would still be expected to be slower than rates under a CO atmosphere. A second possibility is that with the high energy light needed to observe the Soret band transients, multiple reactions may occur, complicating the kinetics.

Despite these problems, it is clear that excitation under ethylene results in a different product than photolysis under an inert atmosphere. Furthermore, although oxygen quenches the triplet excited state, there is no evidence for the substantial red shift normally observed upon binding of dioxygen.⁴ These experiments suggest another possible mechanism that would initiate not with oxygen binding but with olefin binding. RuTFPPCl₈(CO) is not able to catalyze the hydroxylation of alkanes with dioxygen,

suggesting that the electron richness of the carbon - carbon double bond is somehow important. Toluene, which has weak methyl C-H bonds, is not oxidized, either alone or in the presence of olefin to initiate reaction. Cumene or 3-methyl pentane, which is oxidized in low yield by $\text{Fe}(\text{TFPPBr}_8)\text{Cl}$, is also inactive with the ruthenium porphyrin and dioxygen.

Some evidence for olefin binding does exist. The carbonyl stretch in the solution IR of $\text{RuTFPPCl}_8(\text{CO})$ in CCl_4 shifts 2.2 cm^{-1} upon addition of a small amount of cyclohexene. The shift to higher energy is consistent with weak competition by the π^* orbitals of the olefin for backbonding density from the ruthenium ion.

^1H NMR of $\text{RuTFPPCl}_8(\text{CO})$ in acetone- d_6 after 24 hours under an ethylene atmosphere showed a weak resonance at -3.6 ppm. $\text{RuTMP}(\text{C}_2\text{H}_4)$ has a singlet at -3.27 ppm, assigned to a π complex of ethylene,³⁶ suggesting a similar assignment for $\text{RuTFPPCl}_8(\text{C}_2\text{H}_4)$. The carbonyl ligand may remain bound to trans to the olefin, but it is not clear from the NMR data. As the signal is present under an atmosphere of ethylene gas, exchange of the bound ethylene must be slow on the NMR time scale. The ^{19}F NMR of this sample still showed several different porphyrin species, indicating that only a small fraction of the porphyrin has ethylene bound.

UV-Vis data indicates that olefin binding, if occurring, is not highly favored. A solution of $\text{RuTFPPCl}_8(\text{CO})$ with cyclohexene showed no change after 24 hours, suggesting that any olefin complex is of low enough concentration to be swamped by the signal of the carbonyl porphyrin. Alternatively, a weak interaction with olefin might cause only small changes in the UV-Vis spectrum.

If olefin binding is not favored for the ground state, the transient spectroscopy suggests that olefin binding may be more favorable in the excited state. A mechanism for catalytic olefin oxidation via the excited state is shown in Figure 5.22. The mixing of the $^3(\pi - \pi^*)$ and $(d - \pi^*)$ orbitals indicate that visible excitation of $\text{RuTFPPCl}_8(\text{CO})$ might populate the MLCT state which results in an oxidized metal center in the excited state.

Olefin binding to the strongly oxidizing Ru^{III} would then be more likely to occur (Figure 5.22). Once a π olefin complex is formed, it may rearrange to form a ruthenium(IV) alkyl radical complex, which would readily combine with dioxygen. The bound alkyl peroxide radical could abstract a hydrogen atom from another substrate molecule, forming a peroxide complex. From this point, several different pathways could occur. The peroxide could homolytically cleave, either thermally or photochemically, initiating a free radical reaction (not shown). Alternatively, the peroxide could decompose via an intermolecular epoxidation reaction, leaving $\text{Ru}^{\text{III}}\text{TFPPCl}_8(\text{OH})$ (after the formal π radical anion recombines with the ruthenium), which may recombine with another radical, R^\bullet , to form ROH and return the porphyrin to the resting state of the catalytic cycle.

This mechanism has several advantages over the mechanism involving loss of CO . First, spontaneous loss of the π acid carbonyl ligand is not likely for such an electron deficient porphyrin. Second, a partial carbon monoxide mechanism would not inhibit a photochemical reaction. Third, the dramatic increase in reactivity with light is explained by a greater amount of olefin complexation, which decomposes to lead directly to product or free radicals. The branching for a radical mechanism explains the large amount of allylic radical products observed. In addition, the large non-competitive isotope effect suggests that branching for the intermolecular mechanism is favored over C-D bond cleavage by a substantial amount, as is the high percentage of epoxidation formed with cyclohexene- d_{10} .

The peroxide experiments are also consistent with this mechanism. Addition of mCPBA removes the carbonyl ligand, which leads to a less oxidizing MLCT state with less or no affinity for olefin interaction. Addition of small amounts of TBHP may enhance the branching to the radical pathway by providing radicals to propagate radical reactions.

Conclusion

Traditional scientific method has always been at the very best, 20-20 hindsight. It's good for seeing where you've been. It's good for testing the truth of what you think you know, but it can't tell you where you ought to go.

-- Robert M. Pirsig, *Zen and the Art of Motorcycle Maintenance*, (1974).³⁷

RuTFPPClg(CO) has unprecedented ability for a carbonyl porphyrin to catalyze the oxidation of olefins with dioxygen. The mechanism does not appear to be radical decomposition of alkyl peroxides, as observed with Fe(TFPPBr₈)Cl, or the Groves dioxo ruthenium(VI) chemistry observed with RuTMP. Instead, a novel mechanism is proposed that involves an interaction of olefin with a mixed $^3(\pi - \pi^*) - (d - \pi^*)$ excited state. The electron-withdrawing porphyrin ligand creates a highly oxidizing excited state ruthenium center, which can be stabilized by an interaction with a π donor ligand. Photochemically driven oxidation chemistry with such low energy, low intensity light is quite amazing.

The involvement of light in the mechanism is indisputable. The dramatic enhancement of catalysis by even low-energy irradiation clearly favors a photochemical reaction mechanism. This is unprecedented for this class of porphyrin catalysts. RuTFPPClg(CO) is unique in being the first stable, effective photocatalyst for olefin oxidation with dioxygen. Moreover, the catalyst would be extremely interesting for potential commercial applications since it fulfills the desired requirements of intense, low-energy light absorption.

Once olefin binding has occurred, the following steps in the reaction mechanism are not as clear. Although a logical mechanism can be proposed, further work would be necessary to completely understand the decomposition of the bound olefin/oxygen complex to form product. The potential also exists to tune the mechanism to favor one

branches of the proposed mechanism over another to increase the selectivity for epoxidation over hydroxylation. For example, selective photolysis at 420 nm (into the Soret band) could decrease undesired radical side reactions (such as decomposition of the bound alkylperoxide). Other conditions, such as solvent, temperature, and oxygen concentration have obvious potential to change the reaction selectivity. Since phase transfer is not rate limiting, perhaps a lower concentration of oxygen would increase the activity by decreasing unfavorable quenching of the excited state by oxygen (as suggested by the higher activity in the unstirred reactions).

A continuation of this project would include a more thorough investigation of the proposed photochemical activation of olefin. The photophysics of $\text{RuTFPPCl}_8(\text{CO})$ could be better understood, especially the fast excited state decay under an argon atmosphere. Furthermore, if ethylene is quenching the $^3(\pi - \pi^*)$ excited state, varying the concentration of olefin would allow the quenching rate to be determined by Stern-Volmer kinetics. The possibility of a reaction with solvent could also be eliminated by repeating the reaction in a more inert solvent.

Experimental

Materials -- Ruthenium porphyrins were obtained as described in Chapter 2. Iodosobenzene and cyclohexene-*d*₁₀ was purchased from TCI. Cyclohexene, cyclooctene (Aldrich), and methylene chloride (EM Science) were distilled under argon before use. Cyclohexene oxide, 2-cyclohexen-1-ol, 2-cyclohexen-1-one, *m*-chloroperoxybenzoic acid (mCPBA), *tert*-butyl hydroperoxide (TBHP), triethylamine-N-oxide, pyridine, and styrene were purchased from Aldrich. Hydrogen peroxide and acetone were purchased from EM Science. Carbon monoxide, ethylene, and dioxygen lecture bottles were purchased from Matheson.

Methods -- General oxidation reactions were conducted as described in Chapter 4. UV-Vis, NMR, and IR spectra were obtained as described in Chapters 2 and 3.

Reaction with peroxide -- Reactivity with TBHP was only determined in a qualitative fashion. Approximately 0.2 mL TBHP was added to a mM solution of either RuTFPPClg(CO) or Fe(TFPPBr)Cl in methylene chloride and allowed to stir for several hours. During this time, the solution was monitored visually for the evolution of gas that would indicate peroxide decomposition. A similar reaction with hydrogen peroxide was also monitored. In this case, 10 mg of porphyrin in 10 mL acetone was degassed on a high vacuum line. Five mL of 0.6 % hydrogen peroxide in acetone (degassed) was added, and the solution allowed to stir at room temperature. Every hour, the pressure of evolved gas was measured with a Toeppler pump and the number of moles calculated. An IR of the gas indicated that it was not carbon dioxide or carbon monoxide (from the carbonyl ligand of the ruthenium porphyrin), and was assumed to be dioxygen from the recombination of radicals produced from peroxide decomposition by the porphyrin.

Titration with mCPBA -- A solution of RuTFPPClg(CO) in methylene chloride, such that the absorbance at either the Soret or Q band was close to 1, was prepared and

the exact concentration determined by either serial dilution or from the extinction coefficient. A solution of mCPBA (mM) was prepared by serial dilution. The porphyrin solution (2.5 mL) was titrated with 10 to 20 μ L aliquots of mCPBA, and monitored by UV-Vis. The changes in the spectrum were complete after addition of less than 100 μ L mCPBA solution, such that the porphyrin concentration remained relatively constant.

Titration with triphenylphosphine -- Aliquots from a mM solution of PPh_3 were added to the porphyrin solution immediately after addition of mCPBA, and monitored by UV-Vis. The solution was concentrated and spiked with CDCl_3 for NMR analysis.

Initiation with mCPBA or $(\text{Et})_3\text{NO}$ -- Five to ten equivalents of oxidant (approximately 1-3 mg) were added with the porphyrin to the reaction flask. Under argon, 15 mL of methylene chloride were added, and the solution allowed to stir for two minutes. The reaction vessel was flushed with dioxygen as 1 mL of cyclohexene was added to start the oxidation reaction. Product formation was measured as before.

Mixed atmosphere reactions -- $\text{RuTFPPCl}_8(\text{CO})$, solvent, and cyclohexene were mixed together in the reaction flask under argon. A mixture of carbon monoxide and oxygen was used to flush the argon from the flask and start the oxidation reaction.

Pressurized carbon monoxide reaction -- A mM solution of $\text{RuTFPPCl}_8(\text{CO})$ in either methylene chloride or carbon tetrachloride was placed in a glass lined Parr reactor. The reactor was connected to a carbon monoxide tank, and flushed twice before full pressurization to 1100 psi of CO. The reaction was not stirred, but allowed to rest under CO pressure for 2 or 4 days (in CCl_4 or CH_2Cl_2 , respectively). The pressure was let down, the Parr reactor opened and the porphyrin solution transferred to a Teflon capped vial. One mL of solution was used to run an oxidation reaction by injecting it into the reaction just before addition of dioxygen and substrate. The concentration of $\text{RuTFPPCl}_8(\text{CO})$ in the reaction was calculated from the absorbance of the porphyrin solution.

Initiate with TBHP -- Attempts to initiate cyclohexene oxidation reactions with peroxide were accomplished by addition of TBHP to the reaction before addition of substrate. A small amount of a dilute TBHP solution was added to a solution of $\text{RuTFPPCl}_8(\text{CO})$ in methylene chloride. Three separate reactions were run, adding 10, 225, or 380 equivalents of TBHP, respectively.

Stir rate -- The stir rate was lowered to half of normal for these reactions. One reaction was also run without any stirring.

Isotope effect -- The isotope effect was calculated from both competitive and non-competitive experiments. Competitive experiments were run with 15 mL of methylene chloride, 2 mg $\text{RuTFPPCl}_8(\text{CO})$, and 1 mL each of cyclohexene and cyclohexene- d_{10} . The deuterated oxidation products ran slightly slower on the GC, allowing individual determination of deuterated and non-deuterated turnover numbers. Non-competitive experiments were run with 1 mL of cyclohexene- d_{10} , and compared to reactions run with perprotio cyclohexene. The isotope effect was calculated as a ratio of turnover numbers at 24 hours, since actual rates of product formation were not determined from these experiments.

Singlet oxygen generation -- A cyclohexene oxidation reaction was run as described above, with 3 μmol ZnTFPPCl_8 in place of $\text{RuTFPPCl}_8(\text{CO})$.

Light experiments -- A cyclohexene oxidation reaction was run as described above, except the entire reaction flask was wrapped in foil to prevent incidental light from affecting the reaction. The light catalyzed reaction was accomplished by photolysis of an oxidation reaction with a normal 150 watt light bulb. The light was turned on before addition of substrate, and kept on for the duration of the experiment. The reaction was placed in a water bath to maintain ambient temperature.

Laser experiments -- Solutions of $\text{RuTFPPCl}_8(\text{CO})$ in methylene chloride were degassed by three cycles of the freeze/pump/thaw method on a high vacuum line in a quartz laser cuvette. The cuvettes were then backfilled with the desired gas (argon,

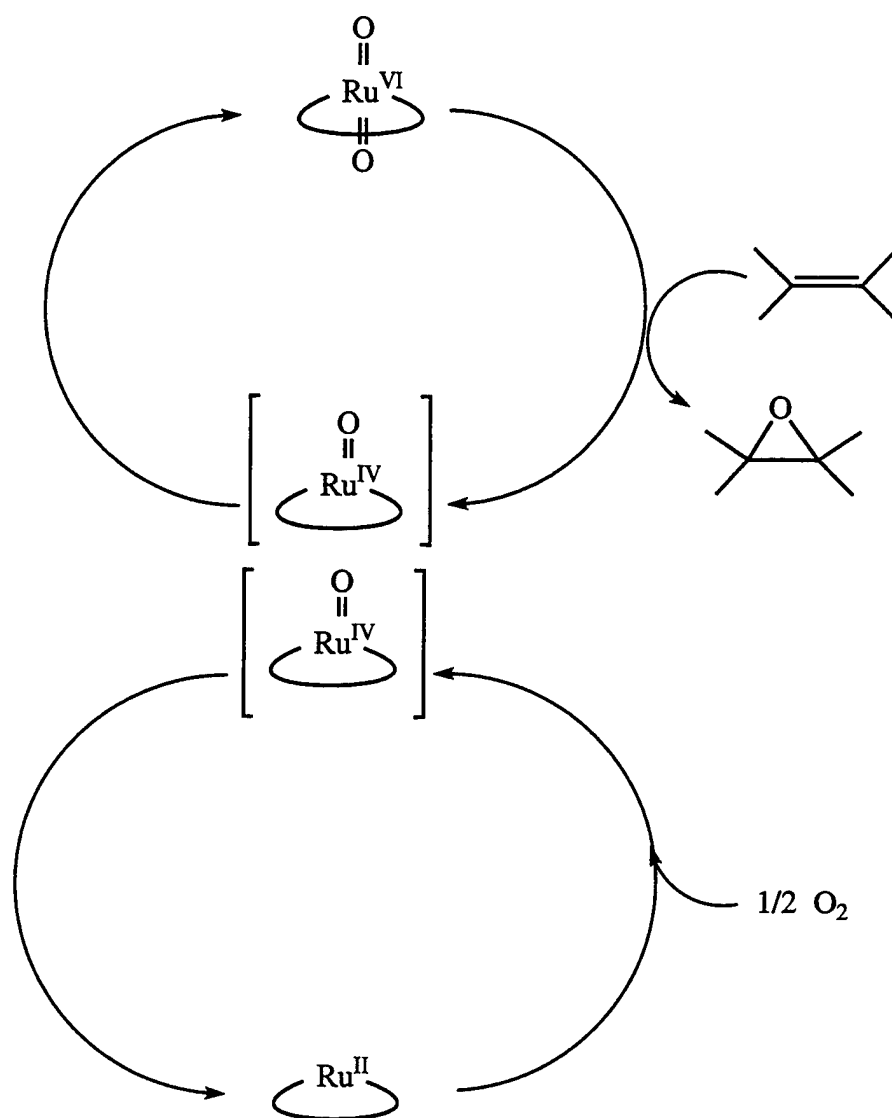
carbon monoxide, oxygen, or ethylene) to 1 atm pressure. The excitation source for the time resolved absorption experiments was the third harmonic of a Quanta-Ray Nd-YAG laser with a 20 nm pulse width; a PTi arc lamp supplied the white probe light source, and a DH 10 SA Inc. monochromator was placed before the R955 Hamamatsu PMT detector. The analog signal was analyzed by a RTD 710A digitizer, and worked up on a 386 PC. The arc lamp power was 68 W, and in the case of weak signals the arc lamp was pulsed at 6 Hz. The signal was amplified with a fast amplifier designed at Brookhaven National Laboratories.³⁸ Further data manipulation was accomplished on either a 486 PC or a Macintosh IISi with computer programs written at Caltech.

References and Notes

- (1) Collman, J. P.; Hutchison, J. E.; Ennics, M. S.; Lopez, M. A.; Guillard, R. *J. Am. Chem. Soc.* **1992**, *114*, 8074-8080.
- (2) Chow, B. C.; Cohen, I. A. *Bioinorg. Chem.* **1971**, *1*, 57-63.
- (3) Antipas, A.; Buchler, J. W.; Gouterman, M.; Smith, P. D. *J. Am. Chem. Soc.* **1978**, *100*, 3015-3024.
- (4) Barringer, L. F.; Rillema, D. P.; Ham, J. H. *J. Inorg. Biochem.* **1984**, *21*, 195-207.
- (5) Brown, G. M.; Hopf, F. R.; Ferguson, J. A.; Meyer, T. J.; Whitten, D. G. *J. Am. Chem. Soc.* **1973**, *95*, 5939-5942.
- (6) Brown, G. M.; Hopf, F. R.; Meyer, T. J.; Whitten, D. G. *J. Am. Chem. Soc.* **1975**, *97*, 5385-5390.
- (7) Eaton, G. R.; Eaton, S. S. *J. Am. Chem. Soc.* **1975**, *97*, 235-236.
- (8) Hopf, F. R.; O'Brien, T. P.; Scheidt, W. R.; Whitten, D. G. *J. Am. Chem. Soc.* **1975**, *97*, 277-281.
- (9) Tsutsui, M.; Ostfeld, D.; Hoffman, L. M. *J. Am. Chem. Soc.* **1971**, *93*, 1820-1823.
- (10) Groves, J. T.; Quinn, R. *Inorg. Chem.* **1984**, *23*, 3844-3846.
- (11) Groves, J. T.; Quinn, R. *J. Am. Chem. Soc.* **1985**, *107*, 5790-5792.
- (12) Groves, J. T.; Ahn, K.-H. *Inorg. Chem.* **1987**, *26*, 3831-3833.
- (13) Ohtake, H.; Higuchi, T.; Hirobe, M. *Tetrahedron Lett.* **1992**, *33*, 2521-2524.
- (14) Higuchi, T.; Ohtake, H.; Hirobe, M. *Tetrahedron Lett.* **1991**, *32*, 7435-7438.
- (15) Ohtake, H.; Higuchi, T.; Hirobe, M. *J. Am. Chem. Soc.* **1992**, *114*, 10660-10662.
- (16) Takagi, S.; Miyamoto, T. K.; Hamaguchi, M.; Sasaki, Y.; Matsurmura, T. *Inorg. Chim. Acta* **1990**, *173*, 215-221.
- (17) Ho, C.; Leung, W.-H.; Chi-Ming-Che *J. Chem. Soc., Dalton Trans.* **1991**, 2933-2939.
- (18) Leung, W.-H.; Chi-Ming-Che *J. Am. Chem. Soc.* **1989**, *111*, 8812-8818.
- (19) Rajapakse, N.; James, B. R.; Dolphin, D. *Catal. Lett.* **1989**, *2*, 219-226.
- (20) Tavares, M.; Ramasseul, R.; Marchon, J.-C.; Maumy, M. *Catal. Lett.* **1991**, *8*, 245-252.
- (21) Tavares, M.; Ramasseul, R.; Marchon, J.-C.; Bachet, B.; Brassy, C.; Marnon, J.-P. *J. Chem. Soc., Perkin Trans. 2* **1992**, 1321-1329.
- (22) Tavares, M.; Ramasseul, R.; Marchon, J.-C. *Catal. Lett.* **1990**, *4*, 163-168.
- (23) Ellis, P. E., Jr.; Lyons, J. E. *Coord. Chem. Rev.* **1990**, *105*, 181-193.

- (24) Lyons, J. E.; Ellis, P. E., Jr.; Myers, H. K., Jr.; Wagner, R. W. *J. Catal.* **1993**, *141*, 311-315.
- (25) Grinstaff, M. W.; Hill, M. G.; Birnbaum, E. R.; Schaefer, W. P.; Labinger, J. A.; Gray, H. B. submitted to *Inorg. Chem.*
- (26) Sugimoto, H.; Higashi, T.; Mori, M.; Nagano, M.; Yoshida, Z.-I.; Ogoshi, H. *Bull. Chem. Soc. Jpn.* **1982**, *55*, 822-828.
- (27) Attempts to repeat this experiment on a larger scale were not successful. Oxidation of RuTFPPCl₈(CO) was not clean, and although product formation was observed, it was impossible to differentiate between oxo transfer from the dioxo ruthenium porphyrin and direct reaction with excess mCPBA.
- (28) Evans, E. W.; Howlader, M. B. H.; Atlay, M. T. *Inorg. Chim. Acta* **1995**, *230*, 193-197.
- (29) Mimoun, H.; Saussine, L.; Daire, E.; Postel, M.; Fischer, J.; Weiss, R. *J. Am. Chem. Soc.* **1983**, *105*, 3101-3110.
- (30) Roecker, L.; Meyer, T. J. *J. Am. Chem. Soc.* **1987**, *109*, 746-754.
- (31) Kalyanasundaram, K. *Photochemistry of Polypyridine and Porphyrin Complexes*; Academic Press, Inc.: San Diego, 1992.
- (32) March, J. *Advanced Organic Chemistry*; 4th ed.; John Wiley & Sons: New York, 1992, pp 708.
- (33) The faster rates are taken from the 5 μ s transient spectra, and the slower rates from the 50 μ s data. The two sets of rates do not show good agreement, suggesting that additional processes are contributing to the kinetics.
- (34) Rillema, D. P.; Nagle, J. K.; Barringer, L. F., Jr.; Meyer, T. J. *J. Am. Chem. Soc.* **1981**, *103*, 57-82.
- (35) Levine, L. M. A.; Holten, D. *J. Phys. Chem.* **1988**, *92*, 714.
- (36) Rajapakse, N.; James, B. R.; Dolphin, D. *Can. J. Chem.* **1990**, *68*, 2274-2277.
- (37) Pirsig, R. *Zen and the Art of Motorcycle Maintenance*; Morrow: New York, 1974, pp 412.
- (38) McCleskey, T. M. Thesis, California Institute of Technology, 1994.

Figure 5.1 -- The Groves mechanism for catalytic oxidation of olefins with dioxygen by $\text{Ru}^{\text{VI}}\text{TMP}(\text{O})_2$. The ruthenium(IV) monooxo porphyrin disproportionates to reform the active ruthenium(VI) catalyst (see reference 11).



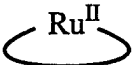
 = Ruthenium tetramesitylporphyrin

Figure 5.2 -- Turnovers of cyclohexene by $\text{RuTFPPCl}_8(\text{CO})$ with iodosobenzene in 24 hours, showing the observed product distribution. Only 25% of the available oxidant is used.

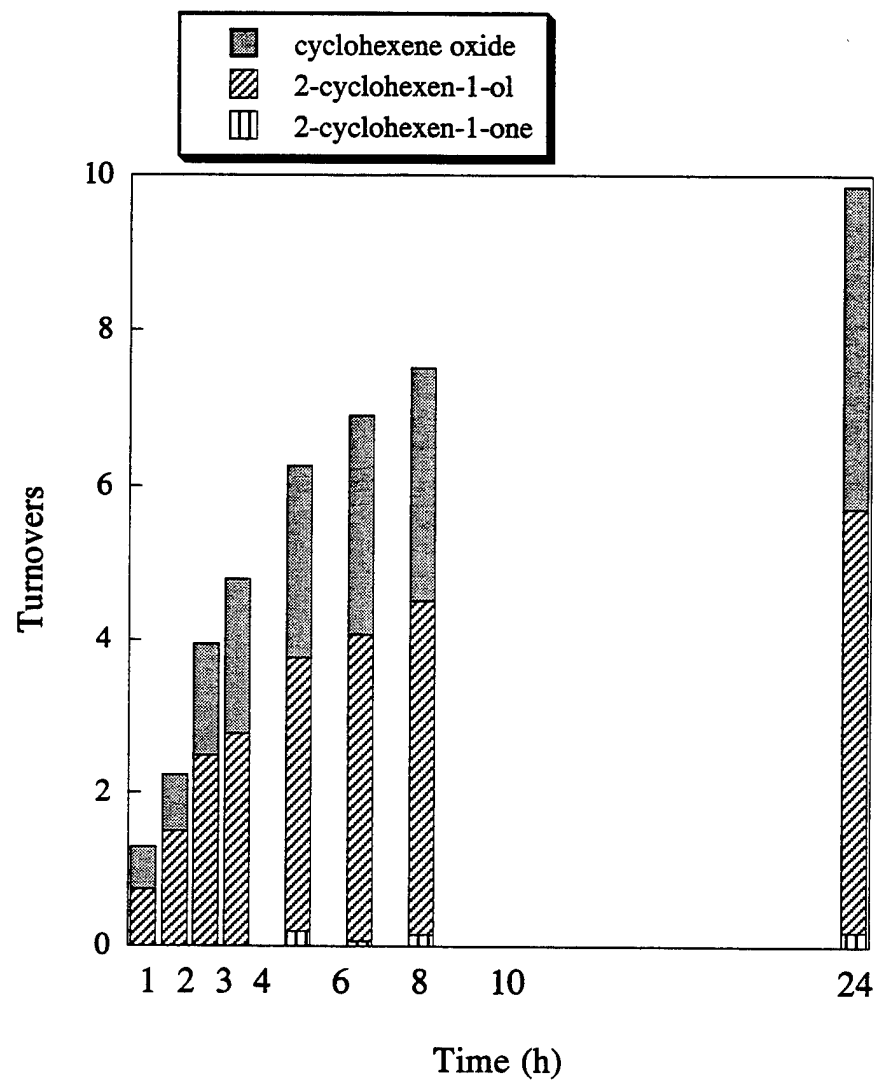


Figure 5.3 -- Turnovers of cyclohexene by $\text{RuTFPPCl}_8(\text{CO})$ with dioxygen in 24 hours, showing the observed product distribution. More allylic oxidation products are observed than with PhIO as the oxidant.

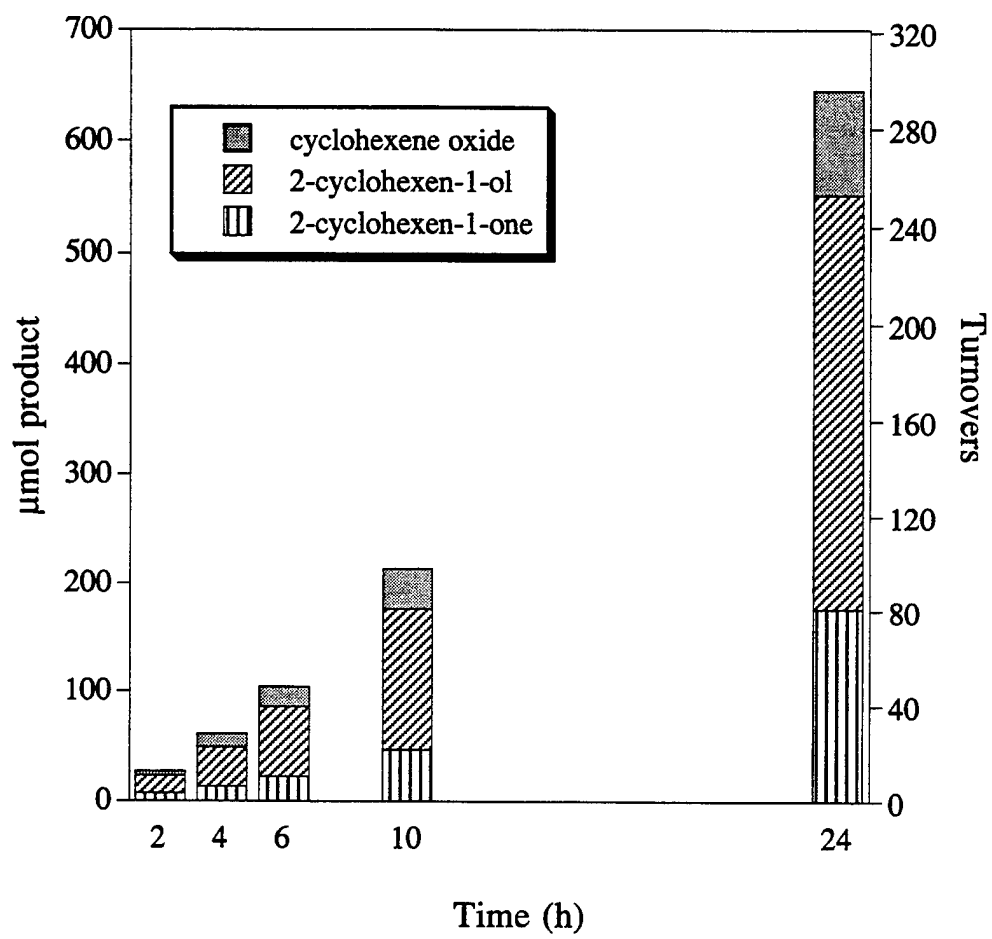


Figure 5.4 -- Hydrogen peroxide decomposition by $\text{RuTFPPCl}_8(\text{CO})$ and $\text{Fe}(\text{TFPPBr}_8)\text{Cl}$ in acetone, as determined by oxygen evolution. The iron porphyrin decomposes 68 turnovers in 4 hours, while the ruthenium porphyrin shows much less activity in the same time period (4.5 TO).

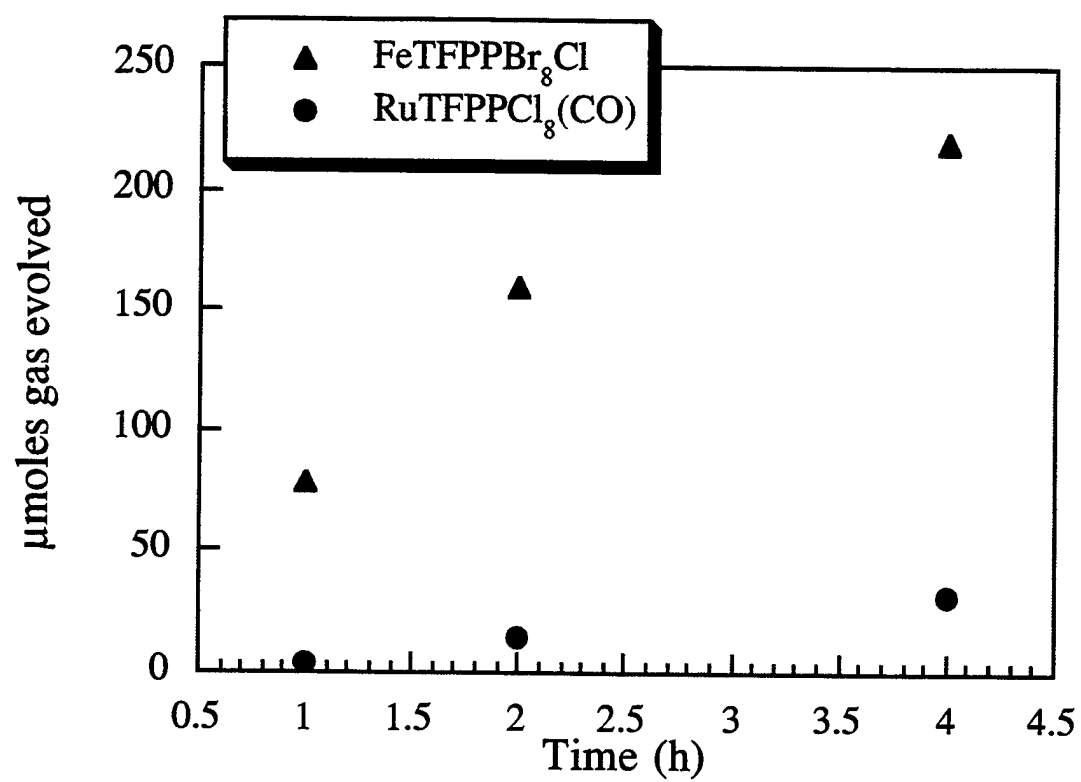


Figure 5.5 -- UV-Vis spectrum of $\text{RuTFPPCl}_8(\text{CO})$ upon titration with 2 equivalents of mCPBA to form $\text{Ru}^{\text{VI}}\text{TFPPCl}_8(\text{O})_2$. The red shift of the Soret band to 420 nm is consistent with dioxo formation.

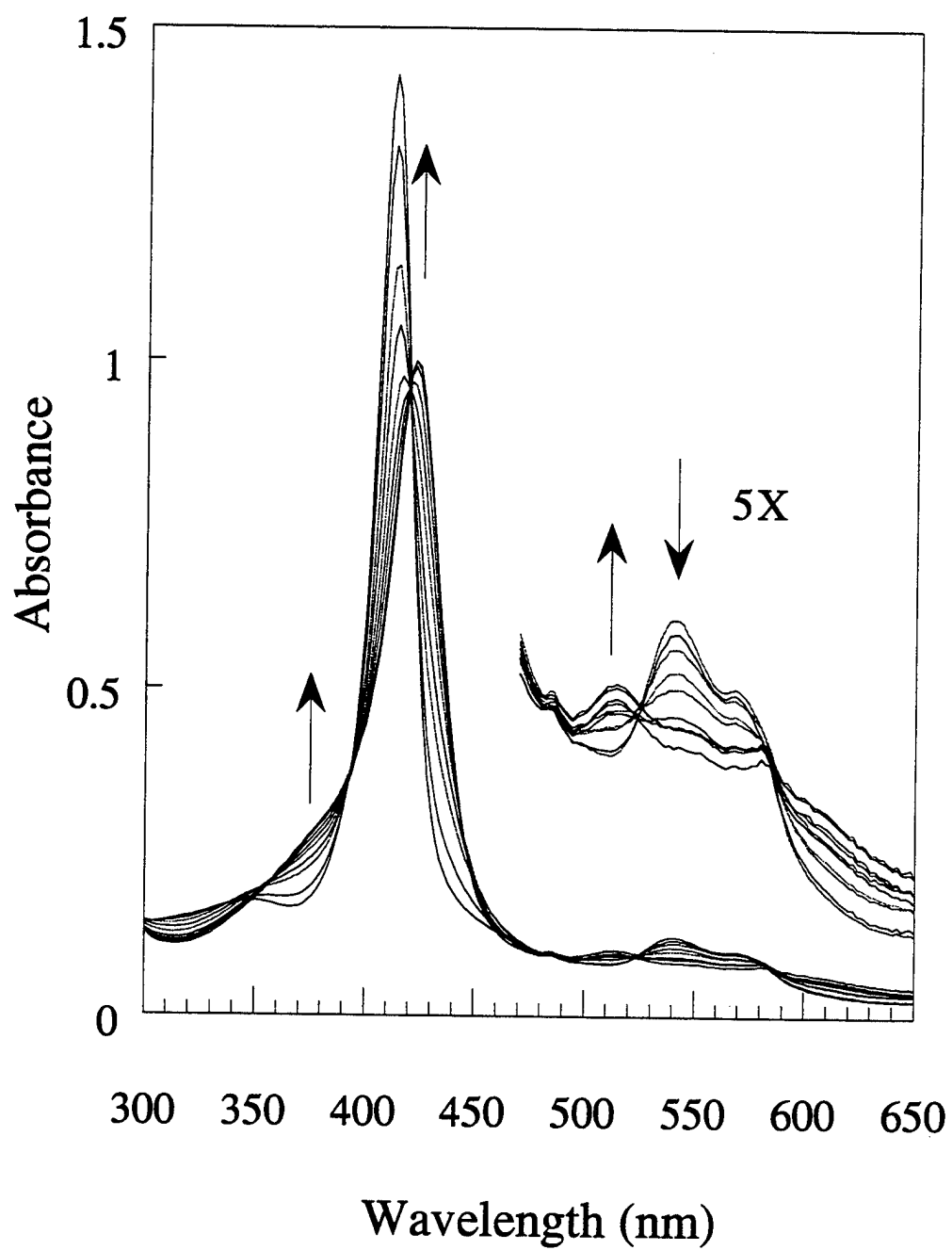


Figure 5.6 -- Addition of cyclohexene to $\text{Ru}^{\text{VI}}\text{TFPPCl}_8(\text{O})_2$. The initial decrease in Soret intensity corresponds to a single oxidation of substrate and formation of $\text{Ru}^{\text{IV}}\text{TFPPCl}_8(\text{O})$. Eventually, the second oxo also transfers, and addition of carbon monoxide gas regenerates the original spectrum of $\text{Ru}^{\text{II}}\text{TFPPCl}_8(\text{CO})$ with 85% of the original intensity.

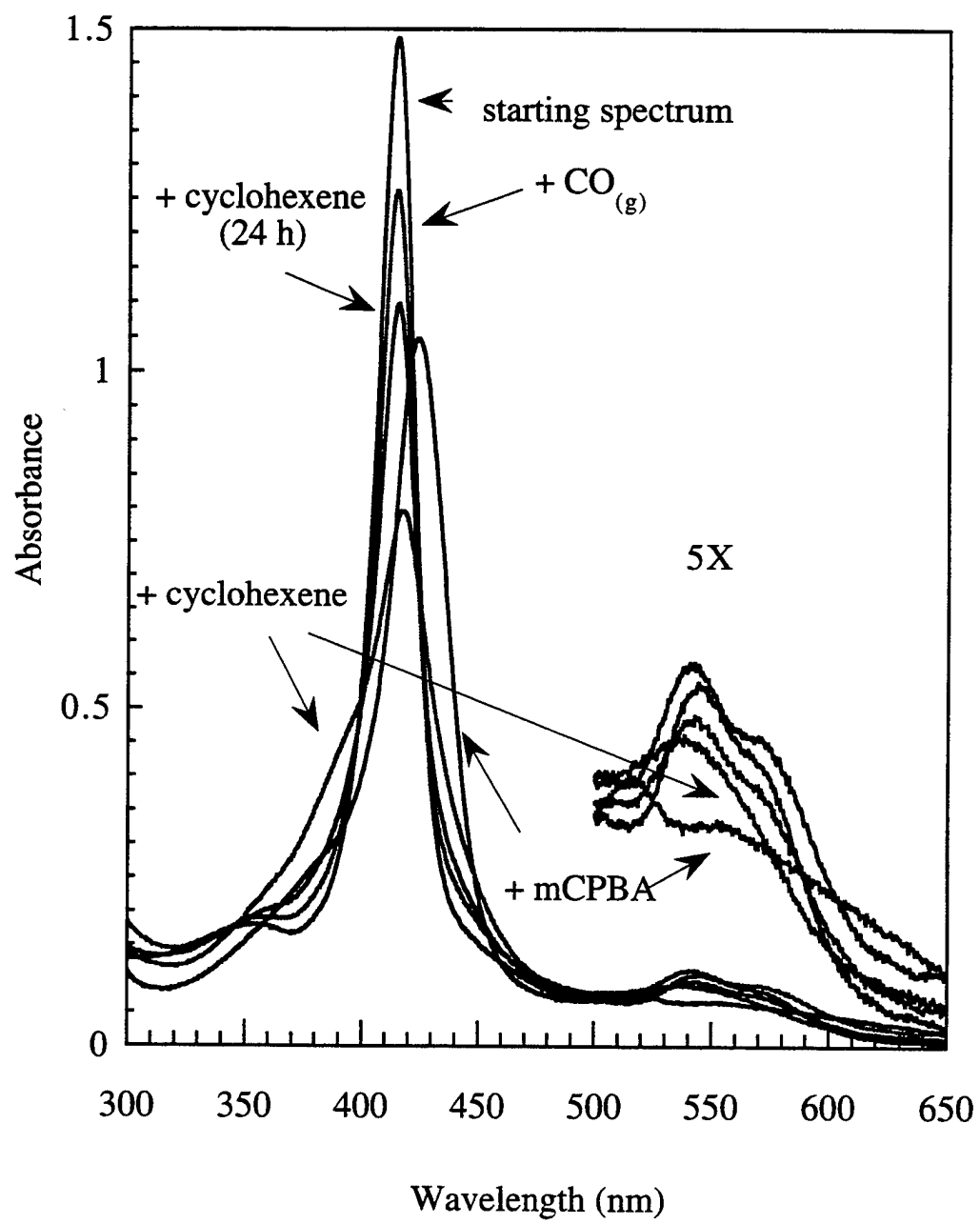


Figure 5.7 -- Addition of triphenylphosphine to $\text{Ru}^{\text{VI}}\text{TFPPCl}_8(\text{O})_2$. The first 2 eq (a) are believed to correspond to transfer of both oxo ligands. Further addition of PPh_3 (2 eq, spectrum b) results in new spectral features consistent with coordination of triphenylphosphine to the ruthenium porphyrin.

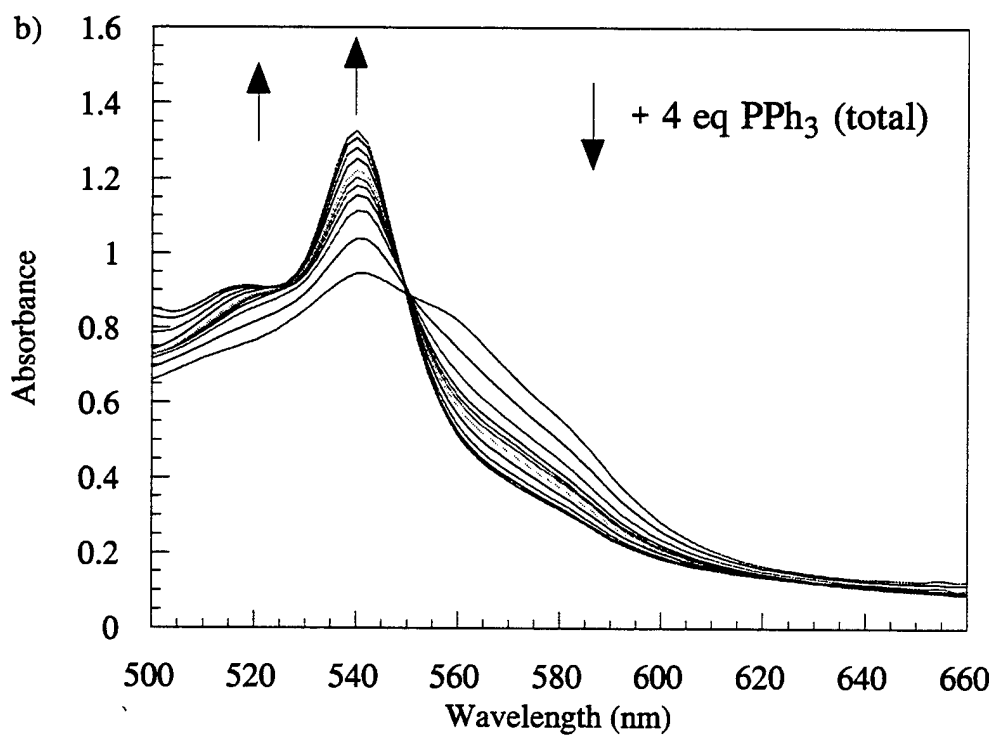
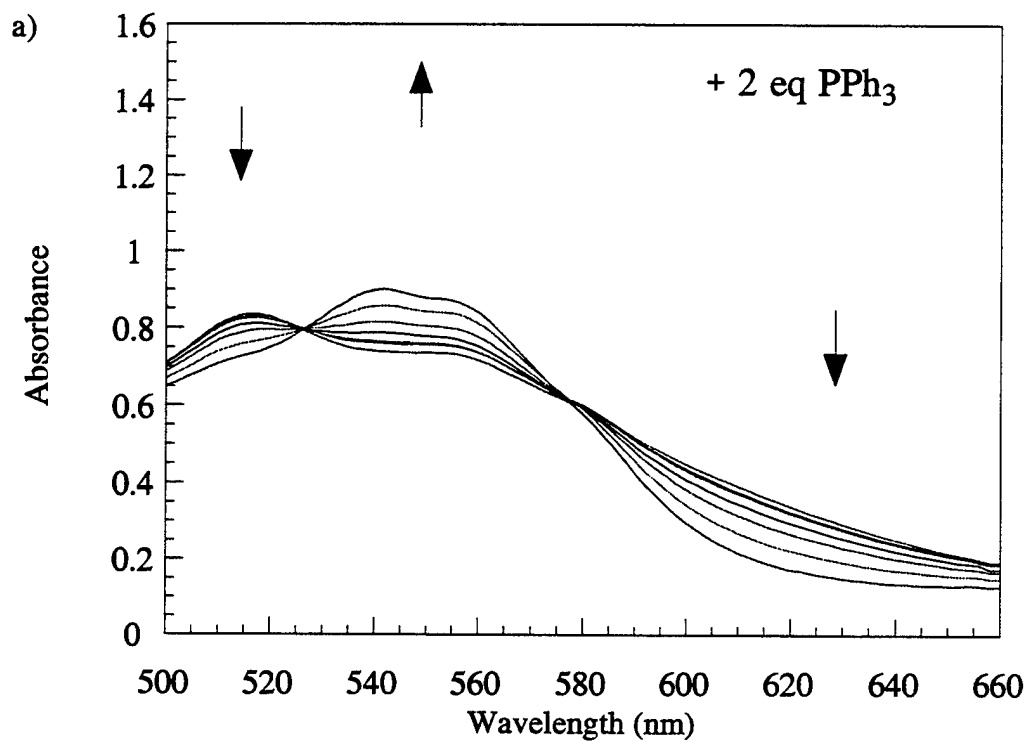


Figure 5.8 -- A potential mechanism for oxidation of olefins by $\text{Ru}^{\text{II}}\text{TFPPCl}_8(\text{CO})$.

Initial loss of CO allows oxygen to bind to the electron poor metal center,
initiating the chemistry.

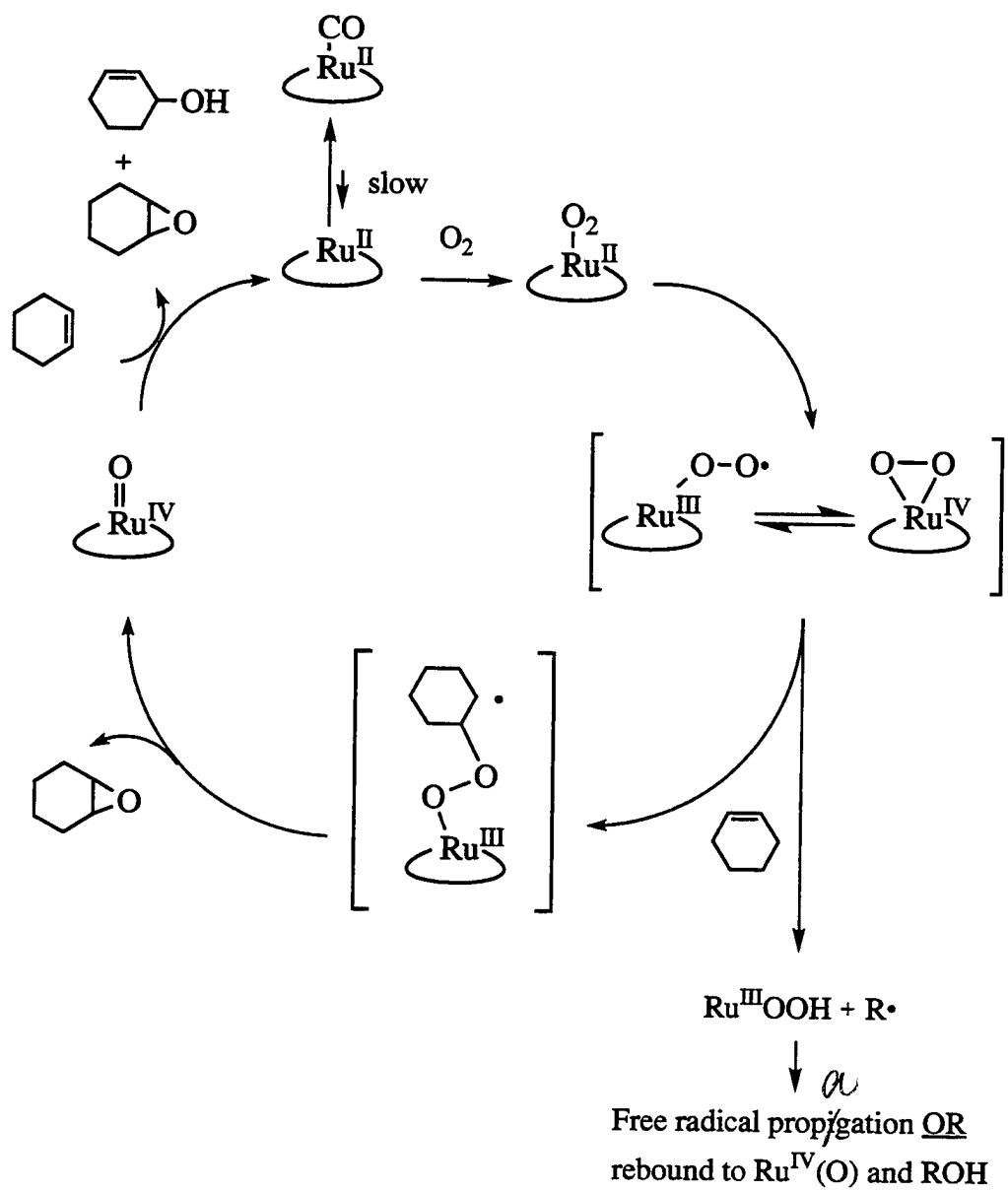


Figure 5.9 -- Relative rates of reaction for $\text{RuTFPPCl}_8(\text{CO})$ with dioxygen (a "normal" reaction) or in the presence of small amounts of $(\text{Et})_3\text{NO}$ or mCPBA before addition of substrate.

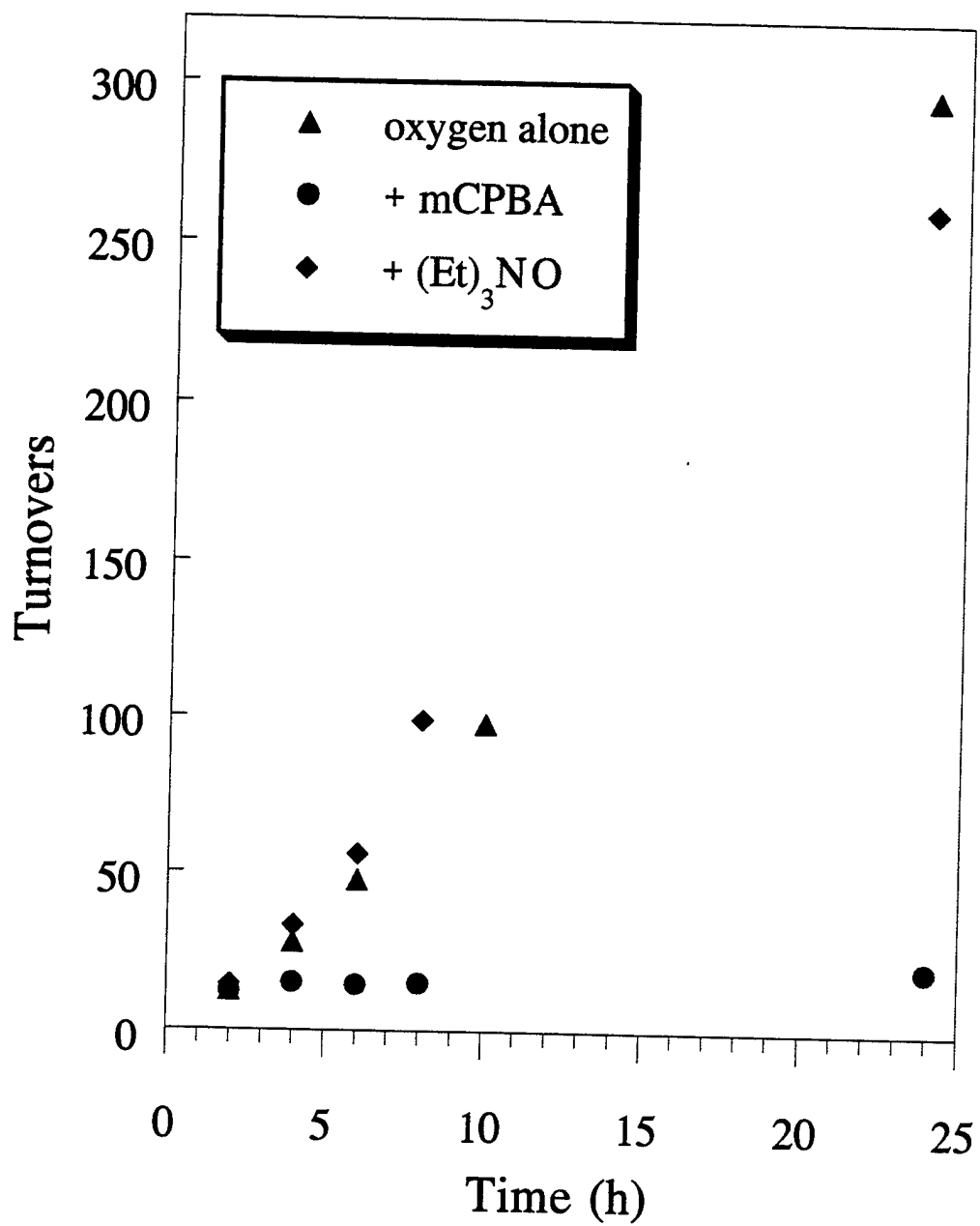


Figure 5.10 -- The relative rates of cyclohexene oxidation after the addition of 10 or 300 equivalents of TBHP. Although a small addition of peroxide only induces a minor enhancement of the chemistry, the large addition appears to initiate a free radical reaction that may not be related to the ruthenium catalyst.

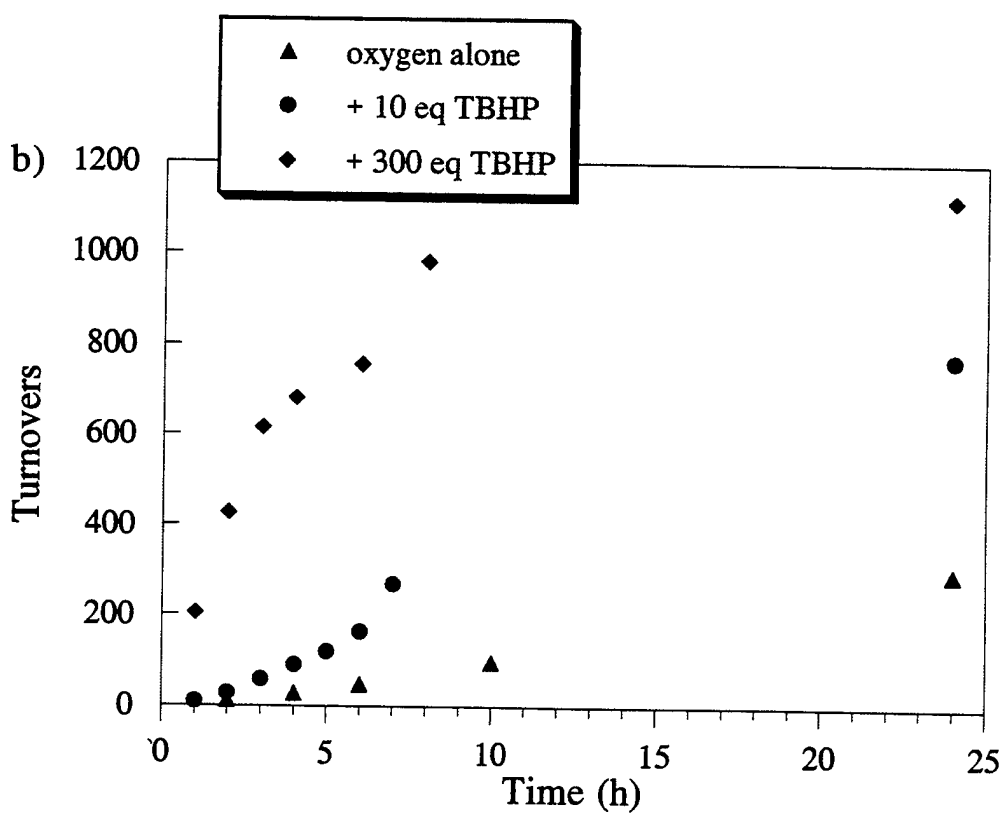
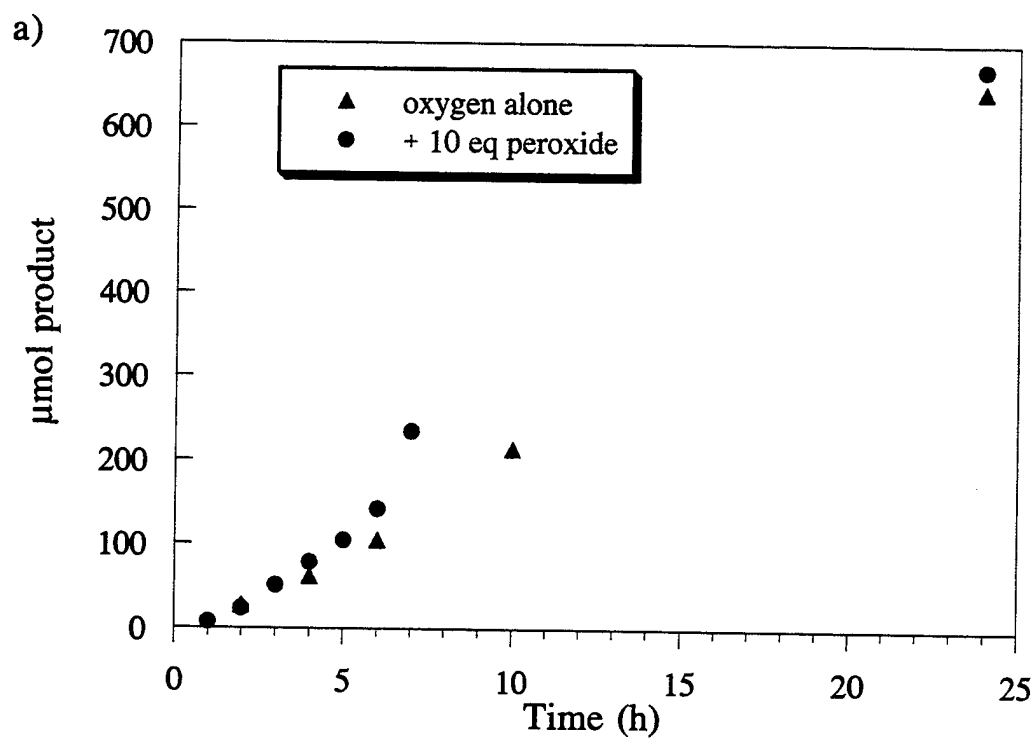


Figure 5.11 -- Relative turnovers in experiments stirred at two different rates indicate that phase transfer was not rate limiting. Experiments that were stirred more slowly showed slightly more activity than average.

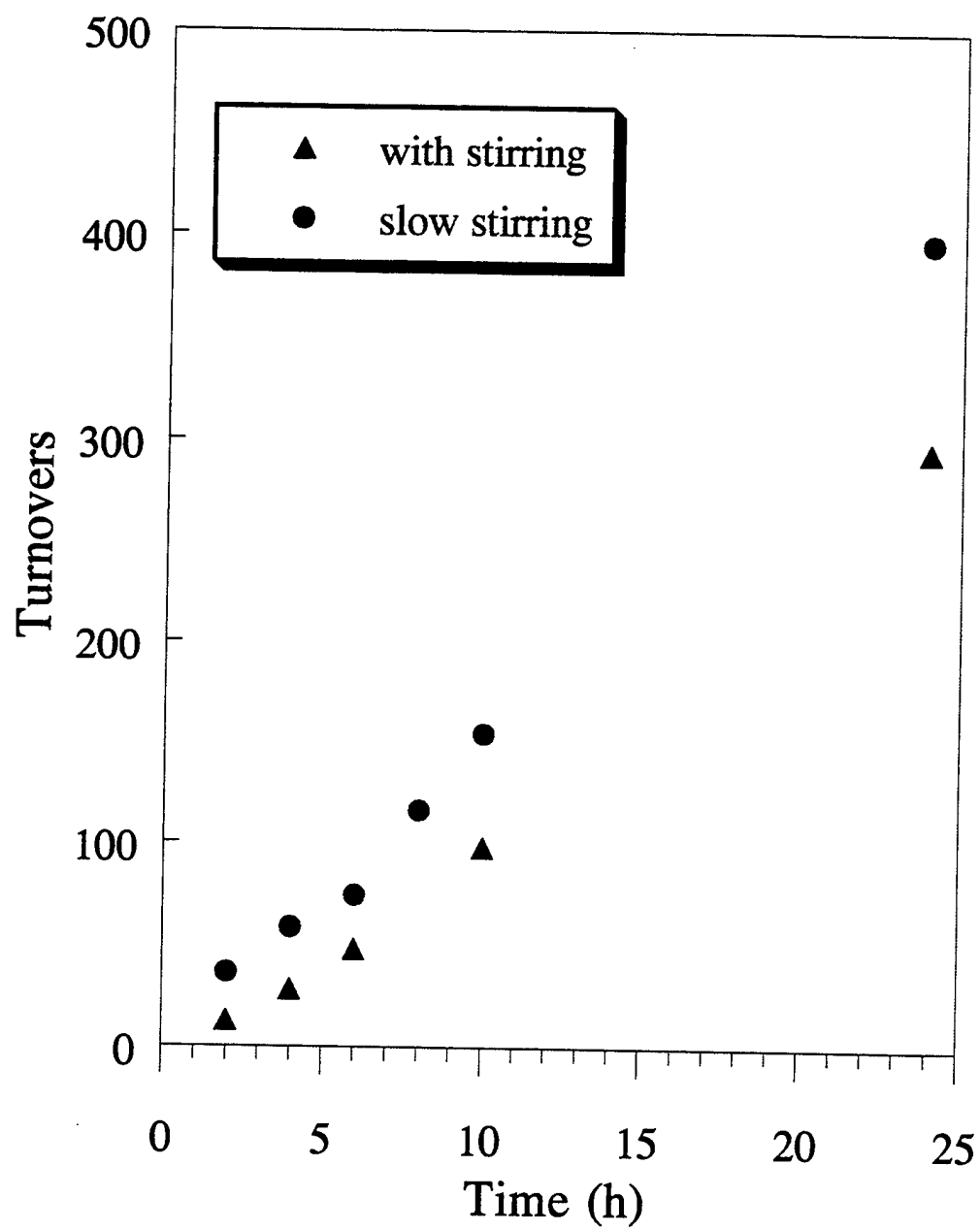


Figure 5.12 -- Relative rates of cyclohexene oxidation under dioxygen or under a mixture of oxygen and carbon monoxide, indicating that CO does not inhibit catalysis by $\text{Ru}^{\text{II}}\text{TFPPCl}_8(\text{CO})$.

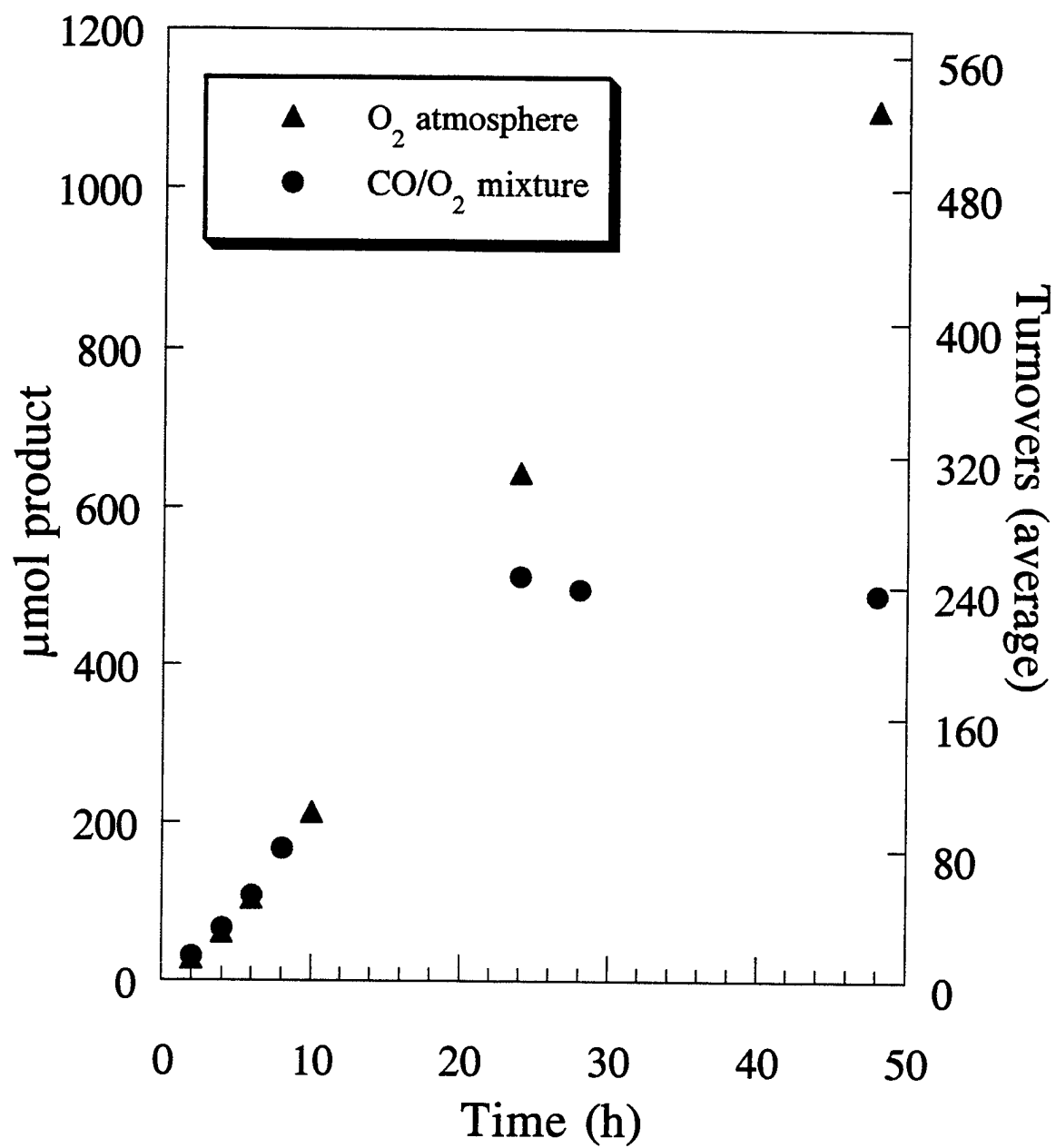


Figure 5.13 -- UV-Vis spectrum of $\text{Ru}^{\text{II}}\text{TFPPCl}_8(\text{CO})$ in carbon tetrachloride after two days in a Parr reactor under 1100 psi of carbon monoxide. The Soret band is slightly red shifted and the Q bands are slightly blue shifted from the spectrum before the Parr reactor. The absorption at 280 nm is believed to be from an organic product (see text).

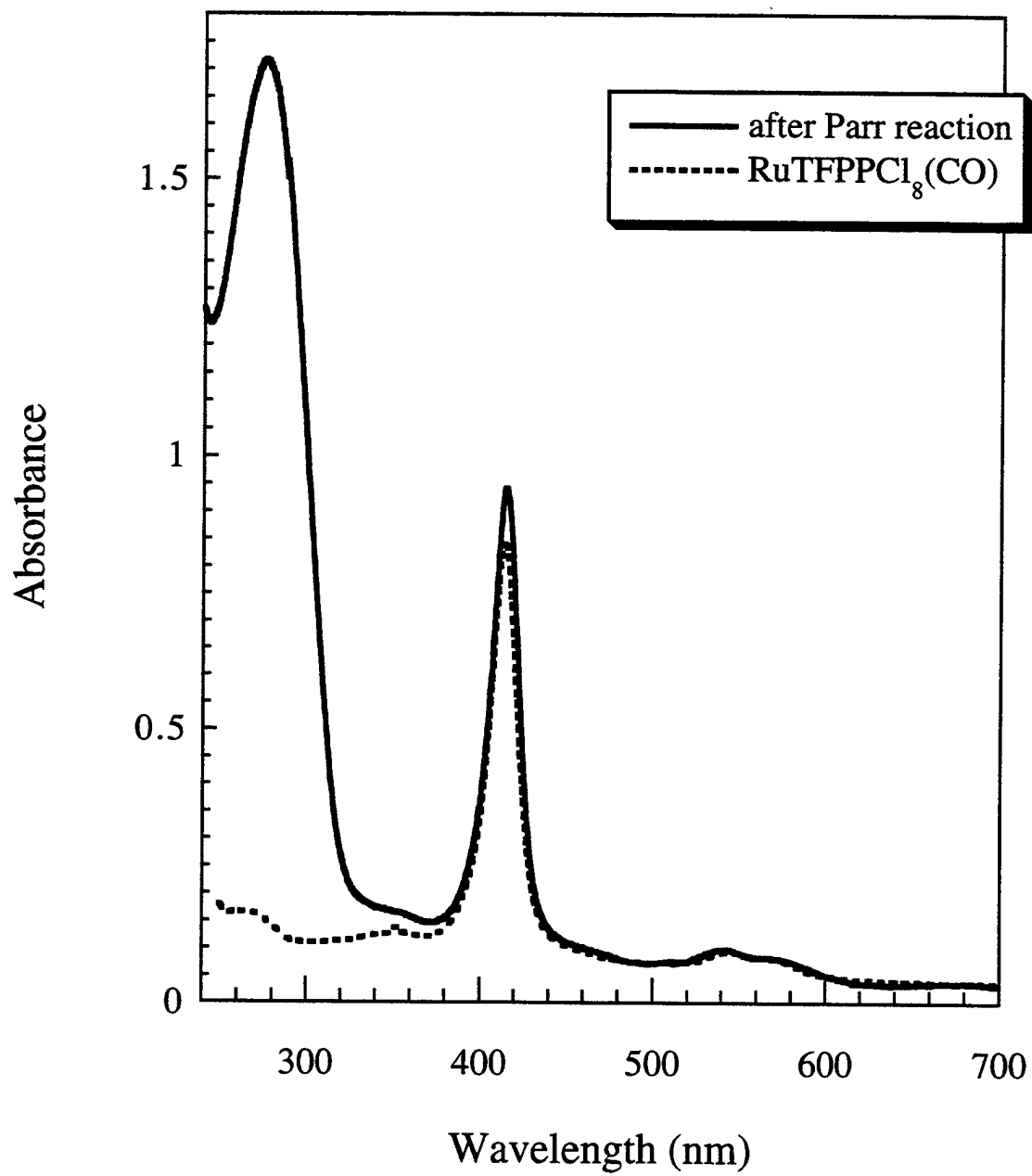


Figure 5.14 -- Relative rates of cyclohexene and cyclohexene-*d*₁₀ oxidation by
Ru^{II}TFPPCl₈(CO) with dioxygen.

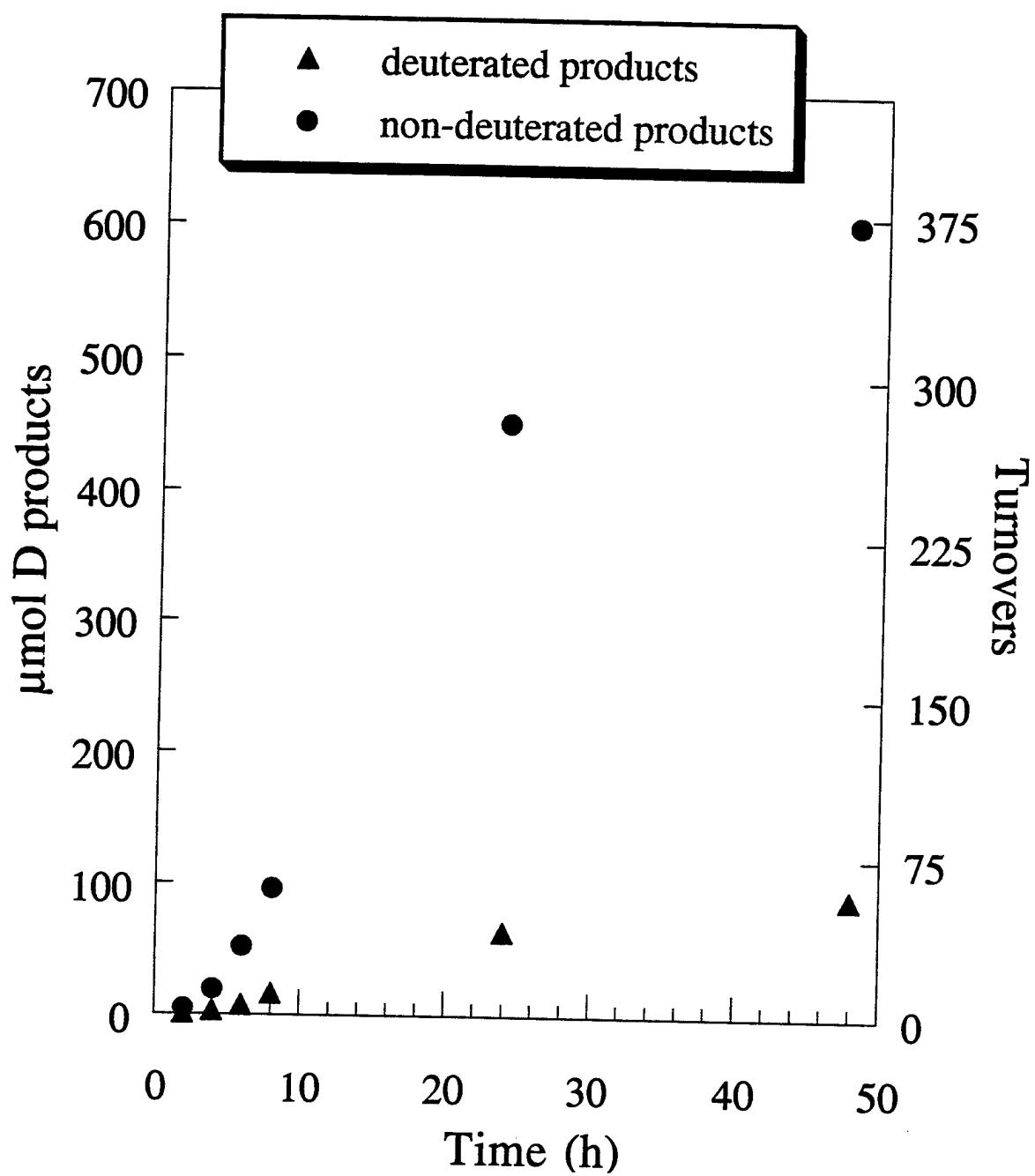


Figure 5.15 -- Cyclohexene oxidation experiments carried out in the dark showed great variability in the initiation period. Eventually both reactions showed significant reactivity.

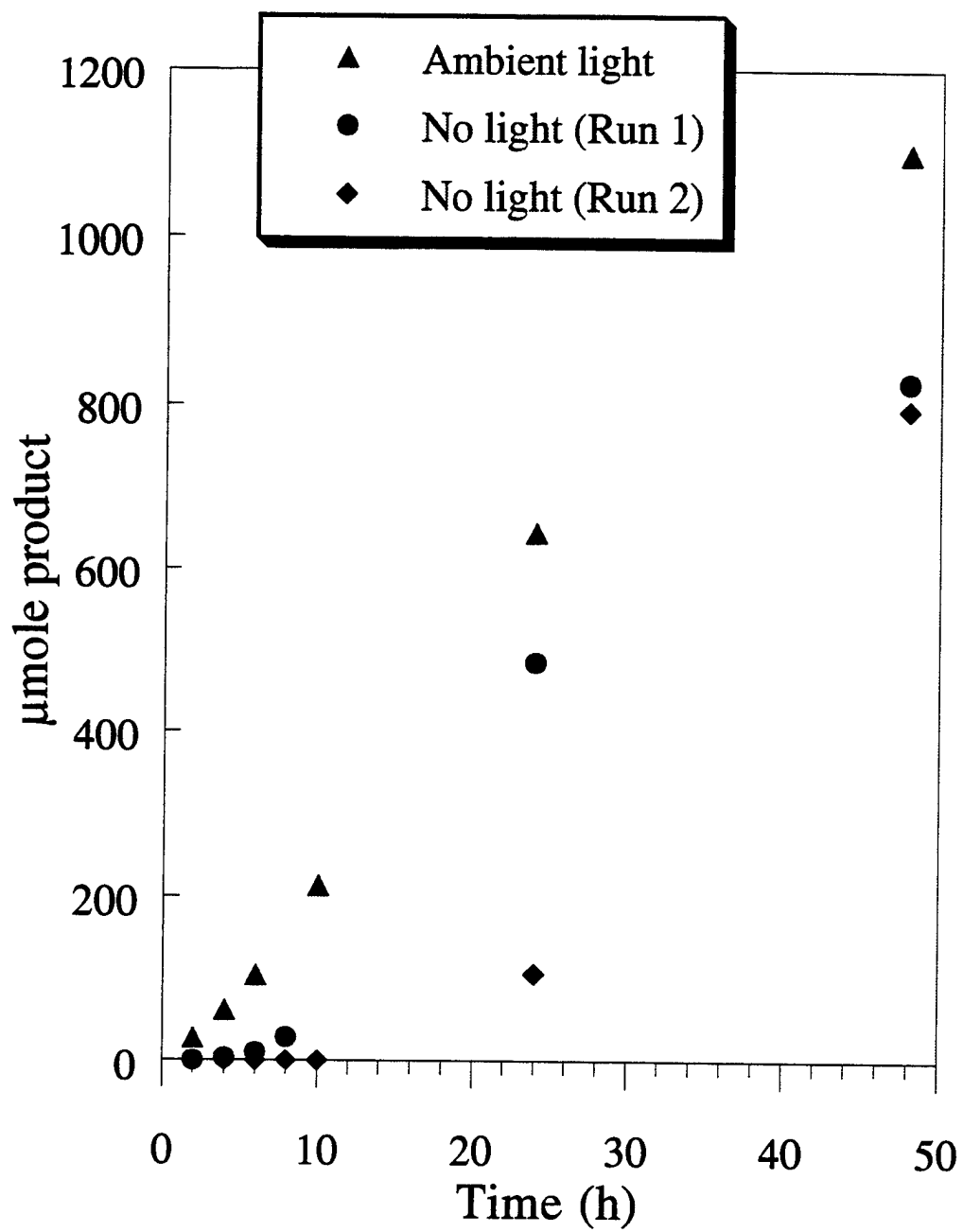


Figure 5.16 -- Photolysis of a cyclohexene oxidation reaction by $\text{Ru}^{\text{II}}\text{TFPPCl}_8(\text{CO})$ with dioxygen with a tungsten lamp dramatically increased the reaction rate.

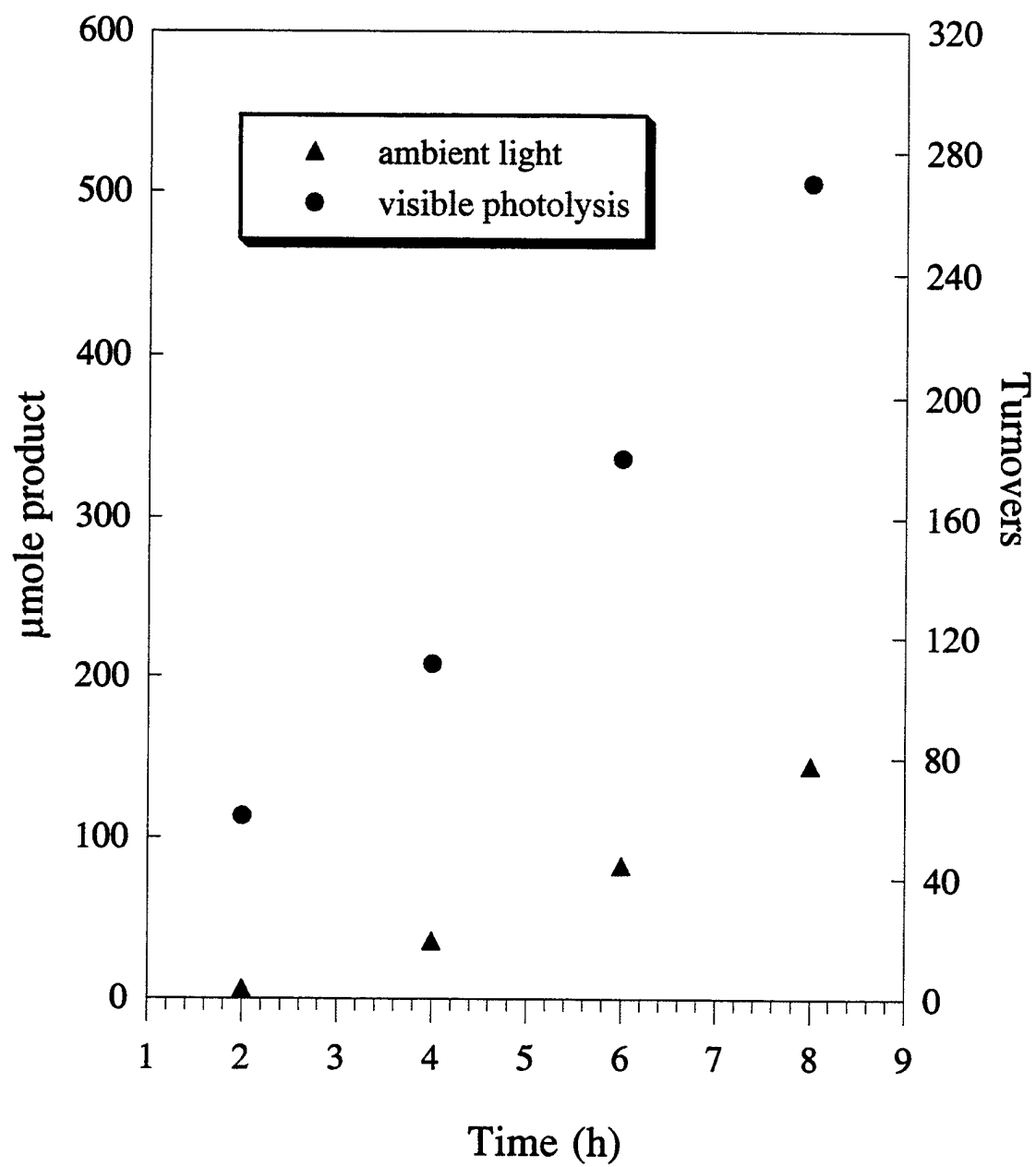


Figure 5.17 -- Transient absorption spectrum in the Q band region immediately following irradiation at 480 nm. The appearance of a low energy band is consistent with formation of a porphyrin triplet excited state.

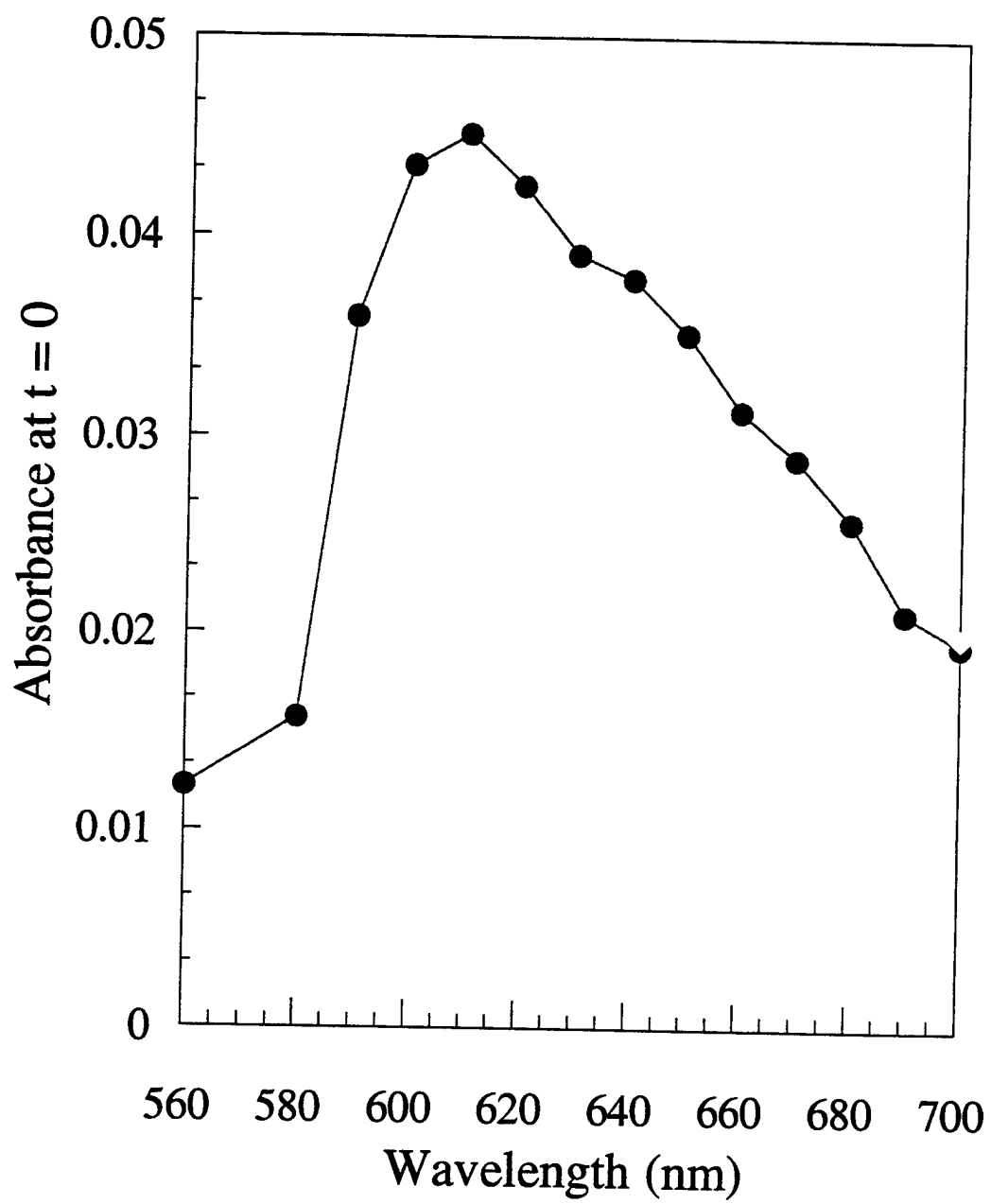


Figure 5.18 -- A 5 μ s transient spectrum at 415 nm for excitation of $\text{Ru}^{\text{II}}\text{TFPPCl}_8(\text{CO})$ with 355 nm light. The sample is in methylene chloride and under an atmosphere of CO. Other transient spectra are in appendix 5.

DATA FILE: RUCO.006

1995-2-23 9:27:49

TIME RANGE: 5.0 μ s

INPUT V RANGE: 0.320V

INPUT OFFSET: 0 %

EXPERIMENT: TRANSIENT ABSORPTION

FAST (200 MHz) QUASI-DIFFERENTIAL AMP

MODE: SINGLE-ENDED

SHOTS PRE CYCLE: 10

CYCLES: 5

PMT VOLTAGE: 702 V

EXCITATION WAVELENGTH: 355 nm OBSERVATION WAVELENGTH: 415 nm

SAMPLE: RuCl₃(CO)SOLVENT: CH₂Cl₂

TEMPERATURE: rt

COMMENT: under CO

COMMENT:

---> FIXED PARAMETER; ! ---> FIXED SIGN

$$y(t) = C0 + C1 \cdot e^{-k1 \cdot t} + C2 \cdot e^{-k2 \cdot t}$$

$$C0 = -1.941E-2$$

$$C1 = -1.023E-1$$

$$C2 = -4.168E-2$$

$$!k1 = 3.951E6 \text{ s}^{-1}$$

$$!k2 = 8.530E5 \text{ s}^{-1}$$

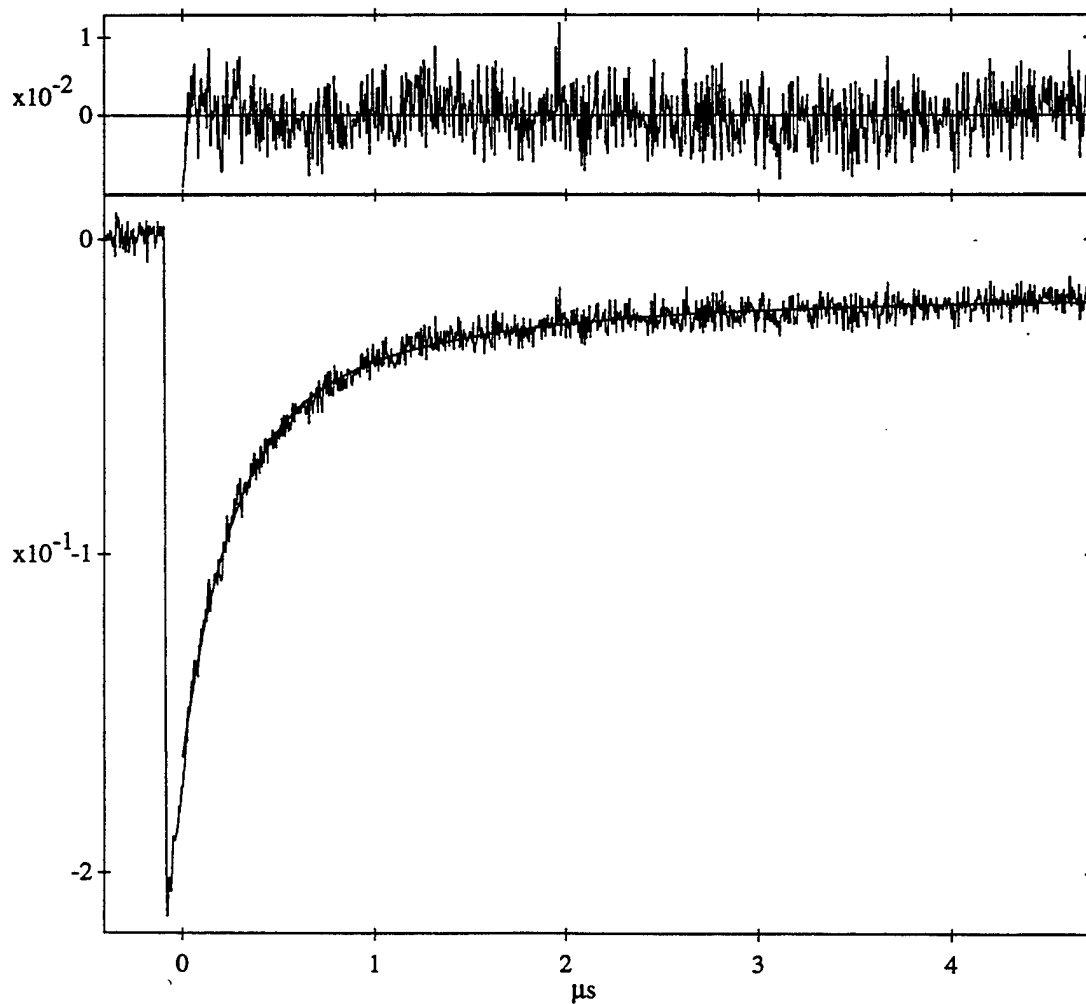


Figure 5.19 -- A 50 μ s transient spectrum at 415 nm for excitation of $\text{Ru}^{\text{II}}\text{TFPPCl}_8(\text{CO})$ with 355 nm light. The sample is in methylene chloride and under an atmosphere of CO. Other transient spectra are in appendix 5.

DATA FILE: RUCO.002

1995-2-23 8:56:56

TIME RANGE: 50 μ s

INPUT V RANGE: 0.320V

INPUT OFFSET: 0 %

EXPERIMENT: TRANSIENT ABSORPTION

FAST (200 MHz) QUASI-DIFFERENTIAL AMP

MODE: SINGLE-ENDED

SHOTS PRE CYCLE: 10

CYCLES: 5

PMT VOLTAGE: 700 V

EXCITATION WAVELENGTH: 355 nm OBSERVATION WAVELENGTH: 415 nmSAMPLE: RuCl₃(CO)SOLVENT: CH₂Cl₂

TEMPERATURE: rt

COMMENT: under CO

COMMENT:

--> FIXED PARAMETER; ! --> FIXED SIGN

$$y(t) = C0 + C1 * e^{-k1 * t} + C2 * e^{-k2 * t}$$

$$C0 = -7.483E-3$$

$$C1 = -7.385E-2$$

$$C2 = -2.381E-2$$

$$!k1 = 2.196E6 \text{ s}^{-1}$$

$$!k2 = 1.318E5 \text{ s}^{-1}$$

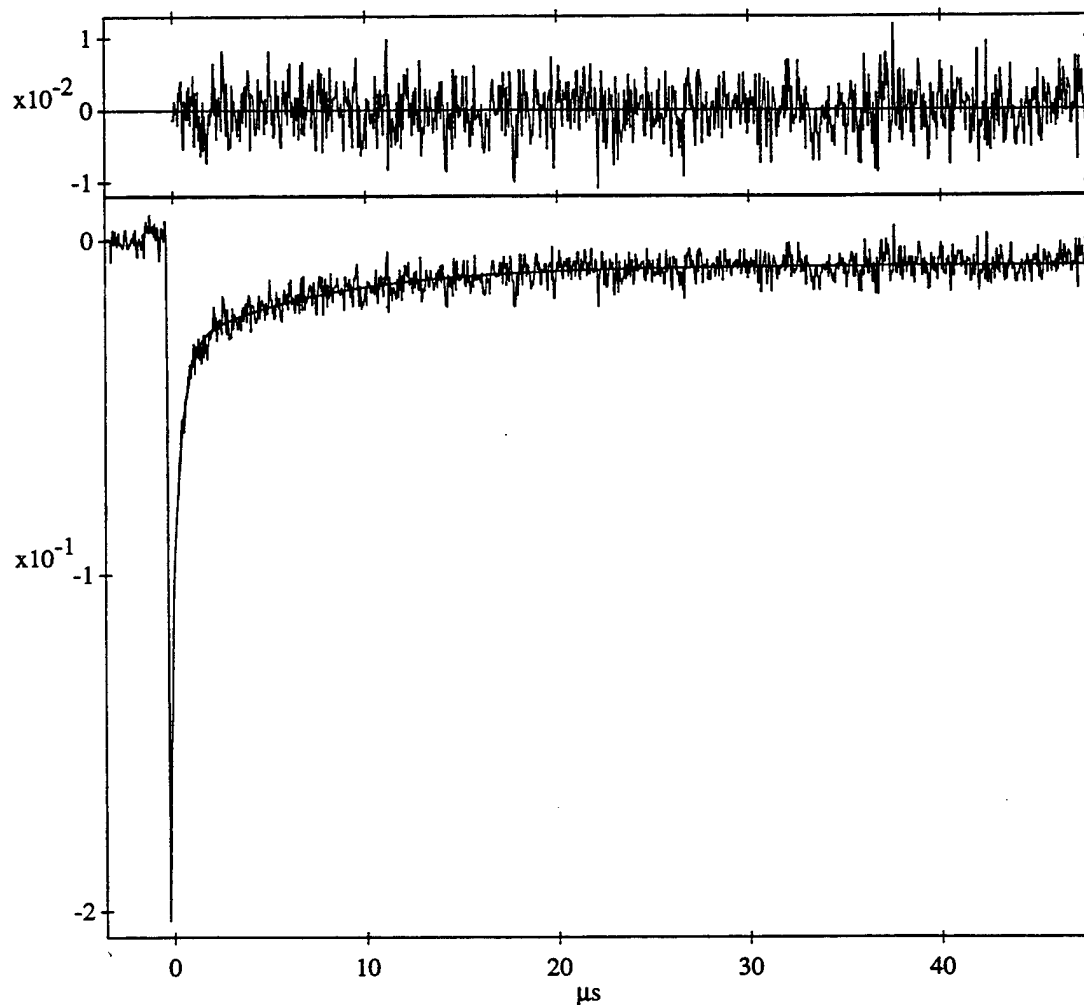


Figure 5.20 -- The 50 μ s transient absorption spectrum after excitation with 355 nm light of equally concentrated solutions of RuTFPPCl₈(CO) in methylene chloride under different atmospheres. The spectra are very similar; only the ethylene spectrum has a larger decrease in Soret intensity relative to the other samples.

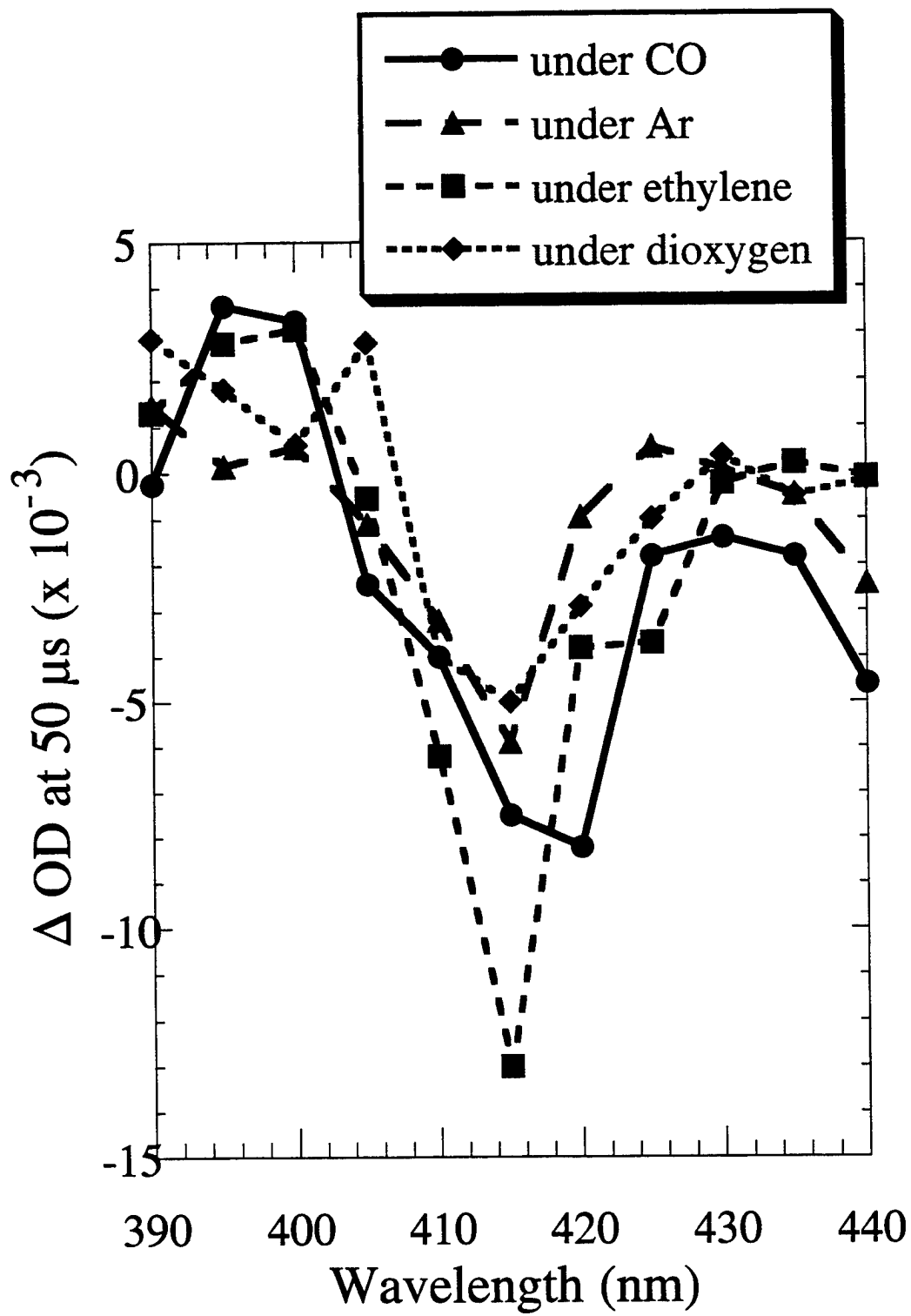


Figure 5.21 -- UV-Vis spectra of the samples shown in Figure 5.20 after the completion of the laser photolysis experiments. The samples under argon and dioxygen show significant broadening and a decrease in the Soret intensity, but CO or ethylene atmospheres protected the porphyrin from decomposition.

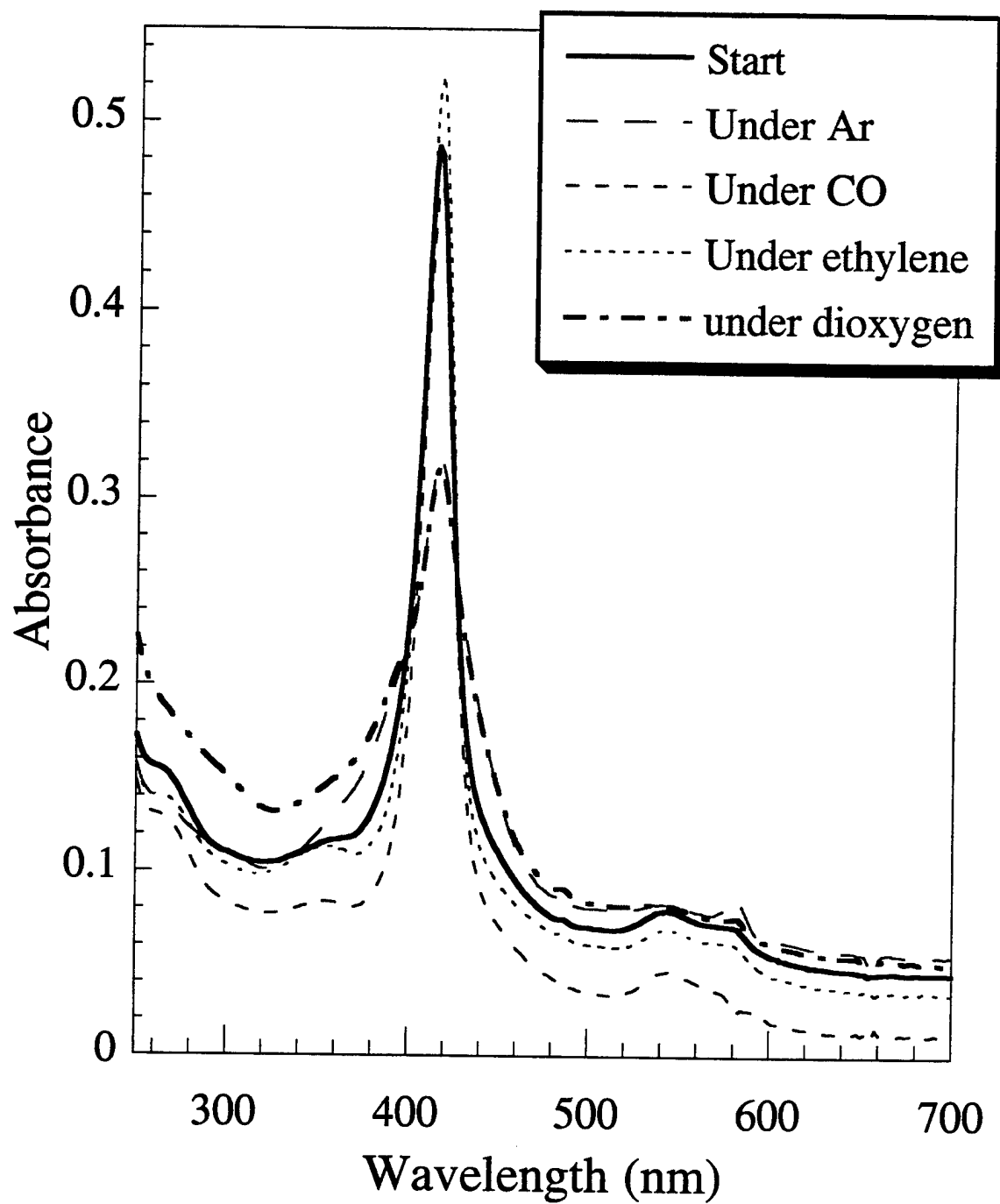


Figure 5.22 -- A mechanism for catalytic olefin oxidation by $\text{RuTFPPCl}_8(\text{CO})$ with dioxygen involving an excited state of the porphyrin. Olefin binding is enhanced in the excited state due to the photochemical oxidation of the metal. The excited state could also be quenched by oxygen, forming singlet oxygen that could also lead to product formation.

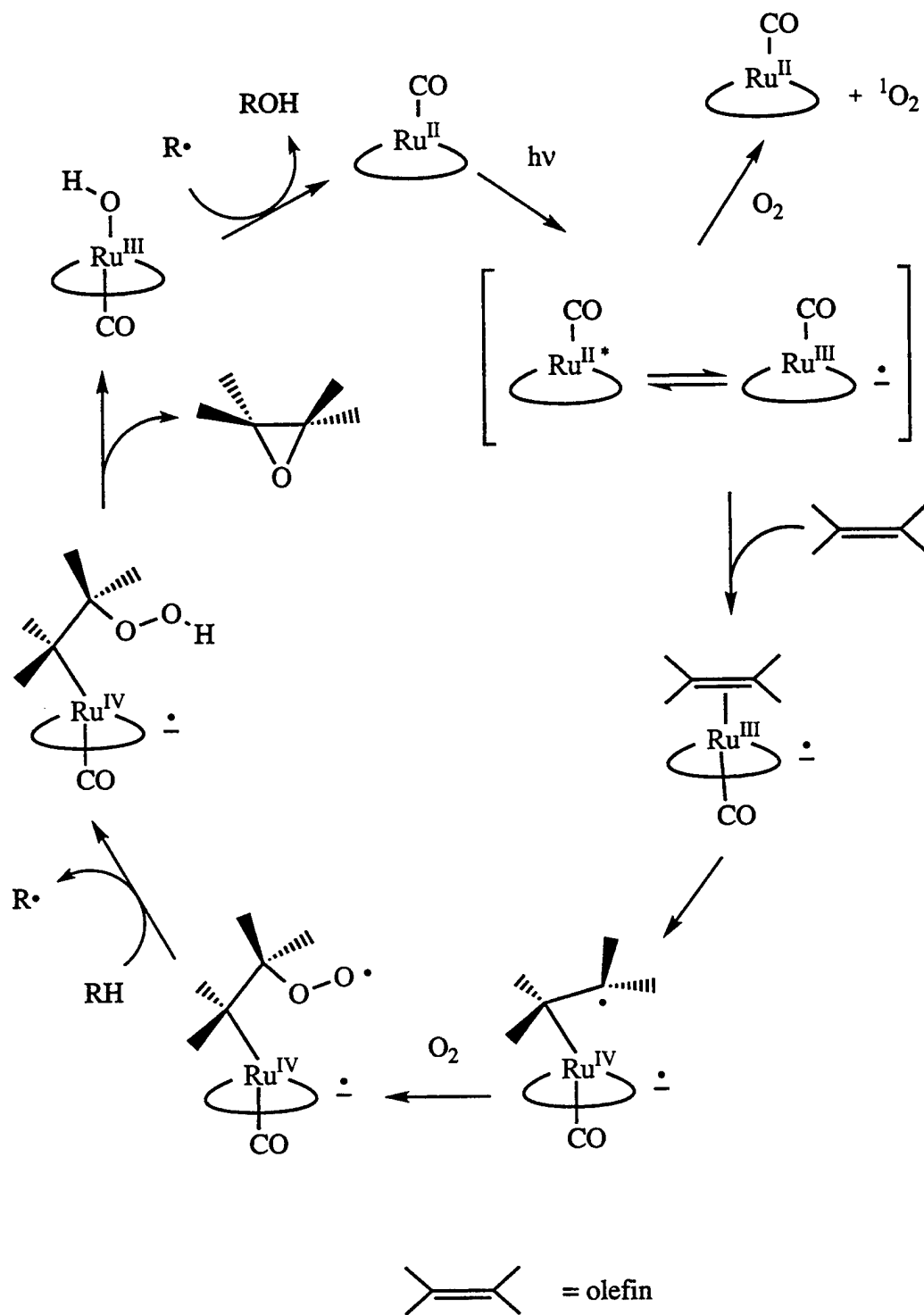
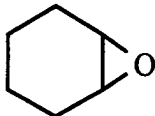
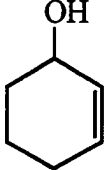
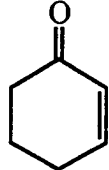


Table 5.1. Oxidation Chemistry with RuTFPPCl₈(CO).

Reaction Conditions ^a	% 	% 	% 	Turnovers
PhIO	42	56	2	9.9
O ₂	15	58	27	296
O ₂ + 10 eq (Et) ₃ NO	7	59	35	260
O ₂ + 5 eq mCPBA	35	52	13	20
O ₂ + 10 eq TBHP	14	54	32	770
O ₂ + 300 eq TBHP	7	65	28	1119
slow str rate	14	61	25	258
CO/O ₂	7	57	36	258
No light	16	59	25	200 (average)
Visible Photolysis	15	61	24	531

a. Reactions run in 15 mL of methylene chloride with approximately 1.5 - 2.0 μ mol of RuTFPPCl₈(CO) and 1 mL of cyclohexene. All reactions were run under 1 atm of dioxygen, except the PhIO reaction, which was under an argon atmosphere. See text and experimental section for more details.

Chapter 6

Solubility and Reactivity of Iron and Ruthenium Halogenated Porphyrins in Supercritical Carbon Dioxide

Introduction

The investigation of biomimetic metalloporphyrin catalysis has two general long range goals: first, to better understand oxidation chemistry *in vivo*, and second, the more economic objective of applying this knowledge to the design of efficient oxidation catalysts for industrial applications. The latter aim of efficiency is not specific to oxygenation, but also drives research in other areas of catalysis. Increasing pressure from the government to reduce waste as well as burgeoning costs of waste disposal have necessitated fundamental changes in catalysis methodology. Consideration of the catalyst efficiency and longevity are no longer sufficient; solvent disposal, waste stream reduction, and chemical toxicity are of increasing importance.

Supercritical carbon dioxide (SC CO₂) has recently received great attention as an environmentally friendly solvent. Non-toxic, inexpensive, and nonflammable, it is currently used for commercial extraction of hops and decaffination of coffee.¹ SC CO₂ is being further explored as a medium for uses ranging from the extraction of lanthanides from nuclear reprocessing waste² to dry-cleaning.³ The primary applications and research related to SC CO₂ have focused on separation technology. The use of supercritical carbon dioxide as a solvent for chemical reactions has not been widely explored, an area where the unique attributes of supercritical fluids (SCFs) could possibly affect the desired enhancements in catalysis.

In general, SCFs have properties that range between those of gases and liquids. Gases are miscible in SCFs, eliminating phase transfer problems during hydrogenation or oxygenation catalysis in homogeneous solution. The density of a SCF is extremely

dependent on the pressure and temperature, and can vary between being "gas-like" or "liquid-like". The polarity of SC CO₂ is similar to that of halogenated hydrocarbons, indicating that it may be an excellent replacement for hazardous solvents such as carbon tetrachloride or methylene chloride.⁴

Carbon dioxide has an unusually low critical point. A phase diagram (Figure 6.1) shows the critical point at 72.8 atm and 31 °C, which is far lower than that of water (218 atm and 374 °C).⁵ These conditions are easily achievable in the laboratory, albeit with care and respect, and are also feasible for industrial applications.

Supercritical carbon dioxide has recently begun to be explored as a medium for catalysis. DiSimone conducted the free radical polymerization of methyl methacrylate in SC CO₂. High yields of quality poly(methyl methacrylate) were obtained from a single phase reaction, avoiding the aqueous and organic dispersing media used in classical polymerization techniques.⁶ Noyori et. al. have achieved formation of dimethylformamide from hydrogen gas, dimethylamine, and supercritical carbon dioxide with a ruthenium phosphine catalyst. The CO₂ serves as both solvent and reactant, driving the reaction at a rate an order of magnitude above that in an organic solvent.⁷ Similarly, the miscibility of H₂ in SC CO₂ leads to very high initial rates of reaction for the formation of formic acid, catalyzed by Ru(PMe₃)₄(H)₂.⁸ Asymmetric hydrogenation reactions with ruthenium and rhodium catalysts have demonstrated that enantioselectivity can be increased by moving from a conventional solvent to supercritical CO₂.³ The above examples demonstrate several methods in which SCFs have improved catalytic processes.

Despite these recent successes, only one oxidative system has been investigated in SC CO₂.⁹ The uncatalyzed free radical oxidation of cyclohexane with dioxygen in SC CO₂ has been reported. The conversion of cyclohexane and the ratio of cyclohexanol and cyclohexanone produced are controlled by the pressure and temperature near the critical region.¹⁰ No other oxidations in supercritical carbon dioxide have been reported. Catalytic olefin oxidation by halogenated metalloporphyrins seems an ideal system for analysis in

SC CO₂. Since dioxygen is the only additive in these reactions (no coreductant is needed), the miscibility of O₂ with SC CO₂ has potential to increase reactivity in the SCF. Furthermore, the different solvation properties of SC CO₂ could lead to different selectivity in the oxidation reactions.

Before investigating reactivity, we determined the solubility of three halogenated porphyrins in SC CO₂. Although the dielectric constant of supercritical carbon dioxide increases with pressure, it remains quite low (only 1.8 at 2000 psi), making SC CO₂ a rather poor solvent.⁴ However, since chlorinated solvents able to dissolve halogenated porphyrins (i.e., CCl₄) also have low dielectric constants, the porphyrins were anticipated to be soluble in the supercritical medium. Fe(TFPP)Cl, Fe(TFPPBr₈)Cl and RuTFPPCl₈(CO) were investigated, since their chemistry in methylene chloride had been previously studied in our laboratory.

Results

Solubility Studies

An apparatus allowing UV-Vis spectroscopy under high pressures is pictured in Figure 6.2. A tank of liquid carbon dioxide was connected to allow flow directly into the cell or into an ISCO syringe pump, which is capable of condensing CO₂ up to 5000 psi. The cell was secured with a stand on top of a stirplate in between the lamp and detector. Rubber heating tape was wrapped around the cell to maintain the temperature at 40°C during the UV-Vis experiments (Figure 6.2).

After the cell was aligned in the spectrophotometer setup, a solution of porphyrin in methylene chloride was injected into the cell through the thermocouple inlet. The thermocouple was then reattached, and the cell evacuated to remove the organic solvent. CO₂ was added, and the absorbance calculated from light intensity measurements taken at 500 psi intervals (Figure 6.3-6.6). A spectrum of each compound in methylene chloride is also displayed in each figure for comparison. The concentration of porphyrin in solution is

calculated assuming the extinction coefficients are similar in methylene chloride and in SC CO₂. Although porphyrin spectra are known to be sensitive to solvent, generally the position of the band shifts more than the extinction coefficient.

In general, solubility was found to increase with pressure. Although the spectra are quite noisy, due to refraction from mixing lines in the large cell, the main features of the porphyrin are still observable. Fe(TFPP)Cl (Figure 6.3) is the least sensitive to pressure, but has the highest solubility, with the concentration only changing from 0.27 to 0.30 μ M from 2000 to 5000 psi CO₂. The Q band region is most distinct in these spectra, with a shoulder at 500 and a stronger band at 610 nm corresponding to the solution spectrum bands at 504 and 620 nm.

The resolution of the Soret band of Fe(TFPPBr₃)Cl is lost in SC CO₂ (Figure 6.4). However, there is a definite increase in absorbance from 1400 to 3500 psi, and the solubility increases from 0.07 to 0.20 μ M. Further increases in pressure do not cause much change in absorbance.

Unlike the iron porphyrins, the Soret band of RuTFPPCl₃(CO) is quite distinct in SC CO₂. The Q band region in this spectrum, however, has a substantial amount of instrument noise (Figure 6.5). The solubility increased from almost nothing in liquid carbon dioxide (800 psi) to 0.16 μ M (5000 psi). The changes of solubility with pressure for all three porphyrins are plotted in Figure 6.6. Although none of the porphyrins were soluble in liquid CO₂ (data not shown), all of them were soluble once the critical point was achieved (> 1200 psi). Surprisingly, little change in the concentration was observed at higher pressures.

Solubility Studies Discussion

The solubility of halogenated porphyrins in supercritical carbon dioxide was significantly less than in halogenated solvents. Although solubility increased with pressure as the dielectric constant increased (became more like that of a halogenated solvent), the

maximum solubility achieved was quite low ($< 1 \mu\text{M}$). Presumably SC CO_2 never became polar enough to dissolve large amounts of porphyrin.

The observed pressure broadening of electronic absorption bands is not unexpected. The $d\sigma^* \rightarrow p\sigma$ transitions in single crystals of Pt_2Cl have been shown to red shift and broaden with pressure.¹¹ However, the rather dramatic change in the shape of the spectrum from room temperature and one atmosphere pressure relative to SC pressure and temperature for both of the iron porphyrins is rather puzzling. The loss of resolution in the Soret bands of $\text{Fe}(\text{TFPP})\text{Cl}$ and $\text{Fe}(\text{TFPPBr}_8)\text{Cl}$ could be ascribed to pressure broadening. Other aspects of the spectra are not as readily explained. A single intense Q band has appeared in the spectrum of $\text{Fe}(\text{TFPPBr}_8)\text{Cl}$; although absorption maxima often shift with solvent, the appearance of a new absorptions suggests that the porphyrin has been chemically altered. A blue shift in the Soret band and an increase in intensity of a band around 600 nm may be attributed to dimerization at high pressures. Relative to the 410, 510, and 620 nm bands in $\text{Fe}(\text{TFPP})\text{Cl}$, $(\text{FeTFPP})_2\text{O}$ has absorption bands at 398 and 600 nm; these values match well with the observed SC CO_2 spectrum ($\lambda_{\text{max}} = 390, 610 \text{ nm}$). Similarly, a μ -oxo dimer of $\text{Fe}(\text{TFPPBr}_8)\text{Cl}$ would be expected to have a blue shifted Soret band and a more intense Q band relative to the monomer. The SC CO_2 spectrum of $\text{Fe}(\text{TFPPBr}_8)\text{Cl}$ has maximum absorbance at 420 and 600 nm, relative to a 442 nm Soret band and weak Q bands in the solution spectrum. Although formation of a μ -oxo dimer should not have been possible in these experiments, since no oxygen was present in the cell, other dimerization modes are possible and could also account for the observed spectral changes. Contaminants from the carbon dioxide are also possible; although high purity carbon dioxide should be fairly free of impurities, no scrubbers were used. Dimerization is further suggested by the lack of pressure shifting with $\text{RuTFPPCl}_8(\text{CO})$; the ruthenium porphyrins are not as susceptible to dimerization as the iron analogs. Higher resolution spectra would have to be obtained to fully address this question.

A second complication was introduced by the use of methylene chloride.

Methylene chloride was found to extract plasticizers from the O-rings used to make the seal between the sapphire windows and the cell. When the pressure was decreased, the plasticizers formed a film on the interior of the cell, possibly causing interference patterns and reducing the quality of the spectra. Furthermore, the plasticizers seem to reduce the solubility of $\text{RuTFPPCl}_8(\text{CO})$. Addition of $\text{RuTFPPCl}_8(\text{CO})$ as a solid to the cell resulted in much higher solubility (Figure 6.7). By 3000 psi, the Soret band had already reached the maximum absorbance able to be measured by the instrument (~ 0.4).

Addition of cyclohexene resulted in a higher quality spectrum for $\text{RuTFPPCl}_8(\text{CO})$ (Figure 6.8). No solubility is observed in liquid carbon dioxide, but the transition limit of the spectrophotometer is reached by 2000 psi, indicating that cyclohexene is an excellent co-solvent for $\text{RuTFPPCl}_8(\text{CO})$. Cyclohexene also reduces the noise level in the ruthenium porphyrin spectrum; this effect is not understood. The structure in the Q band region changes in the presence of olefin, with a slight red shift and different intensity for the Q(1,0) and the Q(0,0) bands relative to the methylene chloride spectrum, indicating that cyclohexene may coordinate at high pressure, since no distinct Q bands were observed with SC CO_2 alone.

Despite the complications and noise levels of the spectra, lower limits for the solubility of the three halogenated porphyrins were determined. The minimal solubility of these complexes is not expected to limit the reactivity of the catalysts in supercritical carbon dioxide since the co-solvent properties of the substrate, cyclohexene, will increase the net solubility of $\text{Fe}(\text{TFPP})\text{Cl}$, $\text{Fe}(\text{TFPPBr}_8)\text{Cl}$, and $\text{RuTFPPCl}_8(\text{CO})$ in the oxidation reaction mixture.

The ability to perform UV-visible spectroscopy at high pressures is a valuable tool for studying reaction intermediates in SCF reactions. This will help determine if reaction pathways change at higher pressures. Further work to enable transient IR and emission spectroscopy in SCF systems is currently in progress at LANL.

Oxidation of Cyclohexene

We investigated the ability of $\text{Fe}(\text{TFPP})\text{Cl}$, $\text{Fe}(\text{TFPPBr}_8)\text{Cl}$, and $\text{RuTFPPCl}_8(\text{CO})$ to oxidize cyclohexene in supercritical carbon dioxide. The oxidation reaction had been studied in methylene chloride (Chapter 4 and 5), providing a comparison for data in a SCF. For oxidations with dioxygen, it was thought that the miscibility of O_2 would increase the reaction rate relative to the solution chemistry.

In order to help separate solvent and pressure effects, oxygenation reactions with iodosobenzene as an oxygen source were also investigated. This chemistry should be relatively unaffected by pressure, and should help isolate the different solvation properties at high pressure.

The oxidation reactions were conducted in a small autoclave reactor (Figure 6.9). Constructed in a similar fashion to the UV-Vis apparatus, this system had an additional inlet for pressurized air. The porphyrin, cyclohexene, and iodosobenzene (if used) were added to the reactor, which was then sealed and connected to the carbon dioxide inlet. As with the UV-Vis cell, the system temperature was maintained at 40 °C and the reaction stirred to maintain equilibrium. All reactions were run at 5000 psi of CO_2 to maximize solubility of the porphyrin. At the end of the batch reaction, the pressure was let down through a metering valve, and volatile organics were collected in cold acetone. The cell was washed with additional acetone, and products were detected by GC/MS.

Two reactions were run in the UV-Vis cell in order to determine the effect of light on the ruthenium porphyrin oxidation reaction. Since irradiation with visible light dramatically enhances catalysis by $\text{RuTFPPCl}_8(\text{CO})$ with dioxygen in methylene chloride, we wanted to determine if light would also enhance cyclohexene oxidation in SC CO_2 .

The results of the oxidation reactions are shown in Figures 6.10 - 6.12. With iodosobenzene, the overall activity was similar to the methylene chloride reactions for $\text{Fe}(\text{TFPP})\text{Cl}$ and $\text{Fe}(\text{TFPPBr}_8)\text{Cl}$. $\text{RuTFPPCl}_8(\text{CO})$ activity was considerably higher in

SC CO₂, with 21 turnovers compared to only 5 in methylene chloride (4 hour points). The product distributions for these reactions showed more variation. Notably, Fe(TFPP)Cl produced only cyclohexene oxide. For the perhalogenated iron and ruthenium complexes, higher oxidation products were observed. While reactions in methylene chloride have only been found to produce 2-cyclohexen-1-ol and 2-cyclohexen-1-one, the SC CO₂ reactions showed large peaks in the GC at later retention times. The first was identified by comparison to a library mass spectrum as 7-oxa-bicyclo[4.1.0]heptan-2-one (Figure 6.13). The second was assumed to be 4-hydroxy-2-cyclohexen-1-one due to a similar relationship in the retention times of cyclohexene oxide and 2-cyclohexen-1-ol, and since it is the logical partitioning product from the oxidation of 2-cyclohexen-1-one. Both Fe(TFPPBr₈)Cl and RuTFPPCl₈(CO) reactions with PhIO showed less 2-cyclohexen-1-ol than in methylene chloride, and more 2-cyclohexen-1-one, as well as 7-oxa-bicyclo[4.1.0]heptan-2-one and 4-hydroxy-2-cyclohexen-1-ol. None of the reactions used more than 30% of the available oxidant in 4 hours. A batch reaction of Fe(TFPPBr₈)Cl run for 12 hours showed no more epoxide formation, but more allylic oxidation products were observed.

With air, the catalyst activities were similar in the two solvents. It is difficult to make a direct comparison, because the batch reactions in SC CO₂ were run for different times than the methylene chloride experiments. Nevertheless, it is clear that all catalysts are quite active in the supercritical solvent. Fe(TFPP)Cl (at 4 hours), Fe(TFPPBr₈)Cl, and RuTFPPCl₈(CO) (at 12 hours) showed 11, 59, and 51 turnovers, respectively. If the higher oxidation products are considered as more than one turnover, the numbers for the latter reactions increase to 127 and 90 turnovers. As with iodosobenzene, substantial amounts of multiple oxidation products were observed in all reactions, with a decrease in the amount of 2-cyclohexen-1-ol produced. Surprisingly, a greater percentage of epoxide was also produced.

Both Fe(TFPPBr₈)Cl and RuTFPPCl₈(CO) had substantial initiation periods in SC CO₂. Batch reactions run for only 4 hours showed no trace of products. After 12

hours, however, significant activity was observed, as described above. Only Fe(TFPP)Cl showed activity with air in the 4 hour time period. Attempts to shorten the initiation period for RuTFPPCl₈(CO) by the addition of light were not successful. Two experiments with RuTFPPCl₈(CO) were conducted in the larger UV-Vis cell. Upon addition of CO₂, the solution turned a bright red, indicating that cyclohexene serves as an excellent co-solvent for the catalyst. A flashlight was used to irradiate the reaction through the cell window for the duration of the batch reaction. However, after only a few hours, the pressure dropped and the solution bleached. A reaction in the UV-Vis cell was attempted twice. The first reaction, with one atmosphere of air, bleached after 20 hours. The second, with 5 atm air, bleached within 6 hours. After bleaching was observed, the cell was let down as previously described. No product formation was detected in either light reaction.

Discussion Oxidation Experiments

The iodosobenzene reactions in supercritical carbon dioxide all showed an increase in the percent epoxide formed relative to reaction in CH₂Cl₂. As discussed in Chapter 4, epoxidation with a high-valent metal-oxo is believed to occur by a different mechanism than hydroxylation. The different solvation properties of SC CO₂ may increase the probability for electron transfer (leading to epoxidation) over hydrogen abstraction (leading to hydroxylation). The success of free radical polymerization reactions conducted in SC CO₂ suggests that radicals are quite stable in a supercritical medium. However, the solvent may change the stability of the caged radical species such that electron transfer becomes more favorable. SC CO₂ may provide a new medium for probing the oxo-transfer step in olefin oxidation reactions.

In addition to the increase in epoxide formation, there is also an increase in multiple oxidations of the same substrate molecule, both with PhIO and dioxygen. The supercritical fluid did not greatly increase the observed turnover numbers, suggesting that phase transfer is not the limiting step in the dioxygen reactions for any of the porphyrins. However, the

different solvent properties of SC CO₂ may be changing the selectivity; perhaps the catalysts are more soluble in the oxidized cyclohexene derivatives than in cyclohexene itself. Therefore, the catalyst could re-oxidize a single substrate multiple times before encountering other substrate molecules.

For RuTFPPCl₈(CO), fewer turnovers are observed in the dark cell, consistent with the photochemical reaction mechanism described in Chapter 5. However, the UV-Vis suggests a greater interaction between the porphyrin and substrate in SC CO₂, indicating that olefin binding may occur in the ground state in this medium, whereas it only is effective in the excited state in a methylene chloride solution. Alternatively, a different reaction mechanism may take precedence in this solvent. Unfortunately, attempts to photolyze the reaction were complicated by the cell design. The Buna-N O-rings used to seal the sapphire windows, while having excellent resistance to supercritical carbon dioxide, are reported to have unsatisfactory resistance to alkanes,¹² suggesting that the "bleach" observed upon photolysis was not due to porphyrin decomposition but a leaking cell.

Conclusion

The preliminary results described above demonstrate that supercritical carbon dioxide is an adequate solvent replacement for methylene chloride for porphyrin-catalyzed oxidation of cyclohexene. Large rate enhancement was not observed, but changes in the reaction selectivity did occur. Most notable was the 100% selectivity observed for epoxidation of cyclohexene with Fe(TFPP)Cl and PhIO, and increased epoxidation selectivity for both RuTFPPCl₈(CO) and Fe(TFPPBr₈)Cl in reactions with either PhIO or O₂. For allylic oxidation products, multiple oxidations of the same substrate molecule was observed, suggesting that destruction of organics in a supercritical medium may be favorable under different conditions. A repeat of the oxidation experiments at different temperatures and pressures would reveal if the selectivity could be tuned to favor one

pathway more completely. Further experiments would be needed to determine the source of these effects.

Methods

$\text{RuTFPPCl}_8(\text{CO})$ and $\text{Fe}(\text{TFPPBr}_8)\text{Cl}$ were synthesized as in Chapter 2. $\text{Fe}(\text{TFPP})\text{Cl}$ was used as received (Aldrich). Cyclohexene was from Aldrich, and distilled under argon before use. Acetone and methylene chloride were used as received from EM Science. Iodosobenzene was from TCI and used as received. Air and carbon dioxide were from Albuquerque Welding. Oxidation products were determined by injection onto an Hewlett Packard GC/MS with an auto injector and a JW Scientific DB-5 30m column. Sample identification was determined by injection of an authentic sample for cyclohexene oxide, 2-cyclohexen-1-ol, and 2-cyclohexen-1-one (Aldrich). The identity of one higher boiling peak was determined by the library on the GC MS.

Standard NPT, Swagelock, and HiP pressure rated valves and connections were used to build the high pressure systems. Stainless steel tubing (1/16" - 1/4") was used for longer connections. An ISCO brand syringe pump was used to pressurize the carbon dioxide. All systems were barricaded behind Lexan shielding, and tubing and valves were secured to the work tables to minimize damage in case of a pressure failure. All systems were equipped with relief valves or rupture discs, so the system would blow at the designed weak point in case of over-pressurization.

UV-Vis spectra were measured on a Hewlett Packard 8452 spectrophotometer. The lamp and detector were removed from the instrument cavity and placed on a laser table to allow room for the large cell. Additional focusing mirrors were placed after the lamp and before the detector to increase light intensity. Intensity data was collected in ASCII format, and loaded onto a Macintosh computer, where absorbance readings were calculated ($A = \log(I_0/I)$). I_0 readings were taken at each pressure since the absorbance of CO_2 was found to change considerably around the supercritical transition. This is due to the variable

density of SC CO₂; the change in the index of refraction between the cell windows and solvent decreased at higher pressures. The stirplate was turned off when spectra were taken, in order to minimize refraction by mixing lines in solution. The large cell volume (≈ 75 mL) made it difficult to maintain a constant temperature in the cell, causing visible sheer lines due to the temperature gradient in solution. Averaging intensity data helped decrease the noise in the spectra.

The cell used for UV-Vis experiments was constructed of 316 stainless steel, with a 13.2 cm path length and 1 inch aperture on each side. The seal between the 1 cm thick sapphire windows and the metal cell was made by a Buna-N rubber O-ring, which was replaced after each use. The cell had three inlets for a thermocouple, an inlet valve, and a t-joint which contained a relief valve, an analog pressure gauge, and an outlet line. The outlet could be directed to a vacuum pump or vented to a hood.

For each sample, the cell was first mounted on the stand and aligned for maximum lamp intensity. A solution of porphyrin in methylene chloride was added through the thermocouple inlet, and then the thermocouple was fastened down. By this method, a known amount of porphyrin could be added, such that the possible absorbance in a 13.2 cm path length cell would not be above 1. The cell was evacuated, removing the solvent, and then carbon dioxide was added. The cell was sealed off at each pressure, and allowed to equilibrate to 40 ± 0.5 °C for each intensity reading. Alternatively, excess solid porphyrin was added to the cell before the windows were sealed down (the large nuts for the windows had to be tightened down on a vise).

Oxidation reactions were conducted in a cell designed by Dave Morgenstern and Sam Borkowsky at Los Alamos National Laboratory. This cell was a single 2.5" cylinder of 316 stainless steel, with a 5/8" hole bored into the center. The only openings were for a rupture disc (rated to 10000 psi), an analog pressure gauge, a thermocouple, and the main reactor valve. The total cell volume was ≈ 12 mL. The inlet lines allowed the sequential addition of compressed air and carbon dioxide to the cell. Air was always added first, so

that the CO₂ would flush any oxygen from the lines before the system was brought up to pressure. Although air or pure oxygen gas could be used with this reactor, air was used for safety reasons.

Solid porphyrin, cyclohexene, and iodosobenzene (if used) were added to the reactor, the valve was sealed on the vise, and the reactor was then attached to the inlet and letdown tubing. Air was added first, up to the pressure of the tank (110 psig) and then CO₂ up to 5000 psi. As with the UV-Vis experiments, the cell rested on a stirplate and the cell temperature was maintained at 40 °C with heating tape. As soon as the pressure reached 5000 psi, the main reactor valve was closed, and the system allowed to stir for the desired reaction time.

Oxidation reactions were let down by a HiP metering valve through 1/16" tubing, and the end of the tubing was crimped with a hammer to reduce the flow rate. The pressure was let down slowly over a period of 1-2 hours into a vial containing approximately 20 mL of cold acetone to catch volatile organics. The vial rested in a cold block of steel to maintain its temperature and reduce loss of organics. The reaction vessel was then opened and rinsed with acetone to remove residual cyclohexene and products. The rinse was collected, and the volume measured. An aliquot was taken, diluted with a known amount of toluene in acetone to standardize the GC/MS analysis, and injected onto the GC. Although there is undoubtedly some loss to evaporation, it is believed that most of the organic products are collected by this method. No mass balance calculation was attempted.

References and Notes

- (1) Kaupp, G. *Angew. Chem., Int. Ed. Eng.* **1994**, *33*, 1452-1455.
- (2) Laintz, K. E.; Tachikawa, E. *Anal. Chem.* **1994**, *66*, 2190-2193.
- (3) Personal communication from William Tumas, Los Alamos National Laboratory, January 1995.
- (4) Wenclawiak, B. In *Analysis with Supercritical Fluids: Extraction and Chromatography*; B. Wenclawiak, Ed.; Springer-Verlag: Berlin, 1992.
- (5) Dickerson, R. E.; Gray, H. B.; Darensbourg, M. Y.; Darensbourg, D. J. *Chemical Principles*; 4th ed.; The Benjamin/Cummings Publishing Co., Inc.: Menlo Park, CA, 1984.
- (6) DeSimone, J. M.; Maury, E. E.; Meneceloglu, Y. Z.; McClain, J. B.; Romack, T. J.; Combes, J. R. *Science* **1994**, *265*, 356-359.
- (7) Jessop, P. G.; Hsiao, Y.; Ikariya, T.; Noyori, R. *J. Am. Chem. Soc.* **1994**, *116*, 8851-8852.
- (8) Jessop, P. G.; Ikariya, T.; Noyori, R. *Nature* **1994**, *368*, 231-233.
- (9) A substantial amount of oxidation chemistry has been investigated in supercritical water. Complete oxidation of organics has been observed under these harsh conditions. For example, see Webley, P. A.; Tester, J. W. *Energy Fuels*. **1991**, *30*, 411.
- (10) Srinivas, P.; Mukhopadhyay, M. *Ind. Eng. Chem. Res.* **1994**, *33*, 3118-3124.
- (11) Stroud, M. A.; Drickamer, H. G.; Zietlow, M. H.; Gray, H. B.; Swanson, B. I. *J. Am. Chem. Soc.* **1989**, *111*, 66-72.
- (12) Seymour, R. S. *Engineering Polymer Source Book*; McGraw-Hill: New York, 1990, pp 102.

Figure 6.1 -- Phase diagram of carbon dioxide (modified from reference 5). The critical point of CO₂ is at relatively low temperature and pressure, facilitating its use as a supercritical solvent.

Phase Diagram of Carbon Dioxide

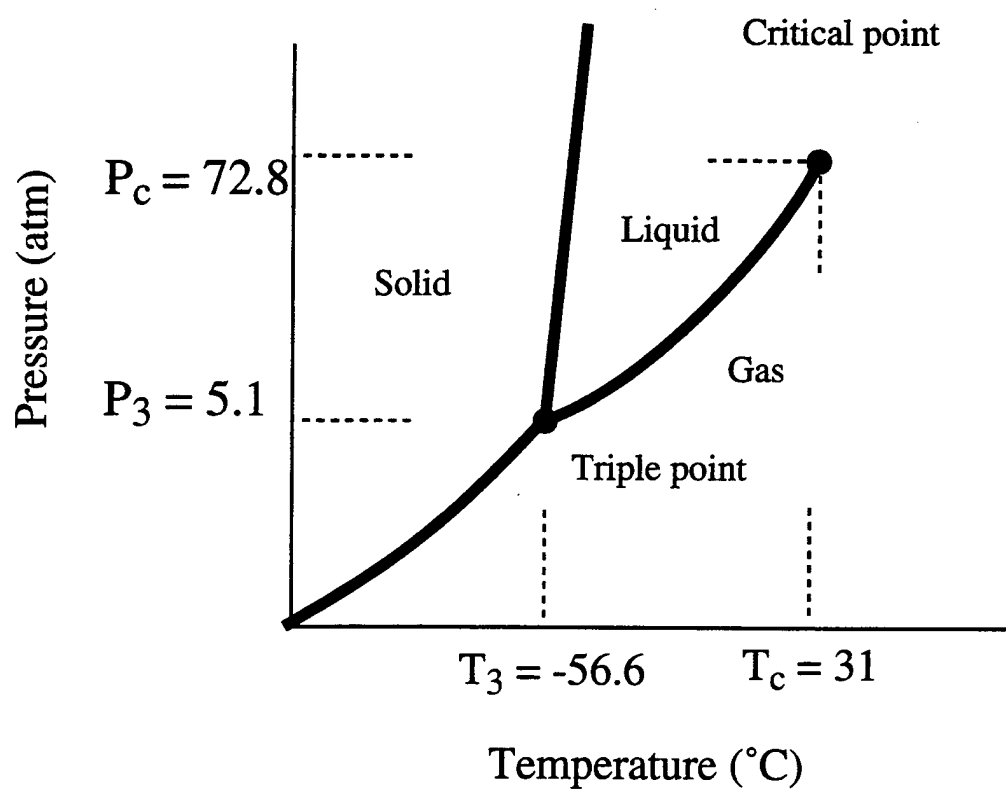
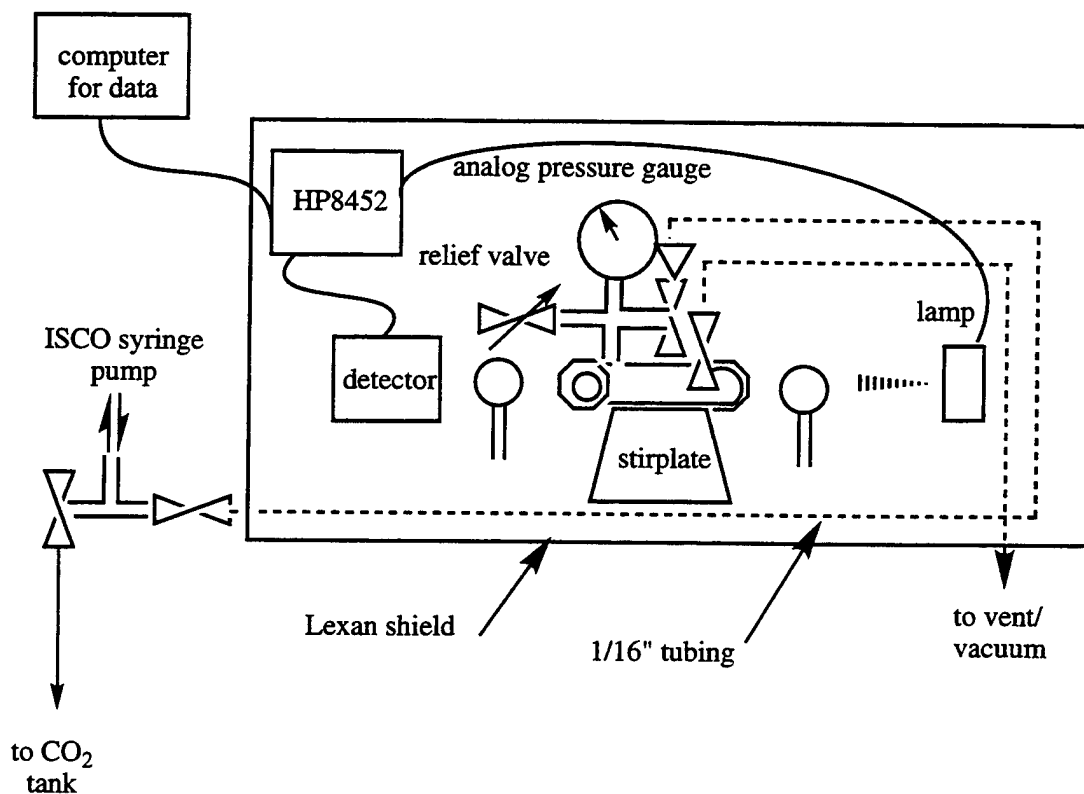


Figure 6.2 -- Apparatus used for UV-Visible spectroscopy in supercritical carbon dioxide.

UV Vis in Supercritical CO₂



Cell characteristics: 6 inches long, 13.2 cm path length
 1 inch diameter aperture with sapphire windows
 75 mL cell volume, including dead space
 316 stainless steel
 rated to 5000 psi

Figure 6.3 -- Spectra of Fe(TFPP)Cl in methylene chloride and carbon dioxide. The spectrum in SC CO₂ is smoothed to remove noise from refracted light. The solubility did not change much with pressure, increasing only from 0.27 to 0.30 μ M from 2000 to 5000 psi of CO₂.

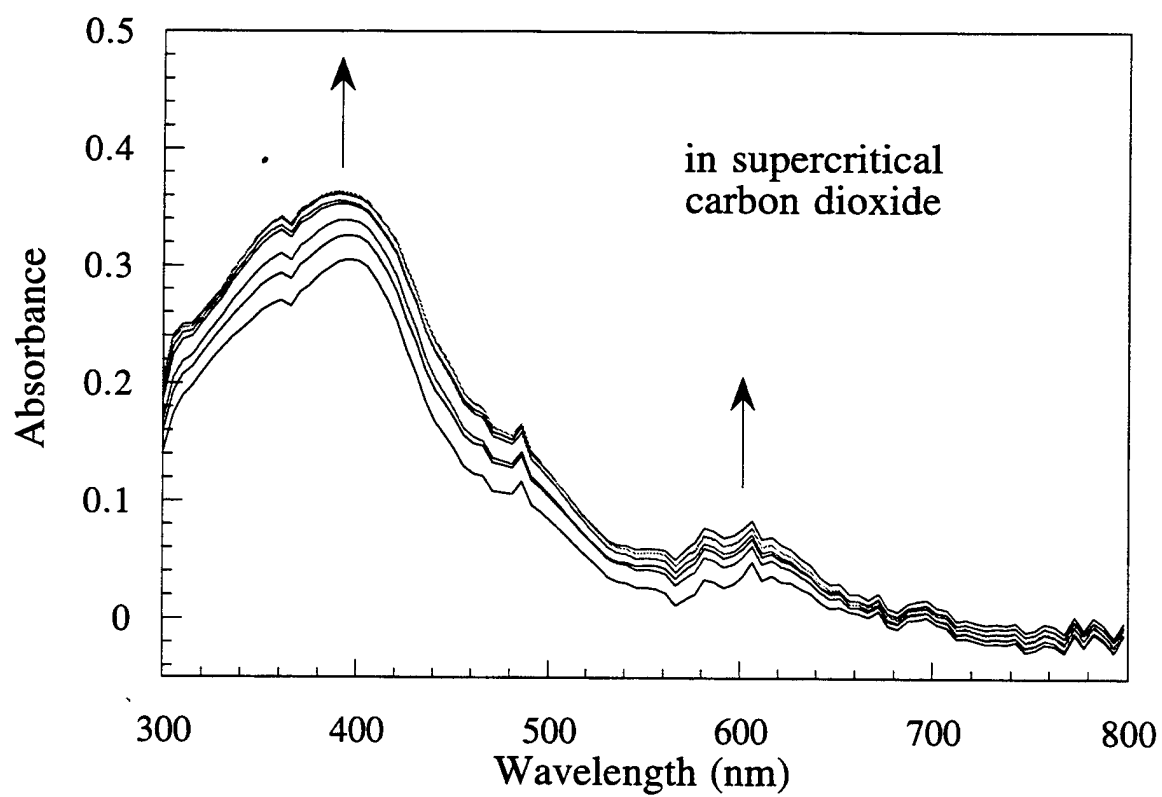
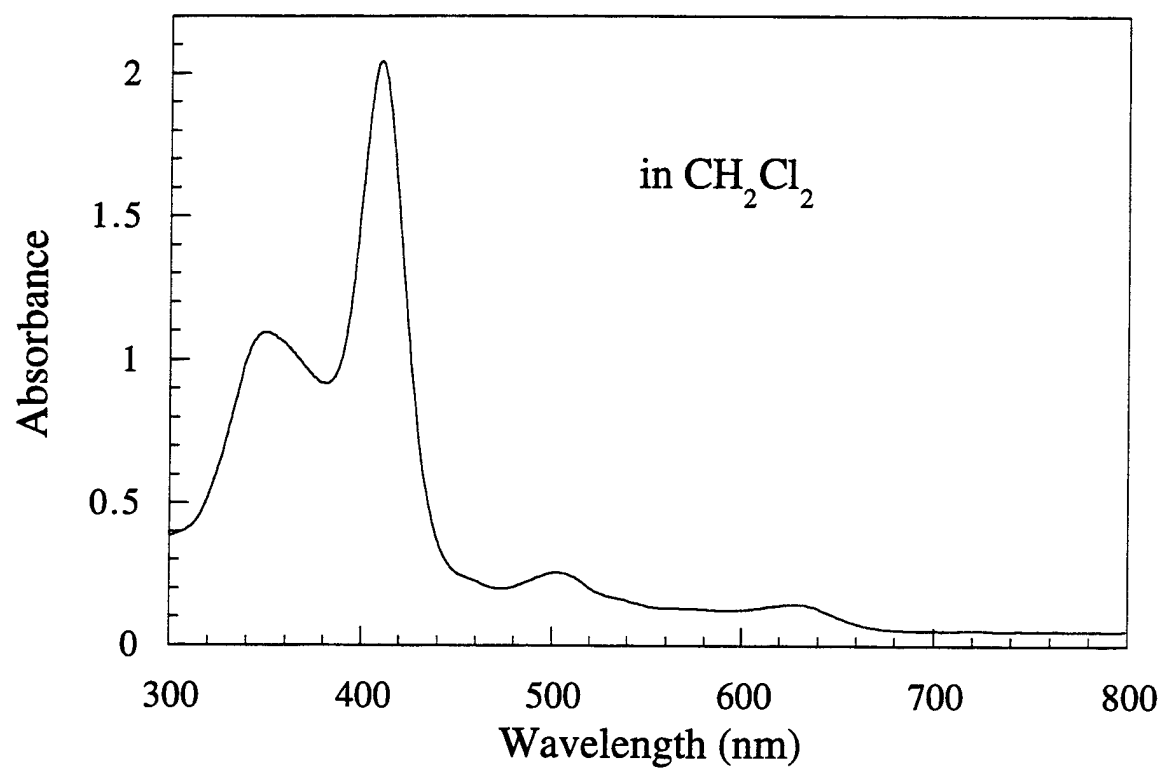


Figure 6.4 -- Spectra of $\text{Fe}(\text{TFPPBr}_8)\text{Cl}$ in methylene chloride and carbon dioxide. The spectrum in SC CO_2 is smoothed to removed noise from refracted light. The solubility increased from 0.07 to 0.20 μM from 2000 to 3500 psi of CO_2 , remaining fairly constant after this pressure.

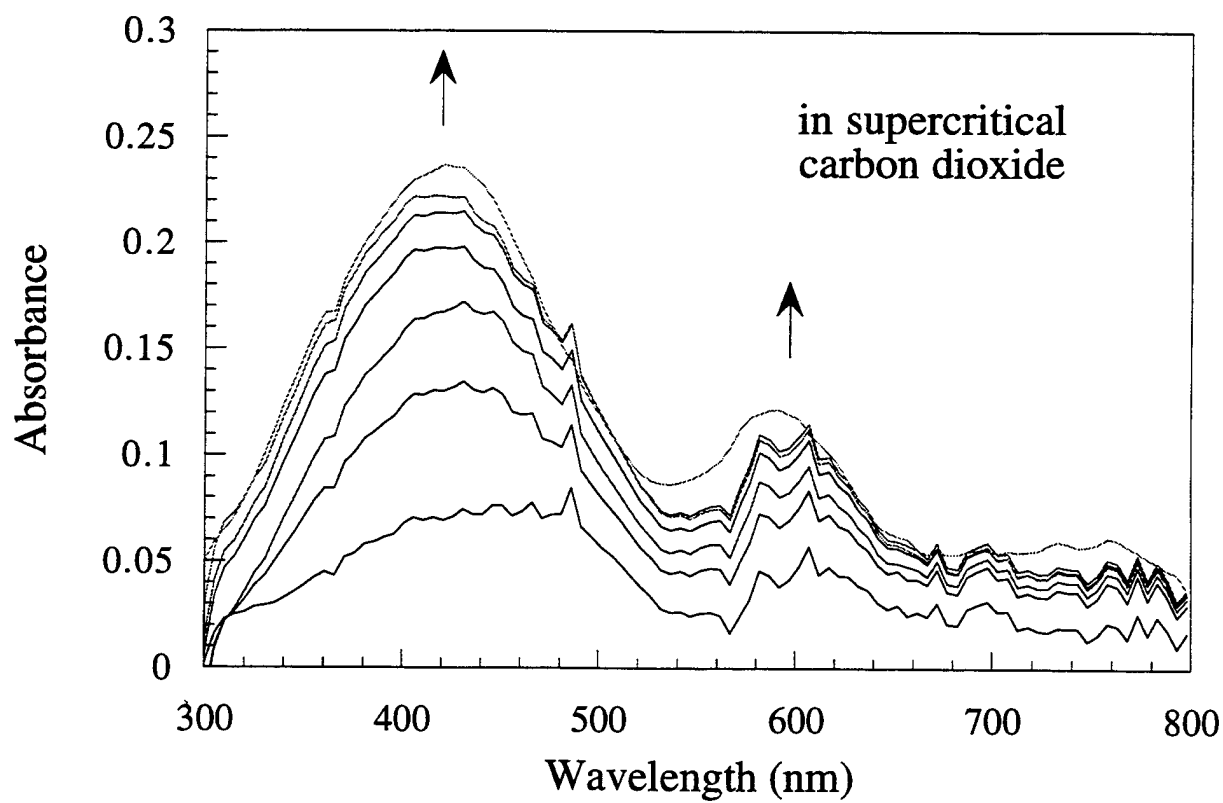
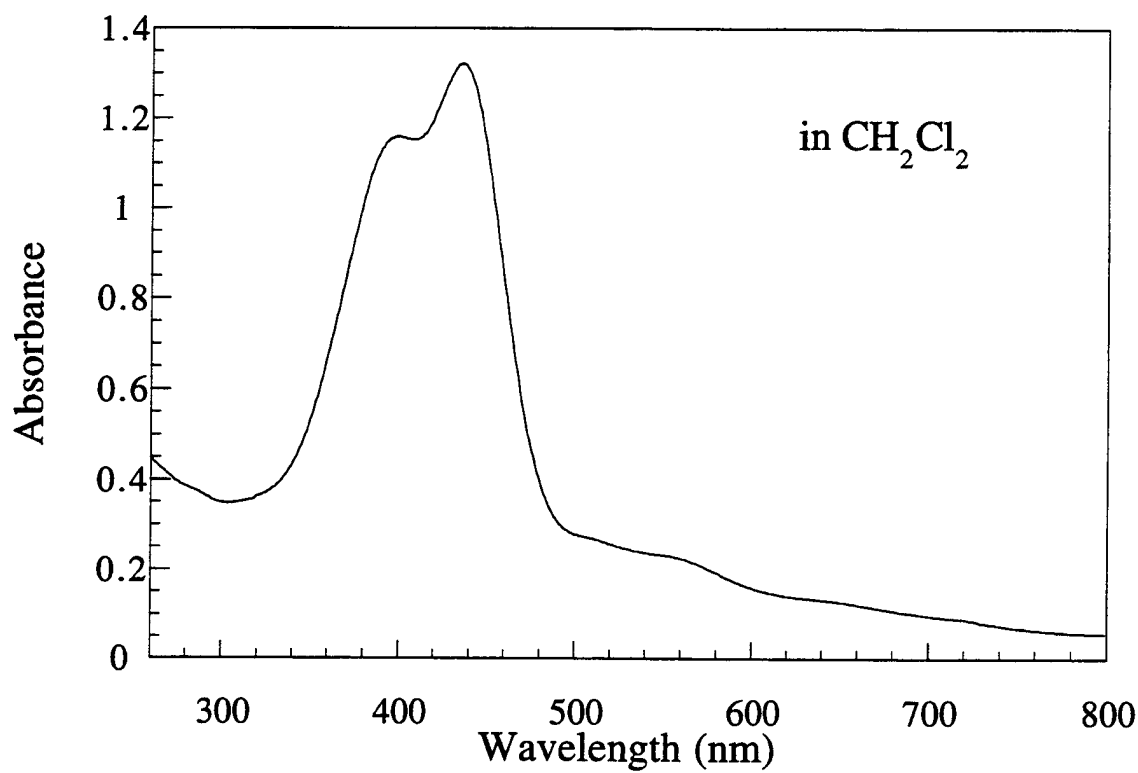


Figure 6.5 – Spectra of RuTFPPCl₈(CO) in methylene chloride and carbon dioxide. The porphyrin is almost insoluble in liquid CO₂, but solubility increased to 0.16 μM at 5000 psi of CO₂. The spectra in the two different solvents match best for RuTFPPCl₈(CO), suggesting no unusual interactions in the supercritical solvent.

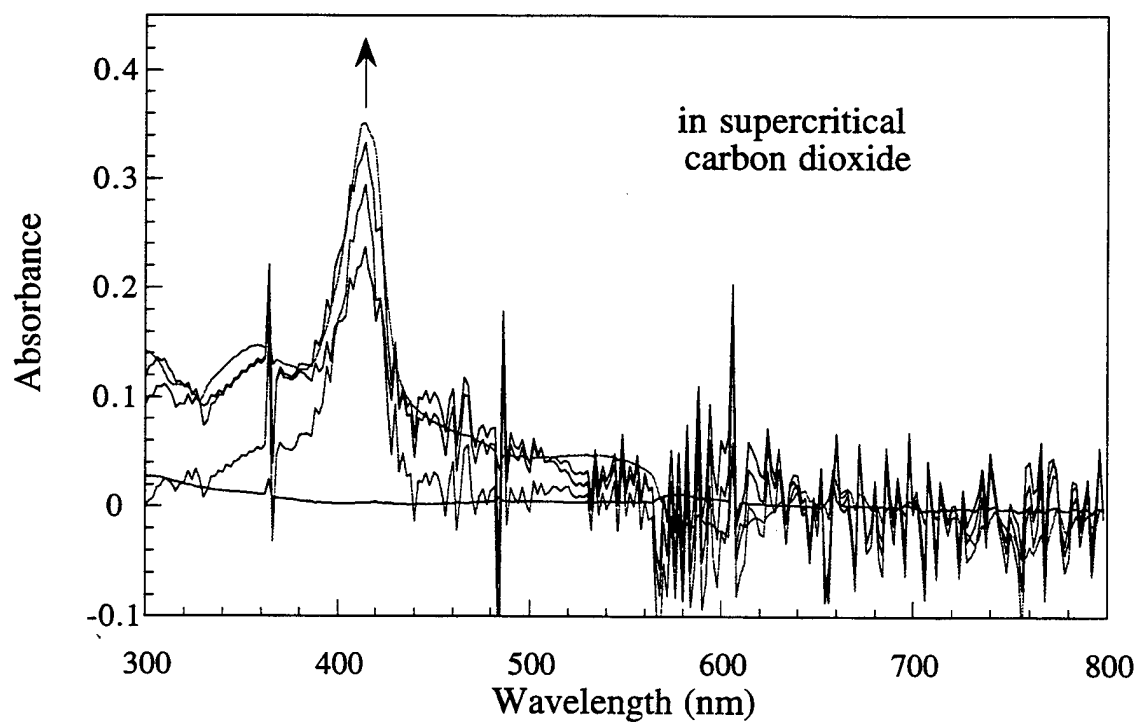
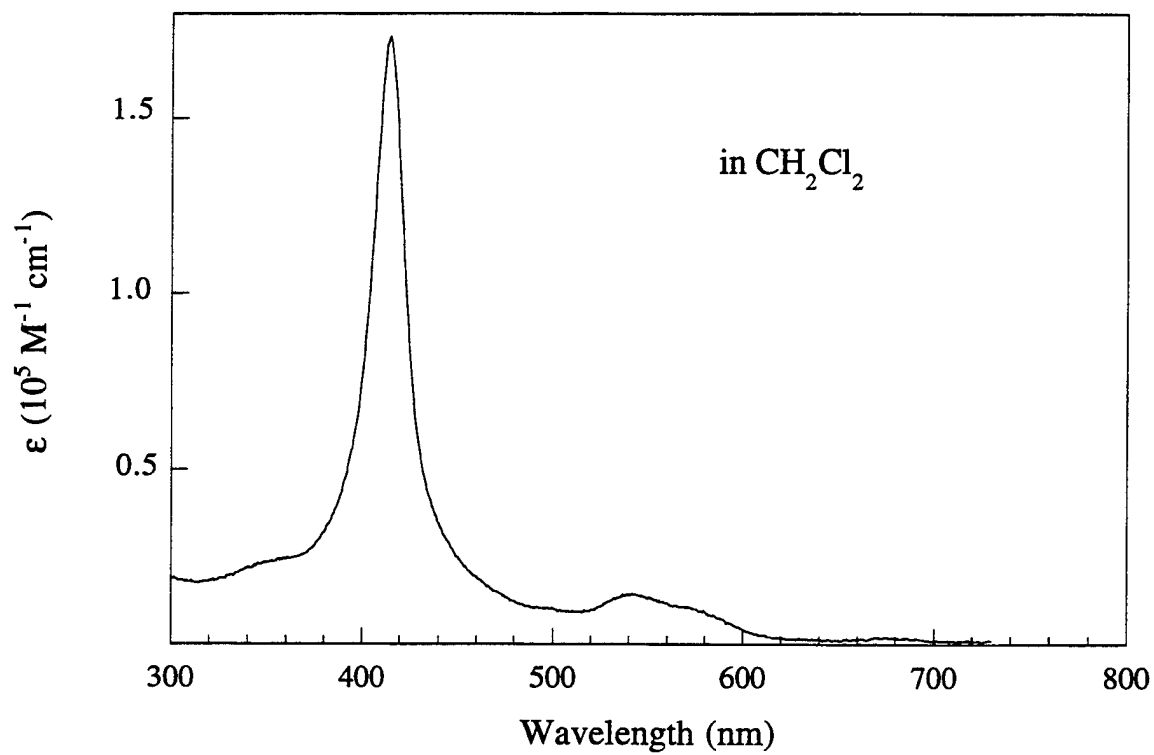


Figure 6.6 -- A plot of solubility versus pressure for the halogenated porphyrins.

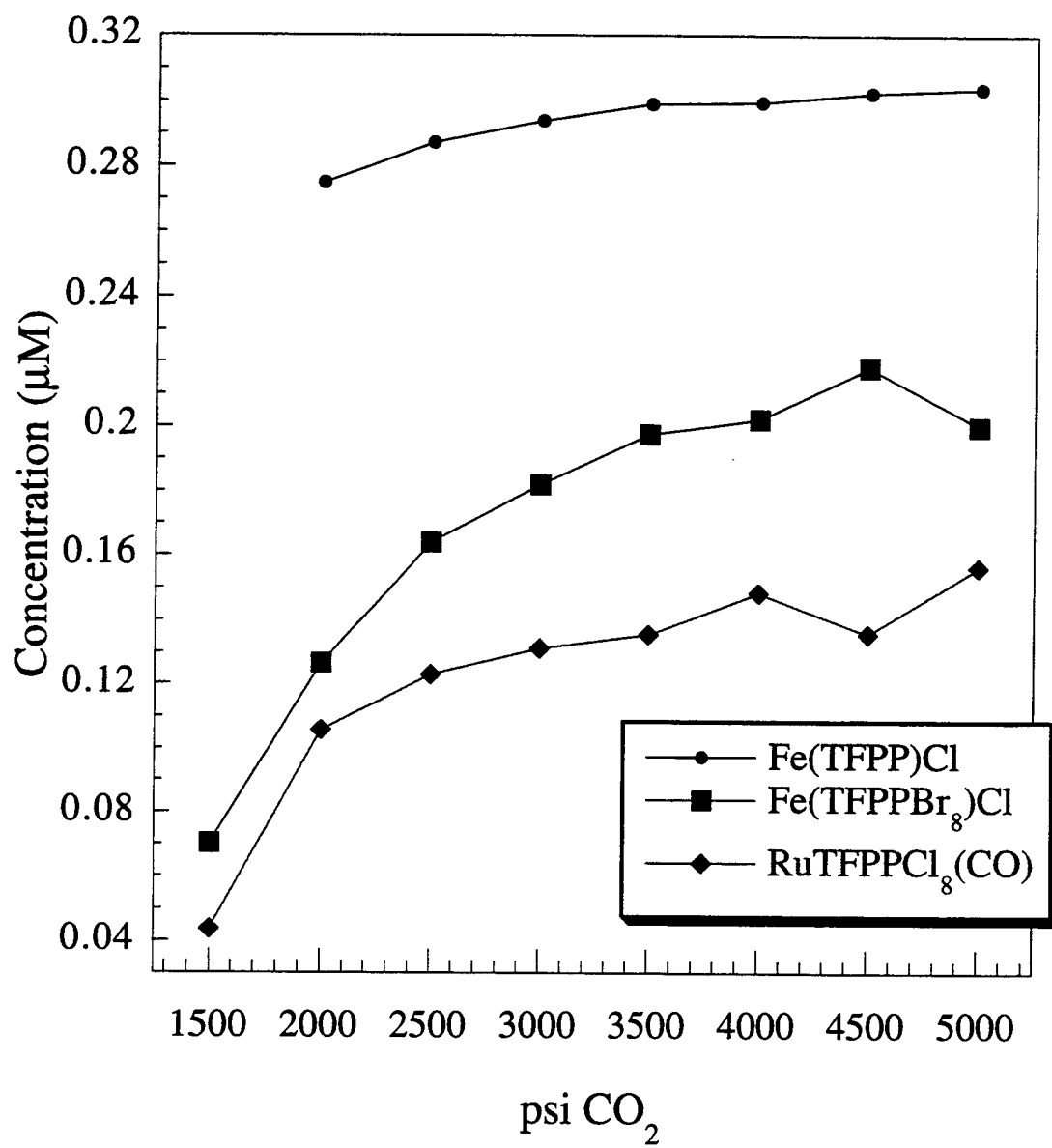


Figure 6.7 -- Spectrum of $\text{RuTFPPCl}_8(\text{CO})$ in carbon dioxide. This differs from the spectrum in Figure 6.3 in that the porphyrin was added as a solid, and not as a methylene chloride solution. The solubility is much higher in this case, reaching the maximum transmission of the instrument by 3000 psi, suggesting that a deleterious interaction occurs when the porphyrin is added as a CH_2Cl_2 solution (data at 2000, 3000, and 4000 psi).

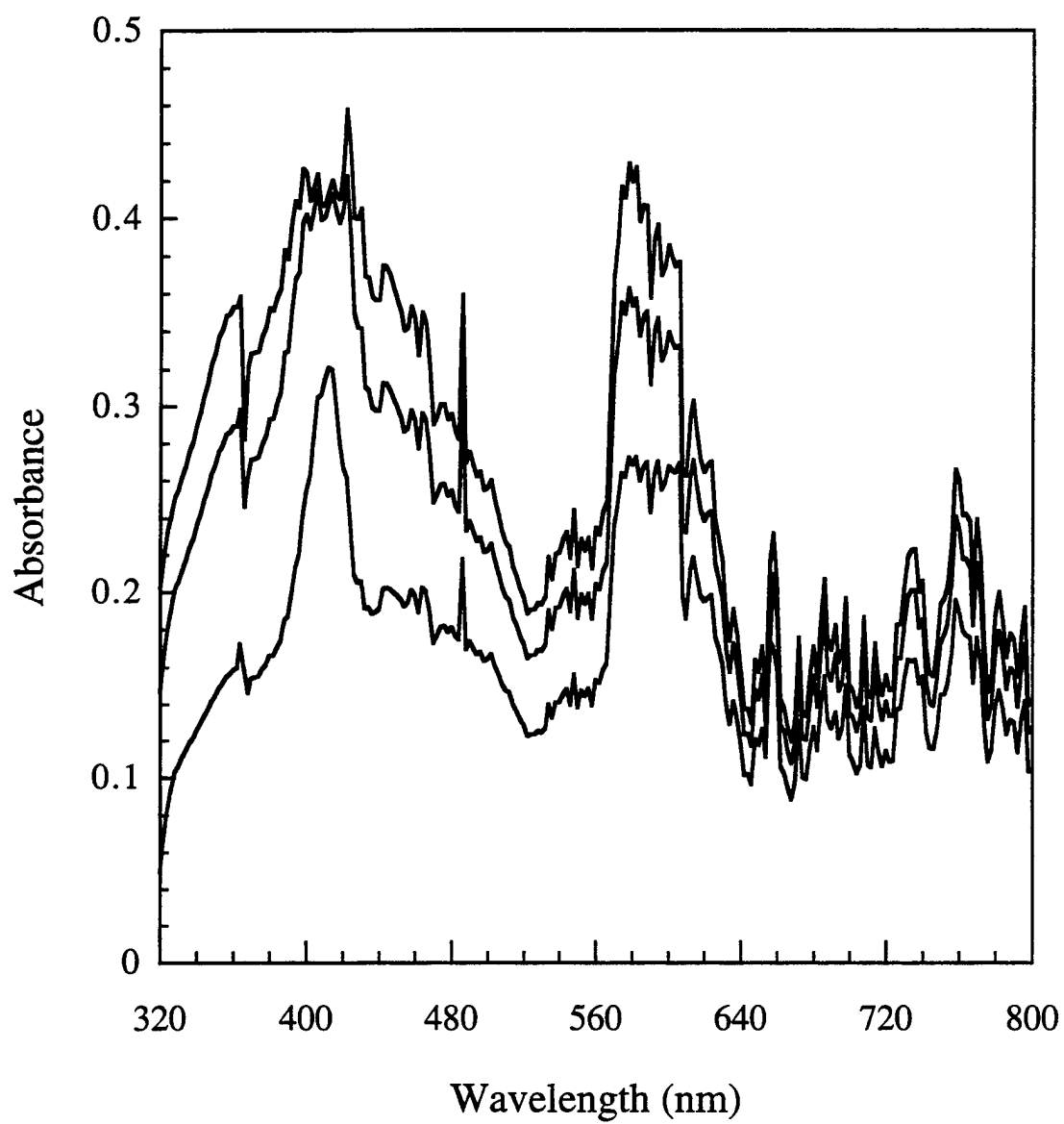


Figure 6.8 -- Spectrum of RuTFPPClg(CO) with cyclohexene in carbon dioxide. The Q band structure is significantly different than without cyclohexene, suggesting a possible interaction or binding of alkene in the supercritical solvent (data at 800, 1200, 2000, 3000, 4000, and 5000 psi).

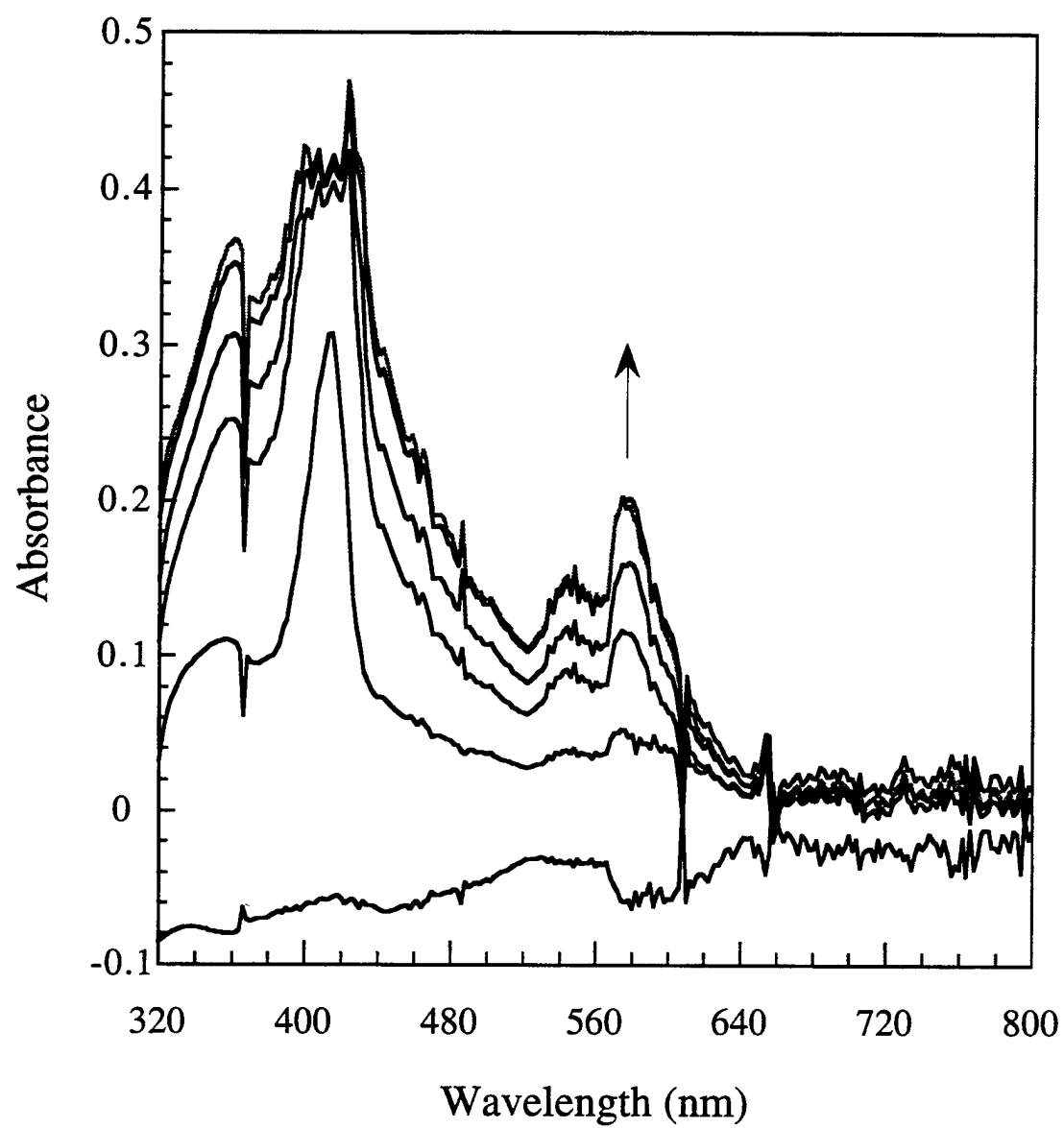


Figure 6.9 -- Cell used for oxidation reactions with iodosobenzene or air by halogenated porphyrins in supercritical carbon dioxide.

Plumbing for High Pressure Oxygen Reactions in Small Cell

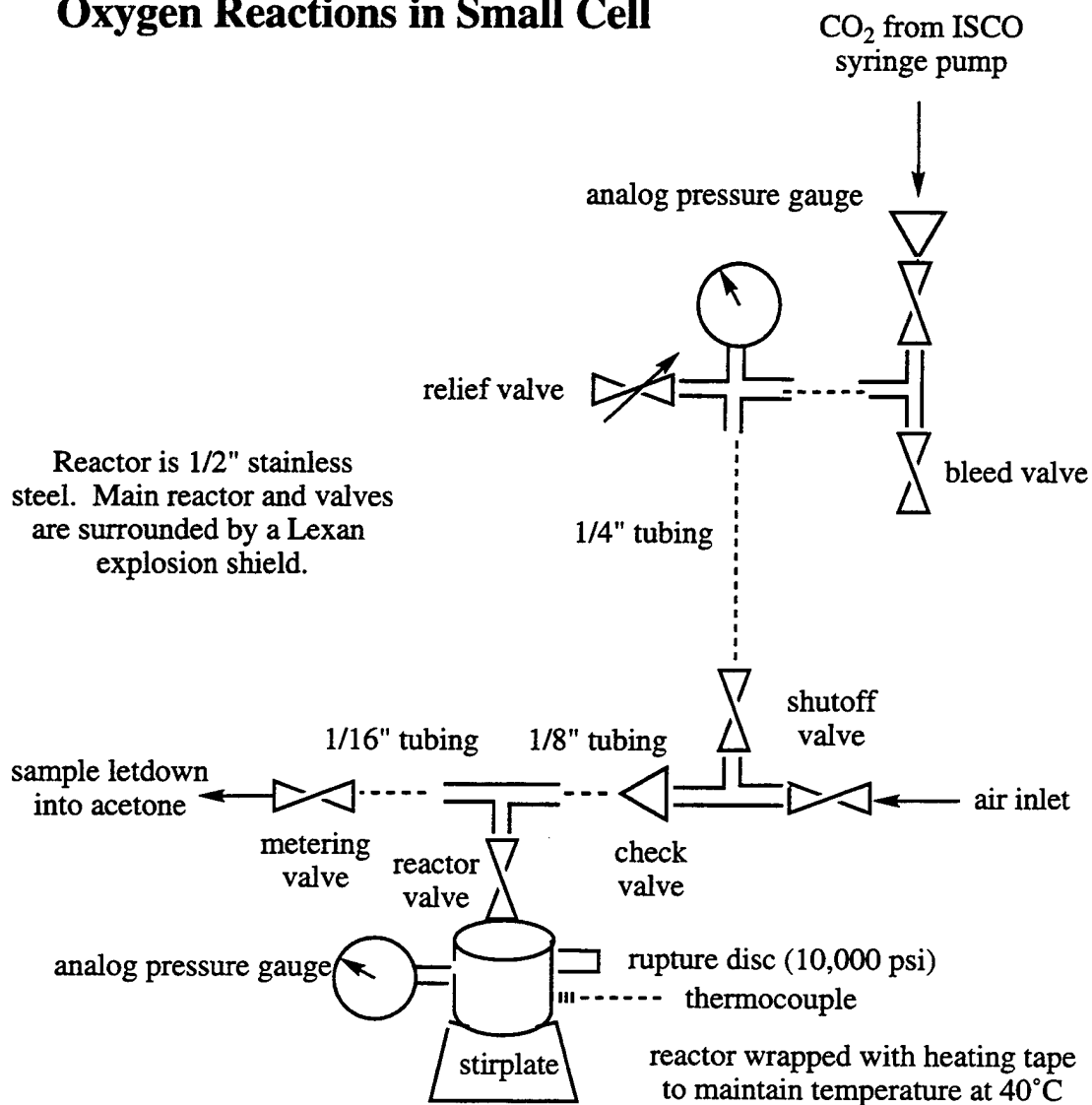


Figure 6.10 -- Turnovers of cyclohexene observed in oxidation reactions with Fe(TFPP)Cl and either iodosobenzene (left) or dioxygen (right). PhIO data is after 4 hours, and the dioxygen results are at 24 hours (CH₂Cl₂) or 12 hours (SC CO₂) in the different solvents. 100% selectivity for epoxide formation is observed with PhIO in SC CO₂.

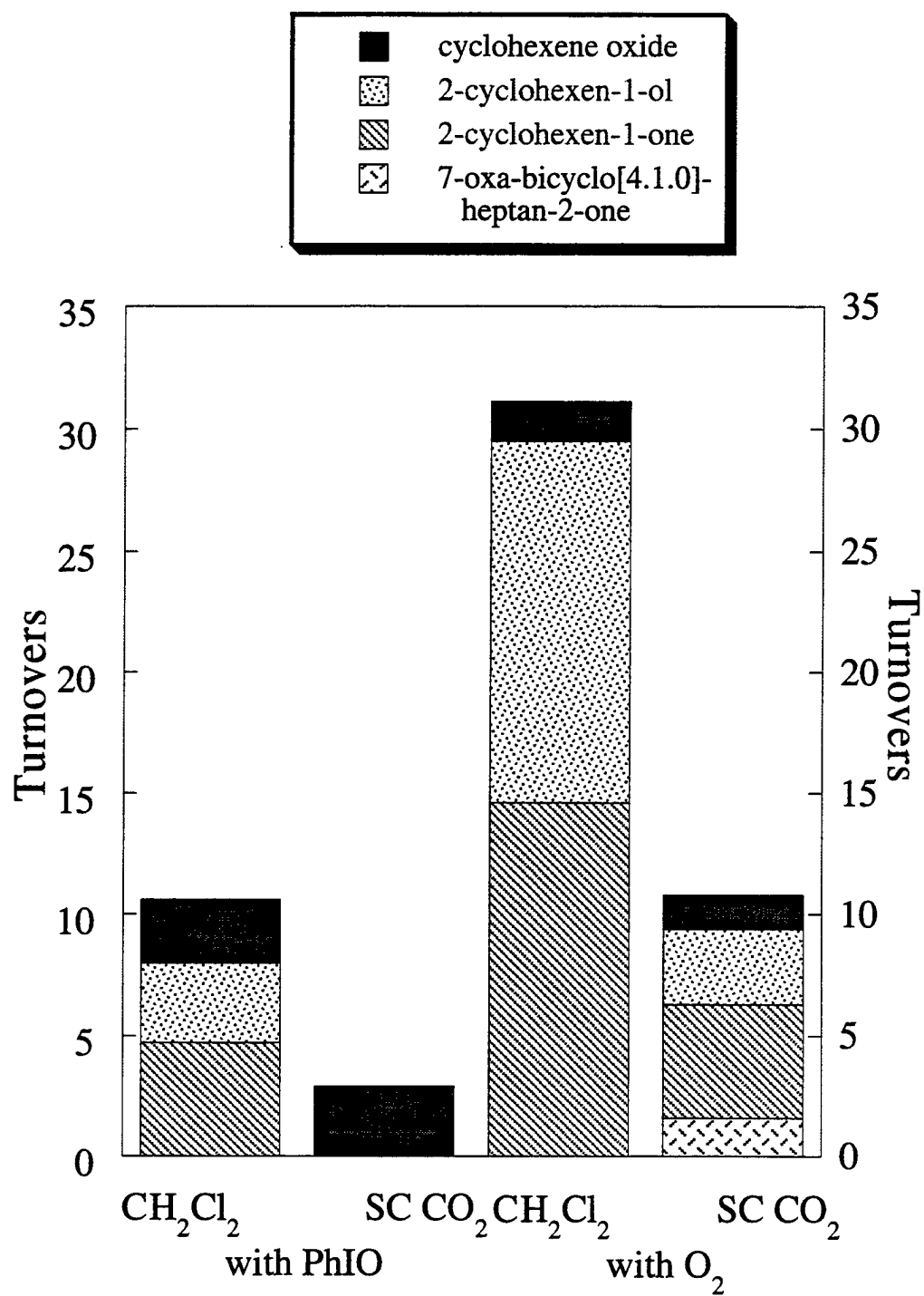


Figure 6.11 -- Turnovers of cyclohexene observed in oxidation reactions with Fe(TFPPBr₈)Cl and either iodosobenzene (left) or dioxygen (right). PhIO data is after 4 hours, and the dioxygen results are at 24 hours (CH₂Cl₂) or 12 hours (SC CO₂) in the different solvents. Higher selectivity for epoxide formation is observed with dioxygen in SC CO₂ relative to CH₂Cl₂. Significant amounts of higher oxidation products are also observed.

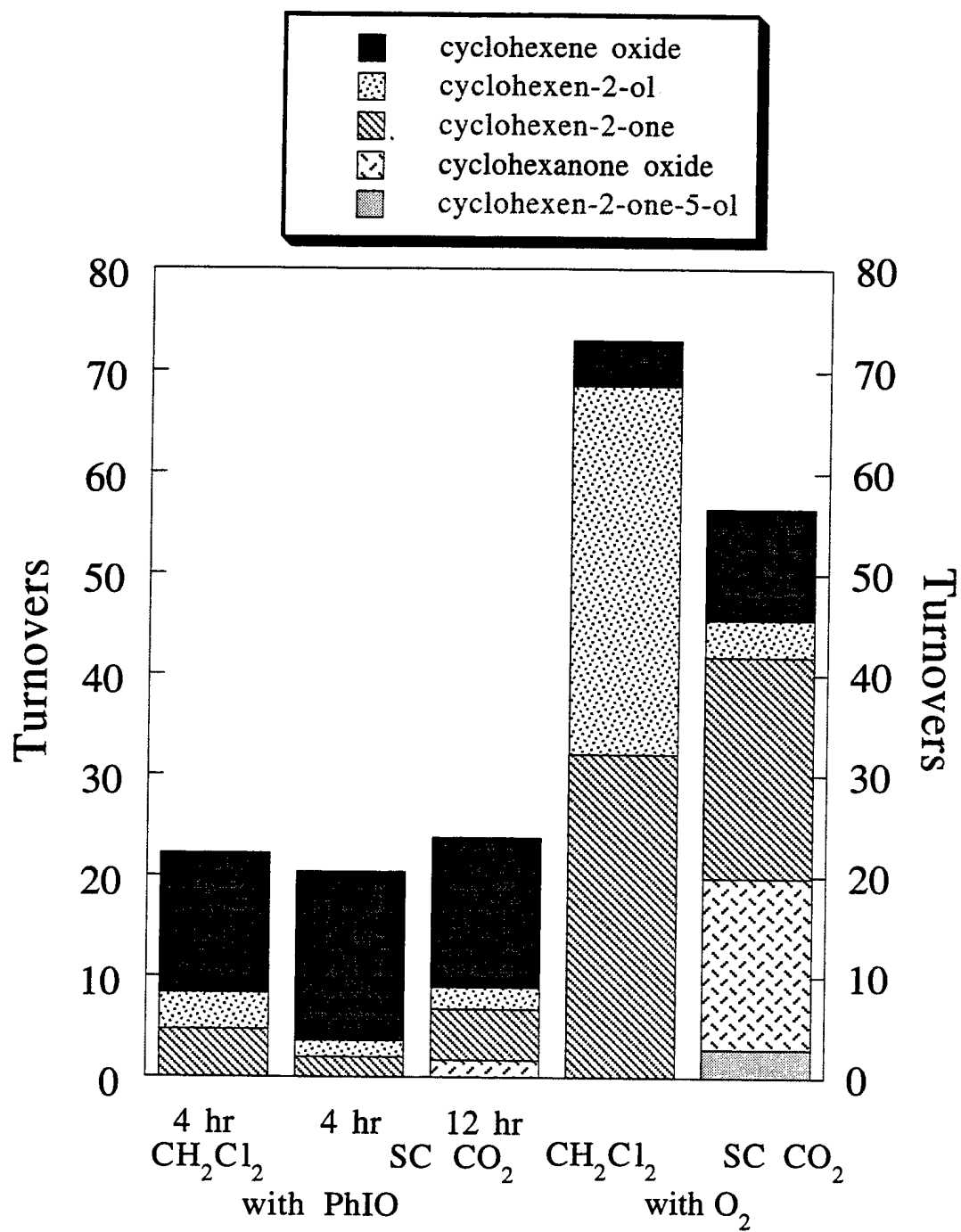


Figure 6.12 -- Turnovers of cyclohexene observed in oxidation reactions with $\text{RuTFPPCl}_8(\text{CO})$ and either iodosobenzene (left) or dioxygen (right). PhIO data is after 4 hours, and the dioxygen results are at 24 hours (CH_2Cl_2) or 12 hours (SC CO_2) in the different solvents. Higher selectivity for epoxide formation is observed with PhIO in SC CO_2 relative to CH_2Cl_2 . The dioxygen reactions are not as effective in the supercritical solvent.

- cyclohexene oxide
- ▤ 2-cyclohexen-1-ol
- ▨ 2-cyclohexen-1-one
- ▧ 7-oxa-bicylo[4.1.0]-heptan-2-one
- ▩ 4-hydroxy-2-cyclohexen-1-one

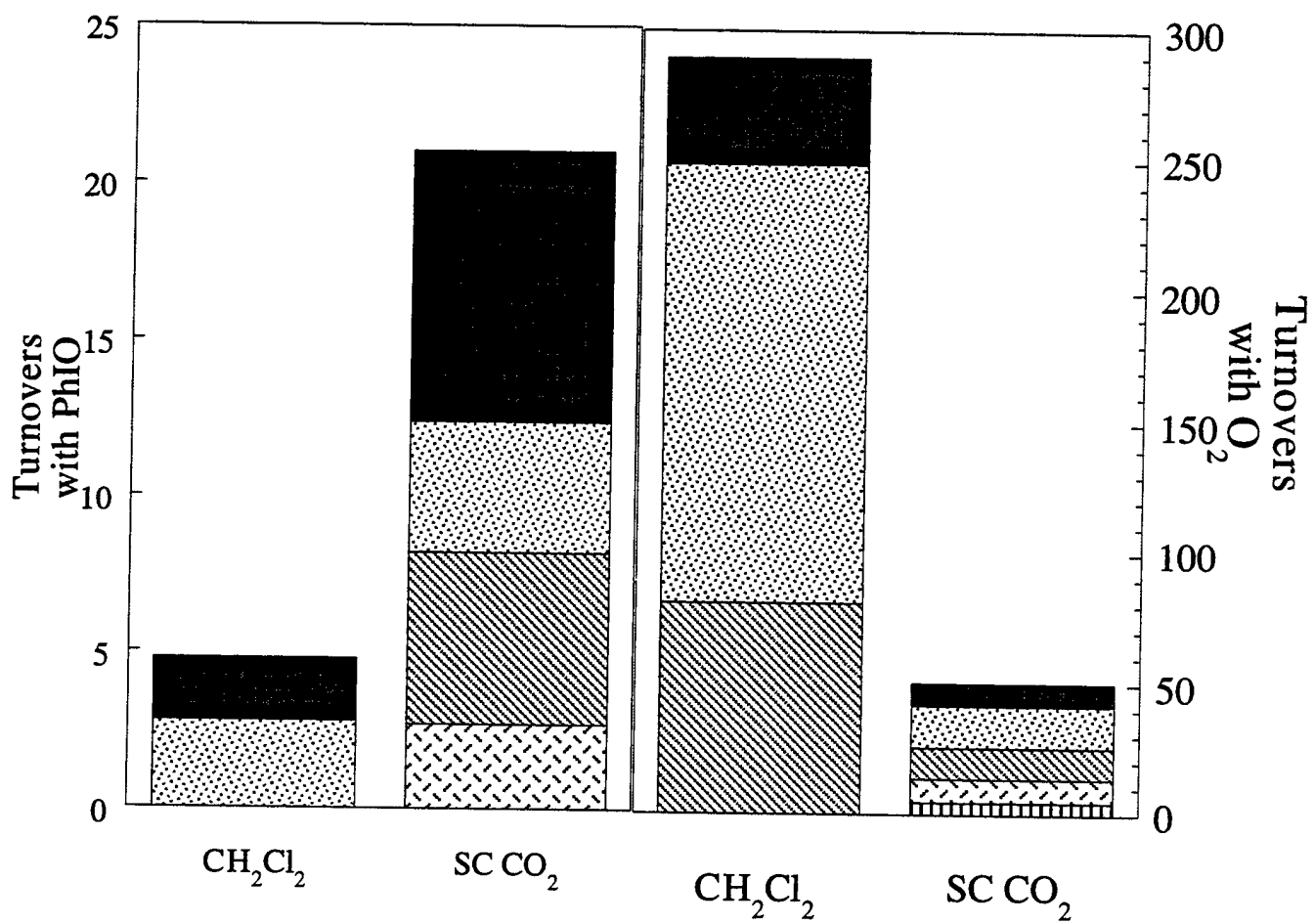
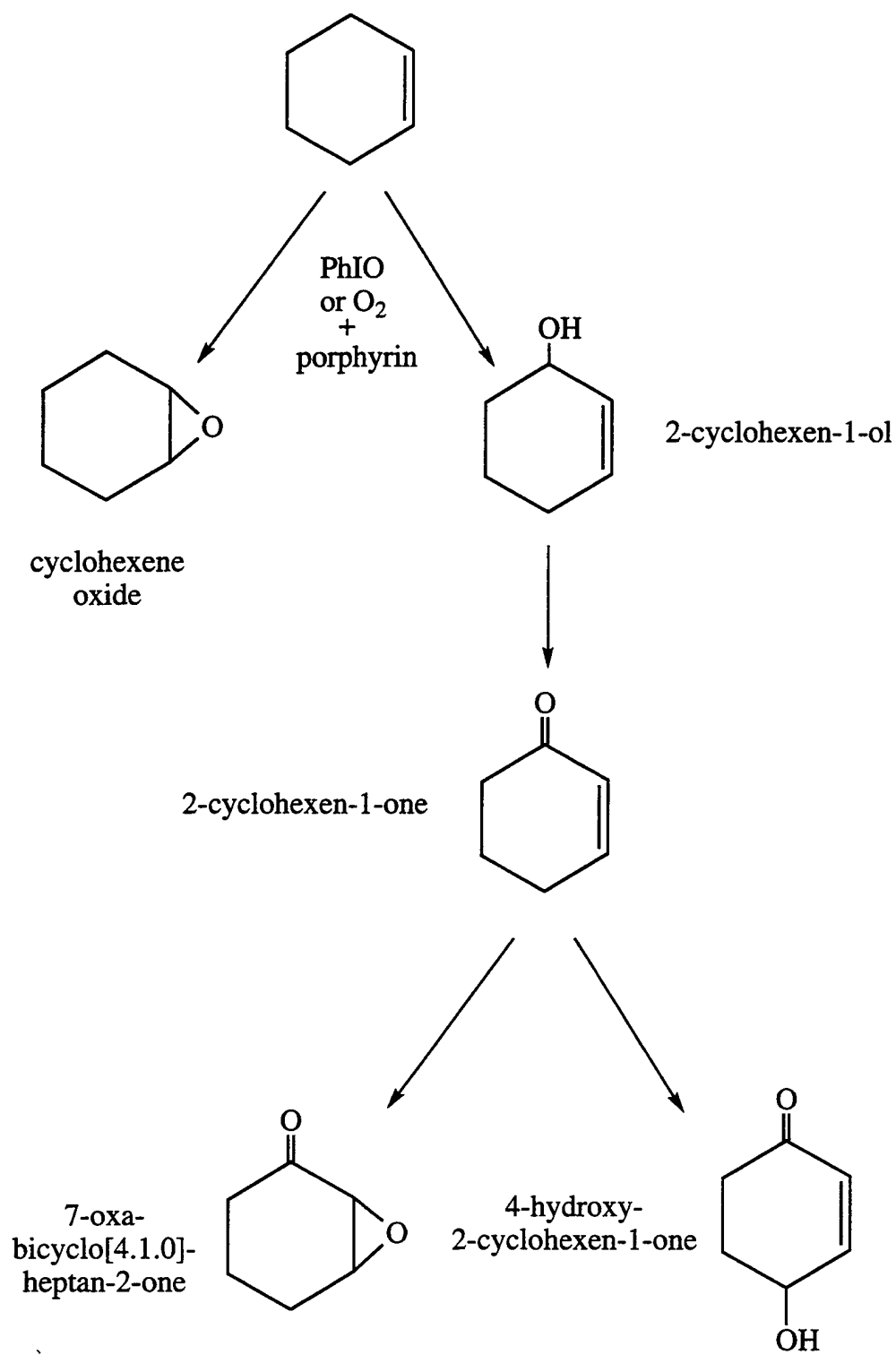
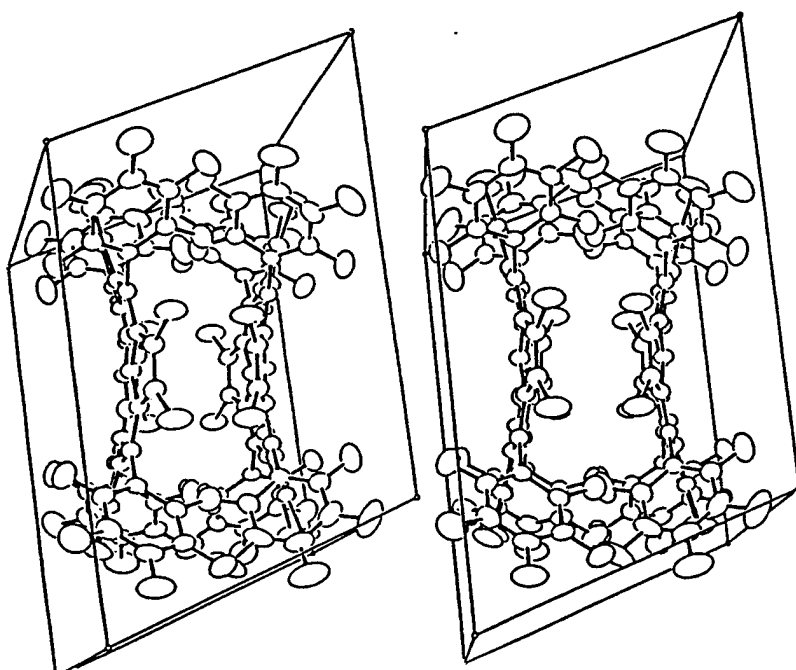
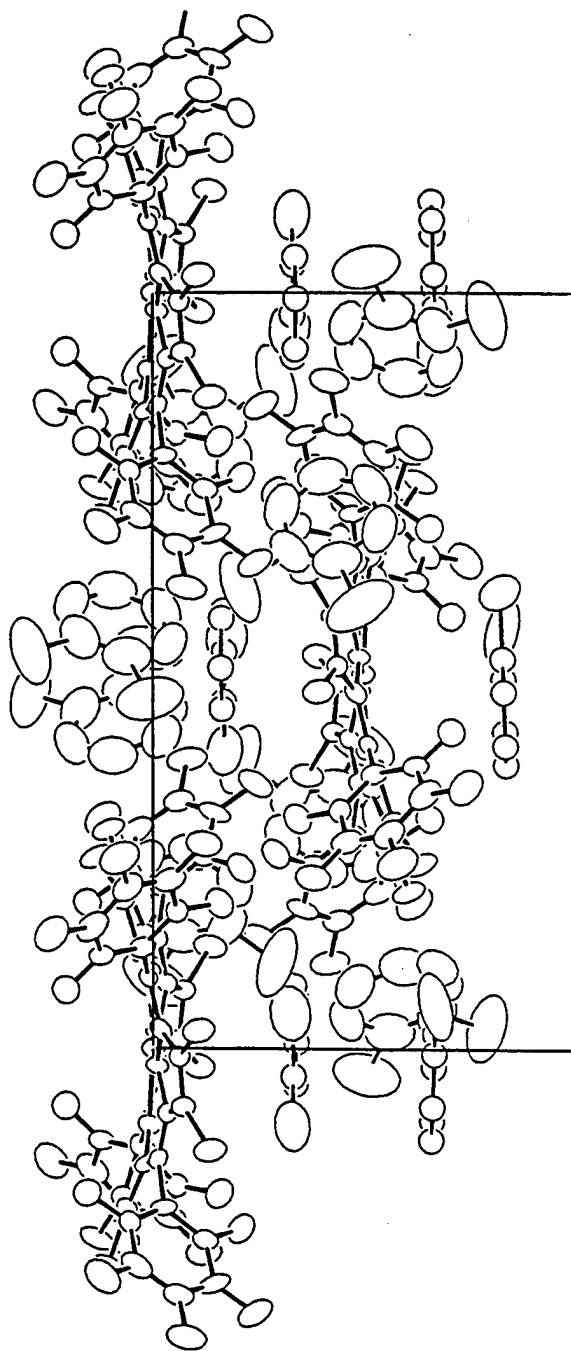


Figure 6.13 -- Partitioning mechanism to higher oxidation products.



Appendix 2
Crystal Structure Data





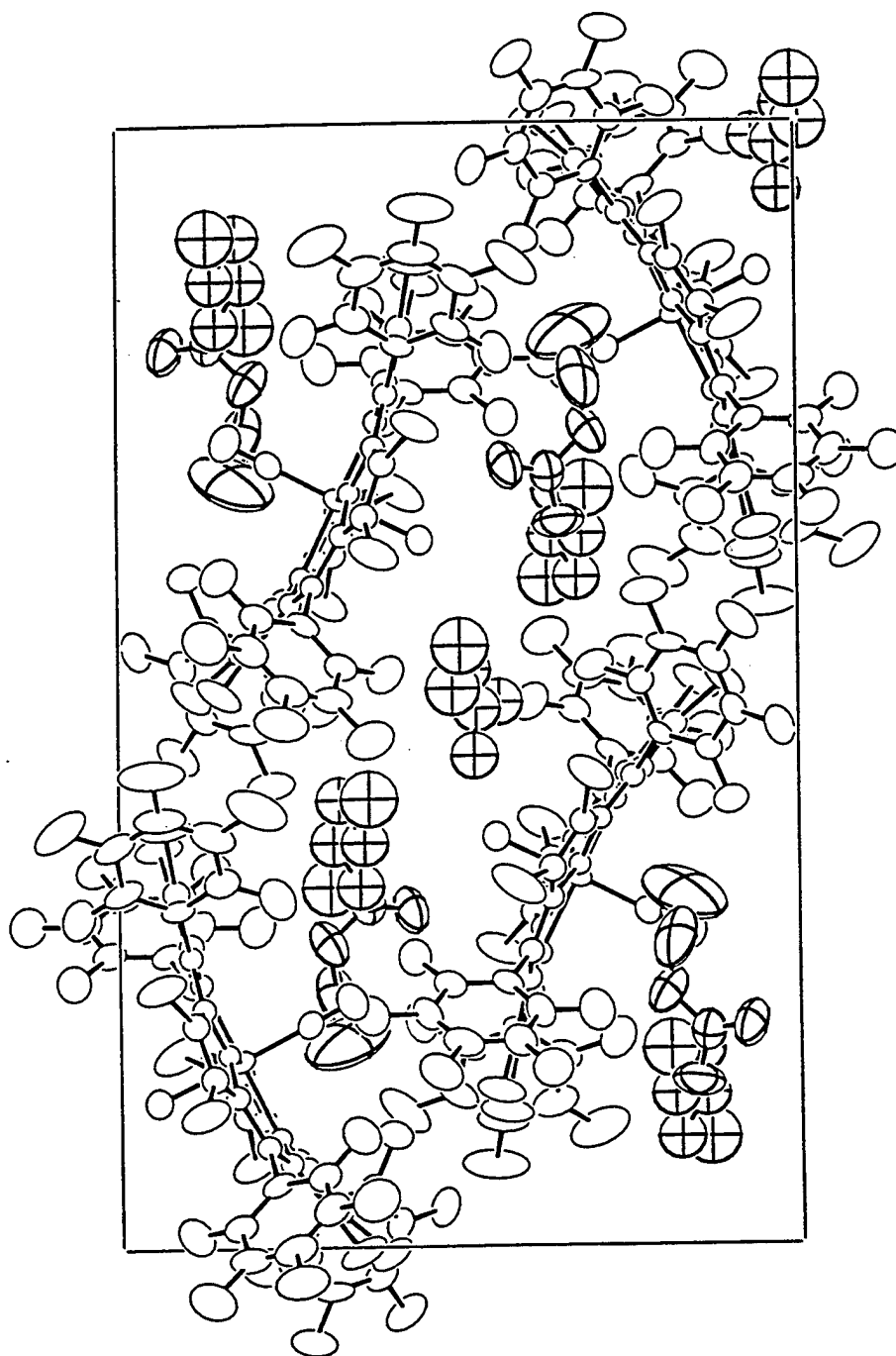


Table 1. Final Heavy Atom Parameters for
Tetrakis(pentafluorophenyl)- β -octachloroporphyrin

Atom	x, y, z and $U_{eq}^a \times 10^4$			
	x	y	z	U_{eq}
Cl1	8772(1)	7676(1)	3695(1)	599(2)
Cl2	9105(1)	7909(1)	5768(1)	564(2)
Cl3	7030(1)	6297(1)	9358(1)	649(3)
Cl4	6863(1)	4203(1)	9784(1)	565(3)
Cl5	8296(1)	666(1)	7251(1)	551(2)
Cl6	8017(1)	388(1)	5189(1)	594(3)
Cl7	5875(1)	3260(1)	2544(1)	610(2)
Cl8	6089(1)	5349(1)	2107(1)	588(2)
N1	7751(2)	5801(2)	5404(2)	322(6)
N2	7639(2)	4666(2)	7079(2)	303(6)
N3	7448(2)	3089(2)	5970(2)	292(6)
N4	7218(2)	4335(2)	4383(2)	311(6)
C1	7855(3)	6171(2)	4534(2)	305(6)
C2	8351(3)	6968(2)	4569(2)	347(7)
C3	8477(3)	7076(2)	5450(2)	349(7)
C4	8058(3)	6354(2)	6001(2)	318(7)
C5	7890(3)	6276(2)	6972(2)	315(7)
C6	7600(3)	5516(2)	7474(2)	305(7)
C7	7306(3)	5446(2)	8484(2)	346(7)
C8	7231(3)	4562(2)	8666(2)	335(7)

Table 1. (Cont.)

Atom	x	y	z	U_{eq}
C9	7464(3)	4046(2)	7771(2)	295(7)
C10	7580(3)	3079(2)	7622(2)	285(6)
C11	7659(3)	2624(2)	6766(2)	287(6)
C12	7889(3)	1611(2)	6566(2)	308(7)
C13	7771(3)	1499(2)	5684(2)	318(7)
C14	7451(3)	2439(2)	5303(2)	278(6)
C15	7112(3)	2674(2)	4449(2)	298(7)
C16	6922(3)	3579(2)	4059(2)	310(6)
C17	6483(3)	3861(2)	3212(2)	349(7)
C18	6571(3)	4745(2)	3031(2)	350(7)
C19	7080(3)	5043(2)	3756(2)	304(7)
C20	7459(3)	5865(2)	3788(2)	299(7)
C21	7988(3)	7087(2)	7529(2)	313(7)
C22	6947(3)	7927(2)	7798(2)	356(7)
C23	6998(3)	8682(2)	8311(2)	417(9)
C24	8127(4)	8587(2)	8595(2)	454(9)
C25	9175(3)	7759(2)	8359(2)	444(8)
C26	9107(3)	7027(2)	7820(2)	390(8)
C31	7581(3)	2476(2)	8462(2)	287(6)
C32	8712(3)	2034(2)	8757(2)	346(7)

Table 1. (Cont.)

Atom	x	y	z	U_{eq}
C33	8719(3)	1485(2)	9522(2)	412(8)
C34	7567(4)	1361(2)	10009(2)	491(10)
C35	6431(3)	1784(2)	9738(2)	465(9)
C36	6446(3)	2343(2)	8980(2)	368(7)
C41	7026(3)	1869(2)	3882(2)	313(7)
C42	8108(3)	1325(2)	3209(2)	388(7)
C43	8109(4)	554(2)	2699(2)	516(9)
C44	7008(4)	292(2)	2873(3)	572(10)
C45	5909(4)	799(3)	3536(3)	573(9)
C46	5909(3)	1603(2)	4018(2)	426(8)
C51	7431(3)	6472(2)	2950(2)	306(6)
C52	8481(3)	6277(2)	2166(2)	387(8)
C53	8433(4)	6815(3)	1389(2)	478(9)
C54	7343(4)	7583(3)	1397(2)	488(9)
C55	6295(3)	7816(2)	2163(3)	454(9)
C56	6344(3)	7253(2)	2920(2)	357(7)
F22	5813(2)	8012(1)	7569(1)	587(5)
F23	5974(2)	9491(1)	8548(2)	679(6)
F24	8193(2)	9314(1)	9096(1)	721(6)
F25	10283(2)	7663(2)	8629(2)	740(6)

Table 1. (Cont.)

Atom	x	y	z	U_{eq}
F26	10183(2)	6251(1)	7549(2)	661(6)
F32	9855(2)	2125(1)	8267(1)	526(5)
F33	9839(2)	1063(1)	9778(1)	670(6)
F34	7552(2)	820(2)	10752(1)	833(7)
F35	5305(2)	1658(2)	10213(2)	825(7)
F36	5305(2)	2795(1)	8753(1)	560(5)
F42	9238(2)	1523(2)	3072(1)	628(6)
F43	9185(2)	56(2)	2043(2)	916(7)
F44	7005(3)	-470(2)	2384(2)	1022(8)
F45	4818(3)	549(2)	3707(2)	985(7)
F46	4808(2)	2121(2)	4628(2)	765(7)
F52	9591(2)	5562(1)	2157(1)	677(6)
F53	9461(2)	6597(2)	639(1)	827(7)
F54	7293(3)	8122(2)	650(2)	864(7)
F55	5208(2)	8568(1)	2179(2)	750(6)
F56	5271(2)	7458(1)	3637(1)	627(6)

$$^a U_{eq} = \frac{1}{3} \sum_i \sum_j [U_{ij}(a_i^* a_j^*)(\vec{a}_i \cdot \vec{a}_j)]$$

Table 2. Selected Distances and Angles for
Tetrakis(pentafluorophenyl)- β -octachloroporphyrin

Distance(Å)		Distance(Å)	
C11 -C2	1.706(3)	C4 -C5	1.400(4)
C12 -C3	1.705(3)	C5 -C6	1.404(4)
C13 -C7	1.708(3)	C6 -C7	1.449(4)
C14 -C8	1.708(3)	C7 -C8	1.341(4)
C15 -C12	1.702(3)	C8 -C9	1.453(4)
C16 -C13	1.706(3)	C9 -C10	1.396(4)
C17 -C17	1.708(3)	C10 -C11	1.402(4)
C18 -C18	1.706(3)	C11 -C12	1.445(4)
N1 -C1	1.372(4)	C12 -C13	1.350(4)
N1 -C4	1.372(4)	C13 -C14	1.446(4)
N2 -C6	1.366(4)	C14 -C15	1.399(4)
N2 -C9	1.370(4)	C15 -C16	1.407(4)
N3 -C11	1.373(4)	C16 -C17	1.448(4)
N3 -C14	1.377(4)	C17 -C18	1.346(4)
N4 -C16	1.373(4)	C18 -C19	1.450(4)
N4 -C19	1.369(4)	C19 -C20	1.400(4)
C1 -C2	1.446(4)		
C1 -C20	1.404(4)		
C2 -C3	1.350(4)		
C3 -C4	1.445(4)		

Table 2. (Cont.)

		Angle(°)			Angle(°)
C4	-N1 -C1	109.9(2)	C6	-C7 -Cl3	129.5(2)
C9	-N2 -C6	109.4(2)	C8	-C7 -Cl3	122.2(2)
C14	-N3 -C11	109.5(2)	C8	-C7 -C6	108.3(3)
C19	-N4 -C16	109.1(2)	C7	-C8 -Cl4	122.6(2)
C2	-C1 -N1	106.8(2)	C9	-C8 -Cl4	129.8(2)
C20	-C1 -N1	125.4(3)	C9	-C8 -C7	107.6(3)
C20	-C1 -C2	127.6(3)	C8	-C9 -N2	107.4(2)
C1	-C2 -Cl1	129.4(2)	C10	-C9 -N2	125.4(3)
C3	-C2 -Cl1	122.5(2)	C10	-C9 -C8	127.1(3)
C3	-C2 -C1	108.1(3)	C11	-C10 -C9	126.0(3)
C2	-C3 -Cl2	122.7(2)	C10	-C11 -N3	125.1(3)
C4	-C3 -Cl2	129.2(2)	C12	-C11 -N3	107.2(2)
C4	-C3 -C2	108.0(3)	C12	-C11 -C10	127.6(3)
C3	-C4 -N1	106.9(2)	C11	-C12 -Cl5	129.2(2)
C5	-C4 -N1	125.9(3)	C13	-C12 -Cl5	122.7(2)
C5	-C4 -C3	127.0(3)	C13	-C12 -C11	108.1(2)
C6	-C5 -C4	125.6(3)	C12	-C13 -Cl6	121.5(2)
C5	-C6 -N2	125.1(3)	C14	-C13 -Cl6	130.4(2)
C7	-C6 -N2	107.3(2)	C14	-C13 -C12	108.0(3)
C7	-C6 -C5	127.4(3)	C13	-C14 -N3	107.1(2)

Table 2. (Cont.)

Angle(°)	
C15 -C14 -N3	125.5(2)
C15 -C14 -C13	127.3(3)
C16 -C15 -C14	125.8(3)
C15 -C16 -N4	125.5(3)
C17 -C16 -N4	107.5(2)
C17 -C16 -C15	126.9(3)
C16 -C17 -C17	129.1(2)
C18 -C17 -C17	122.9(2)
C18 -C17 -C16	107.9(3)
C17 -C18 -C18	122.2(2)
C19 -C18 -C18	130.0(2)
C19 -C18 -C17	107.8(3)
C18 -C19 -N4	107.6(2)
C20 -C19 -N4	125.3(3)
C20 -C19 -C18	127.0(3)
C19 -C20 -C1	125.6(3)

Table S1. Anisotropic Displacement Parameters for
Tetrakis(pentafluorophenyl)- β -octachloroporphyrin

Atom	U_{11}	U_{22}	U_{33}	U_{12}	U_{13}	U_{23}
Cl1	990(8)	710(6)	410(5)	-647(6)	-262(5)	235(4)
Cl2	906(7)	624(6)	459(5)	-589(5)	-259(5)	119(4)
Cl3	1245(9)	425(5)	309(5)	-384(5)	-93(5)	-55(4)
Cl4	1022(8)	439(5)	247(4)	-315(5)	-78(4)	41(4)
Cl5	979(7)	284(4)	484(5)	-179(4)	-401(5)	126(4)
Cl6	1110(8)	252(4)	520(5)	-199(5)	-417(5)	35(4)
Cl7	1028(8)	488(5)	657(6)	-422(5)	-616(6)	178(4)
Cl8	1017(8)	492(5)	554(6)	-402(5)	-552(5)	253(4)
N1	476(16)	288(13)	286(14)	-200(12)	-150(12)	53(11)
N2	421(15)	286(13)	235(13)	-146(11)	-102(12)	13(11)
N3	399(15)	245(13)	269(13)	-126(11)	-127(11)	41(11)
N4	459(16)	271(13)	275(14)	-164(12)	-166(12)	43(11)
C1	385(18)	312(16)	283(16)	-166(14)	-133(14)	53(13)
C2	443(19)	359(17)	320(17)	-226(15)	-118(15)	81(13)
C3	436(19)	323(16)	384(18)	-220(15)	-147(15)	52(14)
C4	408(18)	283(16)	327(17)	-171(14)	-134(14)	49(13)
C5	385(18)	282(16)	328(17)	-146(14)	-132(14)	21(13)
C6	364(18)	274(16)	307(16)	-118(13)	-118(14)	12(13)
C7	468(19)	310(17)	261(16)	-126(14)	-89(14)	-21(13)
C8	427(19)	333(17)	255(16)	-138(14)	-85(14)	40(13)
C9	369(18)	302(16)	236(15)	-129(13)	-93(13)	40(13)
C10	329(17)	293(16)	262(16)	-121(13)	-106(13)	65(12)
C11	301(16)	286(16)	296(16)	-111(13)	-98(13)	60(13)
C12	367(17)	250(15)	338(17)	-113(13)	-131(14)	82(13)
C13	382(18)	258(15)	344(17)	-117(13)	-129(14)	11(13)
C14	318(17)	250(15)	286(16)	-100(13)	-102(13)	12(12)
C15	327(17)	279(16)	311(16)	-122(13)	-91(13)	-2(13)
C16	393(18)	311(16)	287(16)	-159(14)	-135(14)	25(13)
C17	453(19)	343(17)	334(17)	-158(15)	-213(15)	23(13)
C18	451(19)	325(17)	346(17)	-152(15)	-200(15)	100(13)
C19	376(18)	302(16)	280(16)	-142(14)	-126(14)	49(13)
C20	326(17)	299(16)	286(16)	-108(13)	-99(13)	64(12)
C21	425(19)	281(16)	295(16)	-172(14)	-128(14)	44(13)
C22	386(19)	362(18)	404(18)	-200(15)	-150(15)	80(14)
C23	540(22)	253(17)	422(19)	-137(16)	-41(17)	10(14)
C24	740(26)	390(20)	363(19)	-338(19)	-166(18)	10(15)
C25	546(22)	522(22)	432(20)	-299(19)	-264(17)	94(16)
C26	484(21)	316(17)	391(18)	-123(16)	-158(16)	36(14)
C31	399(18)	260(15)	243(15)	-139(13)	-116(14)	42(12)

Table S1. (Cont.)

Atom	U_{11}	U_{22}	U_{33}	U_{12}	U_{13}	U_{23}
C32	411(20)	330(17)	319(17)	-135(15)	-112(15)	13(14)
C33	522(22)	367(18)	347(18)	-51(16)	-239(17)	36(14)
C34	745(27)	373(19)	293(18)	-116(18)	-116(18)	140(15)
C35	490(22)	441(20)	406(20)	-181(17)	29(17)	128(16)
C36	385(19)	330(17)	401(19)	-107(15)	-135(16)	76(14)
C41	413(19)	298(16)	300(16)	-157(14)	-169(15)	45(13)
C42	460(21)	385(18)	381(18)	-145(16)	-207(16)	2(15)
C43	599(24)	436(20)	461(21)	17(19)	-279(19)	-124(17)
C44	871(31)	346(20)	657(26)	-228(21)	-437(24)	-20(18)
C45	745(28)	633(25)	678(26)	-512(23)	-420(23)	217(21)
C46	450(21)	481(20)	416(19)	-219(17)	-145(17)	55(16)
C51	389(18)	301(16)	285(16)	-169(14)	-112(14)	45(13)
C52	387(19)	396(18)	395(19)	-131(16)	-123(16)	28(15)
C53	566(23)	618(23)	307(19)	-332(20)	-22(17)	37(17)
C54	789(28)	526(22)	377(20)	-421(21)	-299(20)	215(17)
C55	559(23)	300(18)	625(24)	-154(17)	-359(20)	105(16)
C56	381(19)	335(17)	376(18)	-122(15)	-124(16)	25(14)
F22	486(12)	505(12)	829(15)	-148(10)	-287(11)	16(10)
F23	746(15)	350(11)	807(15)	-90(11)	-59(12)	-71(10)
F24	1212(19)	508(12)	648(13)	-470(13)	-342(13)	-83(10)
F25	833(16)	822(15)	872(16)	-431(13)	-559(13)	86(12)
F26	543(13)	518(12)	906(16)	-45(10)	-317(12)	-74(11)
F32	403(11)	650(13)	584(12)	-227(10)	-160(10)	108(10)
F33	760(15)	639(13)	603(13)	-28(11)	-433(12)	82(10)
F34	1148(19)	766(15)	455(12)	-179(14)	-165(12)	367(11)
F35	685(15)	841(16)	814(16)	-298(13)	111(13)	347(13)
F36	402(11)	624(12)	681(13)	-178(10)	-181(10)	186(10)
F42	434(12)	861(15)	598(13)	-242(11)	-87(10)	-140(11)
F43	807(17)	874(17)	819(16)	178(14)	-324(14)	-470(14)
F44	1617(25)	521(14)	1228(21)	-413(15)	-803(19)	-154(13)
F45	1173(21)	1190(20)	1143(20)	-981(18)	-508(17)	282(16)
F46	526(14)	1098(18)	679(15)	-393(13)	21(12)	-121(13)
F52	472(12)	650(13)	701(14)	4(11)	-17(10)	13(11)
F53	941(17)	1098(18)	423(13)	-532(15)	142(12)	7(12)
F54	1436(22)	877(16)	590(14)	-641(16)	-494(14)	462(12)
F55	817(16)	459(12)	1065(18)	-88(11)	-575(14)	203(11)
F56	442(12)	663(13)	621(13)	-62(10)	-7(11)	5(10)

$U_{i,j}$ values have been multiplied by 10^4

The form of the displacement factor is:

$$\exp -2\pi^2(U_{11}h^2a^{*2} + U_{22}k^2b^{*2} + U_{33}l^2c^{*2} + 2U_{12}hka^*b^* + 2U_{13}hla^*c^* + 2U_{23}klb^*c^*)$$

Table S2. Hydrogen Atom Parameters for
Tetrakis(pentafluorophenyl)- β -octachloroporphyrin

Atom	x, y and $z \times 10^4$			B
	x	y	z	
H1	7559(53)	5227(40)	5567(38)	3.0
H2	7773(55)	4537(41)	6517(41)	2.9
H3	7317(51)	3747(40)	5918(37)	2.8
H4	7414(55)	4351(40)	4900(40)	2.9

All atoms have a population factor of one-half.

Table S3. Complete Distances and Angles for
Tetrakis(pentafluorophenyl)- β -octachloroporphyrin

Distance(Å)		Distance(Å)	
C11 -C2	1.706(3)	C15 -C41	1.496(4)
C12 -C3	1.705(3)	C16 -C17	1.448(4)
C13 -C7	1.708(3)	C17 -C18	1.346(4)
C14 -C8	1.708(3)	C18 -C19	1.450(4)
C15 -C12	1.702(3)	C19 -C20	1.400(4)
C16 -C13	1.706(3)	C20 -C51	1.506(4)
C17 -C17	1.708(3)	C21 -C22	1.373(4)
C18 -C18	1.706(3)	C21 -C26	1.381(4)
N1 -C1	1.372(4)	C22 -C23	1.372(4)
N1 -C4	1.372(4)	C22 -F22	1.343(4)
N1 -H1	0.94(6)	C23 -C24	1.375(5)
N2 -C6	1.366(4)	C23 -F23	1.331(4)
N2 -C9	1.370(4)	C24 -C25	1.361(5)
N2 -H2	0.82(6)	C24 -F24	1.335(4)
N3 -C11	1.373(4)	C25 -C26	1.375(5)
N3 -C14	1.377(4)	C25 -F25	1.342(4)
N3 -H3	0.93(6)	C26 -F26	1.337(4)
N4 -C16	1.373(4)	C31 -C32	1.380(4)
N4 -C19	1.369(4)	C31 -C36	1.373(4)
N4 -H4	0.84(6)	C32 -C33	1.370(4)
C1 -C2	1.446(4)	C32 -F32	1.342(3)
C1 -C20	1.404(4)	C33 -C34	1.369(5)
C2 -C3	1.350(4)	C33 -F33	1.335(4)
C3 -C4	1.445(4)	C34 -C35	1.363(5)
C4 -C5	1.400(4)	C34 -F34	1.336(4)
C5 -C6	1.404(4)	C35 -C36	1.368(5)
C5 -C21	1.500(4)	C35 -F35	1.340(4)
C6 -C7	1.449(4)	C36 -F36	1.343(4)
C7 -C8	1.341(4)	C41 -C42	1.374(4)
C8 -C9	1.453(4)	C41 -C46	1.380(4)
C9 -C10	1.396(4)	C42 -C43	1.365(5)
C10 -C11	1.402(4)	C42 -F42	1.341(4)
C10 -C31	1.503(4)	C43 -C44	1.359(5)
C11 -C12	1.445(4)	C43 -F43	1.339(4)
C12 -C13	1.350(4)	C44 -C45	1.362(6)
C13 -C14	1.446(4)	C44 -F44	1.338(5)
C14 -C15	1.399(4)	C45 -C46	1.385(5)
C15 -C16	1.407(4)	C45 -F45	1.337(5)

Table S3. (Cont.)

Distance(Å)		Angle(°)	
C46 -F46	1.329(4)	C4 -N1 -C1	109.9(2)
C51 -C52	1.382(4)	H1 -N1 -C1	125.9(35)
C51 -C56	1.377(4)	H1 -N1 -C4	124.1(35)
C52 -C53	1.377(5)	C9 -N2 -C6	109.4(2)
C52 -F52	1.331(4)	H2 -N2 -C6	125.7(42)
C53 -C54	1.357(5)	H2 -N2 -C9	124.9(42)
C53 -F53	1.336(4)	C14 -N3 -C11	109.5(2)
C54 -C55	1.362(5)	H3 -N3 -C11	123.1(35)
C54 -F54	1.341(4)	H3 -N3 -C14	127.4(35)
C55 -C56	1.373(5)	C19 -N4 -C16	109.1(2)
C55 -F55	1.341(4)	H4 -N4 -C16	123.6(40)
C56 -F56	1.337(4)	H4 -N4 -C19	127.3(41)
		C2 -C1 -N1	106.8(2)
		C20 -C1 -N1	125.4(3)
		C20 -C1 -C2	127.6(3)
		C1 -C2 -Cl1	129.4(2)
		C3 -C2 -Cl1	122.5(2)
		C3 -C2 -C1	108.1(3)
		C2 -C3 -Cl2	122.7(2)
		C4 -C3 -Cl2	129.2(2)
		C4 -C3 -C2	108.0(3)
		C3 -C4 -N1	106.9(2)
		C5 -C4 -N1	125.9(3)
		C5 -C4 -C3	127.0(3)
		C6 -C5 -C4	125.6(3)
		C21 -C5 -C4	117.3(2)
		C21 -C5 -C6	117.1(2)
		C5 -C6 -N2	125.1(3)
		C7 -C6 -N2	107.3(2)
		C7 -C6 -C5	127.4(3)
		C6 -C7 -Cl3	129.5(2)
		C8 -C7 -Cl3	122.2(2)
		C8 -C7 -C6	108.3(3)
		C7 -C8 -Cl4	122.6(2)
		C9 -C8 -Cl4	129.8(2)
		C9 -C8 -C7	107.6(3)
		C8 -C9 -N2	107.4(2)
		C10 -C9 -N2	125.4(3)

Table S3. (Cont.)

Angle(°)		Angle(°)	
C10 -C9 -C8	127.1(3)	F22 -C22 -C21	118.9(3)
C11 -C10 -C9	126.0(3)	F22 -C22 -C23	118.0(3)
C31 -C10 -C9	117.0(2)	C24 -C23 -C22	118.8(3)
C31 -C10 -C11	116.9(2)	F23 -C23 -C22	121.3(3)
C10 -C11 -N3	125.1(3)	F23 -C23 -C24	119.9(3)
C12 -C11 -N3	107.2(2)	C25 -C24 -C23	120.1(3)
C12 -C11 -C10	127.6(3)	F24 -C24 -C23	119.6(3)
C11 -C12 -C15	129.2(2)	F24 -C24 -C25	120.3(3)
C13 -C12 -C15	122.7(2)	C26 -C25 -C24	119.7(3)
C13 -C12 -C11	108.1(2)	F25 -C25 -C24	120.5(3)
C12 -C13 -C16	121.5(2)	F25 -C25 -C26	119.8(3)
C14 -C13 -C16	130.4(2)	C25 -C26 -C21	122.2(3)
C14 -C13 -C12	108.0(3)	F26 -C26 -C21	119.7(3)
C13 -C14 -N3	107.1(2)	F26 -C26 -C25	118.1(3)
C15 -C14 -N3	125.5(2)	C32 -C31 -C10	122.1(3)
C15 -C14 -C13	127.3(3)	C36 -C31 -C10	121.4(3)
C16 -C15 -C14	125.8(3)	C36 -C31 -C32	116.5(3)
C41 -C15 -C14	116.5(2)	C33 -C32 -C31	122.4(3)
C41 -C15 -C16	117.7(2)	F32 -C32 -C31	119.1(3)
C15 -C16 -N4	125.5(3)	F32 -C32 -C33	118.5(3)
C17 -C16 -N4	107.5(2)	C34 -C33 -C32	119.0(3)
C17 -C16 -C15	126.9(3)	F33 -C33 -C32	120.4(3)
C16 -C17 -C17	129.1(2)	F33 -C33 -C34	120.6(3)
C18 -C17 -C17	122.9(2)	C35 -C34 -C33	120.3(3)
C18 -C17 -C16	107.9(3)	F34 -C34 -C33	120.1(3)
C17 -C18 -C18	122.2(2)	F34 -C34 -C35	119.6(3)
C19 -C18 -C18	130.0(2)	C36 -C35 -C34	119.6(3)
C19 -C18 -C17	107.8(3)	F35 -C35 -C34	120.2(3)
C18 -C19 -N4	107.6(2)	F35 -C35 -C36	120.2(3)
C20 -C19 -N4	125.3(3)	C35 -C36 -C31	122.2(3)
C20 -C19 -C18	127.0(3)	F36 -C36 -C31	119.0(3)
C19 -C20 -C1	125.6(3)	F36 -C36 -C35	118.7(3)
C51 -C20 -C1	117.4(2)	C42 -C41 -C15	120.2(3)
C51 -C20 -C19	117.0(2)	C46 -C41 -C15	123.3(3)
C22 -C21 -C5	121.4(3)	C46 -C41 -C42	116.5(3)
C26 -C21 -C5	122.5(3)	C43 -C42 -C41	122.9(3)
C26 -C21 -C22	116.1(3)	F42 -C42 -C41	119.2(3)
C23 -C22 -C21	123.1(3)	F42 -C42 -C43	117.8(3)

Table S3. (Cont.)

Angle(°)	
C44 -C43 -C42	119.1(3)
F43 -C43 -C42	120.6(3)
F43 -C43 -C44	120.3(3)
C45 -C44 -C43	120.6(4)
F44 -C44 -C43	119.6(3)
F44 -C44 -C45	119.9(4)
C46 -C45 -C44	119.4(4)
F45 -C45 -C44	121.0(4)
F45 -C45 -C46	119.6(3)
C45 -C46 -C41	121.4(3)
F46 -C46 -C41	119.8(3)
F46 -C46 -C45	118.8(3)
C52 -C51 -C20	122.2(3)
C56 -C51 -C20	121.6(3)
C56 -C51 -C52	116.2(3)
C53 -C52 -C51	122.0(3)
F52 -C52 -C51	119.9(3)
F52 -C52 -C53	118.1(3)
C54 -C53 -C52	119.5(3)
F53 -C53 -C52	120.3(3)
F53 -C53 -C54	120.1(3)
C55 -C54 -C53	120.5(3)
F54 -C54 -C53	120.1(3)
F54 -C54 -C55	119.4(3)
C56 -C55 -C54	119.2(3)
F55 -C55 -C54	121.2(3)
F55 -C55 -C56	119.6(3)
C55 -C56 -C51	122.6(3)
F56 -C56 -C51	119.4(3)
F56 -C56 -C55	118.1(3)

**Table S4. Observed and Calculated Structure Factors for
Tetrakis(pentafluorophenyl)- β -octachloroporphyrin**

The columns contain, in order, ℓ , $10F_{obs}$, $10F_{calc}$ and $10\sigma F_{obs}$. A minus sign preceding F_{obs} indicates that F_{obs}^2 is negative.

Tetrakis(pentafluorophenyl)-beta-octachloroporphyrin

Page 1

-10	1	1	6	117	115	5	5	47	8	9	1	251	257	4
							6	99	105	6	2	142	145	4
							7	102	111	6	3	94	78	5
1	182	227	5	1	132	125	5	-7	6	1	4	131	122	4
2	-14	2	16	2	48	39	8	1	120	118	5	5	10	10
3	42	47	8	3	220	237	4	2	42	17	9	6	51	34
				4	203	203	5	3	96	87	5	7	20	35
-10	2	1		5	79	61	6	4	208	200	5	8	37	48
1	39	41	10	-8	5	1		5	162	160	5	-6	6	1
2	16	28	18					6	116	109	5	1	36	17
				1	60	48	7	-7	7	1		2	133	139
-10	3	1		2	53	29	8	1	79	87	6	3	93	93
1	80	63	6	3	188	189	5	2	232	240	4	4	285	271
				4	65	62	7	3	95	98	6	5	46	27
-9	1	1		-8	6	1		4	61	58	7	6	125	139
1	117	104	5	1	129	128	5	-7	8	1		7	73	72
2	56	31	7	2	149	149	5	1	-21	7	14	-6	7	1
3	142	132	5	3	76	57	7	2	61	88	7	1	249	261
4	-21	8	14	-8	7	1		3	58	77	7	2	33	50
5	11	17	21	1	115	117	5	-6	1	1		3	-29	1
6	73	42	7	-7	1	1		1	343	362	4	4	237	245
-9	2	1		1	26	17	10	2	347	349	4	5	121	117
1	50	31	7	2	46	59	7	3	199	185	4	6	46	43
2	23	46	13	3	84	76	5	4	184	183	4	-6	8	1
3	60	65	7	4	33	7	9	5	66	44	6	1	113	113
4	61	67	8	5	145	141	4	6	73	68	6	2	75	92
5	156	151	5	6	137	137	5	7	209	213	4	3	31	37
-9	3	1		7	54	75	8	8	121	112	5	4	43	39
1	84	81	6	8	73	81	7	9	37	23	11	5	53	21
2	54	47	8	9	-38	10	10	10	119	112	5	-6	9	1
3	71	71	7	-7	2	1		-6	2	1		1	105	124
4	60	77	8	1	111	108	4	1	264	272	4	2	57	61
-9	4	1		2	42	27	8	2	106	120	4	3	-43	6
1	65	88	7	3	284	296	4	3	206	212	4	-6	10	1
2	36	29	11	4	50	51	6	4	99	107	4	1	80	58
3	38	17	11	5	141	139	4	5	39	24	8	-5	1	1
-9	5	1		6	94	104	5	6	264	268	4	1	159	157
1	110	97	5	7	161	140	5	7	76	61	6	2	278	272
				8	67	42	7	8	78	69	6	3	521	517
-8	1	1		9	29	11	13	9	257	257	5	4	539	534
1	931	921	8	-7	3	1		10	47	58	9	5	73	55
2	278	278	4	1	192	194	4	-6	3	1		6	134	126
3	55	47	7	1	97	92	5	1	200	199	4	7	287	277
4	119	122	5	2	105	112	5	2	193	192	4	8	-12	3
5	40	24	8	3	192	190	4	3	125	125	4	9	328	328
6	152	155	5	4	38	29	9	4	233	236	4	10	68	71
7	98	97	6	5	170	162	5	5	111	132	5	11	84	75
8	5	15	26	6	31	5	11	6	166	177	4	12	107	100
-8	2	1		7	116	110	5	7	179	176	4	-5	2	1
1	116	86	4	-7	4	1		8	25	34	13	1	396	399
2	206	201	4	1	116	126	4	9	174	160	5	2	135	130
3	139	122	4	2	162	180	4	10	14	28	20	3	447	450
4	65	59	7	3	50	36	8	-6	4	1		4	230	228
5	12	16	19	4	198	208	4	1	50	26	6	5	41	32
6	196	192	5	5	161	162	4	2	59	17	5	6	289	282
7	130	129	5	6	158	161	5	3	151	148	4	7	32	33
				7	53	56	8	4	50	41	5	8	248	248
-8	3	1		-7	5	1		5	221	222	4	9	136	129
1	288	284	4	1	39	11	9	6	40	27	9	10	8	27
2	261	276	4	2	189	187	4	7	84	74	6	11	71	71
3	174	172	4	3	143	158	4	8	136	154	5	-5	3	1
4	100	85	5	4	70	53	6	9	46	29	8			
5	68	57	7					-6	5	1				

Tetrakis(pentafluorophenyl)-beta-octachloroporphyrin

Page 2

[illegible]

Tetrakis(pentafluorophenyl)-beta-octachloroporphyrin

Page 3

1	713	718	6	-3	13	1	6	297	291	4	1	108	120	5	
2	159	167	3				7	51	74	6	2	67	64	6	
3	84	68	4	1	207	206	5	9	98	88	5	3	63	50	7
4	234	232	4				10	57	64	7	4	330	338	5	
5	410	400	4	-2	1	1	11	66	79	7	5	5	226	220	4
6	151	153	4				12	232	233	5	6	44	15	9	5
7	72	73	6				13	21	7	16	7	158	138	5	5
8	170	187	4	1	1250	1234	10				8	279	260	5	
9	249	243	4				10								
10	135	120	5				-2	6	1		-2	12	1		
11	157	147	5												
-3	7	1					1	307	306	3					
1	388	375	4				2	83	78	4	1	145	150	4	
2	108	106	4				3	552	546	5	2	146	145	5	
3	-12	5	15				4	448	450	4	3	89	104	6	
4	230	230	4				5	57	53	5	4	91	86	6	
5	59	52	6				6	300	298	4	5	42	34	10	
6	231	230	4				7	143	142	4	6	50	65	9	
7	87	78	5				8	40	21	8					
8	139	133	5				9	47	43	8	-2	13	1		
9	54	47	8				10	135	133	5	1	82	80	6	
10	32	51	12				11	106	114	5	2	44	27	9	
11	66	68	7				12	11	4	21	3	101	83	6	
-3	8	1					-2	7	1		4	241	222	5	
1	177	179	4				1	46	38	6	-1	1	1		
2	108	102	4				2	92	87	4					
3	208	219	4				3	146	142	3	1	380	367	3	
4	299	307	4				4	181	181	3	2	729	715	6	
5	281	274	4				5	230	227	4	3	186	190	2	
6	73	60	6				6	232	230	4	4	422	432	4	
7	50	50	6				7	205	211	4	5	41	0	4	
8	193	181	4				8	248	251	4	6	163	163	3	
9	41	67	9				9	136	116	5	7	53	86	5	
10	-50	11	7				10	101	107	5	8	454	465	5	
-3	9	1					11	207	191	5	9	53	52	6	
1	283	265	4				-2	8	1		10	430	433	5	
2	173	169	4				1	-21	27	10	11	59	58	6	
3	167	168	4				2	66	72	5	12	144	139	4	
4	183	197	4				3	119	112	4	13	-46	6	7	
5	203	192	4				4	260	261	4	14	90	96	6	
6	-11	30	19				5	67	54	5	15	107	107	6	
7	86	65	7				6	449	433	5	-1	2	1		
8	115	107	5				7	30	12	11	1	122	125	2	
9	104	108	6				8	400	404	5	2	425	408	4	
-3	10	1					9	219	221	4	3	152	138	2	
1	251	250	4				10	56	49	8	4	783	795	7	
2	107	107	5				11	90	80	6	5	12	4	12	
3	310	307	4				-2	9	1		6	399	387	4	
4	159	132	4				1	149	147	4	7	95	105	4	
5	130	116	5				2	71	74	5	8	803	798	7	
6	84	77	6				3	35	44	8	9	927	926	8	
7	14	12	18				4	43	14	8	10	139	134	4	
8	65	35	7				5	44	21	8	11	280	289	4	
-3	11	1					6	87	87	5	12	307	295	4	
1	189	184	4				7	166	153	4	13	70	87	7	
2	203	199	4				8	157	155	5	14	91	92	6	
3	34	27	9				9	70	67	7	-1	3	1		
4	58	33	7				10	139	133	5	1	446	436	4	
5	32	35	11				-2	10	1		2	207	212	2	
6	129	126	5				1	28	37	9	3	214	212	3	
-3	12	1					2	101	103	5	4	378	385	4	
1	99	88	5				3	151	152	4	5	120	113	3	
2	205	206	5				4	173	167	4	6	31	21	7	
3	101	94	5				5	367	370	5	7	626	617	6	
4	170	157	5				6	138	125	5	8	193	194	3	
-3	12	1					7	243	246	4	9	55	54	6	
1	99	88	5				8	-27	7	12	10	139	142	4	
2	205	206	5				9	157	161	5	11	-36	16	9	
3	101	94	5				-2	11	1		12	318	323	5	
4	170	157	5								13	200	202	5	
											14	201	198	5	

Tetrakis(pentafluorophenyl)-beta-octachloroporphyrin

Page 4

[illegible]

Tetrakis(pentafluorophenyl)-beta-octachloroporphyrin

Page 5

1	770	766	6	-13	95	98	6	7	75	86	6	-3	73	73	6
2	202	200	3	-12	-26	38	11	8	65	69	7	-2	80	88	6
3	680	687	6	-11	122	129	5	9	250	252	4	-1	86	96	6
4	278	279	3	-10	-38	17	8	10	-38	12	9	0	126	121	5
5	389	409	4	-9	67	84	6	11	54	68	8	1	42	30	9
6	284	289	3	-8	258	257	4	0	11	1		2	50	47	8
7	230	231	3	-7	88	84	4	-11	196	191	5	3	171	160	5
8	102	111	4	-6	526	531	5	-10	107	115	5	4	250	238	5
9	227	219	4	-5	358	359	4	-9	-30	13	11	5	24	31	14
10	79	92	5	-4	494	496	5	-8	174	188	4	0	15	1	
11	231	229	4	-3	85	90	4	-7	-27	39	11	-3	124	122	5
12	209	216	4	-2	215	218	3	-6	195	195	4	-2	391	378	5
13	110	103	5	-1	29	38	7	-5	31	52	10	-1	50	67	9
14	25	50	14	0	417	426	4	-4	148	149	4	0	-49	19	7
0	6	1		1	15	27	12	-3	38	48	8	1	141	133	5
-14	166	161	5	2	55	44	5	-2	229	235	4	1	-14	1	
-13	134	133	5	3	425	416	4	-1	395	401	4	0	249	238	5
-12	-14	23	14	4	466	472	5	0	245	249	4	1	25	27	13
-11	339	339	4	5	293	290	4	1	15	35	13	2	108	112	5
-10	529	530	5	6	379	369	4	2	71	71	5	3	-34	25	9
-9	455	446	5	7	263	254	4	3	280	287	4	4	91	91	6
-8	37	76	7	8	331	332	4	4	249	245	4	5	147	130	5
-7	287	289	4	9	101	104	5	5	133	122	4	6	195	188	5
-6	60	50	5	10	139	125	5	6	258	256	4				
-5	300	293	3	11	149	154	5	7	128	136	5	1	-13	1	
-4	360	361	4	12	94	80	6	8	370	348	5	0	183	184	4
-3	435	419	4	0	9	1		9	49	14	7	1	214	220	4
-2	236	215	3	-13	128	140	5	10	56	37	8	2	143	150	5
-1	514	513	5	-12	58	75	8	0	12	1		3	178	166	4
0	348	345	3	-11	-24	30	13	-10	235	229	5	4	214	215	4
1	473	484	4	-10	-44	11	7	-9	58	78	7	5	158	137	5
2	302	316	3	-9	31	64	10	-8	116	121	5	6	157	147	5
3	219	230	3	-8	659	667	6	-7	133	138	5	7	464	456	5
4	220	233	3	-7	92	90	5	-6	189	188	4	8	87	95	6
5	50	18	5	-6	40	22	7	-5	215	218	4	1	-12	1	
6	529	530	5	-5	268	268	4	-4	404	406	5	0	47	25	8
7	50	56	6	-4	319	324	4	-3	416	420	5	1	247	246	4
8	365	378	4	-3	254	253	4	-2	-24	38	11	2	377	380	5
9	165	153	4	-2	83	90	4	-1	258	253	4	3	349	336	5
10	73	84	5	-1	27	6	9	1	390	379	5	4	212	199	4
11	239	238	4	0	163	155	3	2	368	359	5	5	290	299	4
12	155	163	5	1	307	298	4	3	327	330	4	6	305	294	4
13	90	93	6	2	260	264	4	4	82	54	6	7	215	219	4
0	7	1		3	347	344	4	5	106	129	5	8	11	55	20
-14	41	51	9	4	434	434	5	6	-30	9	10	9	-44	26	8
-13	137	142	5	5	487	489	5	7	175	166	5	10	221	210	5
-12	179	179	4	6	31	2	9	8	117	109	5	1	-11	1	
-11	116	116	5	7	13	3	16	-8	38	42	10	0	287	283	4
-10	23	30	12	8	427	425	5	-7	190	174	5	1	122	134	4
-9	908	911	8	9	155	154	4	-6	271	270	4	2	129	147	4
-8	332	340	4	10	54	71	8	-5	67	78	7	3	49	83	7
-7	31	47	8	11	-59	6	5	-4	45	16	8	4	27	30	11
-6	581	585	5	12	7	44	24	-3	345	350	5	5	499	493	5
-5	97	95	4	0	10	1		-2	340	335	5	6	237	225	4
-4	406	412	4	-12	225	208	5	-1	34	22	10	7	89	92	5
-3	84	86	4	-11	127	127	5	0	194	191	4	8	117	125	5
-2	98	119	3	-10	55	59	8	1	224	221	4	9	-49	6	6
-1	171	171	3	-9	64	66	7	2	305	309	4	10	102	101	5
0	467	484	4	-8	-49	5	6	3	250	239	4	11	172	161	5
1	70	79	4	-7	62	85	6	4	124	135	5	1	-10	1	
2	492	509	5	-6	611	602	6	5	-4	0	25	0	19	13	10
3	59	58	4	-5	288	280	4	6	61	60	7	1	254	255	4
4	326	320	4	-4	135	140	4	7	24	18	14	2	202	197	4
5	561	558	5	-3	459	457	5	-7	223	202	5	3	308	309	4
6	408	416	4	-2	147	147	4	-6	123	134	5	4	136	130	4
7	363	364	4	-1	95	92	4	-5	178	184	5	5	-29	23	9
8	205	215	4	0	499	498	5	-4	170	163	5	6	199	211	4
9	225	221	4	1	57	59	6								
10	30	22	11	2	203	210	4								
11	94	91	5	3	457	457	5								
12	225	225	5	4	213	214	4								
13	68	51	7	5	369	361	4								
0	8	1		6	192	182	4								

Tetrakis(pentafluorophenyl)-beta-octachloroporphyrin

Page 6

7	444	445	5					1	313	334	3	12	97	95	5
8	118	119	5	0	35	21	6	2	251	281	2	13	216	213	4
9	-35	9	9	1	238	250	3	3	689	695	6	14	120	118	5
10	252	261	4	2	679	686	6	4	481	477	4	15	99	86	6
11	19	10	16	3	117	123	3	5	209	214	3				
12	99	109	6	4	771	758	7	6	174	168	3	1	2	1	
				5	960	942	8	7	401	395	4				
1	-9	1		6	20	4	10	8	209	212	3	-15	272	266	5
				7	567	551	5	9	538	539	5	-14	50	50	9
0	298	295	4	8	487	483	5	10	474	470	5	-13	45	56	9
1	1022	1015	9	9	186	185	4	11	37	39	7	-12	267	256	4
2	78	81	4	10	-36	1	7	12	317	320	4	-11	131	119	4
3	194	192	3	11	172	175	4	13	75	79	6	-10	217	213	4
4	441	450	5	12	93	108	5	14	379	378	5	-9	180	175	4
5	549	555	5	13	115	125	5	15	109	105	6	-8	-24	4	9
6	118	102	4	14	108	106	6					-7	255	271	3
7	126	118	4	15	239	231	5	1	0	1		-6	772	765	7
8	121	122	4									-5	802	790	7
9	-32	48	9	1	-4	1		-15	186	174	5	-4	1506	1519	13
10	38	27	9	0	397	403	4	-14	-26	31	13	-3	665	641	6
11	-28	34	11	1	301	309	3	-13	271	274	4	-2	529	526	4
12	47	71	9	2	770	782	6	-12	-39	2	8	-1	570	580	5
13	117	122	5	3	187	191	3	-11	77	72	5	0	748	756	6
				4	459	459	4	-10	139	139	4	1	-11	12	10
1	-8	1		5	201	202	3	-9	205	207	4	2	11	23	9
				6	1110	1106	9	-8	47	53	5	3	324	329	3
0	297	304	4	7	369	358	4	-7	999	402	4	4	505	507	4
1	698	683	6	8	158	151	3	-6	472	459	4	5	888	876	7
2	414	420	4	9	183	177	4	-5	257	261	3	6	297	285	3
3	341	354	4	10	57	70	6	-4	232	224	3	7	400	399	4
4	38	43	7	11	57	72	6	-3	43	48	5	8	168	164	3
5	70	73	5	12	72	73	6	-2	1104	1068	9	9	163	167	3
6	228	233	4	13	287	296	5	-1	134	112	2	10	368	363	4
7	39	38	7	14	14	42	18	1	219	207	2	11	338	332	4
8	340	348	4	15	291	285	5	2	860	865	7	12	24	47	13
9	333	327	4					3	969	954	8	13	153	152	4
10	163	164	4	1	-3	1		4	28	14	7	14	-14	21	18
11	357	373	5	0	249	254	3	5	590	587	5	15	269	258	5
12	245	237	5	1	168	171	2	6	633	631	6				
13	167	159	5	2	244	250	3	7	63	72	4	1	3	1	
				3	1852	1859	15	8	719	727	6	-15	147	152	5
1	-7	1		4	227	236	3	9	570	559	5	-14	250	255	5
0	402	417	4	5	565	569	5	10	123	126	4	-13	22	36	13
1	101	82	3	6	475	466	4	11	65	67	6	-12	396	389	5
2	254	257	3	7	646	667	6	12	60	82	6	-11	299	290	4
3	210	209	3	8	118	137	3	13	416	410	5	-10	131	123	4
4	167	153	3	9	472	462	5	14	222	220	4	-9	52	28	6
5	152	149	3	10	273	268	4	15	295	290	5	-8	288	294	4
6	51	30	6	11	252	247	4					-7	257	244	3
7	289	284	4	12	110	124	5	1	1	1		-6	642	623	6
8	368	361	4	13	351	353	5	-15	99	108	6	-5	566	572	5
9	87	79	5	14	-46	19	7	-14	254	241	5	-4	1414	1408	12
10	136	147	4	15	87	98	6	-13	313	304	5	-3	315	322	3
11	72	75	6					-12	299	291	4	-2	158	164	2
12	110	127	5	1	-2	1		-11	125	115	4	-1	755	704	6
13	-35	30	10	0	1175	1149	10	-10	554	555	5	0	885	869	7
14	125	132	5	1	698	683	6	-9	129	130	4	1	542	536	4
				2	243	238	2	-8	138	137	3	2	369	365	3
1	-6	1		3	812	796	7	-7	440	431	4	3	495	492	4
0	206	193	3	4	298	277	3	-6	228	240	3	4	1131	1148	9
1	20	1	9	5	419	434	4	-5	770	765	7	5	124	121	3
2	509	511	5	6	166	165	3	-4	346	336	3	6	633	609	6
3	334	335	4	7	156	159	3	-3	734	725	6	7	173	193	3
4	391	403	4	8	-39	24	5	-2	212	202	2	8	557	573	5
5	394	404	4	9	497	501	5	-1	26	23	6	9	268	264	4
6	321	312	4	10	430	426	5	0	252	256	2	10	572	566	6
7	-21	40	10	11	502	501	5	1	42	0	3	11	131	129	4
8	79	60	4	12	-45	12	7	2	494	506	4	12	76	68	6
9	157	153	4	13	148	161	5	3	809	759	7	13	218	216	4
10	98	101	5	14	284	271	5	4	1322	1325	11	14	74	86	7
11	189	197	4	15	250	245	5	5	207	193	3	15	106	99	6
12	135	135	5					6	1113	1118	9				
13	454	455	5	1	-1	1		7	759	768	7	1	4	1	
14	197	193	5	0	412	436	3	8	284	281	4	-15	-32	34	11
								9	413	413	4	-14	54	58	8
1	-5	1						10	142	139	4	-13	164	186	5
								11	204	190	4				

Tetrakis(pentafluorophenyl)-beta-octachloroporphyrin

Page 7

[illegible]

Tetrakis(pentafluorophenyl)-beta-octachloroporphyrin

Page 8

3	268	260	5	4	467	458	5	10	326	327	4	-3	543	541	5
2	-13	1		5	545	551	5	11	33	56	9	-2	1345	1337	11
0	176	160	5	6	210	209	4	12	-11	38	19	-1	1372	1340	11
1	90	82	6	7	92	88	4	13	217	225	4	0	1956	1968	16
2	39	42	10	8	30	48	8	14	-38	17	9	1	293	284	3
3	265	253	5	9	163	165	4	15	-35	4	11	2	387	340	3
4	136	118	5	10	156	161	4					3	84	84	3
5	108	93	5	11	-21	17	14	2	-3	1		4	184	174	2
6	41	23	10	12	169	177	5	0	936	944	8	5	207	204	3
7	84	66	6	13	53	58	8	1	497	500	4	6	717	707	6
				2	-7	1		2	72	63	3	7	100	66	3
2	-12	1		0	275	274	3	3	628	622	5	8	179	185	3
0	128	120	5	1	572	583	5	4	952	916	8	9	594	599	6
1	205	190	4	2	390	385	4	5	553	567	5	10	-41	15	6
2	-4	29	24	3	485	475	5	6	911	873	8	11	20	32	12
3	46	57	8	4	267	257	3	7	25	23	8	12	-47	4	6
4	227	229	4	5	139	135	3	8	109	119	4	13	387	389	5
5	96	104	5	6	549	555	5	9	276	279	4	14	163	171	5
6	24	42	13	7	6	27	19	10	26	13	10	15	205	206	5
7	302	295	5	8	155	157	4	11	245	244	4	16	91	95	6
8	163	155	5	9	417	405	5	12	262	262	4				
9	291	266	5	10	128	121	4	13	258	263	4	2	1	1	
				11	-36	0	9	14	110	108	5	-14	-20	26	13
2	-11	1		12	112	114	5	2	-2	1		-13	225	231	4
0	41	53	9	13	244	248	5	0	2153	2167	18	-12	122	102	5
1	330	324	4	14	150	146	5	1	91	84	3	-11	71	73	6
2	35	52	9	2	-6	1		2	365	353	3	-10	119	120	4
3	-37	5	7	0	78	86	4	3	900	892	7	-9	368	369	4
4	85	94	5	1	354	355	4	4	1253	1245	10	-8	-34	25	7
5	299	286	4	2	279	262	3	5	863	851	7	-7	257	242	3
6	129	123	5	3	25	18	8	6	246	237	3	-6	81	77	4
7	76	77	6	4	244	243	3	7	314	318	3	-5	555	582	5
8	148	144	5	5	530	534	5	8	-18	34	11	-4	195	197	3
9	44	57	9	6	511	516	5	9	93	99	4	-3	710	700	6
10	32	46	12	7	221	219	3	10	304	309	4	-2	466	453	4
				8	653	641	6	11	650	644	6	-1	438	432	4
2	-10	1		9	353	358	4	12	39	58	9	0	22	11	7
0	392	389	4	10	211	198	4	13	54	91	8	1	144	154	2
1	73	69	5	11	-34	21	9	14	166	167	5	2	288	270	3
2	-11	25	16	12	-4	50	24	15	-30	38	12	3	183	160	2
3	133	143	4	13	61	61	7	13	54	91	8	4	163	160	2
4	139	148	4	14	38	46	10	14	166	167	5	5	604	619	5
5	17	20	15					2	-1	1		6	1114	1128	9
6	44	46	7	2	-5	1		0	1525	1490	13	7	175	187	3
7	301	296	4	0	271	278	3	1	61	45	3	8	597	607	5
8	-30	20	10	1	468	455	4	2	341	330	3	9	637	625	6
9	94	98	5	2	361	354	4	3	300	273	3	10	18	34	12
10	153	151	5	3	210	208	3	4	1261	1271	10	11	197	202	4
11	297	290	5	4	227	243	3	5	986	983	8	12	325	338	4
12	77	74	7	5	58	71	4	6	371	360	4	13	-34	24	9
				6	322	321	4	7	605	582	5	14	125	126	5
2	-9	1		7	154	148	3	8	133	146	3	15	267	269	5
0	-28	2	8	8	270	277	4	9	244	255	4	16	44	49	10
1	158	158	4	9	445	442	5	10	178	184	4				
2	287	292	4	10	265	272	4	11	99	109	4	2	2	1	
3	193	197	4	11	533	524	5	12	276	282	4	-14	291	285	5
4	93	102	4	12	99	117	5	13	168	185	4	-13	138	125	5
5	336	328	4	13	-15	26	17	14	72	74	6	-12	125	120	5
6	537	543	5	14	-22	45	14	15	260	238	5	-11	205	216	4
7	160	161	4	15	122	115	6	16	66	62	8	-10	458	455	5
8	192	183	4									-9	205	214	4
9	109	114	5	2	-4	1		2	0	1		-8	500	486	5
10	265	255	4	0	266	262	3	-14	208	182	5	-7	82	81	4
11	326	311	5	1	465	481	4	-13	209	202	5	-6	135	132	3
12	-13	12	18	2	653	659	6	-12	-30	13	11	-5	258	262	3
				3	906	926	8	-11	-24	18	12	-4	976	968	8
2	-8	1		4	1199	1217	10	-10	27	40	11	-3	640	631	5
0	44	36	6	5	302	321	3	-9	74	67	5	-2	1174	1144	10
1	498	513	5	6	273	264	3	-8	256	249	4	-1	62	51	3
2	88	99	4	7	952	972	8	-7	462	441	5	0	454	399	4
3	56	38	5	8	430	436	4	-6	51	53	5	1	135	144	2
				9	645	652	6	-5	1037	1059	9	2	27	5	7
								-4	455	469	4	3	585	584	5
												4	57	50	4
												5	31	87	3
												6	340	331	3

Tetrakis(pentafluorophenyl)-beta-octachloroporphyrin

Page 9

7	168	169	3	-14	248	239	5	0	25	70	8	-11	235	231	5
8	349	359	4	-13	34	54	11	1	206	193	3	-10	84	81	6
9	328	311	4	-12	188	182	4	2	252	255	3	-9	69	70	6
10	413	413	4	-11	79	85	6	3	365	384	4	-8	121	129	5
11	274	264	4	-10	58	50	6	4	285	291	3	-7	150	149	4
12	153	168	4	-9	312	314	4	5	561	557	5	-6	380	378	4
13	381	369	5	-8	458	459	5	6	233	252	3	-5	448	462	5
14	22	10	13	-7	605	615	6	7	638	640	6	-4	38	1	6
15	135	151	5	-6	569	584	5	8	195	197	4	-3	173	171	4
				-5	620	594	6	9	323	317	4	-2	356	353	4
2	3	1		-4	118	117	3	10	658	649	6	-1	154	154	3
-14	307	296	5	-3	143	131	3	11	87	95	5	0	64	80	5
-13	117	124	5	-2	848	852	7	12	73	71	6	1	185	179	3
-12	291	290	4	-1	743	756	6	13	165	163	5	2	91	93	4
-11	545	539	6	0	358	357	3	14	231	235	5	3	903	917	8
-10	369	378	4	1	124	122	3					4	60	62	5
-9	281	263	4	2	1150	1157	10	2	8	1		5	166	165	4
-8	237	239	4	3	1840	1829	15	-13	100	105	6	6	250	254	4
-7	388	377	4	4	532	534	5	-12	-42	7	8	7	303	280	4
-6	150	176	3	5	810	789	7	-11	263	265	4	8	181	169	4
-5	267	283	3	6	258	259	3	-10	131	131	5	9	83	82	6
-4	298	278	3	7	68	73	4	-9	211	218	4	10	59	63	7
-3	1246	1238	10	8	86	94	4	-8	319	324	4	11	24	51	14
-2	1351	1362	9	9	90	92	4	-7	378	374	4	12	257	249	5
-1	210	198	2	10	66	74	6	-6	247	238	4				
0	157	144	2	11	52	78	7	-5	337	344	4	2	11	1	
1	271	281	3	12	552	562	6	-4	46	33	6	-11	124	105	5
2	1010	968	8	13	173	187	5	-3	413	414	4	-10	86	83	6
3	1283	1277	11	14	274	258	5	-2	114	117	3	-9	77	81	6
4	1052	1060	9	15	72	88	7	-1	631	645	6	-8	200	203	4
5	144	150	3					0	315	319	3	-7	368	369	5
6	-6	12	16	2	6	1		1	-35	14	5	-6	328	327	4
7	355	358	4	-14	6	28	24	2	85	101	4	-5	233	233	4
8	253	245	3	-13	160	174	5	3	41	52	6	-4	61	49	6
9	865	864	8	-12	99	106	5	4	114	109	3	-3	75	90	5
10	115	117	4	-11	227	220	4	5	7	22	16	-2	51	45	6
11	70	76	6	-10	176	188	4	6	713	705	6	-1	105	95	4
12	325	332	4	-9	612	606	6	7	354	364	4	0	84	99	5
13	434	432	5	-8	35	37	8	8	170	175	4	1	255	258	4
14	-17	6	16	-7	48	19	6	9	260	259	4	2	444	442	5
15	38	29	11	-6	69	80	4	10	224	237	4	3	451	443	5
				-5	300	301	3	11	77	74	6	4	447	444	5
2	4	1		-4	387	389	4	12	261	264	5	5	382	383	5
-14	58	61	8	-3	565	546	5	13	355	371	5	6	152	156	4
-13	116	102	5	-2	64	32	4					7	231	236	4
-12	121	120	5	-1	1090	1110	9	2	9	1		8	508	504	5
-11	91	104	5	0	556	557	5					9	261	264	4
-10	102	90	5	1	84	93	3	-12	34	47	11	10	82	74	6
-9	369	377	4	2	87	62	4	-11	103	111	5	11	68	73	7
-8	300	289	4	3	708	687	6	-10	-38	12	8				
-7	572	575	5	4	1794	1778	15	-9	-33	7	8	2	12	1	
-6	73	87	4	5	770	756	7	-8	415	417	5	-10	229	217	5
-5	532	516	5	6	347	345	4	-7	140	131	4	-9	98	105	6
-4	1405	1399	12	7	189	211	3	-6	527	532	5	-8	-39	17	8
-3	638	658	5	8	393	392	4	-5	73	71	5	-7	120	103	5
-2	625	622	5	9	667	674	6	-4	63	73	5	-6	-44	12	7
-1	326	332	3	10	551	551	6	-3	244	250	3	-5	429	448	5
0	482	484	4	11	-26	6	11	-2	542	525	5	-4	263	274	4
1	688	694	6	12	105	95	5	-1	379	356	4	-3	120	130	4
2	1085	1093	9	13	62	82	7	0	970	975	8	-2	216	224	4
3	1598	1604	13	14	146	152	5	1	270	270	3	-1	324	332	4
4	164	162	3					2	-43	3	5	0	59	57	6
5	63	79	4	2	7	1		3	45	52	6	1	215	223	4
6	343	341	4	-13	151	146	5	4	797	818	7	2	154	167	4
7	207	219	3	-12	410	394	5	5	143	165	4	3	167	168	4
8	30	28	8	-11	102	103	5	6	358	360	4	4	302	300	4
9	213	210	4	-10	118	110	5	7	387	387	4	5	71	80	6
10	276	268	4	-9	63	48	6	8	201	193	4	6	-17	35	15
11	122	140	4	-8	287	281	4	9	-34	24	9	7	174	183	4
12	264	260	4	-7	605	601	6	10	160	152	4	8	89	91	6
13	90	96	6	-6	160	170	3	11	118	125	5	9	90	95	6
14	210	198	5	-5	-34	21	5	12	41	58	10	10	123	125	5
15	58	49	8	-4	231	248	3	13	28	29	14				
				-3	355	343	4					2	13	1	
2	5	1		-2	509	510	5	2	10	1		-9	153	155	5
				-1	163	175	3	-12	-37	25	10				

Tetrakis(pentafluorophenyl)-beta-octachloroporphyrin

Page 10

-8	-41	2	8	6	104	120	5	4	310	305	4	7	325	324	4	3
-7	-19	25	15	7	-15	1	17	5	151	139	3	8	240	243	3	4
-6	335	313	5	8	-31	2	10	6	203	222	3	9	8	17	17	
-5	368	363	5	9	149	151	5	7	132	128	4	10	195	194	4	4
-4	13	23	17	10	209	198	5	8	347	333	4	11	560	557	6	6
-3	329	324	4					9	527	536	5	12	108	115	5	5
-2	597	585	6	3	-10	1		10	177	159	4	13	-34	30	9	9
-1	51	42	7					11	252	242	4	14	225	215	5	5
0	122	124	4	0	243	242	4	12	61	85	7	15	260	251	5	5
1	595	597	6	1	372	368	5	13	55	66	8					
2	44	50	8	2	265	263	4	14	281	275	5	3	-1	1		
3	-37	5	8	3	171	186	4									
4	77	82	6	4	-38	6	8	3	-5	1		0	608	608	5	5
5	186	184	4	5	30	15	11	0	1296	1282	11	1	1164	1156	10	7
6	-44	34	7	6	215	195	4	1	256	234	3	2	798	797	7	7
7	161	165	5	7	7	103	96	5	2	470	478	4	3	37	3	5
8	83	108	6	8	-34	32	9	3	180	189	3	4	717	720	6	6
				9	179	182	4	4	654	652	6	5	13	28	11	3
2	14	1		10	69	81	6	5	600	596	5	6	131	137	3	3
				11	40	8	10	6	442	446	4	7	157	161	3	3
-7	50	63	9					7	372	366	4	8	467	469	5	5
-6	141	129	5	3	-9	1		8	151	145	4	9	479	479	5	5
-5	227	222	4					9	43	33	7	10	215	208	4	4
-4	223	225	4	0	336	347	4	10	304	309	4	11	-28	6	9	5
-3	44	33	9	1	245	239	4	11	298	292	4	12	88	99	5	5
-2	99	76	5	2	175	178	4	12	100	103	5	13	84	95	6	6
-1	25	38	13	3	168	171	4	13	8	46	21	14	33	46	11	11
0	221	211	4	4	111	105	4	14	103	95	6	15	330	324	5	5
1	48	48	8	5	144	138	4	15	147	138	5	16	252	234	5	5
2	217	209	4	6	521	504	5									
3	372	373	5	7	34	13	9	3	-4	1		3	0	1		
4	211	220	4	8	54	55	7									
5	64	74	7	9	407	413	5	0	95	103	3	-14	47	22	10	10
6	306	286	5	10	69	66	6	1	291	302	3	-13	-38	15	9	9
7	48	27	9	11	183	194	5	2	155	160	3	-12	281	285	5	5
				12	167	164	5	3	520	521	5	-11	251	252	4	4
								4	508	522	5	-10	166	159	4	4
2	15	1		3	-8	1		5	283	292	3	-9	192	197	4	4
-5	20	25	14					6	115	124	3	-8	88	91	4	4
-4	252	255	5	0	101	103	4	7	556	569	5	-7	116	125	4	4
-3	71	67	7	1	178	177	4	8	362	369	4	-6	348	345	4	4
-2	59	59	7	2	94	114	4	9	91	91	4	-5	360	356	4	4
-1	33	10	11	3	218	216	4	10	-21	0	11	-4	46	38	5	5
0	63	47	7	4	57	63	6	11	321	324	4	-3	830	821	7	7
1	249	241	5	5	583	590	6	12	80	89	7	-2	54	45	4	4
2	83	88	6	6	56	60	6	13	206	211	4	-1	46	6	2	2
3	62	30	7	7	468	470	5	14	98	99	6	0	152	145	2	2
4	174	178	5	8	81	89	5	15	357	345	5	1	2457	2436	20	20
				9	409	389	5					2	384	374	3	3
3	-13	1		10	218	216	4	3	-3	1		3	796	810	7	7
0	124	113	5	11	141	143	5					5	818	810	7	7
1	241	241	5	12	-29	27	11	0	605	591	5	6	445	445	4	4
2	170	165	5	13	231	211	5	1	853	864	7	7	169	163	3	3
3	204	201	5					2	20	20	8	8	762	774	7	7
4	166	156	5	3	-7	1		3	161	159	3	9	230	238	4	4
5	334	314	5	0	50	51	6	4	228	223	3	10	138	124	4	4
				1	40	0	7	5	750	728	6	11	106	103	4	4
3	-12	1		2	3	9	16	6	448	455	4	12	65	93	6	6
				3	-12	2	13	7	107	106	3	13	164	158	4	4
0	49	48	8	4	50	45	6	8	27	34	9	14	62	59	7	7
2	208	211	4	5	42	44	7	9	30	11	7	15	-40	16	9	9
3	129	129	5	6	359	359	4	10	461	459	5	16	85	79	6	6
4	82	83	6	7	319	315	4	11	755	762	7					
5	211	201	4	8	287	291	4	12	100	96	5	3	1	1		
6	29	15	12	9	110	110	5	13	86	96	6					
7	54	46	8	10	409	402	5	14	167	154	5	-14	263	260	5	5
8	21	1	15	11	172	175	4	15	-40	27	8	-12	224	221	5	5
				12	259	276	4					-12	275	260	5	5
3	-11	1		13	108	122	5	3	-2	1		-11	212	208	4	4
				14	190	185	5					-10	8	27	20	20
0	185	173	4					0	576	560	5	-9	-12	8	16	16
1	129	133	5	3	-6	1		1	409	411	4	-8	27	29	10	10
2	129	139	5					2	300	297	3	-7	115	106	4	4
3	-29	18	10	0	138	134	3	3	188	192	3	-6	212	211	3	3
4	308	314	4	1	124	129	3	4	747	758	6	-5	358	365	4	4
5	147	148	4	2	29	38	6	5	357	372	4	-4	67	53	3	3
				3	103	100	3	6	125	144	3	-3	323	321	3	3

Tetrakis(pentafluorophenyl)-beta-octachloroporphyrin

Page 11

-2	227	230	3	8	286	274	4	-11	349	338	5	6	214	216	3
-1	1947	1987	16	9	311	316	4	-10	80	90	6	7	56	52	6
0	1856	1836	15	10	244	237	4	-9	189	184	4	8	9	28	17
1	503	484	3	11	26	50	11	-8	416	417	5	9	243	252	4
2	666	653	6	12	256	258	4	-7	370	367	4	10	35	51	10
3	134	125	3	13	341	330	5	-6	95	90	4	11	23	37	12
4	255	259	3	14	27	6	13	-5	263	261	3	12	65	81	7
5	718	696	6	15	186	182	5	-4	127	114	3	13	236	227	5
6	39	16	6					-3	150	146	3				
7	941	954	8	3	4	1		-2	639	651	6	3	9	1	
8	72	57	4					-1	63	53	4				
9	355	337	4	-14	-22	41	15	0	127	114	3	-12	178	181	5
10	247	240	4	-13	-20	18	15	1	11	13	12	-11	156	175	5
11	234	228	4	-12	23	36	12	2	257	265	3	-10	147	153	5
12	279	279	4	-11	62	45	6	3	541	519	5	-9	134	137	4
13	402	399	5	-10	392	390	5	4	446	430	4	-8	11	1	18
14	201	194	4	-9	555	548	6	5	179	179	3	-7	684	689	6
15	57	71	8	-8	241	248	4	6	590	578	5	-6	216	211	4
16	62	59	8	-7	533	543	5	7	679	682	6	-5	306	312	4
				-6	363	380	4	8	153	162	4	-4	320	319	4
				-5	907	918	8	9	476	465	5	-3	285	295	4
				-4	116	119	3	10	331	322	4	-2	238	224	3
				-3	200	209	3	11	78	97	6	-1	238	234	3
				-2	577	587	5	12	88	89	6	0	461	463	5
				-1	22	23	8	13	208	209	5	1	410	416	4
				0	97	98	3	14	186	175	5	2	237	238	3
				1	360	367	3					3	678	689	6
				2	1819	1805	15	3	7	1		4	68	81	5
				3	611	613	5					5	187	202	3
				4	554	549	5	-13	70	97	7	6	244	243	4
				5	70	65	4	-12	43	0	10	7	258	255	4
				6	64	74	4	-11	475	468	5	8	108	120	4
				7	2	44	19	-10	166	142	4	9	178	173	4
				8	462	460	5	-9	79	83	5	10	44	61	8
				9	460	463	5	-8	180	166	4	11	45	70	9
				10	31	28	9	-7	235	249	4	12	125	122	5
				11	-12	55	17	-6	219	204	3	13	269	267	5
				12	132	137	5	-5	113	116	4				
				13	304	303	5	-4	526	520	5	3	10	1	
				14	276	286	5	-3	556	572	5				
				15	252	252	5	-2	27	29	8	-11	72	68	7
								-1	836	843	7	-10	39	51	10
				3	5	1		0	366	343	4	-9	-15	43	17
								1	641	607	6	-8	19	35	14
				-13	35	54	10	2	60	50	4	-7	155	164	4
				-12	247	256	5	3	570	599	5	-6	220	231	4
				-11	132	137	5	4	188	183	3	-5	108	100	4
				-10	166	181	4	5	4	23	18	-4	108	107	4
				-9	212	208	4	6	289	294	4	-3	446	438	5
				-8	561	555	5	7	93	92	4	-2	569	563	5
				-7	117	88	4	8	296	294	4	-1	208	198	3
				-6	739	735	7	9	240	235	4	0	-31	9	7
				-5	154	158	3	10	262	275	4	1	239	231	4
				-4	95	108	3	11	167	173	4	2	301	309	4
				-3	23	21	8	12	129	124	5	3	132	126	4
				-2	675	679	6	13	109	122	5	4	401	404	4
				-1	905	884	8	14	41	51	10	5	160	155	4
				0	716	711	6					6	209	204	4
				1	693	693	6	3	8	1		7	48	31	7
				2	624	609	5	-12	15	38	18	8	366	356	5
				3	298	303	3	-11	105	108	5	9	103	124	5
				4	288	283	3	-10	11	39	19	10	233	246	4
				5	305	291	3	-9	187	188	4	11	58	52	8
				6	518	531	5	-8	378	392	4	12	55	54	8
				7	225	248	3	-7	-11	21	16	3	11	1	
				8	418	425	4	-6	577	578	5				
				9	59	56	5	-5	88	93	4	-11	221	213	5
				10	37	45	8	-4	442	445	4	-10	193	186	5
				11	127	139	4	-3	331	330	4	-9	28	47	12
				12	197	203	4	-2	242	240	3	-8	195	197	4
				13	103	102	5	-1	191	183	3	-7	212	211	4
				14	-23	8	14	0	473	490	4	-6	96	101	5
				15	98	111	6	1	78	92	4	-5	70	72	6
								2	26	5	8	-4	16	47	14
								3	43	64	5	-3	252	263	4
				-13	-19	34	16	4	172	170	3	-2	383	371	4
				-12	266	272	5	5	423	426	4	-1	192	198	4

Tetrakis(pentafluorophenyl)-beta-octachloroporphyrin

Page 12

0	143	130	4					5	130	127	4	14	193	192	5
1	102	103	4	-5	31	36	12	6	-15	14	13	15	165	176	5
2	269	267	4	-4	-18	20	16	7	223	219	4				
3	191	183	4	-3	-55	9	6	8	643	636	6	4	-3	1	
4	204	197	4	-2	107	110	5	9	93	100	5				
5	409	408	5	-1	381	391	5	10	238	231	4	0	101	99	3
6	235	245	4	0	70	70	7	11	142	135	5	1	149	149	3
7	211	200	4	1	172	160	5	12	93	90	6	2	63	54	4
8	-26	27	11	2	187	170	5					3	166	170	3
9	305	288	5	3	353	349	5	4	-7	1		4	377	371	4
10	208	208	5	4	117	121	5					5	74	59	4
11	79	87	6	5	-29	27	12	0	455	450	5	6	305	288	4
	3	12	1		3	16	1	1	310	312	4	7	213	210	3
-10	45	5	10	-1	53	54	8	2	71	68	5	8	185	189	3
-9	149	136	5	0	-30	0	11	3	56	73	5	9	581	588	6
-8	84	46	7	1	93	87	6	4	-31	3	8	10	7	47	20
-7	89	80	6					5	41	44	7	11	89	72	5
-6	146	152	4	4	-12	1		6	73	70	5	12	158	170	4
-5	14	19	16					7	337	330	4	13	105	111	5
-4	31	41	9	0	49	70	8	8	163	148	4	14	172	182	5
-3	-38	30	8	1	83	86	6	9	224	233	4	15	279	266	5
-2	535	541	5	2	57	46	8	10	179	167	4				
-1	310	321	4	3	101	107	5	11	30	42	12	4	-2	1	
0	145	158	4	4	290	293	5	12	153	155	5				
1	59	61	6	5	46	38	9	13	305	300	5	0	416	408	4
2	-25	19	10	6	132	128	5					1	410	419	4
3	143	148	4					4	-6	1		2	12	9	11
4	41	73	8	4	-11	1		0	175	175	3	3	283	284	3
5	181	179	4					1	-26	1	8	4	379	383	4
6	-10	46	19	0	44	26	9	2	52	34	5	5	298	308	3
7	93	122	5	1	241	254	4	3	321	313	4	6	243	239	3
8	350	340	5	2	174	169	4	4	560	547	5	7	125	126	3
9	201	212	5	3	162	160	4	5	278	273	4	8	183	185	3
10	238	235	5	4	251	257	4	6	222	219	4	9	42	44	7
	3	13	1	5	169	171	5	7	176	177	4	10	386	385	4
-9	115	105	5	6	98	91	5	8	54	51	6	11	375	373	5
-8	72	81	7	7	107	112	5	9	79	82	5	12	-34	6	9
-7	193	184	5	8	-22	23	14	10	177	181	4	13	38	55	9
-6	266	255	4	9	70	78	7	11	379	404	5	14	65	70	7
-5	143	140	5					12	-32	29	8	15	202	201	5
-4	-36	2	9	4	-10	1		13	125	119	5				
-3	305	300	4					14	386	374	5	4	-1	1	
-2	-22	14	13	0	100	96	5								
-1	564	556	6	1	237	238	4	4	-5	1		0	369	344	4
0	143	152	4	2	47	55	7	0	42	19	6	1	426	430	4
1	201	208	4	3	-27	22	10	1	227	224	3	2	652	644	6
2	68	72	6	4	116	119	5	2	718	707	6	3	190	185	3
3	249	259	4	5	131	128	5	3	729	736	6	4	593	598	5
4	19	28	14	6	126	131	5	4	226	214	3	5	412	418	4
5	106	116	5	7	261	262	4	5	-14	32	13	6	-11	54	13
6	190	200	4	8	81	91	6	6	144	148	3	7	538	522	5
7	170	169	5	9	36	38	11	7	210	221	4	8	419	424	4
8	151	148	5	10	93	102	6	8	330	331	4	9	380	372	4
9	39	39	10					9	271	272	4	10	211	216	4
	3	14	1	4	-9	1		10	43	45	8	11	290	284	4
-7	44	57	9	0	32	33	10	11	-18	34	15	12	386	397	5
-6	242	238	5	1	60	62	5	12	160	174	4	13	425	423	5
-5	103	111	5	2	440	430	5	13	-37	28	9	14	135	142	5
-4	-34	4	9	3	54	58	7	14	-33	5	11	15	279	270	5
-3	79	82	6	4	18	10	12					4	0	1	
-2	167	155	4	5	57	38	7	4	-4	1		-13	234	234	5
-1	313	310	4	6	766	777	7	0	118	123	3	-12	198	206	5
0	36	49	10	7	93	71	5	1	26	16	8	-11	-15	14	16
1	249	244	4	8	176	182	4	2	79	81	4	-10	-6	23	23
2	362	362	5	9	268	275	4	3	161	152	3	-9	42	31	8
3	62	54	7	10	41	38	9	4	485	509	5	-8	135	140	4
4	94	102	5	11	14	21	18	5	527	516	5	-7	213	209	4
5	131	131	5					6	165	166	3	-6	511	524	5
6	111	105	5	4	-8	1		7	425	414	4	-5	53	20	5
7	89	86	6	0	117	122	4	8	462	461	5	-4	26	3	8
	3	15	1	1	240	237	4	9	407	395	4	-3	38	29	6
				2	70	75	5	10	523	521	5	-2	733	725	6
				3	141	137	4	11	103	104	5	-1	572	573	5
				4	143	153	4	12	-57	0	5	0	1019	1018	9
								13	182	190	5	1	648	665	6
												2	82	93	3

Tetrakis(pentafluorophenyl)-beta-octachloroporphyrin

Page 13

3	225	221	3	15	37	24	11	-4	271	264	3	11	423	426	5
4	127	134	3	16	115	121	6	-3	161	174	3	12	103	71	5
5	52	60	5					-2	147	137	3	13	248	234	5
6	605	608	5		4	3	1	-1	514	529	5	14		30	23
7	73	83	4					0	236	231	3		8		
8	105	113	4	-13	65	80	7	1	238	258	3	4		1	
9	134	126	4	-12	80	103	6	2	681	682	6				
10	564	551	5	-11	549	555	6	3	388	402	4	-12	29	37	13
11	175	170	4	-10	121	119	5	4	43	13	5	-11	136	133	5
12	113	120	5	-9	140	147	4	5	568	532	5	-10	460	455	5
13	213	230	4	-8	100	112	4	6	221	222	3	-9	85	71	6
14	128	122	5	-7	71	73	5	7	-10	17	15	-8	49	24	8
15	-41	6	7	-6	260	254	4	8	475	484	5	-7	572	577	6
16	-25	31	13	-5	437	445	4	9	250	255	4	-6	258	256	4
				-4	233	225	3	10	408	409	5	-5	294	302	4
4	1	1		-3	153	157	3	11	301	308	4	-4	555	555	5
				-2	214	221	3	12	442	441	5	-3	16	17	12
-13	-39	29	9	-1	139	125	3	13	280	288	5	-2	34	39	9
-12	-19	17	15	0	77	87	3	14	165	173	5	-1	27	30	6
-11	166	170	5	1	11	27	13	15	-33	13	11	0	398	412	4
-10	58	64	7	2	126	132	3					1	411	426	4
-9	171	164	4	3	511	499	5	4	6	1		2	175	173	3
-8	-25	25	10	4	538	561	5					3	93	112	4
-7	127	107	4	5	136	144	3	-13	116	121	6	4	191	193	3
-6	446	457	5	6	100	101	3	-12	-19	8	16	5	453	438	5
-5	130	119	3	7	162	168	3	-11	166	184	5	6	150	126	3
-4	278	263	3	8	221	220	3	-10	222	229	4	7	366	372	4
-3	101	107	3	9	306	310	4	-9	107	93	5	8	298	292	4
-2	29	11	7	10	644	628	6	-8	22	28	11	9	137	147	4
-1	717	712	6	11	157	165	4	-7	371	375	4	10	99	100	5
0	304	278	3	12	-53	41	6	-6	36	42	7	11	329	339	5
1	607	616	5	13	80	76	6	-5	192	200	3	12	-44	49	8
2	696	691	6	14	78	78	6	-4	280	279	3	13	-45	31	8
3	261	264	3	15	15	59	18	-3	328	300	4	14	115	124	6
4	44	34	4					-2	425	428	4				
5	576	582	4	4	4	1		-1	316	334	3	4	9	1	
6	285	310	3					0	576	574	5				
7	76	86	4	-13	73	72	7	1	326	325	3	-11	156	171	5
8	136	134	3	-12	65	87	7	2	413	367	4	-10	164	162	5
9	580	570	5	-11	304	305	5	3	768	727	7	-9	13	35	17
10	317	320	4	-10	171	168	4	4	714	699	6	-8	100	111	5
11	48	61	7	-9	435	428	5	5	59	55	4	-7	43	37	7
12	295	303	4	-8	15	27	15	6	419	408	4	-6	170	172	4
13	415	419	5	-7	-30	3	8	7	587	591	5	-5	101	97	4
14	320	326	5	-6	111	109	4	8	211	208	4	-4	133	135	4
15	242	247	5	-5	348	344	4	9	290	289	4	-3	233	245	4
16	-38	11	10	-4	666	677	6	10	454	457	5	-2	574	573	5
				-3	384	376	4	11	136	151	4	-1	644	638	6
4	2	1		-2	218	208	3	12	-35	41	9	0	289	288	4
				-1	442	449	4	13	144	128	5	1	677	680	6
-13	76	71	7	0	879	898	7	14	47	38	9	2	425	428	4
-12	110	121	5	1	162	160	3	15	-37	25	10	3	43	37	6
-11	138	134	5	2	924	911	8					4	31	36	8
-10	34	15	10	3	451	428	4	4	7	1		5	246	257	4
-9	-11	25	18	4	1423	1427	12					6	194	191	4
-8	125	117	4	5	331	320	4	-12	39	34	11	7	887	885	8
-7	418	411	4	6	482	483	5	-11	274	273	5	8	204	204	4
-6	407	389	4	7	446	450	4	-10	80	69	6	9	126	126	4
-5	405	401	4	8	641	638	6	-9	459	446	5	10	83	91	6
-4	351	343	4	9	676	672	6	-8	362	377	4	11	-50	21	5
-3	364	363	4	10	-30	41	9	-7	312	311	4	12	115	132	5
-2	63	60	4	11	-30	11	9	-6	192	191	4	13	241	234	5
-1	63	67	4	12	114	118	5	-5	63	64	5				
0	435	425	4	13	74	87	6	-4	325	328	4	4	10	1	
1	834	835	5	14	-20	44	15	-3	102	110	3	-11	152	146	5
2	254	249	3	15	87	96	6	-2	222	216	3	-10	29	54	12
3	83	71	3					-1	86	89	4	-9	113	120	5
4	904	894	8	4	5	1		0	-18	12	10	-8	-37	12	7
5	142	142	3					1	112	119	3	-7	-8	38	20
6	528	520	5	-13	-34	30	8	2	423	412	4	-6	302	305	4
7	262	275	3	-12	171	170	5	3	22	23	9	-5	190	189	4
8	93	87	4	-11	151	148	5	4	747	746	7	-4	-23	26	10
9	487	479	5	-10	276	266	4	5	579	562	5	-3	700	697	6
10	262	257	4	-9	108	89	5	6	266	259	4	-2	87	97	4
11	-29	23	9	-8	228	233	4	7	-37	0	6	-1	535	540	5
12	-38	15	8	-7	334	337	4	8	136	149	4	0	318	304	5
13	171	175	4	-6	189	178	3	9	-17	34	13	1	437	440	5
14	57	46	8	-5	273	268	4	10	-41	11	7				

Tetrakis(pentafluorophenyl)-beta-octachloroporphyrin

Page 14

2	473	474	5	8	35	45	11	9	28	60	12	6	317	319	4
3	110	107	4	9	52	66	8	10	162	159	5	7	282	284	4
4	63	57	5									8	382	395	4
5	255	248	4	4	14	1		5	-8	1		9	467	455	5
6	460	458	5									10	534	535	5
7	225	251	4	-7	100	116	6	0	226	221	4	11	339	326	5
8	-37	36	8	-6	122	131	5	1	114	101	4	12	-33	38	9
9	293	284	4	-5	45	57	9	2	354	362	4	13	100	111	6
10	70	86	6	-4	227	235	4	3	89	86	5	14	185	191	5
11	44	60	9	-3	53	43	6	4	334	327	4				
12	248	237	5	-2	203	198	4	5	156	172	4	5	-3	1	
				-1	54	74	7	6	339	340	4				
4	11	1		0	-42	10	7	7	144	146	4	0	557	554	5
				1	112	124	5	8	6	3	21	1	344	350	4
-10	290	279	5	2	282	268	4	9	-35	17	9	2	193	174	3
-9	80	83	6	3	163	143	4	10	357	345	5	3	231	231	3
-8	187	198	4	4	-40	33	8	11	87	95	6	4	21	16	9
-7	113	115	5	5	9	43	20	12	128	132	5	5	140	142	3
-6	104	97	5	6	248	239	5					6	121	117	4
-5	469	486	5	7	111	102	5	5	-7	1		7	456	454	5
-4	10	7	18	8	56	56	8					8	390	403	4
-3	183	197	4					0	97	98	4	9	491	493	5
-2	115	118	4	4	15	1		1	219	216	4	10	229	235	4
-1	70	69	5					2	222	233	4	11	51	47	7
0	197	190	4	-5	24	29	14	3	-17	27	12	12	98	91	5
1	107	111	4	-4	135	131	5	4	200	204	4	13	248	252	5
2	690	698	6	-3	33	26	11	5	91	86	5	14	99	112	6
3	296	296	4	-2	-40	13	8	6	172	174	4	15	19	19	17
4	43	44	7	-1	130	139	5	7	86	75	5				
5	108	114	4	0	63	74	7	8	69	65	6	5	-2	1	
6	177	185	4	1	45	44	8	9	-30	3	8	0	316	308	4
7	100	105	5	2	188	176	5	10	30	25	11	1	308	321	3
8	415	411	5	3	121	113	5	11	314	315	5	2	168	163	3
9	327	346	5	4	300	288	5	12	106	111	6	3	352	343	4
10	99	95	5	5	8	15	22					4	242	237	3
11	117	114	5	6	216	211	5	5	-6	1		5	83	87	4
												6	101	85	4
4	12	1		4	16	1		0	226	223	4	7	263	258	4
								1	133	120	4	8	335	333	4
-9	249	254	5	-1	92	93	6	2	325	324	4	9	294	302	4
-8	118	121	5	0	-54	6	6	3	168	171	4	10	49	49	7
-7	86	91	6	1	80	62	6	4	29	26	8	11	188	188	4
-6	243	252	4					5	166	170	4	12	440	440	5
-5	456	459	5	5	-11	1		6	115	117	4	13	477	462	5
-4	40	30	8					7	487	471	5	14	207	207	5
-3	179	186	4	0	104	107	5	8	60	59	6	15	110	124	6
-2	154	160	4	1	92	79	6	9	132	139	4				
-1	256	267	4	2	107	115	5	10	75	81	6	5	-1	1	
0	162	166	4	3	104	99	5	11	138	129	5	0	167	166	3
1	263	289	4	4	67	81	7	12	11	27	20	1	692	724	6
2	54	57	6	5	87	84	6	13	179	180	5	2	1019	1035	9
3	303	299	4	6	35	29	10					3	68	81	4
4	131	123	4	7	94	99	6	5	-5	1		4	373	369	4
5	74	89	6					0	198	193	3	5	538	540	5
6	97	106	5	5	-10	1		1	272	257	4	6	27	14	8
7	226	242	4	0	81	92	6	2	35	24	7	7	473	464	5
8	117	126	5	1	72	65	6	3	324	320	4	8	-23	27	10
9	205	187	5	2	34	26	11	4	285	282	4	9	35	50	8
10	71	74	7	3	42	45	9	5	329	331	4	10	72	88	5
				4	50	51	8	6	118	116	4	11	110	123	5
4	13	1		5	33	12	9	7	-12	27	14	12	34	24	10
-8	285	274	5	6	-15	3	17	8	508	494	5	13	239	243	4
-7	286	276	5	7	-26	30	12	9	183	185	4	14	46	58	9
-6	70	37	6	8	48	62	9	10	199	188	4	15	67	78	7
-5	64	63	6	9	187	177	5	11	142	142	5				
-4	259	251	4					12	159	173	5				
-3	206	205	4	5	-9	1		13	-30	2	11	5	0	1	
-2	100	105	5					14	-53	11	7				
-1	111	101	5	0	139	156	4					-12	17	48	18
0	115	119	5	1	123	124	5	5	-4	1		-11	44	39	9
1	301	303	4	2	36	41	10					-10	52	50	8
2	-41	9	6	3	-3	14	24	0	528	516	5	-9	48	50	8
3	259	268	4	4	-3	15	25	1	233	239	3	-8	21	45	14
4	445	434	5	5	126	119	5	2	67	66	4	-7	96	83	5
5	31	69	11	6	138	125	5	3	40	51	5	-6	205	201	4
6	45	37	8	7	340	339	5	4	110	105	4	-5	533	530	5
7	160	160	5	8	63	65	7	5	278	281	4	-4	42	16	6

Tetrakis(pentafluorophenyl)-beta-octachloroporphyrin

Page 15

-3	423	419	4	13	522	511	6	-2	40	32	5	14	90	90	6
-2	790	795	7	14	312	301	5	-1	288	262	3				
-1	83	78	4	15	88	83	6	0	697	711	6	5	8	1	
0	35	6	6					1	245	240	3				
1	237	222	3	5	3	1		2	31	17	6	-11	150	140	5
2	284	281	3					3	851	873	7	-10	286	277	5
3	102	123	3	-12	65	53	7	4	703	717	6	-9	107	95	5
4	1166	1150	10	-11	123	125	5	5	130	136	3	-8	45	33	8
5	184	169	3	-10	378	380	5	6	220	221	3	-7	637	640	6
6	219	212	3	-9	43	61	9	7	220	214	3	-6	243	218	4
7	32	29	8	-8	206	221	4	8	123	115	4	-5	258	253	4
8	363	354	4	-7	192	185	4	9	164	155	4	-4	28	0	8
9	66	66	5	-6	114	118	4	10	213	217	4	-3	45	43	6
10	218	219	4	-5	87	93	4	11	248	250	4	-2	551	564	5
11	64	55	6	-4	62	45	5	12	334	346	5	-1	96	100	4
12	438	435	5	-3	91	88	4	13	238	234	4	0	111	127	3
13	124	132	5	-2	589	583	5	14	200	194	5	1	296	302	4
14	276	273	5	-1	38	44	6	15	-59	14	6	2	-19	24	9
15	194	181	5	0	129	125	3					3	37	60	7
				1	24	31	8	5	6	1		4	50	37	5
				2	124	129	3					5	331	331	4
				3	341	333	4	-12	130	149	5	6	270	269	4
				4	263	262	3	-11	93	81	6	7	349	354	4
				5	142	148	3	-10	-31	15	11	8	435	431	5
				6	430	410	4	-9	12	22	18	9	636	639	6
				7	-23	24	9	-8	167	169	4	10	17	50	15
				8	90	86	4	-7	520	511	5	11	339	348	5
				9	162	160	4	-6	67	57	5	12	-35	41	10
				10	594	590	6	-5	205	199	4	13	32	31	10
				11	-46	14	6	-4	18	9	10	14	63	75	8
				12	393	387	5	-3	376	373	4				
				13	291	290	4	-2	77	64	4	5	9	1	
				14	215	204	5	-1	73	59	4				
				15	153	145	5	0	494	486	5	-11	57	60	8
								1	58	65	4	-10	38	35	10
								2	394	396	4	-9	120	121	5
								3	279	292	3	-8	274	279	4
								4	17	13	10	-7	245	229	4
								5	833	838	7	-6	115	107	4
								6	90	89	4	-5	35	32	9
								7	14	27	13	-4	48	50	7
								8	421	426	5	-3	258	267	4
								9	177	181	4	-2	456	462	5
								10	491	490	5	-1	331	332	4
								11	103	112	5	0	60	55	5
								12	86	90	6	1	318	322	4
								13	165	148	5	2	150	150	3
								14	301	292	5	3	98	85	4
								15	227	209	5	4	567	565	5
												5	365	373	4
								5	7	1		6	33	30	9
								-12	94	74	6	7	108	103	4
								-11	347	327	5	8	98	103	5
								-10	97	109	6	9	66	77	6
								-9	75	67	6	10	-45	14	7
								-8	52	45	7	11	18	54	16
								-7	260	252	4	12	145	152	5
								-6	572	590	6	13	118	129	5
								-5	286	274	4	5	10	1	
								-4	-24	9	8				
								-3	61	39	5	-10	112	105	5
								-2	867	878	8	-9	23	68	14
								-1	778	774	7	-8	117	125	5
								0	211	218	3	-7	31	14	11
								1	502	484	5	-6	256	252	4
								2	299	289	3	-5	296	283	4
								3	262	261	3	-4	200	200	4
								4	937	947	8	-3	61	70	6
								5	234	228	3	-2	175	190	4
								6	287	300	4	-1	305	316	4
								7	469	462	5	0	185	185	4
								8	395	391	4	1	234	300	4
								9	-38	25	7	2	234	240	4
								10	-33	25	9	3	465	462	5
								11	402	400	5	4	182	184	4
								12	-27	20	10	5	305	301	4
								13	85	86	6	6	175	178	4

Tetrakis(pentafluorophenyl)-beta-octachloroporphyrin

Page 16

7	46	51	7	-4	372	369	5	6	251	248	4	0	394	394	4
8	38	55	7	-3	252	239	4	7	42	41	9	1	143	134	3
9	237	225	4	-2	254	242	4	8	143	146	5	2	15	4	12
10	400	408	5	-1	225	227	4	9	92	110	6	3	388	392	4
11	89	99	6	0	49	51	6	10	108	97	5	4	77	72	4
12	-47	16	8	1	83	92	6	11	236	229	5	5	533	527	5
5	11	1		2	193	174	4	6	-6	1		6	97	93	4
-9	-30	25	11	3	68	82	6	0	287	291	4	7	153	169	4
-8	204	203	4	4	-3	32	25	1	214	205	4	8	-15	20	14
-7	215	218	4	5	80	74	6	1	214	205	4	9	185	184	4
-6	257	259	4	6	85	95	6	2	119	130	4	10	83	89	5
-5	156	140	4	7	206	199	5	3	74	68	5	11	251	254	4
-4	426	427	5	8	103	96	6	4	226	238	4	12	485	484	5
-3	85	84	5	5	15	1		5	82	89	5	13	68	67	7
-2	220	214	4	-4	76	80	7	6	258	257	4	14	70	65	7
-1	189	199	4	-3	265	262	5	7	89	64	6	6	-1	1	
0	80	87	5	-2	142	134	5	8	287	284	4	0	23	23	9
1	220	214	4	-1	91	93	6	9	167	154	4	1	376	385	4
2	419	420	5	0	121	110	5	10	67	69	7	2	492	484	5
3	625	641	6	1	336	321	5	11	140	136	5	3	87	81	4
4	134	151	4	2	311	302	5	12	-31	4	11	4	445	454	4
5	714	715	7	3	26	38	13	6	-5	1		5	491	485	5
6	237	242	4	4	32	36	12	0	37	35	8	6	484	475	5
7	-12	47	18	5	-2	19	25	1	199	196	4	7	226	230	4
8	-23	44	12	6	147	138	5	2	142	141	4	8	176	175	4
9	-15	21	17	5	16	1		3	248	245	4	9	261	257	4
10	75	102	6	1	242	235	5	4	197	194	4	10	-35	7	8
11	190	198	5	6	-10	1		5	230	230	4	11	-19	5	12
5	12	1		7	179	182	4	6	27	34	10	12	425	435	5
-9	49	65	9	8	272	268	4	7	179	182	4	13	196	186	5
-8	319	331	5	9	372	365	5	8	272	268	4	14	22	16	15
-7	270	258	5	0	15	27	18	9	372	365	5	15	129	120	5
-6	345	330	5	1	87	83	6	10	300	290	6	6	0	1	
-5	228	235	4	2	32	20	11	11	77	89	6	-11	120	109	5
-4	332	349	4	3	133	127	5	12	-44	0	8	-10	44	57	9
-3	159	158	4	4	-44	7	8	13	-31	50	11	-9	80	95	6
-2	-21	5	13	5	110	116	5	6	-4	1		-8	114	113	5
-1	357	354	4	6	-15	43	17	7	57	63	8	-7	79	84	6
0	175	192	4	7	57	63	8	0	257	250	4	-6	198	189	4
1	357	349	4	6	-9	1		1	223	218	4	-5	232	230	4
2	78	81	5	0	291	270	5	2	92	74	4	-4	40	30	7
3	221	216	4	1	264	258	4	3	202	205	4	-3	232	242	4
4	35	39	9	2	97	98	5	4	668	695	6	-2	245	249	3
5	98	102	5	3	56	56	7	5	327	323	4	-1	187	179	3
6	171	168	4	4	160	154	5	6	-31	11	8	0	214	206	3
7	-50	0	6	5	182	172	4	7	79	87	4	1	229	226	3
8	77	94	6	6	-22	14	13	8	69	69	6	2	876	866	8
9	-4	35	23	7	44	59	9	9	443	434	5	3	103	85	3
10	174	163	5	8	124	115	5	10	440	447	5	4	102	85	3
5	13	1		9	94	107	6	11	272	278	4	5	112	104	3
-7	126	134	5	6	-8	1		12	79	94	6	6	309	315	4
-6	18	23	16	7	99	100	5	13	142	144	5	7	141	134	4
-5	262	248	4	0	59	58	7	14	-27	23	13	8	67	80	5
-4	50	61	7	1	59	58	7	6	-3	1		9	223	232	4
-3	265	268	4	2	-31	6	10	0	245	243	4	10	443	437	5
-2	447	440	5	3	85	91	5	1	198	201	3	11	177	173	4
-1	203	206	4	4	41	46	8	2	34	37	7	12	288	287	4
0	365	363	5	5	168	162	4	3	118	124	4	13	268	268	5
1	193	199	4	6	236	237	4	4	112	118	4	14	254	262	5
2	68	81	6	7	73	59	6	5	-11	22	15	15	-14	22	19
3	123	131	5	8	115	111	5	6	204	199	4	6	1	1	
4	281	287	4	9	92	68	6	7	125	135	4	-11	117	113	6
5	-37	13	8	10	283	266	5	8	114	116	4	-10	106	92	6
6	462	465	5	6	-7	1		9	62	72	6	-9	-27	9	12
7	120	127	5	7	76	74	6	10	48	56	8	-8	-28	50	11
8	52	58	8	0	139	134	4	11	124	122	5	-7	67	50	6
9	70	79	7	1	40	37	9	12	39	35	9	-6	127	120	4
5	14	1		2	143	151	4	13	62	53	7	-5	27	22	10
-6	42	72	9	3	-34	21	9	14	331	329	5	-4	83	82	5
-5	193	179	5	4	93	83	5	6	-2	1		-3	109	116	4
				5								-2	85	65	4
												-1	209	206	3

Tetrakis(pentafluorophenyl)-beta-octachloroporphyrin

Page 17

[illegible]

Tetrakis (pentafluorophenyl)-beta-octa¹chloroporphyrin

Page 18

[illegible]

Tetrakis(pentafluorophenyl)-beta-octachloroporphyrin

Page 19

[illegible]

Tetrakis(pentafluorophenyl)-beta-octachloroporphyrin

Page 20

10	40	8	10	-1	169	165	4	-3	341	342	4	-6	152	133	5
11	13	6	19	0	106	109	4	-2	257	266	4	-5	85	82	6
				1	268	267	4	-1	25	10	11	-4	109	112	5
8	-4	1		2	157	165	4	0	301	284	4	-3	150	142	4
0	88	91	5	3	95	82	4	1	200	202	4	-2	113	111	4
1	38	28	9	4	385	376	4	2	78	81	5	-1	133	127	4
2	325	325	4	5	288	296	4	3	132	127	4	0	38	15	7
3	100	111	5	6	39	29	7	4	120	124	4	1	47	38	7
4	399	395	5	7	294	299	4	5	151	147	4	2	33	1	8
5	119	117	5	8	87	86	5	6	70	88	6	3	51	13	6
6	93	100	5	9	218	223	4	7	113	106	4	4	141	138	4
7	242	246	4	10	133	126	5	8	124	121	4	5	124	135	4
8	233	220	4	11	116	115	5	9	80	88	6	6	228	232	4
9	37	14	9	12	256	243	5	10	-39	12	8	7	115	95	4
10	35	29	11	13	107	107	6	11	90	89	6	8	71	59	5
11	82	85	6	14	47	54	10	12	96	114	6	9	85	65	6
12	144	132	5	8	1	1		13	125	119	5	10	77	61	6
								14	144	148	5	11	27	14	13
8	-3	1		-8	41	62	10	8	4	1		12	54	57	8
0	64	49	6	-7	37	30	11					13	139	144	5
1	134	138	4	-6	83	78	6	-9	108	96	6	8	7	1	
2	37	6	9	-5	356	354	5	-8	1	21	29	-8	27	8	14
3	199	194	4	-4	67	59	6	-7	110	111	5	-7	25	17	14
4	165	155	4	-3	144	155	4	-6	184	190	4	-6	275	263	5
5	192	191	4	-2	373	377	4	-5	138	133	5	-5	151	151	4
6	-33	6	9	-1	314	317	4	-4	45	9	9	-4	76	76	5
7	145	142	4	0	83	80	5	-3	285	271	4	-3	252	255	4
8	110	105	5	1	117	121	4	-2	354	353	4	-2	195	193	4
9	361	337	5	2	126	128	4	-1	197	197	4	-1	-12	3	16
10	54	38	8	3	377	382	4	0	307	308	4	0	245	240	4
11	180	195	5	4	63	58	4	1	44	0	7	1	111	101	4
12	-8	32	23	5	128	119	4	2	308	308	4	2	152	153	4
				6	88	103	5	3	586	590	6	3	164	173	4
8	-2	1		7	115	111	4	4	68	51	5	4	38	44	8
0	155	160	4	8	194	190	4	5	85	74	5	5	274	258	4
1	137	161	4	9	130	135	5	6	158	165	4	6	632	622	6
2	298	308	4	10	156	155	4	7	68	72	6	7	41	35	8
3	139	114	4	11	76	64	6	8	212	208	4	8	116	107	5
4	82	85	5	12	124	129	5	9	148	158	4	9	412	406	5
5	59	70	6	13	49	47	9	10	220	226	4	10	106	118	5
6	34	41	9	14	92	82	6	11	-24	25	13	11	33	39	11
7	54	51	7	8	2	1		12	34	38	10	12	477	469	6
8	212	219	4	-9	102	101	6	13	140	142	5	13	193	177	5
9	8	10	21	-8	39	31	11	14	87	95	6				
10	431	424	5	-7	191	201	5	8	5	1		8	8	1	
11	148	157	5	-6	285	285	5	-9	51	69	8	-8	-11	16	21
12	105	117	6	-5	68	42	6	-8	13	30	20	-7	51	67	9
13	67	61	7	-4	134	133	5	-7	59	38	7	-6	110	111	5
				-3	104	88	5	-6	110	114	5	-5	37	40	9
8	-1	1		-2	180	70	5	-5	13	30	16	-4	43	55	8
0	204	206	4	-1	108	113	4	-4	29	34	11	-3	225	228	4
1	256	269	4	0	233	230	4	-3	110	112	5	-2	378	377	5
2	284	270	4	1	35	4	8	-2	203	207	4	-1	250	252	4
3	351	361	4	2	136	135	4	-1	49	33	7	0	103	97	4
4	44	1	7	3	175	173	4	0	135	143	4	1	129	125	4
5	189	188	4	4	63	47	5	1	244	235	4	2	24	10	10
6	32	45	9	5	224	221	4	2	49	7	5	3	86	99	5
7	65	65	6	6	312	306	4	3	334	331	4	4	526	523	5
8	162	157	4	7	192	193	4	4	391	386	4	5	255	244	4
9	141	142	4	8	409	416	5	5	265	270	4	6	412	405	5
10	74	86	6	9	118	120	5	6	-29	1	9	7	313	313	4
11	232	226	4	10	111	131	5	7	149	147	4	8	359	360	5
12	56	66	8	11	-15	16	17	8	46	30	7	9	103	100	5
13	165	163	5	12	11	15	18	9	252	241	4	10	144	150	5
				13	-22	22	15	10	390	371	5	11	80	84	6
8	0	1		14	354	326	5	11	367	366	5	12	261	270	5
-8	116	113	6					12	66	77	7	13	-26	24	13
-7	57	73	8	8	3	1		13	245	242	5				
-6	81	78	6	-9	159	147	5	14	187	197	5	8	9	1	
-5	128	113	5	-8	31	55	12	8	6	1		-8	82	65	7
-4	99	108	5	-7	103	94	6	-9	47	49	10	-7	219	233	5
-3	139	153	4	-6	67	58	6	-8	120	132	5	-6	171	189	5
-2	93	83	5	-5	83	73	6	-7	413	421	5	-5	198	196	4

Tetrakis(pentafluorophenyl)-beta-octachloroporphyrin

Page 21

-3	91	89	5	-4	82	91	6	0	119	108	5	-7	36	32	11
-2	75	60	6	-3	176	160	5	1	409	430	5	-6	125	117	5
-1	209	214	4	-2	15	3	17	2	96	86	5	-5	57	45	8
0	52	44	6	-1	8	30	21	3	206	216	4	-4	148	168	5
1	233	229	4	0	122	122	5	4	59	52	7	-3	181	182	4
2	33	27	9	1	65	47	7	5	104	112	5	-2	169	161	4
3	52	32	7	2	67	51	6	6	211	225	4	-1	93	70	5
4	34	12	9	3	305	300	5	7	26	43	10	0	115	99	4
5	74	67	6	4	64	66	7	8	100	99	5	1	222	218	4
6	278	291	4	5	50	59	8	9	50	55	8	2	374	364	4
7	208	208	4	6	58	52	8	10	55	52	8	3	144	145	4
8	500	511	5	7	375	368	5	11	125	110	5	4	197	197	4
9	208	219	4	8	228	218	5	9	-1	1		5	49	57	7
10	37	55	10									6	165	161	4
11	91	98	6	8	14	1		0	145	118	4	7	442	443	5
12	12	27	21	-2	177	161	5	1	241	246	4	8	81	75	6
	8	10	1	-1	7	2	23	2	165	156	4	9	-34	9	10
-7	134	113	5	0	247	245	5	3	54	36	7	10	123	131	5
-6	68	76	6	1	69	83	7	4	182	179	4	11	262	257	5
-5	152	165	5	2	267	263	5	5	260	252	4	12	-14	35	19
-4	146	136	6	3	339	346	5	6	63	50	6	13	281	275	5
-3	82	98	6	4	-27	23	12	7	373	378	5				
-2	118	128	5	5	189	177	5	8	95	100	5	9	3	1	
-1	-7	0	20	6	204	202	5	9	-8	33	22	-7	141	134	5
0	225	226	4	9	-6	1		10	42	26	9	-6	74	77	7
1	156	157	4					11	32	44	12	-5	6	9	24
2	52	44	6	1	79	68	6	12	266	267	5	-4	147	140	5
3	72	61	6	2	40	40	10					-3	85	70	6
4	45	13	8	3	28	18	13	9	0	1		-2	28	4	12
5	311	299	4	4	86	81	6					-1	79	81	6
6	157	147	4	5	41	26	10	-6	55	74	8	0	256	256	4
7	139	145	4	6	143	136	5	-5	-5	0	24	1	216	215	4
8	-25	1	12					-4	-24	6	13	2	51	14	7
9	127	132	5	9	-5	1		-3	194	189	4	3	272	283	4
10	126	111	5	0	84	101	6	-2	56	7	7	4	268	251	4
11	294	290	5	1	39	43	10	-1	98	49	5	5	25	35	12
	8	11	1	2	19	5	15	0	114	78	5	6	118	109	5
-6	55	61	8	3	14	2	16	1	76	36	6	7	23	11	14
-5	152	168	5	4	91	86	6	2	125	116	4	8	38	25	10
-4	103	102	5	5	140	148	5	3	105	88	5	9	-27	4	12
-3	173	164	4	6	82	95	6	4	36	10	9	10	44	38	9
-2	33	37	10	7	70	60	7	5	41	57	8	11	89	90	6
-1	46	57	8	8	51	53	8	6	246	261	4	12	261	248	5
0	77	79	6					7	83	69	5	13	234	228	5
1	292	289	4	9	-4	1		8	57	66	6				
2	101	86	5	0	40	21	10	9	-16	18	15	9	4	1	
3	352	349	5	1	44	23	9	10	25	13	14	-7	44	45	9
4	172	177	4	2	212	201	4	11	-12	9	20	-6	111	125	6
5	77	96	6	3	56	36	7	12	59	48	11	-5	-19	9	16
6	441	448	5	4	96	100	5	9	1	1		-4	81	77	6
7	301	306	5	5	145	151	5					-3	206	198	4
8	113	110	5	6	31	2	11	-7	30	14	13	-2	21	7	15
9	143	166	5	7	48	69	9	-6	28	17	12	-1	148	133	4
10	265	263	5	8	172	163	5	-5	182	175	5	0	141	100	4
	8	12	1	9	97	85	6	-4	69	66	7	1	58	12	7
-5	34	9	11	10	61	54	6	-3	337	339	5	2	133	139	4
-4	248	224	5					-2	110	71	5	3	82	62	5
-3	117	123	5	9	-3	1		-1	291	299	4	4	281	287	4
-2	69	69	6	0	80	78	5	0	164	159	4	5	53	43	7
-1	89	108	6	1	132	113	5	1	292	300	4	6	153	153	4
0	25	37	13	2	171	160	4	2	134	121	4	7	280	284	4
1	308	311	4	3	187	190	4	3	149	163	4	8	104	99	5
2	193	179	4	4	104	121	5	4	256	250	4	9	11	26	20
3	23	21	13	5	24	8	11	5	168	171	4	10	288	298	5
4	98	90	5	6	-20	33	13	6	120	122	5	11	83	88	6
5	164	169	4	7	27	4	12	7	28	22	11	12	55	38	8
6	137	150	5	8	91	98	6	8	109	92	5	13	173	165	5
7	64	77	7	9	-11	7	17	9	344	360	5				
8	33	14	11	10	52	53	8	10	105	124	5	-7	88	104	6
9	125	138	5	11	52	56	8	11	462	450	5	-6	79	68	7
	8	13	1					12	110	122	6	-5	95	87	6
-5				9	-2	1		13	95	83	6	-4	179	183	5
-4								9	2	1		-3	280	281	4
-3												-2	42	28	9

Tetrakis(pentafluorophenyl)-beta-octachloroporphyrin

Page 22

-1	207	209	4	8	275	279	4	9	13	1	7	292	286	5
0	157	164	4	9	52	32	8				8	106	106	5
1	128	114	4	10	141	151	5				9	82	72	6
2	358	359	4	11	-24	31	14	-2	61	64	10	163	164	5
3	42	6	8	12	90	85	6	-1	174	173	11	82	81	6
4	78	75	5					0	172	165				
5	131	141	4	9	9	1		1	75	71	10	1	1	
6	-19	28	14					2	27	18				
7	106	123	5	-6	55	65	7	3	85	86	-4	94	107	6
8	32	0	11	-5	57	51	8	4	-21	33	-3	76	52	6
9	330	326	5	-4	40	36	8	5	152	165	-2	72	74	6
10	-26	35	13	-3	116	130	5	6	199	202	-1	218	235	4
11	189	176	5	-2	302	309	4				0	286	292	4
12	67	63	7	-1	37	30	9	9	14	1	1	335	348	5
13	139	133	5	0	16	10	16	2	28	9	2	183	186	4
				1	107	106	5	3	64	59	3	72	86	6
9	6	1		2	97	97	5	10	-4	1	4	71	71	5
				3	487	487	5				5	90	73	5
-7	46	45	8	4	230	232	4				6	53	51	8
-6	-37	4	10	5	179	173	4	2	-36	8	7	208	204	4
-5	39	21	10	6	54	44	7	3	66	51	8	67	72	7
-4	156	154	5	7	100	72	5	4	52	70	9	38	53	10
-3	83	73	6	8	291	283	5	5	61	50	10	219	216	5
-2	266	268	4	9	260	265	5	6	55	37	11	70	56	6
-1	104	86	5	10	121	127	5							
0	39	45	9	11	206	194	5	10	-3	1	10	2	1	
1	57	58	6								-5	51	46	9
2	77	76	5	9	10	1		0	-9	36	-4	168	146	5
3	91	91	5	-5	-30	3	11	1	45	43	-3	61	38	7
4	134	127	4	-4	86	102	6	2	56	66	-2	160	162	5
5	150	149	4	-3	78	74	6	3	128	112	-1	121	116	5
6	200	182	4	-2	21	5	13	4	134	131	0	62	48	7
7	364	361	5	-1	122	117	5	5	116	121	1	163	151	4
8	553	555	6	0	30	28	9	6	86	111	2	286	286	4
9	191	186	4	1	206	211	4	7	33	41	3	310	305	4
10	213	211	5	2	195	183	4	8	54	13	4	84	81	5
11	48	44	9	3	490	501	5				5	40	28	9
12	158	166	5	4	149	123	4	10	-2	1	6	204	205	4
				5	287	303	4				7	105	91	5
9	7	1		6	95	100	5	0	-21	27	8	84	78	6
				7	82	97	6	1	12	31	9	147	137	5
-7	84	80	7	8	22	9	14	2	27	9	10	39	25	11
-6	29	37	13	9	-1	33	28	3	54	27	11	85	80	6
-5	194	187	5	10	178	170	5	4	146	131				
-4	63	72	7					5	219	219	10	3	1	
-3	264	274	4	9	11	1		6	44	30				
-2	59	34	6					7	116	112	-5	100	85	6
-1	310	301	4	-5	134	131	5	8	120	128	-4	58	53	8
0	113	109	5	-4	123	127	5	9	94	87	-3	118	101	5
1	114	98	4	-3	292	295	5				-2	80	81	6
2	17	4	15	-2	313	300	5	10	-1	1	-1	29	7	12
3	114	123	4	-1	-31	15	10				0	187	175	4
4	66	72	6	0	271	270	4	0	46	3	1	313	312	4
5	29	30	11	1	164	163	4	1	117	138	2	133	107	4
6	105	85	5	2	227	214	4	2	177	174	3	118	129	5
7	159	160	4	3	48	68	8	3	94	69	4	90	85	5
8	67	72	7	4	242	254	4	4	31	15	5	207	220	4
9	290	285	5	5	316	318	5	5	43	21	6	57	57	7
10	105	115	5	6	289	289	5	6	29	12	7	153	160	5
11	63	57	8	7	66	62	6	7	131	141	8	110	108	5
12	56	9	8	8	132	138	5	8	78	76	9	-6	18	24
				9	19	0	16	9	26	19	10	181	188	5
9	8	1						10	-40	5	11	55	56	9
											12	-15	38	19
-6	13	9	20	9	12	1		10	0	1	10	4	1	
-5	58	32	8					-4	60	31				
-4	51	51	8	-3	48	46	9	-3	38	64	-5	58	62	8
-3	46	25	8	-2	62	41	7	-2	33	39	-4	118	135	5
-2	72	38	6	-1	170	171	5	-1	51	19	-3	90	88	6
-1	178	181	4	0	58	50	7	0	89	54	-2	42	15	10
0	66	58	6	1	151	148	5	1	168	181	-1	72	72	7
1	262	274	4	2	84	90	6	2	63	62	0	49	48	8
2	214	220	4	3	21	28	12	3	76	57	1	191	186	4
3	43	19	8	4	49	61	8	4	55	54	2	138	114	4
4	19	1	14	5	-28	25	9	5	104	93	3	305	300	5
5	16	7	15	6	24	2	14	6	128	138	4	148	140	5
6	48	43	8	7	103	110	5							
7	196	198	4	8	117	120	5							

Tetrakis(pentafluorophenyl)-beta-octachloroporphyrin

Page 23

5	87	76	6	2	70	60	5	11	0	1	-2	52	60	9	
6	122	125	5	3	350	356	4	0	43	11	-1	34	38	12	
7	137	111	5	4	165	154	4	1	32	47	0	88	79	6	
8	84	83	6	5	221	228	4	0	43	11	8	1	43	20	8
9	96	100	6	6	144	135	5	1	32	47	10	2	149	158	5
10	-20	14	15	7	110	108	5	2	72	62	7	3	71	59	7
11	188	196	5	8	47	48	7	3	54	63	7	4	76	49	6
12	75	87	7	9	-18	16	16	4	165	158	5	5	64	38	7
				10	-18	12	17	5	26	40	13	6	154	135	5
								6	135	123	5	7	103	98	6
								7	56	45	8	8	108	106	6
								8	122	112	5	9	124	122	6
												10	-23	25	15
10	5	1		10	9	1		11	1	1		11	6	1	
-5	73	99	7	-4	111	126	5	-1	84	83	6	-3	117	122	6
-4	-31	6	12	-3	40	22	10	0	89	17	6	-2	160	149	5
-3	21	9	16	-2	90	84	6	1	54	44	8	-1	74	87	7
-2	193	157	5	-1	90	77	6	2	62	43	7	0	37	37	9
-1	35	33	11	0	46	5	8	3	87	89	6	1	33	35	11
0	94	101	5	1	112	122	5	4	194	189	5	2	64	55	7
1	47	37	8	2	329	330	5	5	40	18	10	3	103	77	5
2	51	41	7	3	60	47	6	6	96	93	6	4	64	41	7
3	101	78	5	4	42	13	9	7	37	12	10	5	101	98	5
4	175	161	4	5	127	127	5	8	104	96	6	6	347	357	5
5	72	65	6	6	68	73	7	9	45	28	10	7	72	71	7
6	312	309	5	7	47	47	9					8	32	31	12
7	186	182	5	8	202	200	5	11	2	1		9	77	89	7
8	186	191	5	9	143	153	5	-2	119	111	5	11	7	1	
9	84	88	6	10	78	70	7	-1	46	43	9	-2	42	29	9
10	196	197	5					0	36	35	11	-1	36	37	11
11	29	42	13	10	10	1		1	-21	0	14	0	21	57	13
				-3	80	85	6	2	142	116	5	1	30	27	12
10	6	1		-2	106	101	5	3	96	78	5	2	34	24	11
-5	26	52	13	0	42	38	9	4	47	38	9	3	61	31	7
-4	106	115	6	1	80	105	6	5	37	30	10	4	119	124	5
-3	91	75	6	2	117	115	5	6	64	79	7	5	58	42	8
-2	55	44	7	3	82	83	6	7	-12	44	20	6	157	143	5
-1	90	89	6	4	248	253	4	8	30	24	12	7	56	31	7
0	128	129	5	5	76	85	6	9	100	84	6	8	46	54	10
1	239	256	4	6	55	41	8					9	-10	27	21
2	32	31	10	7	483	454	6	11	3	1					
3	259	250	4	8	97	90	6	-2	60	49	7	11	8	1	
4	258	254	4	9	189	186	5	-1	27	30	13	-2	110	85	6
5	48	5	8	10	11	1		0	32	1	12	-1	47	42	8
6	233	226	4	-2	88	66	6	1	186	169	5	0	82	88	6
7	120	120	5	-1	-20	11	13	2	90	86	6	1	72	86	7
8	90	96	6	0	70	47	7	3	112	119	5	2	78	70	6
9	145	152	5	1	172	169	5	4	72	55	6	3	240	243	4
10	9	13	22	2	193	198	5	5	-18	1	16	4	68	66	6
11	258	256	5	3	10	8	20	6	107	101	5	5	175	171	5
				4	-6	18	23	7	116	116	5	6	41	51	10
10	7	1		5	50	51	8	8	208	205	5	7	160	145	5
-5	25	32	14	6	236	238	5	9	42	23	9	8	66	64	7
-4	38	43	11	7	163	161	5	10	25	26	15				
-3	121	114	5	8	203	196	5	11	4	1					
-2	277	279	5					-3	204	216	5	11	9	1	
-1	115	110	5	10	12	1		-2	230	231	5	-1	-14	14	18
0	119	114	5	-1	44	47	9	-1	193	191	5	0	157	137	5
1	114	111	5	0	244	256	5	0	81	76	7	1	51	66	8
2	288	279	4	1	36	17	11	1	155	150	5	2	106	102	5
3	175	165	4	2	135	123	5	2	55	43	8	3	-24	7	13
4	58	10	7	3	109	91	5	3	61	43	7	4	-3	8	26
5	346	351	5	4	-20	15	13	4	154	154	5	5	77	70	6
6	85	84	6	5	64	66	7	5	78	89	7	6	61	23	7
7	61	10	7	6	103	102	6	6	35	41	10	7	68	30	7
8	286	291	5	7				7	56	85	8	8	92	99	6
9	-16	29	17	8				8	-16	4	18				
10	39	39	11	9				9	131	137	5	11	10	1	
11	230	224	5	10				10	69	53	8				
												0	86	98	6
10	8	1		11	-1	1		11	5	1		1	59	56	8
-5	69	66	6	1	65	51	7					2	-6	27	24
-4	56	13	8	2	117	120	5	-3	88	62	7	3	20	0	13
-3	36	2	11	3	78	72	6								
-2	59	51	7	4	240	255	5								
-1	68	36	6	5	72	79	7								
0	142	154	5	6	73	75	7								
1	110	92	5	7	76	36	7								

Tetrakis(pentafluorophenyl)-beta-octachloroporphyrin

Page 24

4	20	5	15	3	44	41	9	12	5	1	4	222	228	5	
5	130	132	5	4	94	91	6	2	25	17	5	139	125	5	
6	49	21	9	5	39	1	10	3	83	90	7	6	-6	3	25
11	11	1		12	4	1		4	39	19	12	12	7	1	
2	138	132	5	2	68	82	7	5	182	185	5	3	152	154	5
3	25	10	14	3	59	14	7	6	110	118	6	4	108	93	6
4	30	42	12	4	50	51	8	12	6	1		5	86	74	6
12	3	1		5	29	29	13	2	62	53	7				
				6	13	5	17	3	180	163	5				

Table 1. Final Heavy Atom Parameters for
Tetrakis(pentafluorophenyl)octachloroporphinato Zinc(II) · 6(C₆H₄Cl₂).

x, y, z and $U_{eq}^a \times 10^4$					
Atom	x	y	z	U_{eq} or B	Pop [†]
Zn	0	0	0	291(4)	
N	1015(4)	231(4)	95(9)	268(20)	
C1	2135(5)	108(6)	626(10)	286(26)	
C2	1542(5)	-246(5)	180(10)	297(26)	
C3	1475(5)	-943(5)	-120(11)	264(25)	
C4	1296(6)	861(6)	338(10)	287(28)	
C5	1989(6)	776(6)	720(10)	326(28)	
Cl1	2909(2)	-235(2)	1075(3)	484(8)	
Cl2	2544(2)	1359(2)	1352(3)	506(9)	
C6	2123(5)	-1340(6)	-259(11)	325(30)	
C7	2322(6)	-1829(6)	564(11)	346(29)	
F7	1935(4)	-1938(4)	1575(7)	547(20)	
C8	2900(7)	-2243(7)	393(14)	524(39)	
F8	3050(4)	-2723(4)	1207(8)	714(24)	
C9	3288(7)	-2138(8)	-611(14)	513(39)	
F9	3850(4)	-2525(5)	-810(8)	767(27)	
C10	3140(6)	-1612(7)	-1458(14)	533(41)	
F10	3529(4)	-1512(5)	-2431(8)	743(25)	
C11	2554(6)	-1232(5)	-1240(12)	329(28)	
F11	2406(4)	-770(4)	-2088(7)	549(20)	

Table 1. (Cont.)

Atom	<i>x</i>	<i>y</i>	<i>z</i>	<i>U</i> _{eq} or <i>B</i>	Pop [†]	
Cl3	4428(9)	6030(8)	1705(11)	1957(66)	0.50	
Cl4	3904(6)	4528(8)	1753(12)	1411(45)	0.50	
Cl5	5339(3)	910(4)	74(9)	2172(35)		
Cl6	4712(11)	1149(11)	2927(13)	2586(92)	0.47	
Cl7	4300(10)	2220(11)	−277(23)	3762(115)	0.53	
C31	4769	1516	620	1226	0.47	
C32	4520	1628	1741	1229	0.47	
C33	4060	2202	1935	1230	0.47	
C34	3895	2612	964	1226	0.47	
C35	4159	2490	−201	1229	0.47	
C36	4608	1930	−396	1230	0.47	
C41	4845	1295	1233	1225	0.53	
C42	4449	1874	964	1229	0.53	
C43	4104	2128	2010	1230	0.53	
C44	4173	1816	3130	1225	0.53	
C45	4602	1219	3265	1229	0.53	
C46	4933	976	2264	1230	0.53	
C14	5068	5371	1677	3.5	•	0.75
C15	4797	4709	1695	3.5	•	0.75
C16	5239	4163	1670	3.5	•	0.75

Table 1. (Cont.)

Atom	<i>x</i>	<i>y</i>	<i>z</i>	<i>U</i> _{eq} or <i>B</i>	Pop [†]
C17	5961	4262	1626	3.5 *	0.75
C18	6215	4923	1609	3.5 *	0.75
C19	5773	5469	1634	3.5 *	0.75
C21	4657	5072	1727	3.5 *	0.25
C22	4555	5782	1716	3.5 *	0.25
C23	5106	6237	1726	3.5 *	0.25
C24	5775	5977	1746	3.5 *	0.25
C25	5863	5255	1756	3.5 *	0.25
C26	5311	4818	1746	3.5 *	0.25

$$^* U_{eq} = \frac{1}{3} \sum_i \sum_j [U_{ij}(a_i^* a_j^*)(\vec{a}_i \cdot \vec{a}_j)]$$

* Isotropic displacement parameter, *B*

† Population Parameter, if different from 1.0

Table 2. Anisotropic Displacement Parameters for
Tetrakis(pentafluorophenyl)octachloroporphinato Zinc(II) · 6(C₆H₄Cl₂).

Atom	U_{11}	U_{22}	U_{33}	U_{12}	U_{13}	U_{23}
Zn	246(8)	246(8)	381(15)	0	0	0
N	262(45)	193(44)	348(55)	-13(38)	-37(47)	31(47)
C1	265(59)	302(70)	290(62)	30(52)	-71(51)	-5(53)
C2	214(54)	337(62)	341(72)	12(47)	82(54)	104(56)
C3	299(61)	255(59)	239(64)	55(49)	52(58)	46(55)
C4	337(68)	274(64)	251(71)	-58(52)	-36(51)	-9(51)
C5	317(68)	269(63)	393(72)	-40(56)	-23(58)	-8(56)
Cl1	325(17)	409(18)	719(23)	64(14)	-208(17)	-66(17)
Cl2	378(18)	370(18)	769(25)	10(15)	-259(19)	-79(18)
C6	181(55)	290(61)	503(85)	31(48)	30(57)	-65(59)
C7	336(69)	372(70)	329(71)	42(58)	-33(58)	-11(59)
F7	509(48)	603(51)	529(45)	31(38)	27(41)	112(41)
C8	469(86)	385(80)	718(113)	121(71)	-235(82)	-134(74)
F8	797(59)	461(48)	885(65)	288(45)	-309(53)	66(47)
C9	315(74)	569(97)	654(99)	161(72)	-90(74)	-204(84)
F9	407(46)	766(60)	1128(75)	328(45)	-143(46)	-271(57)
C10	272(71)	624(94)	702(109)	-27(69)	196(75)	-262(88)
F10	529(52)	879(64)	822(59)	-3(45)	305(50)	-253(54)
C11	272(63)	260(63)	455(74)	-66(53)	-46(63)	-31(60)
F11	586(50)	543(48)	519(48)	-5(43)	156(41)	18(42)
Cl3	3244(222)	1771(143)	855(85)	799(149)	664(122)	-94(89)
Cl4	901(81)	2158(150)	1174(90)	-365(93)	261(71)	-130(98)
Cl5	1313(57)	1979(76)	3224(114)	-271(55)	510(69)	-1399(84)
Cl6	3216(276)	3402(265)	1139(111)	-2200(230)	-667(138)	947(142)
Cl7	2496(199)	3595(275)	5194(352)	-1801(195)	-2386(228)	3455(273)
C31	1002	925	1751	260	5	-205
C32	1368	1214	1105	-116	-302	437
C33	1272	1561	857	-193	286	-264
C34	1002	925	1751	260	5	-205
C35	1368	1214	1105	-116	-302	437
C36	1272	1561	857	-193	286	-264

Table 2. (Cont.)

Atom	U_{11}	U_{22}	U_{33}	U_{12}	U_{13}	U_{23}
C41	1156	1426	1093	-67	334	-410
C42	1426	1368	893	-222	-200	377
C43	1060	867	1763	250	-162	16
C44	1156	1426	1093	-67	334	-410
C45	1426	1368	893	-222	-200	377
C46	1060	867	1763	250	-162	16

$U_{i,j}$ values have been multiplied by 10^4

The form of the displacement factor is:

$$\exp -2\pi^2(U_{11}h^2a^{*2} + U_{22}k^2b^{*2} + U_{33}l^2c^{*2} + 2U_{12}hka^*b^* + 2U_{13}hla^*c^* + 2U_{23}k\ell b^*c^*)$$

Table 3. Complete Distances and Angles for
Tetrakis(pentafluorophenyl)octachloroporphinato Zinc(II) · 6(C₆H₄Cl₂).

		Distance(Å)			Distance(Å)
Zn	-N	2.032	C23	-C24	1.401
N	-C2	1.390(13)	C24	-C25	1.419
N	-C4	1.371(14)	C25	-C26	1.373
C1	-C2	1.431(15)	C15	-C31	1.728
C1	-C5	1.337(15)	C15	-C41	1.758
C1	-C11	1.722(11)	C16	-C32	1.640
C2	-C3	1.405(15)	C17	-C42	1.541
C3	-C6	1.490(15)	C31	-C32	1.334
C3	-C4	1.401(16)	C31	-C36	1.407
C4	-C5	1.423(16)	C32	-C33	1.449
C5	-C12	1.716(12)	C33	-C34	1.367
C6	-C7	1.365(16)	C34	-C35	1.393
C6	-C11	1.378(16)	C35	-C36	1.416
C7	-F7	1.354(14)	C41	-C42	1.399
C7	-C8	1.399(18)	C41	-C46	1.297
C8	-F8	1.324(16)	C42	-C43	1.415
C8	-C9	1.35(2)	C43	-C44	1.372
C9	-F9	1.349(17)	C44	-C45	1.441
C9	-C10	1.41(2)	C45	-C46	1.355
C10	-F10	1.320(16)			
C10	-C11	1.381(18)			
C11	-F11	1.324(14)			
C13	-C14	1.792			
C13	-C26	1.732			
C14	-C15	1.779			
C14	-C21	1.813			
C14	-C15	1.395			
C14	-C19	1.389			
C15	-C16	1.370			
C16	-C17	1.422			
C17	-C18	1.381			
C18	-C19	1.370			
C21	-C22	1.398			
C21	-C26	1.368			
C22	-C23	1.394			

Table 3. (Cont.)

Angle(°)				Angle(°)			
N	-Zn	-N	90.2	C10	-C11	-C6	123.8(11)
N	-Zn	-N	174.1	F11	-C11	-C6	121.0(10)
Zn	-N	-C2	125.2	F11	-C11	-C10	115.2(11)
Zn	-N	-C4	42.4	C15	-C14	-Cl3	113.5
C4	-N	-C2	106.9(8)	C19	-C14	-Cl3	126.2
C5	-C1	-C2	108.8(10)	C19	-C14	-C15	120.2
Cl1	-C1	-C2	128.2(8)	C14	-C15	-Cl4	123.8
Cl1	-C1	-C5	122.9(9)	C16	-C15	-Cl4	117.5
C1	-C2	-N	107.4(9)	C16	-C15	-C14	118.7
C3	-C2	-N	124.2(9)	C17	-C16	-C15	121.2
C3	-C2	-C1	128.4(10)	C18	-C17	-C16	118.8
C6	-C3	-C2	116.5(9)	C19	-C18	-C17	120.0
C4	-C3	-C2	126.5(10)	C18	-C19	-C14	121.1
C4	-C3	-C6	116.9(10)	C22	-C21	-Cl4	117.6
C3	-C4	-N	122.4(10)	C26	-C21	-Cl4	122.9
C5	-C4	-N	109.4(9)	C26	-C21	-C22	119.5
C5	-C4	-C3	128.0(10)	C23	-C22	-C21	121.3
C4	-C5	-C1	107.1(10)	C24	-C23	-C22	119.1
Cl2	-C5	-C1	122.9(9)	C25	-C24	-C23	118.3
Cl2	-C5	-C4	129.7(9)	C26	-C25	-C24	121.3
C7	-C6	-C3	122.5(10)	C21	-C26	-Cl3	128.3
C11	-C6	-C3	121.2(10)	C25	-C26	-Cl3	111.2
C11	-C6	-C7	116.4(11)	C25	-C26	-C21	120.4
F7	-C7	-C6	119.2(10)	C32	-C31	-Cl5	131.5
C8	-C7	-C6	123.0(11)	C36	-C31	-Cl5	105.3
C8	-C7	-F7	117.8(11)	C36	-C31	-C32	123.2
F8	-C8	-C7	119.8(12)	C31	-C32	-Cl6	123.2
C9	-C8	-C7	118.2(13)	C33	-C32	-Cl6	117.8
C9	-C8	-F8	121.9(13)	C33	-C32	-C31	119.1
F9	-C9	-C8	120.1(13)	C34	-C33	-C32	119.0
C10	-C9	-C8	121.9(13)	C35	-C34	-C33	121.4
C10	-C9	-F9	118.0(12)	C36	-C35	-C34	119.8
F10	-C10	-C9	121.1(12)	C35	-C36	-C31	117.5
C11	-C10	-C9	116.5(12)	C42	-C41	-Cl5	119.7
C11	-C10	-F10	122.3(12)	C46	-C41	-Cl5	110.3

Table 3. (Cont.)

Angle(°)	
C46 - C41 - C42	129.9
C41 - C42 - Cl7	129.9
C43 - C42 - Cl7	117.8
C43 - C42 - C41	112.1
C44 - C43 - C42	121.2
C45 - C44 - C43	120.4
C46 - C45 - C44	118.5
C45 - C46 - C41	118.0

Table 4. Intermolecular Distances Less Than 3.5 Å for
Tetrakis(pentafluorophenyl)octachloroporphinato Zinc(II) · 6(C₆H₄Cl₂).

Distance(Å)		Distance(Å)	
C2 -Cl4	3.487(17)	C24 -C34	2.952
C4 -C17	3.387		
Cl1 -F10	3.122(9)		
Cl2 -C33	3.441		
Cl2 -C43	3.467		
Cl2 -F8	3.413(9)		
C7 -F10	3.234(15)		
F7 -C24	3.463		
F7 -C33	3.038		
F7 -C34	3.257		
F7 -C43	3.133		
F7 -C44	3.268		
F7 -F9	3.408(11)		
F7 -F10	3.344(11)		
C8 -F10	3.038(16)		
F8 -C34	3.401		
F8 -C35	3.199		
F8 -C10	3.125(16)		
F8 -F10	2.985(12)		
F8 -C11	3.165(14)		
F8 -F11	2.970(11)		
F9 -C24	3.485		
F9 -Cl4	3.168(15)		
F9 -C36	3.254		
F10 -C46	3.244		
F11 -Cl6	3.49(2)		
F11 -C32	3.336		
F11 -C44	3.473		
F11 -Cl3	3.014(17)		
F11 -C22	3.484		
F11 -C23	3.128		
C17 -C35	3.404		
C18 -C35	3.311		
C23 -C33	3.460		
C23 -C34	3.087		

Table 5. Observed and Calculated Structure Factors for
Tetrakis(pentafluorophenyl)octachloroporphinato Zinc(II) · 6(C₆H₄Cl₂).

The columns contain, in order, h , $10F_{obs}$, $10F_{calc}$ and $10\sigma F_{obs}$. A minus sign preceding F_{obs} indicates that F_{obs}^2 is negative.

Tetrakis(C₆F₅)-Octachloroporphinato Zinc 6(C₆H₄Cl₂)

Page 1

h	0	0	13	445	457	11	9	292	356	10	13	-69	98	31	
2	221	238	14	372	365	12	10	315	308	11	14	377	325	14	
4	1480	1421	13	15	176	189	16	11	336	330	11	15	50	115	36
6	504	483	8	16	157	141	18	12	26	63	45	16	276	291	13
8	1446	1447	14	17	341	323	13	13	142	193	18	17	249	255	14
10	845	796	11	18	274	273	15	14	143	121	19	18	210	175	16
12	46	65	31	19	240	163	14	15	211	188	15	19	120	114	24
14	197	298	14	20	181	153	17	16	564	480	13				
16	-115	48	17	21	174	160	18	17	-106	16	22	h	13	0	
18	487	566	13	22	-30	40	50	18	285	315	13				
20	237	146	14	h	4	0		19	217	252	15	13	186	40	25
22	94	102	27					20	97	43	26	14	144	187	18
				4	2581	2483	26	21	183	160	18	15	107	133	23
h	1	0	5	6	670	620	8	22	-43	26	44	16	180	177	17
1	935	921	10	6	665	753	9	h	8	0		17	131	103	21
2	749	904	7	7	600	625	9					18	10	104	65
3	1185	1178	11	8	75	80	20	8	1230	1226	17	19	144	183	21
4	1176	986	11	9	104	172	16	9	972	949	12	h	14	0	
5	506	423	7	10	1814	1844	17	10	38	41	36				
6	368	422	7	11	133	227	15	11	20	86	48	14	-97	10	30
7	380	446	8	12	591	598	11	12	261	279	13	15	-77	61	28
8	714	754	9	13	58	30	31	13	943	904	13	16	124	56	22
9	822	768	10	14	805	822	12	14	252	221	14	17	140	105	21
10	71	55	22	15	258	226	14	15	21	31	55	18	-93	18	25
11	481	618	10	16	102	148	24	16	454	398	13	h	15	0	
12	712	783	11	17	-37	111	45	17	-35	4	42				
13	231	315	12	18	450	433	13	18	-30	40	47				
14	245	203	13	19	314	241	12	19	57	100	36	15	461	424	17
15	192	155	15	20	-56	133	35	20	293	284	14	16	292	288	14
16	-88	2	23	21	135	113	21	21	92	24	28	17	-64	34	34
17	360	249	13	22	213	203	16	h	9	0		h	16	0	
18	88	110	29	h	5	0		9	107	22	26	16	412	433	18
19	121	64	20	5	1191	1145	15	10	291	238	12				
20	221	191	15	6	1467	1486	14	11	419	309	11	h	0	1	
21	237	222	15	7	460	453	9	12	-98	41	20				
22	141	137	21	8	1066	1029	12	13	352	301	12	1	1588	1641	12
23	25	91	56	9	494	501	9	14	53	47	36	2	48	41	13
h	2	0	10	10	156	118	13	15	484	503	13	3	1174	1085	9
2	830	891	10	11	509	469	10	16	-82	132	28	4	581	561	6
3	464	452	6	12	363	374	11	17	193	199	15	5	531	534	6
4	659	625	7	13	199	236	14	18	166	141	18	6	496	500	6
5	437	456	7	14	128	165	19	19	225	204	15	7	1182	1156	10
6	244	290	8	15	345	337	12	20	206	178	16	8	485	495	6
7	-54	31	21	16	-28	183	48	21	198	152	17	9	692	687	7
8	591	611	9	17	603	567	13	h	10	0		10	404	399	7
9	276	254	9	18	64	25	36					11	499	494	7
10	573	637	9	19	124	83	21	10	425	438	16	12	72	92	17
11	48	67	29	20	156	160	19	11	478	509	11	13	686	644	8
12	344	317	10	21	479	413	12	12	145	139	18	14	-80	48	22
13	-65	97	25	22	214	180	16	13	150	121	19	15	496	440	8
14	110	189	21	h	6	0		14	214	205	16	16	-84	35	17
15	593	652	12	6	570	647	12	15	447	477	13	17	291	248	10
16	141	176	19	7	-69	11	19	16	-41	54	39	18	121	107	17
17	232	123	15	8	112	109	16	17	101	90	24	19	131	90	14
18	546	505	13	9	367	280	10	18	211	189	15	20	213	227	11
19	117	171	21	10	640	638	10	19	-90	98	25	21	121	153	16
20	629	582	12	11	350	301	11	20	-116	12	20	22	193	221	12
21	67	11	33	12	493	473	11	h	11	0		23	148	126	15
22	102	70	26	13	421	414	11					h	1	1	
23	-85	2	28	14	402	342	12	11	145	251	26	2	379	384	4
h	3	0	14	15	238	244	14	12	-38	84	42	3	880	808	7
3	1291	1299	14	16	207	206	16	13	477	319	12	4	1079	1050	9
4	1344	1356	12	17	44	76	44	14	127	105	22	5	1051	968	9
5	359	373	7	18	384	368	12	15	144	115	21	6	1281	1289	10
6	431	208	8	19	231	211	14	16	-54	87	34	7	538	591	6
7	1798	1826	16	20	369	366	13	17	103	177	24	8	475	491	6
8	-100	197	16	21	131	122	22	18	126	110	22	9	233	212	7
9	140	196	13	22	-109	13	22	19	-57	65	36	10	593	513	7
10	-33	36	34	h	7	0		20	-31	11	51	11	320	257	7
11	-53	39	26	7	431	553	13	h	12	0		12	692	715	8
12	481	459	10	8	90	29	18	12	233	195	21	13	445	425	8
												14	433	428	8
												15	-39	44	30

Tetrakis(C₆F₅)-Octachloroporphinato Zinc 6(C₆H₄Cl₂)

Page 2

[illegible]

Tetrakis(C6F5)-Octachloroporphinato Zinc 6(C6H4Cl2)

Page 4

16	344	331	10	14	46	138	32	4	190	190	8	15	172	141	13
17	78	95	23	15	447	367	8	5	952	918	9	16	519	528	9
18	206	199	11	16	187	176	11	6	783	698	8	17	72	86	21
19	253	218	10	17	186	188	12	7	392	330	7	18	314	302	9
20	161	168	13	18	-38	65	34	8	83	37	14	19	71	40	23
21	-91	4	18	19	-20	74	46	9	694	630	8	20	372	361	9
22	74	89	45	20	92	127	21	10	199	150	9	21	118	89	17
h 6 3			h 11 3			h 5 4									
7	375	408	7	12	455	395	9	14	-69	90	21	5	656	716	10
8	352	377	7	13	145	173	15	15	205	171	11	6	446	431	7
9	754	792	8	14	73	104	25	16	34	47	37	7	765	808	8
10	-28	152	32	15	154	181	13	17	42	48	34	8	361	313	7
11	204	146	10	16	196	209	11	18	-76	20	19	9	319	330	8
12	285	266	9	17	239	238	10	19	185	201	12	10	233	240	9
13	438	456	8	18	133	153	15	20	214	229	11	11	225	238	9
14	224	247	10	19	-39	59	35	21	95	89	20	12	246	194	9
15	192	213	12				h 2 4								
16	218	173	12	h 12 3											
17	88	141	19	13	-72	112	23	2	741	739	9	13	103	151	17
18	-40	26	31	14	172	190	12	3	142	155	9	14	272	283	10
19	189	184	12	15	91	47	19	4	263	303	7	15	332	298	10
20	-22	64	43	16	228	197	11	5	500	479	7	16	171	193	14
21	137	143	15	17	159	95	13	6	758	718	8	17	-73	22	20
h 7 3			h 13 3			h 3 4									
8	630	593	8	14	197	165	11	7	259	283	7	18	86	101	20
9	438	404	8	h 14 3				8	908	881	9	19	92	119	20
10	629	585	8	15	110	91	17	9	470	433	7	21	-46	40	32
11	208	240	10	16	205	175	11	10	256	248	8	h 6 4			11
12	384	312	8	17	90	103	21	11	493	441	8	6	788	762	
13	268	224	10	18	-80	36	21	12	265	286	9	7	138	203	10
14	307	281	9	h 15 3				13	262	227	9	8	689	612	8
15	227	171	11	16	405	384	9	14	138	155	14	9	473	442	8
16	-46	118	32	17	218	198	11	15	87	69	20	10	342	320	8
17	185	180	11	18	168	168	14	16	428	441	9	11	232	191	10
18	353	351	9	h 14 3				17	-29	43	41	12	276	220	9
19	148	132	14	15	405	384	9	18	134	84	14	13	140	167	14
20	193	195	12	16	218	198	11	19	227	187	10	14	299	296	10
21	-82	52	21	17	168	168	14	20	105	103	18	15	276	291	10
h 8 3			h 15 3			h 3 4									
9	166	206	10	16	74	102	24	3	668	703	9	16	329	269	10
10	180	129	10	h 0 4				4	565	546	7	17	32	58	35
11	820	836	9	0	525	515	8	5	937	914	9	18	102	158	18
12	100	122	17	1	748	788	7	6	234	272	7	19	116	91	17
13	125	128	15	2	1660	1612	13	7	166	132	9	20	179	166	13
14	225	193	11	3	680	754	7	8	266	237	7	21	51	45	31
15	386	380	9	4	639	616	7	9	291	314	8	h 7 4			11
16	87	115	22	5	257	270	7	10	310	272	8	7	786	741	
17	72	91	22	6	380	335	6	11	73	98	19	8	442	520	8
18	-107	13	14	7	158	177	9	12	582	592	8	9	847	819	9
19	270	269	10	8	253	279	7	13	326	326	9	10	206	219	10
20	-28	17	41	9	416	457	7	14	38	112	32	11	531	523	8
21	133	144	16	10	214	238	9	15	563	540	9	12	256	241	10
h 9 3			h 1 4			h 3 4									
10	395	382	8	11	392	341	8	16	259	207	11	13	179	213	12
11	367	379	9	12	687	698	9	17	114	97	18	14	264	232	10
12	37	94	33	13	57	153	24	18	78	97	21	15	137	158	16
13	110	92	17	14	464	476	9	19	521	535	9	16	187	200	11
14	317	325	10	15	44	92	31	20	115	132	17	17	211	217	11
15	281	234	11	16	361	359	9	21	173	183	13	18	165	160	13
16	308	281	9	17	221	253	12	h 4 4							
17	135	149	14	18	392	381	8	4	986	897	11	19	300	289	10
18	207	219	11	19	117	128	16	5	380	371	7	20	23	16	44
19	-105	39	15	20	198	182	12	6	778	800	8	8	493	474	11
20	55	96	29	21	-37	27	36	7	545	561	7	9	487	492	8
h 10 3			h 1 4			h 3 4									
11	211	281	11	1	284	259	8	10	60	117	21	10	862	894	10
12	287	231	10	2	545	483	6	11	143	200	12	11	423	457	9
13	712	607	10	3	225	224	7	12	1167	1160	11	12	324	350	9

Tetrakis(C6F5)-Octachloroporphinato Zinc 6(C6H4Cl2)

Page 5

20	63	81	27	5	608	658	7	17	292	282	9					
	h	9	4	6	189	204	8	18	363	354	9		9	479	461	8
9	526	509	11	7	371	383	7	19	143	125	14		10	158	149	12
10	76	119	20	8	191	162	9	20	271	267	10		11	492	485	9
11	141	56	14	9	748	644	8	21	112	129	18		12	-47	49	29
12	441	411	9	10	-48	30	24		h	4	5		13	256	240	11
13	362	335	9	11	298	192	9						14	253	260	11
14	381	380	10	12	522	494	8	5	509	486	7		15	137	129	13
15	178	168	11	13	659	553	9	6	459	478	7		16	205	226	11
16	183	155	11	14	202	190	11	7	243	223	8		17	213	219	11
17	324	334	9	15	-60	20	25	8	383	416	8		18	39	37	35
18	150	123	14	16	40	51	35	9	270	251	8		19	164	146	14
19	112	114	18	17	167	170	12	10	383	395	8		h	9	5	
20	202	216	12	18	-57	69	25	11	479	511	8					
	h	10	4	19	296	299	10	12	154	149	13		10	304	295	9
				20	-49	3	30	13	127	141	15		11	390	367	9
				21	177	199	13	14	141	136	14		12	199	230	12
10	228	245	14		h	1	5	15	395	415	10		13	-69	123	24
11	299	307	9					16	380	322	9		14	401	410	8
12	192	209	12	2	298	355	7	17	139	170	14		15	193	209	11
13	-48	59	31	3	553	618	7	18	285	278	9		16	294	298	9
14	201	209	12	4	274	214	7	19	501	460	9		17	108	61	17
15	92	133	18	5	681	715	8	20	94	97	20		18	87	95	21
16	463	465	8	6	854	845	9	21	73	82	34		19	19	62	47
17	115	119	17	7	321	383	7		h	5	5		h	10	5	
18	77	114	23	8	773	747	8	6	524	474	7		11	153	137	14
19	-70	54	24	9	598	640	8	7	432	426	7		12	117	180	17
	h	11	4	10	292	271	8	8	461	386	8		13	205	222	12
				11	252	234	9	9	341	334	8		14	232	193	10
11	393	401	13	12	480	481	8	10	298	249	9		15	468	447	8
12	170	201	13	13	161	190	12	11	282	261	9		16	155	156	13
13	202	210	12	14	19	123	44	12	202	243	11		17	226	231	11
14	196	171	11	15	-86	38	19	13	376	371	9		18	244	211	11
15	247	278	10	16	235	234	11	14	142	163	15					
16	390	376	9	17	-48	10	28	15	235	264	11		h	11	5	
17	207	181	11	18	90	128	19	16	200	217	10		12	361	399	10
18	114	133	17	19	-19	85	45	17	-71	69	21		13	229	235	10
19	251	253	11	20	62	91	27	18	84	102	21		14	103	143	17
	h	12	4	21	97	63	20	19	62	88	26		15	114	132	17
				h	2	5		20	149	144	15		16	264	250	10
12	409	448	13	3	596	605	7		h	6	5		17	125	86	16
13	107	148	16	4	537	485	7						18	224	211	12
14	59	86	25	5	928	929	9	7	132	151	12					
15	-51	53	28	6	207	213	8	8	484	413	8		h	12	5	
16	104	117	18	7	705	671	8	9	289	304	9		13	52	145	28
17	-53	43	29	8	345	299	7	10	291	281	9		14	144	180	14
18	-63	31	26	9	606	633	8	11	380	364	9		15	-79	95	20
	h	13	4	10	210	201	9	12	282	296	10		16	160	127	14
				11	354	356	8	13	177	188	12		17	99	129	20
13	134	158	20	12	231	224	10	14	166	216	13					
14	-72	35	21	13	469	462	9	15	289	257	10		h	13	5	
15	198	216	12	14	232	228	11	16	96	147	18					
16	70	99	25	15	418	375	9	17	197	231	11		14	241	271	10
17	182	206	13	16	37	75	37	18	210	224	11		15	102	103	19
	h	14	4	17	181	143	11	19	208	214	12		16	191	201	12
				18	187	183	12	20	69	35	25		17	37	39	48
				19	180	213	12		h	7	5		h	14	5	
14	523	478	12	20	157	116	14									
15	92	79	20	21	117	119	18	8	85	87	17		15	150	162	14
16	201	187	12		h	3	5	9	128	100	13		16	183	186	13
17	109	86	26		4	396	387	7	10	472	448	8				
	h	15	4		5	456	480	7	11	393	348	9		h	0	6
					6	467	481	7	12	450	455	9				
15	-97	50	24		7	271	274	8	13	112	100	17		0	1466	1440
16	205	194	12		8	432	412	7	14	432	426	9		1	691	627
	h	0	5		9	315	286	8	15	-42	77	29		2	1081	1032
					10	337	373	8	16	103	130	17		3	365	390
					11	435	426	8	17	108	114	17		4	77	46
1	316	294	6		12	703	667	9	18	355	342	9		5	151	58
2	381	327	6		13	97	73	18	19	106	63	18		6	46	42
3	512	502	7		14	205	175	11	20	243	219	11		7	92	159
4	184	233	8		15	186	118	12		h	8	5		8	282	355
					16	449	442	10								

Tetrakis(C₆F₅)-Octachloroporphinato Zinc 6(C₆H₄Cl₂)

Page 6

[illegible]

Tetrakis(C₆F₅)-Octachloroporphinato Zinc 6(C₆H₄Cl₂)

Page 8

[illegible]

Tetrakis(C6F5)-Octachloroporphinato Zinc 6(C6H4Cl2)

Page 9

9	159	149	14	8	148	132	15	1	287	299	14	4	-23	46	44
10	-73	50	23	9	102	103	19	2	69	9	24	5	-37	46	36
11	205	199	12	10	192	205	18	3	179	150	13	6	127	139	16
h	5	11		h	8	11		4	100	103	19	7	136	131	16
6	-45	39	31	9	159	194	14	5	122	138	16	8	103	104	19
7	120	125	16	h	0	12		6	88	30	21	h	4	12	
8	90	125	20	h	0	12		7	95	109	20	4	207	179	16
9	123	96	16	0	77	145	31	h	2	12		5	57	29	28
10	126	97	16	1	30	37	39	2	245	234	15	6	85	95	22
11	86	53	22	2	330	332	9	3	88	57	21	7	113	120	18
h	6	11		3	68	5	25	4	82	82	22	h	5	12	
7	205	203	12	4	84	25	22	5	126	126	16	5	-42	51	44
8	69	27	25	5	244	264	11	6	109	105	18	6	56	106	29
9	167	130	13	6	269	233	10	7	115	71	18	7	91	74	21
10	81	31	23	7	156	125	14	8	126	128	17	h	6	12	
h	7	11		8	75	33	24	h	3	12		6	131	137	23
				h	1	12		3	197	174	17				

Table 1. Final Refined Parameters for
Aquo, Carbonyl Tetrakis(Pentafluorophenyl)octachloroporphyrin Ruthenium(II).

Atom	x, y, z and $U_{eq}^a \times 10^4$			
	x	y	z	U_{eq} or B
Ru	2126(.5)	1763(.5)	1683(.3)	291(2)
Cl1	2662(2)	3927(2)	-61(1)	647(9)
C1	2188(6)	3188(6)	328(3)	2.8(2) *
C2	2635(6)	2714(6)	722(3)	2.3(2) *
N1	1953(5)	2315(4)	990(3)	2.1(1) *
C3	3597(6)	2573(6)	795(3)	2.5(2) *
C4	3997(6)	2090(5)	1169(3)	2.3(2) *
N2	3546(5)	1785(5)	1581(3)	2.1(1) *
C5	4960(6)	1836(6)	1202(4)	3.1(2) *
Cl2	5843(2)	1956(2)	773(1)	748(11)
C6	5069(7)	1380(6)	1619(4)	3.4(2) *
Cl3	6082(2)	876(3)	1761(1)	992(14)
C7	4191(6)	1364(6)	1874(4)	2.8(2) *
C8	4026(6)	1052(6)	2355(4)	2.8(2) *
C9	3163(6)	1023(6)	2593(4)	2.7(2) *
N3	2306(5)	1189(5)	2367(3)	2.4(2) *
Cl10	2978(7)	796(6)	3109(4)	3.2(2) *
Cl4	3744(2)	581(2)	3587(1)	695(10)
C11	2051(7)	828(6)	3186(4)	3.1(2) *
Cl5	1570(2)	663(3)	3763(1)	813(12)

Table 1. (Cont.)

Atom	x	y	z	U_{eq} or B
C12	1613(6)	1046(6)	2710(4)	2.8(2) *
C13	659(6)	1038(6)	2602(3)	2.5(2) *
C14	261(6)	1224(6)	2135(3)	2.5(2) *
N4	715(5)	1586(4)	1736(3)	2.1(1) *
C15	-708(7)	1098(6)	1993(4)	3.3(2) *
C16	-1575(2)	602(2)	2313(1)	767(11)
C16	-798(7)	1367(6)	1519(4)	3.4(2) *
C17	-1825(2)	1228(3)	1192(1)	805(11)
C17	82(6)	1708(6)	1360(3)	2.5(2) *
C18	263(6)	2147(6)	908(3)	2.5(2) *
C19	1108(6)	2475(6)	757(3)	2.3(2) *
C20	1280(6)	3034(6)	342(4)	2.8(2) *
C18	500(2)	3514(2)	-50(1)	718(10)
C21	4245(6)	2982(6)	425(4)	309(24)
C22	4358(7)	2698(7)	-51(4)	460(30)
C23	4973(8)	3078(8)	-388(4)	532(39)
C24	5459(7)	3762(8)	-242(5)	494(34)
C25	5369(7)	4056(7)	223(4)	418(31)
C26	4771(6)	3684(6)	558(4)	347(26)
C31	4834(6)	696(7)	2634(4)	390(29)

Table 1. (Cont.)

Atom	<i>x</i>	<i>y</i>	<i>z</i>	<i>U</i> _{eq} or <i>B</i>
C32	4985(7)	-153(7)	2647(4)	460(30)
C33	5726(7)	-491(8)	2911(4)	521(32)
C34	6323(7)	34(9)	3166(4)	564(41)
C35	6179(7)	870(8)	3155(4)	497(34)
C36	5457(7)	1178(7)	2890(4)	485(33)
C41	14(6)	853(7)	3025(4)	375(30)
C42	-182(7)	60(9)	3185(4)	548(36)
C43	-756(8)	-63(10)	3598(5)	655(40)
C44	-1151(9)	600(13)	3840(5)	801(57)
C45	-984(9)	1377(11)	3683(5)	758(46)
C46	-419(7)	1509(8)	3273(4)	544(34)
C51	-564(6)	2279(7)	567(4)	403(29)
C52	-1167(7)	2958(7)	633(4)	472(32)
C53	-1943(7)	3056(8)	342(5)	581(38)
C54	-2128(7)	2515(10)	-26(5)	613(48)
C55	-1549(8)	1857(9)	-110(4)	626(38)
C56	-765(7)	1723(8)	184(4)	487(30)
F22	3874(5)	2015(4)	-195(2)	706(20)
F23	5056(5)	2762(5)	-849(3)	832(25)
F24	6020(5)	4122(5)	-576(3)	818(22)

Table 1. (Cont.)

Atom	<i>x</i>	<i>y</i>	<i>z</i>	<i>U</i> _{eq} or <i>B</i>
F25	5857(4)	4728(4)	369(3)	648(19)
F26	4692(4)	4006(4)	1018(2)	581(18)
F32	4412(4)	-675(4)	2400(3)	665(19)
F33	5841(5)	-1327(4)	2922(3)	768(21)
F34	7021(4)	-306(5)	3428(3)	789(23)
F35	6777(4)	1349(4)	3402(3)	763(22)
F36	5338(4)	2009(4)	2890(3)	741(22)
F42	198(5)	-592(4)	2962(3)	776(23)
F43	-939(5)	-852(6)	3747(3)	1120(29)
F44	-1711(5)	483(7)	4237(3)	1269(38)
F45	-1382(6)	2026(7)	3920(3)	1343(35)
F46	-259(5)	2311(5)	3120(3)	886(24)
F52	-994(4)	3506(4)	1002(3)	714(21)
F53	-2506(5)	3710(5)	414(3)	969(27)
F54	-2872(4)	2604(5)	-321(3)	936(29)
F55	-1730(5)	1297(5)	-476(3)	996(26)
F56	-218(5)	1070(4)	112(3)	801(22)
C61	2044(7)	2772(7)	1999(4)	380(27)
O61	1983(6)	3394(5)	2200(3)	727(27)
O1	2165(4)	550(4)	1319(3)	455(18)

Table 1. (Cont.)

Atom	<i>x</i>	<i>y</i>	<i>z</i>	<i>U</i> _{eq} or <i>B</i>
C71	6734(14)	1512(12)	8525(6)	1339(72)
C72	7369(10)	1351(10)	8083(6)	810(47)
O2	7836(7)	727(6)	8029(4)	1052(36)
O3	7307(8)	1937(6)	7730(5)	1123(39)
C73	7799(23)	1823(15)	7264(11)	2118(126)
C74	7208(30)	1689(27)	6858(12)	3385(205)

$$^a U_{eq} = \frac{1}{3} \sum_i \sum_j [U_{ij} (a_i^* a_j^*) (\vec{a}_i \cdot \vec{a}_j)]$$

^a Isotropic displacement parameter, *B*

Table 2. Assigned Parameters for
Aquo, Carbonyl Tetrakis(Pentafluorophenyl)octachloroporphyrin Ruthenium(II).

x, y, z and $U_{eq}^a \times 10^4$					
Atom	x	y	z	B	
C81	2113	608	117	10.0	*
C82	3110	277	177	10.0	*
O4	3395	244	596	10.0	*
O5	3902	140	-172	10.0	*
C83	4801	-74	1	13.5	*
C84	5482	37	-378	15.0	*
C91A	4182	1901	8228	15.0	*
C92A	3256	1464	8232	10.0	*
C93A	2614	1851	8622	10.0	*
C94A	1677	1396	8619	10.0	*
C95A	1024	1765	9002	10.0	*
C96A	98	1328	9006	15.0	*
C91B	4073	2287	8474	15.0	*
C92B	3311	1674	8335	10.0	*
C93B	2440	1827	8656	10.0	*
C94B	1666	1226	8527	10.0	*
C95B	806	1382	8845	10.0	*
C96B	44	784	8715	15.0	*
C91C	3801	2164	8479	15.0	*
C92C	3028	1549	8341	10.0	*
C93C	2156	1671	8645	10.0	*
C94C	1405	1091	8521	10.0	*
C95C	545	1247	8840	10.0	*
C96C	-240	644	8712	15.0	*
H71A	6799	1075	8765	10.0	*
H71B	6886	2030	8677	10.0	*
H71C	6100	1528	8413	10.0	*
H73A	8214	1373	7293	10.0	*
H73B	8120	2321	7183	10.0	*
H74A	7585	1586	6569	10.0	*
H74B	6889	1151	6928	10.0	*

Table 2. (Cont.)

Atom	x	y	z	B	
H74C	6796	2099	6818	10.0	*
H81A	1811	602	432	10.0	*
H81B	2131	1164	-8	10.0	*
H81C	1780	265	-113	10.0	*
H83A	4956	271	279	10.0	*
H83B	4801	-643	103	10.0	*
H84A	6077	-112	-249	10.0	*
H84B	5335	-308	-657	10.0	*
H84C	5489	605	-480	10.0	*
H91A	4572	1652	7983	10.0	*
H91B	4093	2474	8150	10.0	*
H91C	4467	1853	8549	10.0	*
H91D	4606	2185	8274	10.0	*
H91E	3859	2841	8419	10.0	*
H91F	4233	2219	8818	10.0	*
H91G	4331	2059	8277	10.0	*
H91H	3589	2719	8423	10.0	*
H91I	3963	2098	8822	10.0	*
H92A	3349	891	8309	10.0	*
H92B	2975	1512	7910	10.0	*
H92D	3528	1121	8391	10.0	*
H92E	3154	1742	7991	10.0	*
H92G	3250	998	8396	10.0	*
H92H	2877	1619	7997	10.0	*
H93A	2518	2424	8546	10.0	*
H93B	2892	1803	8945	10.0	*
H93D	2227	2381	8600	10.0	*
H93E	2600	1759	8999	10.0	*
H93G	1937	2224	8590	10.0	*
H93H	2311	1603	8989	10.0	*
H94A	1777	823	8695	10.0	*

Table 2. (Cont.)

Atom	<i>x</i>	<i>y</i>	<i>z</i>	<i>B</i>	
H94B	1403	1444	8295	10.0	*
H94D	1878	672	8582	10.0	*
H94E	1505	1293	8183	10.0	*
H94G	1616	537	8577	10.0	*
H94H	1243	1158	8178	10.0	*
H95A	927	2338	8926	10.0	*
H95B	1301	1717	9325	10.0	*
H95D	593	1936	8790	10.0	*
H95E	967	1314	9189	10.0	*
H95G	334	1801	8784	10.0	*
H95H	708	1180	9183	10.0	*
H96A	-292	1577	9251	10.0	*
H96B	-187	1376	8685	10.0	*
H96C	187	755	9084	10.0	*
H96D	-483	893	8918	10.0	*
H96E	-122	850	8372	10.0	*
H96F	252	228	8771	10.0	*
H96G	-762	759	8918	10.0	*
H96H	-410	708	8370	10.0	*
H96I	-36	87	8769	10.0	*

Population Parameters: C91A to C96A, 0.302; C91B to C96B, 0.298; C91C to C96C, 0.236. Hydrogen atoms have same population as attached carbon atom; hydrogen atoms A, B and C are on 'A' carbon atoms, D, E and F on 'B' carbon atoms and G, H and I on 'C' carbon atoms. C81, C82, C83, C84 O4 and O5 have population parameter 0.5.

Table 3. Anisotropic Displacement Parameters for
Aquo, Carbonyl Tetrakis(Pentafluorophenyl)octachloroporphyrin Ruthenium(II).

Atom	U_{11}	U_{22}	U_{33}	U_{12}	U_{13}	U_{23}
Ru	172(4)	413(5)	289(4)	-13(4)	-3(3)	76(4)
Cl1	392(16)	884(24)	664(21)	-5(16)	37(15)	444(18)
Cl2	327(16)	1175(30)	744(22)	194(17)	208(15)	461(21)
Cl3	358(18)	1677(40)	944(28)	362(21)	171(18)	729(28)
Cl4	400(17)	1312(30)	373(17)	47(18)	-99(13)	225(18)
Cl5	468(19)	1627(37)	343(17)	-69(21)	11(14)	200(20)
Cl6	333(16)	1384(32)	585(21)	-289(18)	-35(14)	397(21)
Cl7	341(16)	1413(34)	659(22)	-267(19)	-130(15)	389(22)
Cl8	350(16)	1152(29)	650(21)	17(17)	-67(14)	526(20)
C21	266(53)	354(63)	308(59)	38(45)	-4(44)	123(47)
C22	519(70)	408(71)	453(75)	-24(57)	-35(59)	-16(58)
C23	464(70)	910(105)	223(62)	222(70)	90(52)	87(65)
C24	286(62)	606(86)	590(86)	28(59)	60(59)	193(70)
C25	226(56)	415(70)	613(83)	-21(51)	-39(54)	117(61)
C26	244(54)	421(66)	374(65)	27(49)	-64(47)	36(53)
C31	261(58)	562(76)	347(64)	-15(54)	17(47)	126(56)
C32	314(60)	643(85)	421(68)	-79(60)	-48(51)	73(61)
C33	414(71)	536(82)	612(81)	238(62)	51(61)	180(65)
C34	243(62)	976(112)	473(76)	62(69)	-74(54)	155(74)
C35	263(62)	645(87)	581(79)	-54(61)	-104(56)	75(67)
C36	290(62)	505(79)	660(82)	-35(58)	-21(58)	134(65)
C41	230(53)	626(79)	268(60)	-47(53)	-1(45)	91(56)
C42	323(66)	863(103)	458(75)	-84(67)	-36(55)	299(73)
C43	458(77)	947(115)	560(91)	-146(77)	-133(67)	361(85)
C44	494(87)	1562(174)	348(83)	-291(103)	55(66)	90(93)
C45	473(82)	1218(137)	583(94)	11(87)	136(70)	-257(95)
C46	355(65)	759(98)	517(78)	-95(63)	49(57)	90(70)
C51	231(54)	608(77)	371(65)	21(53)	6(47)	209(58)
C52	312(63)	629(85)	477(74)	-37(57)	62(55)	100(62)
C53	339(69)	747(102)	656(89)	148(66)	-20(63)	183(75)
C54	186(60)	1063(115)	590(88)	76(71)	-90(60)	235(82)
C55	540(79)	955(106)	380(71)	-247(82)	-187(60)	63(74)
C56	410(65)	628(80)	423(69)	-6(64)	-71(53)	100(66)

Table 3. (Cont.)

Atom	U_{11}	U_{22}	U_{33}	U_{12}	U_{13}	U_{23}
F22	679(45)	876(56)	565(44)	-213(40)	65(35)	-180(39)
F23	767(50)	1276(67)	454(45)	40(46)	170(37)	-103(43)
F24	640(46)	968(57)	849(55)	-34(41)	372(41)	453(45)
F25	495(39)	514(43)	934(54)	-152(34)	45(36)	178(38)
F26	571(41)	698(46)	474(42)	-144(34)	35(32)	-85(35)
F32	564(43)	638(47)	790(51)	8(36)	-206(38)	0(39)
F33	645(47)	747(53)	910(56)	247(40)	-110(40)	54(43)
F34	435(40)	1121(61)	809(52)	162(39)	-250(37)	254(45)
F35	466(41)	945(56)	874(55)	-133(38)	-276(38)	-16(44)
F36	493(42)	722(53)	1007(59)	-118(36)	-222(39)	97(43)
F42	705(51)	603(49)	1021(62)	54(41)	119(44)	131(44)
F43	807(58)	1426(79)	1125(70)	-334(54)	-101(49)	810(63)
F44	741(55)	2569(118)	500(50)	-408(65)	317(43)	118(61)
F45	1057(70)	1987(108)	989(70)	72(69)	472(57)	-628(71)
F46	876(57)	758(57)	1028(63)	22(46)	263(48)	-212(49)
F52	466(40)	839(54)	835(53)	186(36)	-48(37)	-165(43)
F53	533(46)	1258(69)	1115(67)	474(48)	-72(44)	168(54)
F54	385(40)	1701(81)	718(52)	63(46)	-247(37)	208(52)
F55	813(56)	1311(73)	859(60)	-68(50)	-386(47)	-240(54)
F56	776(51)	780(53)	844(56)	201(44)	-269(42)	-226(43)
C61	310(59)	389(69)	442(70)	27(53)	3(50)	66(56)
O61	807(64)	587(63)	787(66)	50(49)	51(50)	-143(51)
O1	438(43)	417(44)	511(47)	-6(35)	-44(35)	3(36)
C71	1856(192)	1558(179)	601(107)	552(146)	-273(118)	-139(112)
C72	777(107)	679(106)	974(127)	5(86)	-104(92)	35(100)
O2	1119(87)	724(72)	1314(95)	293(65)	222(72)	231(67)
O3	1238(94)	876(85)	1255(100)	194(68)	-35(78)	386(75)
C73	3124(411)	1029(170)	2221(315)	292(215)	2029(317)	446(201)
C74	4265(600)	4101(521)	1808(322)	-2050(429)	1958(371)	-1157(350)

$U_{i,j}$ values have been multiplied by 10^4

The form of the displacement factor is:

$$\exp -2\pi^2(U_{11}h^2a^{*2} + U_{22}k^2b^{*2} + U_{33}l^2c^{*2} + 2U_{12}hka^*b^* + 2U_{13}hla^*c^* + 2U_{23}k\ell b^*c^*)$$

Table 4. Complete Distances and Angles for
Aquo, Carbonyl Tetrakis(Pentafluorophenyl)octachloroporphyrin Ruthenium(II).

Distance(Å)		Distance(Å)	
Ru -N1	2.063(7)	C15 -Cl6	1.711(10)
Ru -N2	2.060(7)	C15 -C16	1.340(14)
Ru -N3	2.059(7)	C16 -Cl7	1.724(11)
Ru -N4	2.052(7)	C16 -C17	1.443(13)
Ru -C61	1.828(10)	C17 -C18	1.420(13)
Ru -O1	2.172(7)	C18 -C19	1.384(12)
Cl1 -C1	1.717(10)	C18 -C51	1.507(13)
C1 -C2	1.446(13)	C19 -C20	1.448(13)
C1 -C20	1.327(13)	C20 -Cl8	1.710(10)
C2 -N1	1.373(11)	C21 -C22	1.359(14)
C2 -C3	1.411(13)	C21 -C26	1.400(13)
N1 -C19	1.385(11)	C22 -C23	1.404(16)
C3 -C4	1.385(13)	C22 -F22	1.350(13)
C3 -C21	1.510(13)	C23 -C24	1.354(16)
C4 -N2	1.368(11)	C23 -F23	1.335(13)
C4 -C5	1.444(13)	C24 -C25	1.334(16)
N2 -C7	1.384(12)	C24 -F24	1.336(13)
C5 -Cl2	1.724(10)	C25 -C26	1.377(14)
C5 -C6	1.340(14)	C25 -F25	1.341(12)
C6 -Cl3	1.705(11)	C26 -F26	1.338(11)
C6 -C7	1.437(14)	C31 -C32	1.376(15)
C7 -C8	1.398(13)	C31 -C36	1.363(15)
C8 -C9	1.396(13)	C32 -C33	1.384(16)
C8 -C31	1.489(14)	C32 -F32	1.342(12)
C9 -N3	1.393(12)	C33 -C34	1.378(16)
C9 -C10	1.452(14)	C33 -F33	1.349(13)
N3 -C12	1.374(12)	C34 -C35	1.354(16)
C10 -Cl4	1.714(10)	C34 -F34	1.336(14)
C10 -C11	1.349(14)	C35 -C36	1.345(16)
C11 -Cl5	1.710(10)	C35 -F35	1.324(13)
C11 -C12	1.456(13)	C36 -F36	1.341(13)
C12 -C13	1.398(13)	C41 -C42	1.370(15)
C13 -C14	1.400(13)	C41 -C46	1.391(15)
C13 -C41	1.493(13)	C42 -C43	1.393(18)
C14 -N4	1.379(11)	C42 -F42	1.321(14)
C14 -C15	1.455(13)	C43 -C44	1.37(2)
N4 -C17	1.365(11)	C43 -F43	1.352(16)

Table 4. (Cont.)

Distance(Å)			Distance(Å)		
C44	-C45	1.33(2)	C91C	-C92C	1.528
C44	-F44	1.347(18)	C92C	-C93C	1.507
C45	-C46	1.382(19)	C93C	-C94C	1.461
C45	-F45	1.345(17)	C94C	-C95C	1.524
C46	-F46	1.367(14)	C95C	-C96C	1.520
C51	-C52	1.402(15)	C71	-H71A	0.953
C51	-C56	1.384(15)	C71	-H71B	0.948
C52	-C53	1.365(16)	C71	-H71C	0.957
C52	-F52	1.340(13)	C73	-H73A	0.938
C53	-C54	1.333(18)	C73	-H73B	0.947
C53	-F53	1.338(14)	C74	-H74A	0.959
C54	-C55	1.360(18)	C74	-H74B	0.993
C54	-F54	1.333(15)	C74	-H74C	0.890
C55	-C56	1.387(17)	C81	-H81A	0.950
C55	-F55	1.351(15)	C81	-H81B	0.950
C56	-F56	1.323(13)	C81	-H81C	0.950
C61	-O61	1.134(13)	C83	-H83A	0.950
C71	-C72	1.52(2)	C83	-H83B	0.950
C72	-O2	1.213(19)	C84	-H84A	0.950
C72	-O3	1.331(19)	C84	-H84B	0.950
O3	-C73	1.44(3)	C84	-H84C	0.950
C73	-C74	1.39(5)	C91A	-H91A	0.950
C81	-C82	1.535	C91A	-H91B	0.950
C82	-O4	1.191	C91A	-H91C	0.950
C82	-O5	1.490	C92A	-H92A	0.950
O5	-C83	1.411	C92A	-H92B	0.950
C83	-C84	1.421	C93A	-H93A	0.950
C91A	-C92A	1.503	C93A	-H93B	0.950
C92A	-C93A	1.526	C94A	-H94A	0.950
C93A	-C94A	1.530	C94A	-H94B	0.950
C94A	-C95A	1.512	C95A	-H95A	0.950
C95A	-C96A	1.503	C95A	-H95B	0.950
C91B	-C92B	1.515	C96A	-H96A	0.950
C92B	-C93B	1.539	C96A	-H96B	0.950
C93B	-C94B	1.507	C96A	-H96C	0.950
C94B	-C95B	1.524	C91B	-H91D	0.950
C95B	-C96B	1.494	C91B	-H91E	0.950

Table 4. (Cont.)

Distance(Å)		Angle(°)	
C91B -H91F	0.950	N1 -Ru -N2	89.3(3)
C92B -H92D	0.950	N1 -Ru -N3	178.8(3)
C92B -H92E	0.950	N1 -Ru -N4	90.4(3)
C93B -H93D	0.950	N1 -Ru -C61	91.6(4)
C93B -H93E	0.950	N1 -Ru -O1	89.2(3)
C94B -H94D	0.950	N2 -Ru -N3	90.3(3)
C94B -H94E	0.950	N2 -Ru -N4	172.2(3)
C95B -H95D	0.950	N2 -Ru -C61	96.4(4)
C95B -H95E	0.950	N2 -Ru -O1	85.9(3)
C96B -H96D	0.950	N3 -Ru -N4	89.8(3)
C96B -H96E	0.950	N3 -Ru -C61	89.6(4)
C96B -H96F	0.950	N3 -Ru -O1	89.7(3)
C91C -H91G	0.950	N4 -Ru -C61	91.4(4)
C91C -H91H	0.950	N4 -Ru -O1	86.3(3)
C91C -H91I	0.950	C61 -Ru -O1	177.6(4)
C92C -H92G	0.950	Ru -C61 -O61	178.9(9)
C92C -H92H	0.950	Ru -N1 -C2	125.7(6)
C93C -H93G	0.950	Ru -N1 -C19	125.6(6)
C93C -H93H	0.950	Ru -N2 -C4	125.8(6)
C94C -H94G	0.950	Ru -N2 -C7	125.2(6)
C94C -H94H	0.950	Ru -N3 -C9	125.0(6)
C95C -H95G	0.950	Ru -N3 -C12	125.2(6)
C95C -H95H	0.950	Ru -N4 -C14	125.6(6)
C96C -H96G	0.950	Ru -N4 -C17	125.7(6)
C96C -H96H	0.950	C2 -C1 -Cl1	128.7(7)
C96C -H96I	0.950	C20 -C1 -Cl1	122.5(7)
		C20 -C1 -C2	108.4(8)
		N1 -C2 -C1	107.9(7)
		C3 -C2 -C1	127.9(8)
		C3 -C2 -N1	123.7(8)
		C19 -N1 -C2	107.9(7)
		C4 -C3 -C2	126.2(8)
		C21 -C3 -C2	116.6(8)
		C21 -C3 -C4	117.3(8)
		N2 -C4 -C3	125.5(8)
		C5 -C4 -C3	126.5(8)
		C5 -C4 -N2	107.9(8)

Table 4. (Cont.)

Angle(°)				Angle(°)			
C7	-N2	-C4	108.1(7)	C17	-C16	-C15	108.6(9)
C12	-C5	-C4	129.5(7)	C17	-C16	-C17	130.4(8)
C6	-C5	-C4	108.2(8)	C16	-C17	-N4	108.1(8)
C6	-C5	-C12	122.0(8)	C18	-C17	-N4	124.8(8)
C13	-C6	-C5	122.6(8)	C18	-C17	-C16	127.0(8)
C7	-C6	-C5	107.7(9)	C19	-C18	-C17	126.8(8)
C7	-C6	-C13	129.6(8)	C51	-C18	-C17	115.7(8)
C6	-C7	-N2	108.0(8)	C51	-C18	-C19	117.4(8)
C8	-C7	-N2	125.3(8)	C18	-C19	-N1	124.6(8)
C8	-C7	-C6	126.4(9)	C20	-C19	-N1	107.8(7)
C9	-C8	-C7	125.7(9)	C20	-C19	-C18	127.7(8)
C31	-C8	-C7	117.5(8)	C19	-C20	-C1	107.9(8)
C31	-C8	-C9	116.8(8)	C18	-C20	-C1	122.7(7)
N3	-C9	-C8	125.7(8)	C18	-C20	-C19	129.2(7)
C10	-C9	-C8	127.4(9)	C22	-C21	-C3	122.9(9)
C10	-C9	-N3	106.9(8)	C26	-C21	-C3	121.1(8)
C12	-N3	-C9	108.9(7)	C26	-C21	-C22	116.0(9)
C14	-C10	-C9	129.5(8)	C23	-C22	-C21	122.1(10)
C11	-C10	-C9	108.7(9)	F22	-C22	-C21	118.2(9)
C11	-C10	-C14	121.7(8)	F22	-C22	-C23	119.7(9)
C15	-C11	-C10	122.2(8)	C24	-C23	-C22	119.4(10)
C12	-C11	-C10	107.5(9)	F23	-C23	-C22	119.0(10)
C12	-C11	-C15	130.3(7)	F23	-C23	-C24	121.6(10)
C11	-C12	-N3	108.0(8)	C25	-C24	-C23	120.1(11)
C13	-C12	-N3	125.2(8)	F24	-C24	-C23	117.9(10)
C13	-C12	-C11	126.6(9)	F24	-C24	-C25	122.0(10)
C14	-C13	-C12	125.2(8)	C26	-C25	-C24	121.0(10)
C41	-C13	-C12	117.2(8)	F25	-C25	-C24	120.1(10)
C41	-C13	-C14	117.5(8)	F25	-C25	-C26	119.0(9)
N4	-C14	-C13	125.7(8)	C25	-C26	-C21	121.4(9)
C15	-C14	-C13	126.1(8)	F26	-C26	-C21	119.6(8)
C15	-C14	-N4	108.2(8)	F26	-C26	-C25	119.0(9)
C17	-N4	-C14	108.2(7)	C32	-C31	-C8	120.9(9)
C16	-C15	-C14	129.2(7)	C36	-C31	-C8	122.8(9)
C16	-C15	-C14	106.8(9)	C36	-C31	-C32	116.3(10)
C16	-C15	-C16	123.6(8)	C33	-C32	-C31	121.3(10)
C17	-C16	-C15	120.9(8)	F32	-C32	-C31	120.4(9)

Table 4. (Cont.)

Angle(°)		Angle(°)	
F32 -C32 -C33	118.2(9)	C54 -C53 -C52	120.2(11)
C34 -C33 -C32	119.1(11)	F53 -C53 -C52	120.0(11)
F33 -C33 -C32	119.5(10)	F53 -C53 -C54	119.8(11)
F33 -C33 -C34	121.3(10)	C55 -C54 -C53	120.3(12)
C35 -C34 -C33	119.9(11)	F54 -C54 -C53	121.3(11)
F34 -C34 -C33	118.2(10)	F54 -C54 -C55	118.3(11)
F34 -C34 -C35	121.9(10)	C56 -C55 -C54	121.5(11)
C36 -C35 -C34	119.4(11)	F55 -C55 -C54	121.2(11)
F35 -C35 -C34	117.6(10)	F55 -C55 -C56	117.3(11)
F35 -C35 -C36	123.0(10)	C55 -C56 -C51	118.9(10)
C35 -C36 -C31	123.9(10)	F56 -C56 -C51	119.6(10)
F36 -C36 -C31	118.5(9)	F56 -C56 -C55	121.5(10)
F36 -C36 -C35	117.6(10)	O2 -C72 -C71	124.5(15)
C42 -C41 -C13	123.3(9)	O3 -C72 -C71	113.1(14)
C46 -C41 -C13	119.4(9)	O3 -C72 -O2	122.2(14)
C46 -C41 -C42	117.3(10)	C73 -O3 -C72	119.2(16)
C43 -C42 -C41	120.1(11)	C74 -C73 -O3	113.0(26)
F42 -C42 -C41	120.4(10)	O4 -C82 -C81	115.5
F42 -C42 -C43	119.5(11)	O5 -C82 -C81	134.5
C44 -C43 -C42	120.8(13)	O5 -C82 -O4	108.6
F43 -C43 -C42	118.8(12)	C83 -O5 -C82	122.2
F43 -C43 -C44	120.3(12)	C84 -C83 -O5	111.7
C45 -C44 -C43	120.0(14)	C93A -C92A -C91A	110.7
F44 -C44 -C43	121.0(13)	C94A -C93A -C92A	109.7
F44 -C44 -C45	119.0(13)	C95A -C94A -C93A	111.0
C46 -C45 -C44	119.9(13)	C96A -C95A -C94A	112.0
F45 -C45 -C44	119.8(13)	C93B -C92B -C91B	110.5
F45 -C45 -C46	120.3(12)	C94B -C93B -C92B	111.8
C45 -C46 -C41	121.8(11)	C95B -C94B -C93B	111.5
F46 -C46 -C41	119.4(10)	C96B -C95B -C94B	111.1
F46 -C46 -C45	118.8(11)	C93C -C92C -C91C	113.1
C52 -C51 -C18	121.2(9)	C94C -C93C -C92C	114.3
C56 -C51 -C18	121.1(9)	C95C -C94C -C93C	111.8
C56 -C51 -C52	117.7(9)	C96C -C95C -C94C	111.9
C53 -C52 -C51	121.4(10)	H71A -C71 -C72	109.9
F52 -C52 -C51	119.2(9)	H71B -C71 -C72	110.1
F52 -C52 -C53	119.4(10)	H71C -C71 -C72	109.6

Table 4. (Cont.)

Angle(°)			Angle(°)		
H71B -C71	-H71A	109.4	H92A -C92A -C91A		109.2
H71C -C71	-H71A	108.7	H92B -C92A -C91A		109.2
H71C -C71	-H71B	109.1	H92A -C92A -C93A		109.2
H73A -C73	-O3	109.9	H92B -C92A -C93A		109.2
H73B -C73	-O3	109.3	H92B -C92A -H92A		109.5
H73A -C73	-C74	109.4	H93A -C93A -C92A		109.4
H73B -C73	-C74	104.4	H93B -C93A -C92A		109.4
H73B -C73	-H73A	110.7	H93A -C93A -C94A		109.4
H74A -C74	-C73	107.9	H93B -C93A -C94A		109.4
H74B -C74	-C73	105.6	H93B -C93A -H93A		109.5
H74C -C74	-C73	112.7	H94A -C94A -C93A		109.1
H74B -C74	-H74A	105.3	H94B -C94A -C93A		109.1
H74C -C74	-H74A	114.0	H94A -C94A -C95A		109.1
H74C -C74	-H74B	110.8	H94B -C94A -C95A		109.1
H81A -C81	-C82	109.5	H94B -C94A -H94A		109.5
H81B -C81	-C82	109.5	H95A -C95A -C94A		108.8
H81C -C81	-C82	109.5	H95B -C95A -C94A		108.8
H81B -C81	-H81A	109.5	H95A -C95A -C96A		108.8
H81C -C81	-H81A	109.5	H95B -C95A -C96A		108.8
H81C -C81	-H81B	109.5	H95B -C95A -H95A		109.5
H83A -C83	-O5	108.9	H96A -C96A -C95A		109.5
H83B -C83	-O5	108.9	H96B -C96A -C95A		109.5
H83A -C83	-C84	108.9	H96C -C96A -C95A		109.5
H83B -C83	-C84	108.9	H96B -C96A -H96A		109.5
H83B -C83	-H83A	109.5	H96C -C96A -H96A		109.5
H84A -C84	-C83	109.5	H96C -C96A -H96B		109.5
H84B -C84	-C83	109.5	H91D -C91B -C92B		109.5
H84C -C84	-C83	109.5	H91E -C91B -C92B		109.5
H84B -C84	-H84A	109.5	H91F -C91B -C92B		109.5
H84C -C84	-H84A	109.5	H91E -C91B -H91D		109.5
H84C -C84	-H84B	109.5	H91F -C91B -H91D		109.5
H91A -C91A -C92A		109.5	H91F -C91B -H91E		109.5
H91B -C91A -C92A		109.5	H92D -C92B -C91B		109.2
H91C -C91A -C92A		109.5	H92E -C92B -C91B		109.2
H91B -C91A -H91A		109.5	H92D -C92B -C93B		109.2
H91C -C91A -H91A		109.5	H92E -C92B -C93B		109.2
H91C -C91A -H91B		109.5	H92E -C92B -H92D		109.5

Table 4. (Cont.)

Angle(°)		Angle(°)	
H93D -C93B -C92B	108.9	H94H -C94C -C93C	108.9
H93E -C93B -C92B	108.9	H94G -C94C -C95C	108.9
H93D -C93B -C94B	108.9	H94H -C94C -C95C	108.9
H93E -C93B -C94B	108.9	H94H -C94C -H94G	109.5
H93E -C93B -H93D	109.5	H95G -C95C -C94C	108.9
H94D -C94B -C93B	108.9	H95H -C95C -C94C	108.9
H94E -C94B -C93B	108.9	H95G -C95C -C96C	108.9
H94D -C94B -C95B	108.9	H95H -C95C -C96C	108.9
H94E -C94B -C95B	108.9	H95H -C95C -H95G	109.5
H94E -C94B -H94D	109.5	H96G -C96C -C95C	109.5
H95D -C95B -C94B	109.1	H96H -C96C -C95C	109.5
H95E -C95B -C94B	109.1	H96I -C96C -C95C	109.5
H95D -C95B -C96B	109.1	H96H -C96C -H96G	109.5
H95E -C95B -C96B	109.1	H96I -C96C -H96G	109.5
H95E -C95B -H95D	109.5	H96I -C96C -H96H	109.5
H96D -C96B -C95B	109.5		
H96E -C96B -C95B	109.5		
H96F -C96B -C95B	109.5		
H96E -C96B -H96D	109.5		
H96F -C96B -H96D	109.5		
H96F -C96B -H96E	109.5		
H91G -C91C -C92C	109.5		
H91H -C91C -C92C	109.5		
H91I -C91C -C92C	109.5		
H91H -C91C -H91G	109.5		
H91I -C91C -H91G	109.5		
H91I -C91C -H91H	109.5		
H92G -C92C -C91C	108.6		
H92H -C92C -C91C	108.6		
H92G -C92C -C93C	108.6		
H92H -C92C -C93C	108.6		
H93G -C93C -C92C	108.3		
H93H -C93C -C92C	108.3		
H93G -C93C -C94C	108.3		
H93H -C93C -C94C	108.3		
H93H -C93C -H93G	109.5		
H94G -C94C -C93C	108.9		

Table 5. Intermolecular Distances Less Than 3.5 Å for
Aquo, Carbonyl Tetrakis(Pentafluorophenyl)octachloroporphyrin Ruthenium(II).

Distance(Å)		Distance(Å)	
Cl1 -F25	3.140(7)	F23 -F36	3.411(10)
C1 -F43	3.423(12)	F24 -F53	3.439(10)
N1 -F43	3.353(11)	F24 -F54	2.981(10)
C4 -O4	3.436	F24 -F44	3.359(11)
N2 -F33	3.415(10)	F24 -F35	3.036(10)
N3 -O2	3.250(13)	F24 -F25	3.314(9)
Cl4 -C91B	3.460	F24 -F26	3.378(9)
Cl4 -F25	3.152(7)	F25 -F53	2.862(10)
C18 -F43	3.471(12)	F25 -F25	3.264(9)
C19 -F43	2.998(12)	F26 -F33	2.982(9)
C20 -F43	3.057(12)	F26 -F34	3.080(9)
C23 -F54	3.191(13)	F32 -C71	3.249(19)
C24 -F53	3.400(14)	F32 -C72	3.057(17)
C24 -F54	3.039(13)	F32 -O2	3.422(12)
C24 -F25	3.087(13)	F32 -O3	3.208(13)
C25 -F53	3.140(13)	F32 -C74	3.47(4)
C25 -C25	3.417(15)	F32 -C91A	3.283
C25 -F25	3.060(12)	F33 -C91A	3.203
C33 -F26	3.032(13)	F33 -C92A	3.353
C34 -F26	3.100(13)	F33 -C61	3.369(12)
C35 -F24	3.394(13)	F33 -O61	3.176(11)
C43 -F34	3.246(15)	F34 -F43	3.170(11)
C44 -F34	3.189(17)	F34 -F44	3.088(11)
C44 -F35	3.409(17)	F34 -O61	3.035(11)
C45 -F35	3.300(16)	F35 -F44	3.400(11)
C54 -F45	3.104(16)	F35 -F45	3.169(11)
C55 -C96A	3.456	F35 -C71	3.442(19)
C55 -F45	3.157(15)	F35 -O3	3.367(13)
C56 -C96A	3.444	F36 -O3	3.323(13)
F22 -C81	3.490	F36 -C91A	2.576
F22 -C82	3.154	F36 -C91B	2.652
F22 -O5	3.004	F36 -C91C	3.022
F23 -F54	3.296(10)	F42 -F52	3.318(10)
F23 -C91A	3.083	F43 -F52	3.033(11)
F23 -C91B	2.409	F43 -C61	3.362(13)
F23 -C91C	2.711	F43 -O61	3.170(12)
F23 -F35	3.491(10)	F45 -F54	3.013(12)

Table 5. (Cont.)

Distance(Å)	
F45 -F55	3.174(12)
F45 -C96A	3.393
F46 -C95A	3.328
F46 -C96A	3.253
F46 -C95B	3.230
F46 -C96B	3.465
F46 -C95C	3.214
F52 -C74	3.47(4)
F55 -C96A	2.975
F55 -C96B	3.448
F55 -C96C	3.228
F55 -C71	3.47(2)
F55 -C81	3.245
F55 -C82	3.305
F55 -O4	3.449
F56 -C81	3.428
F56 -C96A	3.017
O61 -C92A	3.305
O61 -C92C	3.389
O1 -C81	3.210
O1 -C82	3.371
O1 -O4	2.668
O1 -C96C	3.362
O1 -O2	2.683(12)
O2 -C96C	3.306
O4 -C83	3.060
O5 -O5	3.309
O5 -C84	2.343
C84 -C84	2.453

Table 6. Observed and Calculated Structure Factors for
Aquo, Carbonyl Tetrakis(pentafluorophenyl)porphyrin Ruthenium(II)

The columns contain, in order, ℓ , $10F_{obs}$, $10F_{calc}$ and $10\sigma F_{obs}$. A minus sign preceding F_{obs} indicates that F_{obs}^2 is negative.

Aquo. Carbonyl Tetrakis(pentafluorophenyl)octachloroporphyrin Ru(II)

Page 1

-15 0 1	3 715 697 18	-13 2 1	9 72 66 59	9 -147 92 29	9 253 252 25
2 893 807 26	4 863 866 18	1 785 759 17	10 794 773 18	10 -126 112 34	10 396 387 20
4 347 396 32	5 762 743 18	2 389 339 20	11 405 409 21	11 278 300 23	11 150 195 36
6 424 432 30	6 87 109 51	3 1205 1179 18	-13 7 1	12 257 233 24	12 503 488 19
-15 1 1	7 197 146 30	4 406 444 19	1 205 155 29	13 313 316 22	13 217 267 29
1 433 380 21	8 194 122 31	5 215 114 27	2 248 257 26	14 225 230 27	14 -52 84 68
2 879 871 19	9 1018 994 19	6 292 264 23	3 -29 75 81	15 111 137 44	15 148 222 39
3 427 440 21	10 247 253 27	7 330 316 21	4 181 237 32	16 531 522 19	-12 7 1
4 383 358 22	11 237 266 28	8 78 163 52	5 123 23 42	17 614 587 19	1 147 167 35
5 547 531 20	-14 4 1	9 391 413 20	6 571 556 19	-12 3 1	2 51 26 64
6 504 495 20	1 335 336 22	10 493 517 19	7 24 62 87	1 -135 50 30	3 232 261 26
-15 2 1	2 321 347 23	11 228 197 27	8 514 441 20	2 321 309 20	4 432 392 19
1 41 25 75	3 277 229 25	12 79 136 54	9 92 27 52	3 985 1035 17	5 -49 47 65
2 -74 23 56	4 208 126 29	13 -17 19 91	10 267 237 27	4 602 620 17	6 543 487 18
3 507 479 20	5 282 255 24	14 464 443 20	-13 8 1	5 -91 64 43	7 147 119 36
4 404 373 21	6 176 7 33	15 790 766 19	1 223 183 28	6 563 575 17	8 945 886 18
5 418 405 21	7 648 672 19	-13 3 1	2 470 491 20	7 184 202 29	9 223 96 28
6 227 259 29	8 300 281 24	1 383 344 20	3 229 207 28	8 452 450 18	10 543 523 19
-15 3 1	9 345 326 23	2 390 390 20	4 399 466 21	9 513 551 18	11 305 288 24
1 608 584 19	10 150 201 38	3 268 179 24	5 143 196 39	10 -176 34 24	12 160 160 36
2 127 58 43	-14 5 1	4 187 4 29	6 76 108 58	11 -185 27 23	13 269 242 26
3 417 424 21	1 107 0 46	5 945 930 17	7 146 131 39	12 -85 58 48	-12 8 1
4 179 108 34	2 911 870 18	6 380 400 20	8 62 37 65	13 193 176 30	1 470 441 19
-15 4 1	3 694 705 18	7 113 133 42	-13 9 1	14 140 121 37	2 369 309 21
1 170 77 35	4 650 608 18	8 -76 42 51	1 472 444 20	15 752 755 18	3 355 365 21
-14 0 1	5 325 341 23	9 156 66 34	2 195 188 32	16 148 112 37	4 439 438 20
2 663 641 25	6 451 495 20	10 459 385 19	3 -156 77 31	17 279 156 26	5 210 112 29
4 170 231 45	7 126 55 42	11 760 760 18	4 84 7 55	-12 4 1	6 797 803 18
6 897 867 25	8 735 663 19	12 106 133 46	-12 0 1	1 526 550 17	7 295 285 24
8 179 205 44	-14 6 1	13 481 515 20	2 222 218 40	2 466 433 18	8 196 178 31
10 631 579 26	1 489 514 20	14 458 438 20	4 -229 18 22	3 372 327 19	9 438 377 20
12 600 555 27	2 39 71 76	-13 4 1	6 1027 1071 23	4 399 408 19	10 683 713 19
-14 1 1	3 69 24 60	1 278 281 23	8 -112 115 50	5 437 492 18	11 214 140 30
1 246 217 26	4 165 201 35	2 349 326 21	10 -207 6 27	6 35 139 73	12 364 379 23
2 523 485 19	5 -43 42 73	3 664 655 17	12 808 773 24	7 422 373 19	-12 9 1
3 153 195 35	6 459 466 21	4 140 131 36	14 663 568 25	8 232 235 25	1 151 55 36
4 304 293 23	7 366 335 22	5 277 260 23	16 462 422 28	9 -59 18 59	2 222 255 28
5 67 80 58	-14 7 1	6 238 243 26	18 287 340 35	10 196 117 29	3 178 188 32
6 608 574 18	1 222 157 29	7 235 220 26	-12 1 1	11 372 378 20	4 374 312 21
7 242 157 26	2 550 537 19	8 519 445 19	1 84 77 53	12 293 325 23	5 94 62 50
8 711 719 18	3 422 360 21	9 906 911 18	2 320 402 24	13 563 549 18	6 389 425 21
9 301 271 24	-13 0 1	10 151 70 36	3 -166 21 28	14 -139 64 33	7 386 356 22
10 337 298 23	1 1663 1611 26	11 359 393 22	4 293 374 21	15 154 108 36	8 426 427 21
11 234 169 28	2 537 544 25	12 -124 2 38	5 99 171 43	16 262 261 26	9 559 556 20
12 -155 38 31	3 216 157 37	13 355 337 23	6 68 127 54	-12 5 1	10 157 10 38
-14 2 1	4 262 310 34	14 433 420 21	7 405 378 19	1 -113 138 37	-12 10 1
1 80 89 53	5 79 8 69	-13 5 1	8 -122 125 34	2 86 27 48	1 355 296 22
2 189 204 30	6 459 466 21	1 -155 24 28	9 -115 21 36	3 514 516 18	2 202 145 31
3 249 263 26	7 366 335 22	2 120 203 40	10 257 315 24	4 453 476 18	3 110 84 46
4 144 54 37	8 127 85 34	3 321 301 22	11 127 167 38	5 74 88 53	4 182 146 33
5 548 521 19	9 -119 100 36	4 -66 27 56	12 270 243 23	6 309 239 22	5 743 724 19
6 434 396 20	10 205 173 28	5 189 262 30	13 85 78 50	7 931 879 17	6 231 154 29
7 540 507 19	11 696 607 18	6 360 355 21	14 800 746 18	8 527 496 18	7 677 568 19
8 351 383 22	12 917 852 18	7 456 418 19	15 419 370 20	9 811 785 17	-11 0 1
9 250 252 26	13 85 35 52	8 271 250 25	16 654 654 18	10 140 163 37	2 1295 1283 26
10 164 44 35	14 186 27 32	9 235 205 27	17 294 299 24	11 -72 11 54	4 536 490 26
11 722 695 19	15 256 170 27	10 247 265 27	18 255 206 27	12 399 389 20	6 -183 112 32
-14 3 1	-13 1 1	11 -92 66 48	-12 2 1	13 180 151 32	8 455 547 28
1 600 610 18	1 548 503 18	12 490 529 20	1 117 222 41	14 431 386 20	10 508 466 24
2 132 108 39	2 699 657 17	13 716 750 19	2 -131 87 31	15 694 702 19	12 762 748 23
	3 193 118 29	-13 6 1	3 187 196 28	16 470 436 20	14 788 760 24
	4 835 757 17	1 -127 24 35	4 -95 51 41	-12 6 1	16 390 466 28
	5 1153 1104 18	2 121 236 41	5 650 686 17	1 354 324 20	18 201 258 42
	6 799 725 17	3 -129 70 34	6 227 234 25	2 -189 53 22	20 638 603 27
	7 268 280 24	4 315 296 22	7 519 528 17	3 -10 144 93	-11 1 1
	8 -127 85 34	5 -47 74 68	8 -117 1 36	4 -126 47 34	1 -113 24 38
	9 -119 100 36	6 -73 67 54		5 481 503 18	
	10 205 173 28	7 143 45 37		6 415 396 19	
	11 696 607 18	8 510 516 19		7 233 208 26	
	12 917 852 18			8 -67 47 56	
	13 85 35 52				
	14 186 27 32				
	15 256 170 27				

Aquo. Carbonyl Tetrakis(pentafluorophenyl)octachloroporphyrin Ru(II)

2	51	99	65	13	563	562	18	9	369	325	21	10	97	148	46	16	-142	125	31	5	625	572	17	
3	88	139	60	14	28	123	79	10	249	285	26	11	402	445	21	17	332	397	22	6	452	482	18	
4	830	744	18	15	155	245	35	11	298	255	24	12	455	418	20	18	235	277	27	7	202	225	28	
5	166	260	33	16	-156	47	29	12	-75	63	55	13	244	240	23	19	58	97	64	8	140	162	36	
6	573	572	19	17	-174	34	27	13	201	138	31	14	879	901	17	20	-21	108	90	9	640	652	17	
7	52	178	65	18	112	131	45	14	464	465	20	15	128	142	37					10	-37	22	31	
8	-85	57	49	19	299	276	25	15	153	143	38	16	-123	35	35	-10	5	1		11	-145	32	31	
9	-176	1	25									17	-137	70	32					12	255	249	25	
10	561	601	17	-11	5	1		-11	9	1		18	-134	93	33	1	83	121	50	13	152	194	35	
11	601	590	17									19	176	227	32	2	810	810	18	14	-74	8	55	
12	382	249	29	1	427	412	21	1	605	609	18	20	632	639	19	3	591	600	18	15	111	126	45	
13	135	35	20	2	151	6	36	2	153	96	34					4	53	18	64	16	355	376	22	
14	-141	35	30	3	1008	1030	19	3	136	233	37	-10	2	1		5	525	526	19	17	-146	117	34	
15	337	351	21	4	178	207	33	4	128	91	39					6	192	66	22					
16	538	523	18	5	156	117	31	5	-65	38	57					7	190	304	31	-10	9	1		
17	-174	49	26	6	797	785	16	6	-156	90	29	1	322	331	21	8	-75	13	54					
18	237	293	27	7	286	358	22	7	412	377	20	2	143	57	33	9	95	95	49	1	-97	11	42	
19	-51	41	68	8	522	558	17	8	-30	42	80	3	1529	1480	20	10	-95	32	41	2	219	140	26	
20	167	130	36	9	321	256	21	9	282	263	25	4	414	393	19	11	-89	72	44	3	673	663	17	
				10	408	394	19	10	178	255	33	5	909	871	18	12	94	103	46	4	-112	103	38	
				11	659	665	17	11	288	231	25	6	-108	23	37	13	270	299	23	5	219	146	27	
				12	85	110	50	12	311	355	24	7	-68	29	53	14	666	624	17	6	550	572	18	
				13	229	231	26	13	394	377	22	8	705	693	18	15	283	274	23	7	674	656	17	
				14	-150	46	30	-11	10	1		9	252	268	25	16	-62	166	58	8	343	275	21	
				15	216	281	28																	
				16	-66	144	59	-11	10	1		10	305	305	23	17	-168	61	27	9	587	575	18	
				17	531	535	19	1	440	418	20	11	614	621	19	18	-107	141	42	10	-131	101	34	
				18	371	380	22	2	110	77	44	12	627	616	19	19	237	268	28	11	-108	36	41	
								3	193	208	30	13	103	145	42	20	137	268	28	12	242	262	27	
								4	-87	5	49	14	-119	15	35	20	211	243	29	13	307	341	24	
								5	121	39	42	15	39	100	70	21	146	185	39	14	477	454	20	
								6	404	459	21	16	526	533	18	-10	6	1		15	102	150	49	
								7	391	415	21	17	758	721	17	2	205	272	29	16	-77	3	57	
								8	-100	78	46	18	29	161	79	1	-75	51	52					
								9	208	221	30	19	-164	60	28	2	293	329	24	-10	10	1		
								10	35	102	81	20	211	243	29	3	397	407	21	1	505	552	18	
								11	-123	116	40	21	146	185	39	4	293	329	24	2	218	243	27	
																5	44	55	71	3	-132	68	33	
																6	-106	62	42	4	216	205	37	
																7	291	298	25	5	281	327	24	
																8	802	805	19	6	199	232	29	
																9	111	79	40	7	318	303	62	
																10	877	857	17	8	-54	83	64	
																11	49	35	65	9	-155	2	30	
																12	446	443	19	10	-42	41	72	
																13	230	273	26	11	442	377	20	
																14	108	205	43	12	397	360	21	
																15	209	230	28	13	-139	4	35	
																16	378	420	21	14	-135	3	37	
																17	-120	95	38					
																18	-140	81	34					
																19	-176	78	28	-10	11	1		
																				1	338	334	22	
																				2	202	219	29	
																				3	550	529	19	
																				4	99	43	47	
																				5	346	317	22	
																				6	363	393	22	
																				7	216	252	29	
																				8	259	242	26	
																				9	284	265	25	
																				10	-74	7	57	
																				11	-105	70	46	
																				12	217	241	31	

Aquo. Carbonyl Tetrakis(pentafluorophenyl)octachloroporphyrin Ru(II)

Page 3

1 53 119 70	6 682 627 17	10 157 70 36	-9 10 1	1 1135 1158 16	24 237 249 29
2 172 189 35	7 41 89 66	11 773 775 19		2 1035 1115 16	-8 4 1
3 197 279 32	8 455 448 18	12 339 321 20	1 148 146 34	3 571 562 15	1 189 163 24
-9 0 1	9 459 453 19	13 286 308 22	2 289 329 22	4 467 485 16	2 39 153 61
2 854 902 22	10 163 187 32	14 606 615 17	3 309 287 22	5 425 447 16	3 729 755 16
4 277 302 28	11 1098 1085 19	15 308 296 22	4 146 155 35	6 362 361 17	4 425 453 17
6 486 488 24	12 -164 73 26	16 145 172 36	5 369 389 20	7 571 581 16	5 483 522 17
8 1656 1685 26	13 -129 76 35	17 -147 62 30	6 264 305 24	8 1250 1175 17	6 469 438 17
10 649 625 24	14 442 413 21	18 521 517 19	7 537 511 18	9 364 339 18	7 1020 1004 17
12 594 649 25	15 -121 184 34	19 149 187 37	8 454 490 19	10 711 768 16	8 597 587 17
14 470 511 28	16 153 185 33	20 466 492 20	9 252 334 25	11 1347 1289 19	9 1305 1351 19
16 347 401 28	17 836 845 17	21 -163 27 30	10 134 185 38	12 585 602 17	10 186 114 28
18 -58 94 77	18 267 300 24	-9 7 1	11 305 317 23	13 333 378 21	11 1071 1082 18
20 147 226 49	19 184 214 31	1 158 186 33	12 -188 21 24	14 699 747 18	12 392 355 20
22 399 350 30	20 99 183 47	2 477 461 19	13 306 317 24	15 -41 165 71	13 156 245 34
-9 1 1	21 237 270 27	3 -37 35 72	14 -36 55 78	16 -103 109 43	14 188 160 31
1 585 621 16	22 128 158 42	4 838 800 18	15 117 181 45	17 38 119 69	15 597 597 19
2 439 396 17	-9 4 1	5 473 470 20	-9 11 1	18 561 557 17	16 264 233 22
3 462 451 17	1 1110 1053 17	6 295 270 24	1 212 208 27	19 407 367 19	17 -31 54 75
4 431 390 17	2 335 333 19	7 254 236 26	2 393 389 20	20 581 579 18	18 146 225 35
5 287 306 20	3 963 950 17	8 513 512 20	3 255 241 25	21 -66 29 56	19 -111 15 39
6 1237 1133 18	4 460 382 18	9 314 357 24	4 231 230 26	22 89 59 51	20 32 116 77
7 191 248 26	5 -72 11 48	10 249 276 23	5 665 592 18	23 -86 119 51	21 454 464 20
8 220 222 24	6 772 774 17	11 476 435 18	6 259 249 25	24 146 183 39	22 224 208 29
9 122 133 37	7 655 647 17	12 460 522 18	7 158 123 34	-8 2 1	23 -35 122 80
10 -66 81 52	8 477 472 19	13 80 171 51	8 158 161 34	1 998 1086 16	-8 5 1
11 139 195 35	9 514 544 19	14 -88 138 46	9 320 374 23	2 223 260 21	1 513 511 16
12 57 99 61	10 -99 35 42	15 114 122 42	10 29 69 81	3 806 907 15	2 -148 58 24
13 131 191 38	11 152 170 35	16 337 360 22	11 144 178 38	4 -52 102 52	3 124 140 34
14 -119 26 38	12 210 195 29	17 243 260 26	12 -99 123 46	5 706 719 15	4 446 479 17
15 746 747 19	13 -156 57 29	18 625 672 19	13 -149 0 33	6 1047 1000 16	5 567 572 17
16 148 221 33	14 277 269 22	19 66 243 61	14 50 207 72	7 582 624 16	6 340 373 19
17 475 538 18	15 494 541 18	20 122 160 44	-9 8 1	8 302 276 19	7 153 102 31
18 444 490 19	16 708 725 17	-9 8 1	1 816 782 18	9 241 207 22	8 86 22 46
19 -164 79 27	17 62 79 59	1 816 782 18	2 645 607 19	10 1245 1260 18	9 849 854 17
20 99 137 46	18 448 503 19	2 645 607 19	3 165 163 34	11 557 589 17	10 -109 19 38
21 211 252 29	19 739 749 18	3 165 163 34	4 195 221 31	12 -120 42 33	11 -152 3 28
22 328 350 23	20 149 93 37	4 195 221 31	5 190 111 31	13 329 376 21	12 230 289 27
23 32 109 83	21 475 494 20	5 190 111 31	6 609 587 19	14 578 586 18	13 671 669 19
-9 2 1	22 32 34 83	6 609 587 19	7 186 150 33	15 265 329 25	14 477 463 20
1 262 219 21	-9 5 1	8 342 385 20	8 342 385 20	16 244 265 27	15 394 413 19
2 -139 133 25	1 354 391 19	9 -82 125 47	9 -82 125 47	17 679 652 16	16 -95 138 42
3 23 10 74	2 -110 27 35	10 -138 65 31	10 -138 65 31	18 256 231 24	17 51 182 63
4 -74 9 44	3 1127 1121 18	11 112 153 42	11 112 153 42	19 336 323 21	18 -122 94 36
5 559 540 17	4 450 481 18	12 456 457 19	12 456 457 19	20 438 445 19	19 192 216 30
6 287 283 21	5 538 501 18	13 -126 0 35	13 -126 0 35	21 581 556 18	20 357 360 21
7 1408 1397 19	6 742 737 17	14 14 142 91	14 14 142 91	22 156 67 35	21 129 212 41
8 626 666 17	7 277 310 23	15 469 509 19	15 469 509 19	23 688 678 19	22 15 58 94
9 421 363 19	8 146 148 35	16 302 308 23	16 302 308 23	24 -166 34 30	23 261 257 27
10 -107 77 38	9 994 944 18	17 102 157 48	17 102 157 48	-8 3 1	-8 6 1
11 194 153 29	10 626 663 19	18 205 251 31	18 205 251 31	1 766 835 15	1 417 412 18
12 -126 44 34	11 60 55 62	19 -169 12 29	19 -169 12 29	2 115 164 33	2 375 353 19
13 562 542 19	12 411 408 21	-9 9 1	-9 9 1	3 425 441 16	3 800 791 17
14 -85 82 49	13 -70 78 51	1 444 456 21	1 444 456 21	4 131 69 31	4 546 526 17
15 -154 93 26	14 523 514 17	2 454 380 21	2 454 380 21	5 1564 1565 19	5 683 669 17
16 551 600 17	15 398 379 19	3 543 571 17	3 543 571 17	6 89 82 40	6 1123 1174 18
17 -78 122 49	16 825 786 17	4 95 115 44	4 95 115 44	7 372 422 18	7 518 485 18
18 460 488 19	17 212 232 28	5 253 328 23	5 253 328 23	8 61 128 52	8 749 710 18
19 72 112 55	18 152 134 35	6 190 218 28	6 190 218 28	9 936 996 17	9 217 184 27
20 423 433 20	19 374 452 21	7 283 256 22	7 283 256 22	10 811 780 17	10 776 770 18
21 29 185 82	20 44 114 72	8 602 649 17	8 602 649 17	11 578 595 17	11 -33 56 76
22 43 157 74	21 184 260 33	9 580 550 18	9 580 550 18	12 105 157 42	12 193 219 31
23 91 77 53	-9 6 1	10 93 153 47	10 93 153 47	13 599 593 18	13 193 240 31
-9 3 1	1 64 127 55	11 290 280 23	11 290 280 23	14 72 180 55	14 729 720 16
1 292 288 20	2 500 533 18	12 -73 111 53	12 -73 111 53	15 479 543 20	15 420 437 19
2 183 157 26	3 185 184 29	13 214 328 28	13 214 328 28	16 416 435 21	16 241 288 25
3 85 77 43	4 34 37 73	14 -115 45 39	14 -115 45 39	17 423 456 18	17 -149 16 29
4 1165 1147 18	5 470 463 19	15 -99 81 45	15 -99 81 45	18 -86 116 46	18 -48 92 66
5 1395 1411 19	6 327 335 22	16 -18 147 92	16 -18 147 92	19 499 527 18	19 348 357 21
	7 418 434 20	17 349 358 23	17 349 358 23	20 49 126 66	20 103 150 26
	8 497 531 19			21 460 510 19	21 336 265 23
	9 -74 0 54			22 -101 98 44	22 326 338 24
				23 448 430 20	

Aquo. Carbonyl Tetrakis(pentafluorophenyl)octachloroporphyrin Ru(II)

Page 4

-8 7 1	7 -31 25 75	8 989 935 21	11 716 692 16	7 112 132 37	10 146 155 38
1 522 455 18	8 122 89 39	10 389 402 24	12 226 174 24	8 249 233 23	11 160 150 31
2 737 755 17	9 563 548 18	12 871 903 23	13 98 188 43	9 254 278 23	12 436 465 18
3 -81 70 46	10 488 511 18	14 1338 1319 25	14 793 816 18	10 593 552 18	13 141 87 35
4 331 289 21	11 442 418 19	16 898 948 25	15 1613 1621 21	11 39 21 70	14 19 98 85
5 512 476 18	12 67 120 58	18 1251 1322 27	16 555 556 19	12 1059 1051 18	15 180 150 31
6 405 414 20	13 113 153 43	20 235 225 35	17 491 434 20	13 328 248 22	16 167 136 33
7 449 419 19	14 -96 66 45	22 -81 19 66	18 318 287 20	14 534 500 19	17 91 18 49
8 798 731 18	15 649 674 18	24 -80 93 70	19 531 561 17	15 141 59 38	18 -140 4 33
9 421 447 20	16 -78 79 54	-7 1 1	20 126 93 39	16 64 20 56	19 -58 107 64
10 129 44 40	17 381 359 22	1 716 694 14	21 213 314 28	17 177 226 30	20 -48 29 72
11 347 365 22	18 250 310 28	2 1355 1316 17	22 -49 173 67	18 557 562 18	-7 10 1
12 940 973 19	-8 11 1	3 556 485 14	23 -102 14 44	19 -80 66 50	1 694 650 18
13 438 429 18	1 466 456 18	4 1792 1683 19	24 -119 83 40	20 487 474 19	2 460 484 20
14 452 454 18	2 327 309 21	5 498 468 15	25 -82 49 55	21 91 242 50	3 128 54 40
15 257 265 24	3 151 83 33	6 607 539 15	-7 4 1	22 215 225 29	4 190 154 31
16 51 161 65	4 322 316 21	7 -110 53 29	1 869 861 15	23 132 157 42	5 725 724 19
17 -148 44 30	5 83 60 50	8 693 664 15	2 111 73 33	-7 7 1	6 194 115 31
18 519 548 19	6 240 174 25	9 539 468 16	3 453 441 16	1 308 366 20	7 969 962 19
19 85 138 52	7 763 748 17	10 -116 85 29	4 634 651 15	2 748 710 16	8 196 27 27
20 276 266 25	8 92 38 48	11 474 491 17	5 888 912 16	3 219 171 24	9 101 112 43
21 120 102 44	9 211 166 28	12 770 807 16	6 278 270 19	4 786 777 17	10 133 141 36
-8 8 1	10 151 183 35	13 480 514 18	7 280 259 20	5 40 92 65	11 555 564 18
1 153 25 33	11 -32 106 78	14 382 391 19	8 399 405 17	6 163 195 30	12 445 437 19
2 807 819 18	12 460 391 20	15 401 416 20	9 128 50 33	7 177 132 29	13 636 625 18
3 764 821 18	13 542 536 19	16 1040 1013 18	10 151 153 30	8 954 937 18	14 237 264 26
4 683 670 18	14 44 65 73	17 168 128 33	11 788 798 17	9 295 311 22	15 110 120 44
5 152 175 35	15 130 157 42	18 379 334 22	12 242 250 24	10 621 614 18	16 301 314 23
6 -55 114 62	16 118 21 45	19 303 313 21	13 777 763 17	11 120 62 41	17 -135 60 35
7 104 164 45	-8 12 1	20 989 1031 17	14 524 453 19	12 301 273 23	18 217 211 29
8 287 302 24	1 151 183 35	21 611 606 18	15 934 955 18	13 1012 1017 19	19 563 574 20
9 -130 61 35	2 448 448 19	22 -149 55 30	16 247 245 26	14 801 819 19	-7 11 1
10 553 521 20	3 -28 21 79	23 -109 50 43	17 550 511 20	15 830 777 17	1 243 253 27
11 113 41 40	4 230 236 26	24 -144 133 35	18 654 640 17	16 624 607 17	2 499 499 18
12 618 622 17	5 395 379 20	-7 2 1	19 691 632 17	17 222 212 26	3 621 636 16
13 267 252 23	6 -14 13 91	1 590 574 14	20 442 468 19	18 163 263 33	4 318 275 20
14 127 186 39	7 163 204 33	2 892 880 15	21 -117 38 38	19 31 93 78	5 438 414 18
15 -86 115 47	8 266 251 25	3 907 954 15	22 -173 16 26	20 281 257 24	6 320 353 21
16 403 420 20	9 399 364 21	4 502 463 15	23 426 423 21	21 208 190 30	7 290 308 22
17 125 100 40	10 569 539 19	5 491 373 15	24 -105 60 45	22 736 725 19	8 621 620 17
18 137 196 39	11 410 433 21	6 495 507 15	-7 5 1	-7 8 1	9 559 593 18
19 -118 53 40	12 169 242 35	7 1459 1413 18	1 609 542 15	1 342 369 20	10 69 35 55
20 -144 92 34	13 -114 108 42	8 294 329 19	2 913 863 16	2 116 191 38	11 601 571 18
-8 9 1	14 -100 98 48	9 550 568 16	3 1336 1337 18	3 -200 17 18	12 -136 37 33
1 707 671 18	-8 13 1	10 252 301 21	4 741 745 16	4 -20 129 81	13 -61 94 60
2 414 381 20	1 115 1 42	11 281 320 20	5 151 97 28	5 847 824 18	14 -97 3 45
3 560 492 19	2 115 139 42	12 313 319 20	6 -79 45 41	6 1712 1676 21	15 219 177 29
4 565 598 19	3 186 230 31	13 964 1020 17	7 952 963 17	7 478 496 19	16 -62 141 62
5 187 197 32	4 385 402 21	14 350 312 20	8 600 563 16	8 330 253 22	17 192 159 33
6 168 199 34	5 -94 115 46	15 -48 105 65	9 1439 1431 19	9 98 63 46	-7 12 1
7 410 445 21	6 317 310 23	16 305 276 23	10 350 360 20	10 121 77 41	1 329 307 21
8 116 152 42	7 156 180 36	17 1441 1411 20	11 -67 21 52	11 356 355 22	2 130 83 37
9 190 240 28	8 499 542 20	18 549 572 20	12 36 3 71	12 681 667 19	3 99 81 45
10 -111 58 38	9 137 74 40	19 130 202 37	13 547 550 18	13 389 376 19	4 128 193 38
11 749 686 17	10 119 92 44	20 273 268 23	14 1628 1638 21	14 643 579 17	5 186 54 29
12 658 643 17	11 64 40 64	21 296 350 23	15 1397 1384 20	15 43 85 69	6 841 784 17
13 476 476 19	-8 14 1	22 209 284 28	16 502 498 20	16 448 501 19	7 576 565 18
14 222 280 27	1 -84 69 51	23 -131 40 35	17 451 495 18	17 143 118 36	8 205 211 28
15 142 163 37	2 244 316 27	24 495 436 20	18 330 287 21	18 65 96 59	9 -79 8 51
16 72 17 57	3 117 5 44	25 262 305 27	19 343 314 21	19 297 307 23	10 -147 74 31
17 558 562 19	4 305 211 24	-7 3 1	20 374 381 20	20 203 285 30	11 91 88 50
18 244 281 27	5 -139 67 35	1 620 607 14	21 387 411 20	21 228 155 29	12 376 372 21
19 192 228 33	6 105 16 48	2 90 3 36	22 -75 122 54	-7 9 1	13 307 328 24
-8 10 1	7 178 227 34	3 1856 1778 20	23 144 164 39	1 -93 87 43	14 47 50 71
1 397 394 22	-7 0 1	4 581 568 15	24 124 93 44	2 236 236 25	15 78 101 58
2 205 111 30	2 1548 1528 23	5 555 548 15	-7 6 1	3 1049 1057 18	16 -148 28 34
3 671 655 19	3 1553 1548 23	6 392 394 16	1 713 689 16	4 1124 1049 19	-7 13 1
4 320 322 20	4 1166 1122 21	7 545 552 16	2 1043 1023 17	5 128 97 39	1 90 122 47
5 382 391 19	6 1086 1074 17	8 1086 1074 17	3 146 181 29	6 143 204 36	2 258 197 24
6 439 448 18	7 1084 1098 17	9 1084 1098 17	4 211 203 24	7 176 182 32	3 106 85 43
	8 191 117 25	10 191 117 25	5 689 737 16	8 317 324 23	
			6 872 889 17	9 876 847 19	

Aquo. Carbonyl Tetrakis(pentafluorophenyl)octachloroporphyrin Ru(II)

Page 5

4 600 560 18	1 628 635 13	20 170 172 31	15 259 266 26	18 75 189 56	-6 15 1
5 144 192 36	2 1118 1077 15	21 740 774 17	16 237 243 24	19 303 289 24	1 291 265 23
6 254 280 25	3 1065 999 15	22 468 492 19	17 229 251 25	20 171 149 35	2 449 461 20
7 41 16 72	4 1705 1481 18	23 137 207 38	18 753 736 17		3 131 63 39
8 195 169 30	5 284 254 17	24 -111 76 42	19 92 99 48	-6 11 1	4 108 132 44
9 208 96 29	6 120 140 29	25 169 124 36	20 61 102 60	1 84 158 50	5 303 300 23
10 477 487 20	7 921 949 15		21 -70 47 56	2 211 224 28	6 303 396 24
11 -75 100 56	8 616 546 15	-6 5 1	22 253 227 26	3 125 130 40	7 244 128 27
12 104 59 48	9 1380 1365 17	1 83 65 38	23 -57 75 65	4 318 313 23	8 259 226 27
13 -174 77 28	10 1080 1076 16	2 630 574 15	-6 8 1	5 740 716 19	
-7 14 1	11 628 605 16	3 261 196 19	1 97 13 40	6 157 89 36	-5 0 1
1 184 65 30	12 106 209 36	4 78 99 41	2 465 461 17	7 714 683 19	2 157 236 30
2 270 280 24	13 932 947 17	5 675 610 15	3 1114 1094 17	8 238 266 24	4 2323 2319 27
3 128 192 39	14 201 189 26	6 2024 1934 21	4 136 28 33	9 256 298 23	6 1313 1409 20
4 61 99 61	15 812 812 17	7 741 662 15	5 287 329 21	10 267 337 23	8 2245 2154 27
5 209 201 29	16 698 686 18	8 734 751 16	6 123 83 36	11 451 473 19	10 1062 974 21
6 245 305 27	17 871 852 18	9 203 216 24	7 178 40 29	12 577 575 18	12 245 259 26
7 251 266 27	18 368 356 22	10 33 44 67	8 976 965 18	13 369 378 20	14 585 464 23
8 383 395 22	19 237 280 28	11 771 757 17	9 966 924 18	14 -97 134 44	16 713 656 24
9 127 103 43	20 795 800 17	12 820 803 17	10 613 581 18	15 -66 106 57	18 633 666 25
10 266 231 27	21 172 135 31	13 525 559 18	11 -47 68 67	16 -129 48 36	20 1034 1058 26
-7 15 1	22 -128 107 35	14 382 393 20	12 279 291 24	17 291 304 24	22 484 386 26
1 180 117 32	23 502 520 19	15 253 251 25	13 135 154 39	18 294 284 25	24 577 617 26
2 187 250 32	24 106 195 46	16 431 519 20	14 288 251 25	19 402 369 22	26 408 373 30
3 181 191 33	25 364 368 22	17 506 563 20	15 413 422 18	-6 12 1	-5 1 1
4 275 218 25	26 101 26 50	18 416 424 18	16 449 422 18	1 510 493 17	1 2075 2044 20
5 266 198 26	-6 3 1	19 530 535 17	17 76 154 53	2 534 455 17	2 1555 1467 17
-6 0 1	1 1122 1083 15	20 196 247 29	18 -15 34 90	3 339 353 20	3 2047 1929 20
2 507 605 19	2 224 329 19	21 128 142 39	19 41 96 71	4 350 320 20	4 939 840 13
4 2720 2526 31	3 62 112 43	22 172 138 32	20 432 459 20	5 365 360 19	5 532 525 13
6 534 521 19	4 256 229 18	23 477 490 20	21 495 512 20	6 -77 44 50	6 -53 35 44
8 836 806 20	5 894 816 15	24 512 509 20	22 326 329 23	7 99 46 45	7 1141 1232 15
10 1836 1820 26	6 485 516 15	25 214 223 31	-6 9 1	8 518 506 18	8 928 908 14
12 524 490 23	7 1657 1650 19	-6 6 1	1 410 396 19	9 498 533 18	9 371 356 15
14 395 412 26	8 1212 1253 16	1 373 350 17	2 153 218 32	10 231 226 26	10 352 365 16
16 1207 1232 25	9 474 381 16	2 1330 1291 17	3 216 232 26	11 -31 27 77	11 -95 28 33
18 293 351 33	10 584 510 16	3 237 221 21	4 226 228 25	12 -108 66 41	12 654 653 15
20 -26 91 96	11 954 927 16	4 912 907 16	5 937 958 18	13 379 419 21	13 1373 1370 18
22 488 480 26	12 -186 23 18	5 55 10 52	6 -93 134 43	14 -80 154 52	14 1198 1164 17
24 -142 98 45	13 892 882 17	6 195 147 24	7 613 643 18	15 -67 116 59	15 1007 967 17
26 724 674 26	14 421 426 18	7 391 437 17	8 350 348 21	16 298 298 25	16 1026 1046 18
-6 1 1	15 291 327 22	8 907 850 16	9 207 131 29	17 340 359 23	17 764 777 18
1 1650 1536 18	16 -32 18 75	9 266 212 21	10 215 260 28	-6 13 1	18 791 816 18
2 538 537 13	17 690 693 18	10 1318 1350 18	11 510 539 20	1 455 478 18	19 154 191 35
3 1686 1532 18	18 462 424 20	11 394 303 19	12 397 393 22	2 306 314 21	20 223 148 29
4 214 86 19	19 701 685 19	12 33 40 73	13 300 314 21	3 213 245 26	21 359 296 20
5 1084 998 15	20 124 169 38	13 102 57 43	14 222 210 26	4 306 306 21	22 958 994 17
6 1619 1481 18	21 -168 33 26	14 764 752 18	15 243 262 25	5 264 244 24	23 108 114 43
7 600 593 14	22 -108 71 40	15 347 341 22	16 -151 10 29	6 592 643 18	24 214 210 28
8 173 199 23	23 302 327 23	16 599 643 19	17 -58 25 61	7 265 300 24	25 101 168 48
9 903 882 15	24 138 172 39	17 73 139 51	18 467 427 19	8 289 323 23	26 503 503 20
10 1074 1112 16	25 598 573 19	18 154 130 33	19 246 284 26	9 151 53 35	27 197 159 33
11 1027 960 16	26 173 142 36	19 12 48 91	20 155 215 36	10 381 395 21	-5 2 1
12 689 714 16	-6 4 1	20 596 564 18	21 290 303 25	11 124 73 41	1 1900 1870 19
13 267 273 21	1 750 700 14	21 145 107 36	-6 10 1	12 247 323 27	2 694 768 13
14 292 242 21	2 381 418 15	22 549 577 19	1 378 332 20	13 25 159 86	3 2875 2797 26
15 650 635 17	3 1301 1305 16	23 -77 10 55	2 73 86 53	14 305 259 24	4 392 421 14
16 884 875 18	4 483 451 15	24 123 152 44	3 381 435 20	15 109 116 48	5 1421 1323 16
17 622 635 18	5 1035 1045 15	-6 7 1	4 -20 45 84	-6 14 1	6 1587 1567 17
18 506 494 19	6 303 259 18	1 530 454 16	5 273 285 24	1 177 63 30	7 193 255 20
19 443 484 21	7 821 829 15	2 111 12 35	6 140 118 37	2 309 337 22	8 786 691 14
20 552 582 17	8 874 883 16	3 527 561 16	7 751 751 18	3 392 368 20	9 313 241 17
21 142 197 35	9 1460 1459 18	4 139 188 30	8 254 179 26	4 514 544 18	10 771 854 15
22 568 577 18	10 631 681 16	5 166 113 27	9 918 970 19	5 -82 102 49	11 35 87 61
23 -100 12 43	11 515 507 17	6 992 990 17	10 152 39 37	6 123 21 40	12 1427 1438 18
24 -149 114 31	12 1013 1005 17	7 497 530 17	11 119 101 39	7 232 196 27	13 1235 1284 17
25 -192 49 24	13 225 294 24	8 -52 72 57	12 185 231 29	8 468 506 20	14 339 272 19
26 429 398 21	14 574 547 18	9 306 338 21	13 266 282 24	9 -138 75 34	15 18 65 80
-6 2 1	15 862 841 18	10 254 295 24	14 364 399 20	10 182 226 33	16 232 333 25
	16 391 347 20	11 617 589 18	15 120 162 40	11 103 176 48	17 203 226 28
	17 566 525 19	12 1316 1314 19	16 -106 9 41	12 126 216 43	18 423 326 20
	18 -76 76 54	13 160 139 34	17 -142 127 32		
	19 571 514 17	14 69 69 57			

Aquo. Carbonyl Tetrakis(pentafluorophenyl)octachloroporphyrin Ru(II)

19	1395	1373	20	10	314	393	19	5	536	498	17	8	491	478	20	7	357	394	21	18	82	142	50	
20	-83	6	52	11	893	882	16	6	711	706	16	9	586	576	20	8	294	258	24	19	354	403	22	
21	72	117	53	12	576	536	16	7	-75	61	45	10	120	163	38	9	167	117	35	20	827	805	19	
22	421	391	19	13	654	711	17	8	145	144	32	11	-56	59	59	10	-60	73	64	21	186	218	33	
23	332	321	22	14	-76	138	47	9	415	430	19	12	357	275	20	-5 16 1					22	378	441	20
24	190	220	31	15	100	113	43	10	638	652	17	13	434	484	19						23	249	289	25
25	284	334	25	16	333	408	22	11	506	492	18	14	239	231	25	1 243 238 27					24	89	24	50
26	37	113	79	17	688	707	18	12	484	459	19	15	420	472	20						25	635	608	18
-5 3 1				18	346	325	23	13	155	166	35	16	-103	89	42	2 52 130 67					26	610	326	21
				19	271	321	22	14	280	288	25	17	-79	100	52						27	236	256	29
1 2216 2117 21				20	193	184	28	15	193	202	31	18	106	131	47	3 212 251 29					-4 3 1			
				21	610	658	17	16	545	548	17	19	163	154	36									
2	966	901	14	22	338	355	21	17	352	353	20	20	214	287	31	2 1019 617 17					1	668	613	12
3	697	745	13	23	81	161	53	18	233	281	26	-4 0 1					2	3098	2866	33	2	828	833	13
4	1401	1522	16	24	235	253	28	19	111	133	42						3	634	814	17	3	1023	969	13
5	1322	1368	16	25	-88	155	51	20	313	356	22						4	814	914	33	4	218	156	18
6	854	855	14	-5 6 1				21	12	88	94	1	546	510	19	5	571	595	13					
7	229	310	19					22	160	209	36	2	384	343	21	6	562	595	13					
8	-114	139	27	-5 9 1				23	384	357	22	3	322	361	23	7	1324	1272	16					
9	496	559	15					1	209	203	24	4	277	230	25	8	-122	175	24					
10	253	212	19	2	-70	99	41	-5 9 1				5	445	526	17	12	-145	61	30					
11	1007	950	16	3	582	570	15					1	209	203	24	6	422	328	18	14	526	491	22	
12	670	632	16	4	450	376	15	2	258	213	22	7	394	401	19	16	105	87	52					
13	650	662	16	5	1554	1532	18	3	1064	1047	17	9	198	219	28	18	910	892	24					
14	62	120	52	6	561	635	15	4	115	47	37	10	586	579	17	22	239	345	34					
15	659	670	17	7	679	717	15	5	515	495	17	11	468	470	19	24	353	342	30					
16	63	221	56	8	103	97	37	6	-35	2	69	12	540	520	18	26	589	624	26					
17	390	342	23	9	466	421	17	7	488	479	18	13	160	158	34	-4 1 1								
18	297	318	23	10	1123	1189	17	8	590	537	18	14	-100	101	43									
19	225	215	28	11	1472	1413	19	9	1347	1345	19	15	86	160	52	1	-97	46	28					
20	51	91	62	12	784	736	17	10	689	609	18	16	417	350	21	2	815	875	12					
21	389	444	19	13	230	198	25	11	119	85	41	17	262	243	26	3	1587	1474	16					
22	14	70	91	14	45	179	65	12	357	423	22	18	392	366	22	4	1194	1246	14					
23	474	446	19	15	-95	79	43	13	177	171	33	-5 13 1					5	194	336	18				
24	-72	42	55	16	459	460	20	14	1125	1130	20						6	512	550	12				
25	463	428	20	17	12	139	95	15	277	262	22	7	186	61	20	10	-58	40	44					
26	182	180	34	18	193	242	29	16	372	426	20	1	111	115	39	11	356	361	16					
-5 4 1				19	-128	104	33	17	-117	73	37	2	246	290	23	12	366	321	16	-4 4 1				
				20	322	353	21	18	-97	35	44	3	-119	61	34	3	-130	27	31					
1	750	671	13	22	563	543	18	19	346	362	21	5	207	271	26	13	699	680	15	1	1754	1700	18	
2	148	232	24	23	280	316	25	20	84	10	50	6	286	293	22	14	888	860	16	2	1699	619	13	
3	-47	23	49	24	614	595	19	21	411	426	21	7	147	41	34	15	847	896	17	3	742	771	13	
4	97	36	33	25	138	237	41	22	338	291	23	8	633	652	17	16	1069	1087	17	4	657	655	13	
5	1010	968	15	-5 7 1				-5 10 1				10	218	116	27	17	-90	37	42	5	199	208	15	
6	499	533	14									1	269	206	19	1	335	346	20	11	168	181	33	18
7	455	388	15	2	891	895	15	2	86	198	46	12	307	284	23	19	-93	137	45	6	1057	973	19	
8	1222	1180	16	3	553	545	15	3	328	380	21	13	-44	81	71	19	-92	467	20	8	171	147	23	
9	326	379	17	4	467	412	16	4	156	82	32	14	563	599	19	20	436	138	20	9	587	528	14	
10	1800	1749	20	5	309	346	19	5	674	736	18	15	124	50	43	21	-38	91	33	10	37	143	58	
11	1800	1749	20	6	100	143	37	6	-121	8	34	16	410	424	22	22	156	191	33	11	92	104	38	
12	190	187	25	7	504	551	16	7	554	528	18	23	443	389	19	23	327	335	22	12	-89	70	36	
13	734	711	16	8	1041	1055	17	8	673	644	18	24	343	389	19	25	216	270	28	13	427	454	17	
14	-99	88	37	9	341	288	19	9	284	292	24	26	292	292	24	27	158	186	37	14	383	391	18	
15	84	115	47	10	797	786	17	10	125	113	41	1	266	242	23	15	889	889	14	15	989	1031	17	
16	345	400	21	11	325	340	20	11	738	750	19	2	166	156	31	16	1695	1626	17	16	267	290	23	
17	351	378	21	12	340	321	20	12	417	408	21	3	-112	76	37	17	-90	37	42	17	469	462	19	
18	434	407	20	13	366	386	20	13	138	93	35	4	388	344	19	18	324	360	22	18	324	360	22	
19	172	165	34	14	223	270	27	14	308	315	21	5	78	104	51	19	677	665	19	19	677	665	19	
20	451	504	18	15	333	374	22	15	-125	48	35	6	280	306	23	20	1695	1626	17	20	61	126	64	
21	219	166	27	16	-149	66	31	16	-72	25	53	7	233	172	26	21	1293	908	13	21	694	703	17	
22	405	400	20	17	152	164	32	17	561	519	18	8	223	132	27	22	295	263	14	22	429	388	19	
23	641	675	18	18	122	214	38	18	-30	35	79	9	288	297	24	23	1284	1274	15	23	152	161	35	
24	-165	3	28	19	208	265	27	19	261	205	26	10	412	404	20	24	718	779	13	24	99	204	47	
25	292	286	25	20	585	600	18	20	-82	164	52	11	144	87	38	25	2087	2099	21	25	348	361	22	
26	-165	15	30	21	110	145	43	21	78	51	58	12	327	319	23	26	1210	1123	15	26	164	114	36	
-5 5 1				22	562	590	19	-5 11 1				13	193	203	32	9	238	195	18	-4 5 1				
				23	8	89	100					10	869	898	14									
1	-74	7	37	24	23	5	90	1	333	255	21	11	63	31	59	11	430	458	15	1	307	322	15	
2	495	546	14	-5 8 1				2	159	13	32	2	397	398	20	12	1625	1673	19	2	911	985	14	
3	427	423	15					3	648	631	18	3	249	142	25	3	249	142	25	13	301	333	19	3
4	954	940	15	1	279	258	19	4	713	630	19	4	308	354	22	14	472	550	17	4	382	331	15	
5	1142	930	16	2	193	176	24	5	496	527	18	5	135	121	38	15	825	840	17	5	856	902	14	
6	664	711	15	3	156	78	28	6	345	319	22	6	-78	82	52	16	-85	154	53	6	991	970	15	
7	373	343	16	4	677	670	16	7	706	642	19													
8	439	1801	16																					
9	1131	1201	16																					

Aquo. Carbonyl Tetrakis(pentafluorophenyl)octachloroporphyrin Ru(II)

[illegible]

Aquo. Carbonyl Tetrakis(pentafluorophenyl)octachloroporphyrin Ru(II)

Page 8

8 726 774 15	5 264 251 21	12 -92 108 44	7 2415 2383 22	23 381 382 20	10 416 435 16
9 380 397 17	6 567 549 17	13 164 206 33	8 943 875 13	24 -77 38 52	11 149 182 28
10 270 381 20	7 -73 14 48	14 407 414 20	9 1799 1844 18	25 -136 3 34	12 786 832 16
11 -70 51 46	8 267 278 23	15 185 165 31	10 1063 1068 14	26 69 94 60	13 537 552 16
12 628 626 17	9 335 301 21	16 292 282 24	11 401 317 14	27 234 229 28	14 683 725 16
13 454 435 18	10 493 480 19	17 332 347 23	12 959 961 15	28 -133 135 38	15 -100 1 38
14 1057 1028 18	11 732 651 18	18 418 358 21	13 980 932 15		16 -57 79 57
15 105 87 42	12 122 57 41		14 549 557 15	-2 4 1	17 209 177 27
16 -59 73 59	13 136 152 39	-3 14 1	15 51 50 54		18 -73 105 53
17 529 446 19	14 -45 63 71		16 1050 1075 17	1 1437 1247 15	19 -107 103 42
18 114 137 44	15 89 17 47	1 124 151 37	17 519 524 17	2 591 602 11	20 304 351 21
19 109 2 41	16 183 212 29	2 247 286 24	18 148 166 32	3 1179 991 14	21 -90 83 45
20 674 717 17	17 535 544 18	3 207 154 26	19 390 444 20	4 223 114 17	22 -148 53 30
21 132 154 38	18 223 245 27	4 547 544 17	20 479 430 19	5 2627 2637 24	23 -44 53 69
22 247 295 25	19 522 505 18	5 160 1 32	21 -126 12 36	6 565 476 12	24 406 386 20
23 113 149 44	20 105 11 45	6 502 460 18	22 476 507 21	7 36 63 54	25 278 253 25
24 245 180 27	21 659 589 18	7 -95 163 42	23 238 227 25	8 894 856 14	26 580 537 19
25 174 200 35	22 339 318 23	8 163 158 32	24 357 352 21	9 631 548 13	
		9 184 198 29	25 501 506 19	10 194 92 21	-2 7 1
		10 145 91 35	26 104 103 46	11 1270 1248 16	
		11 430 370 19	27 237 254 28	12 505 412 15	1 203 200 19
		12 332 363 22	28 346 277 24	13 724 697 15	2 828 779 14
		13 126 30 41		14 244 225 21	3 1029 1070 15
		14 157 118 36	-2 2 1	15 883 904 16	4 916 972 14
		15 258 161 27		16 505 488 17	5 606 513 14
				17 100 121 42	6 666 671 14
				18 -70 79 52	7 834 772 15
				19 212 258 28	8 1168 1185 16
				20 109 182 45	9 425 450 16
				21 -131 0 36	10 414 399 17
				22 549 544 17	11 192 268 24
				23 32 61 77	12 544 515 16
				24 45 69 69	13 -116 26 32
				25 651 572 18	14 637 616 17
				26 235 172 28	15 188 212 28
				27 396 382 22	16 419 426 20
					17 613 657 19
				-2 5 1	18 237 216 27
					19 -147 60 28
				1 129 0 24	20 366 418 20
				2 783 652 12	21 194 262 29
				3 900 788 13	22 437 408 19
				4 199 298 19	23 161 47 34
				5 1668 1655 18	24 876 823 18
				6 1136 1117 15	25 336 304 23
				7 1145 1034 15	
				8 334 370 15	-2 8 1
				9 1040 992 15	
				10 350 268 16	1 478 444 15
				11 1133 1144 16	2 1586 1642 18
				12 1191 1198 17	3 834 828 15
				13 45 135 57	4 157 3 25
				14 823 842 16	5 215 101 21
				15 919 914 17	6 1320 1304 17
				16 670 701 17	7 479 408 16
				17 57 55 59	8 872 921 16
				18 229 221 26	9 772 740 16
				19 -80 108 51	10 439 445 17
				20 114 239 44	11 575 567 17
				21 91 97 46	12 338 350 20
				22 570 566 17	13 240 251 24
				23 730 678 17	14 417 459 19
				24 208 121 29	15 97 17 46
				25 128 132 41	16 186 244 31
				26 297 257 25	17 53 46 66
				27 149 155 39	18 443 450 18
					19 -125 32 34
				-2 6 1	20 428 444 19
					21 296 305 23
				1 809 732 13	22 314 313 22
				2 1333 1342 15	23 500 514 19
				3 1108 1163 14	24 278 234 25
				4 558 488 13	25 254 217 28
				5 838 934 14	
				6 438 416 14	-2 9 1
				7 871 933 14	
				8 737 727 14	1 466 424 15
				9 210 231 21	2 339 345 17

Aquo. Carbonyl Tetrakis(pentafluorophenyl)octachloroporphyrin Ru(II)

Page 9

3	360	416	17	4	455	431	19	3	176	187	32	16	816	825	16	2	1067	1059	13	21	478	522	18
4	977	911	16	5	282	299	23	4	210	185	28	17	115	129	36	3	380	383	13	22	322	338	27
5	1533	1568	16	6	296	308	23	5	247	296	26	18	271	267	22	4	2124	2167	20	23	225	263	27
6	507	505	16	7	486	496	19	6	258	241	25	19	90	41	44	5	1266	1253	15	24	415	396	20
7	260	126	20	8	511	539	19	7	370	356	21	20	383	405	21	6	771	921	14	25	110	106	46
8	25	4	71	9	460	488	20	8	-84	21	51	21	904	919	19	7	305	325	15	26	217	258	30
9	418	451	18	10	164	195	20	9	197	178	31	22	346	309	23	8	1056	1109	15				
10	284	296	21	11	184	246	28					23	44	148	68	9	738	707	14	-1	8	1	
11	299	336	21	12	403	409	19	-2	17	1		24	287	338	23	10	113	20	30				
12	-58	121	57	13	535	527	17					25	407	416	20	11	778	802	15	1	244	331	18
13	379	390	20	14	22	4	82	1	109	15	45	26	284	252	24	12	367	418	17	2	400	340	15
14	195	252	30	15	-144	46	30	2	153	23	36	27	642	549	19	13	610	591	15	3	527	560	14
15	234	256	27	16	-136	47	32					28	111	104	48	14	543	568	16	4	501	445	15
16	75	184	56	17	140	141	37	-1	0	1						15	738	698	16	5	630	616	15
17	207	188	26	18	268	284	25					-1	3	1		16	246	299	23	6	52	59	51
18	-141	104	30	19	326	334	23					17	623	597	17	17	987	969	18	7	235	258	20
19	-145	27	30	20	114	164	46					18	3087	969	18	18	987	969	18	8	456	462	16
20	262	226	24									19	1863	1882	17	19	624	592	19	9	642	613	16
21	444	485	19	-2	13	1						2	696	731	11	20	503	539	20	10	144	16	29
22	140	31	38									3	1502	1195	15	21	337	341	20	11	1032	980	17
23	587	524	19									4	1478	1488	15	22	504	496	18	12	290	357	21
24	177	150	35									5	116	174	26	23	-63	132	58	13	211	224	26
												6	1064	1031	13	24	341	360	22	14	-130	22	31
-2	10	1										7	1060	998	13	25	615	585	18	15	316	334	22
												8	2123	2108	21	26	117</						

Aquo. Carbonyl Tetrakis(pentafluorophenyl)octachloroporphyrin Ru(II)

Page 10

15 407 390 21		3 215 231 13	18 503 448 18	3 1974 1997 20	22 113 158 43
16 161 285 31		4 149 340 19	19 300 314 22	4 740 794 13	23 338 324 22
17 -129 83 33		5 334 85 12	20 273 286 25	5 902 803 14	24 349 376 22
18 265 330 24		6 582 518 11	21 808 765 19	6 2164 2172 21	25 231 263 29
19 373 355 20		7 673 622 11	22 72 104 53	7 780 802 14	
20 125 92 40		8 193 272 19	23 157 137 33	8 807 783 14	0 9 1
21 521 528 19		9 858 856 13	24 -91 84 46	9 835 910 14	1 682 684 15
22 157 87 36		10 1824 1724 19	25 216 153 28	10 1174 1169 16	2 70 23 43
23 276 244 26		11 400 410 14	26 80 75 55	11 408 431 16	3 682 748 15
		12 287 278 17	27 486 496 20	12 765 750 15	4 170 128 25
		13 720 688 14	28 -135 7 37	13 344 285 18	5 944 886 16
		14 623 577 15		14 294 346 20	6 428 441 16
		15 1030 1040 16		15 135 154 33	7 372 430 17
		16 1200 1153 17		16 1111 1122 18	8 1017 981 17
		17 573 592 17	0 3937 3959 34	17 379 388 20	9 893 982 16
		18 174 137 29	1 164 248 19	18 844 829 18	10 548 504 17
		19 230 39 25	2 2025 2015 19	19 -74 61 54	11 445 411 18
		20 549 534 19	3 725 701 11	20 371 396 22	12 335 361 20
		21 674 598 19	4 420 449 12	21 446 473 18	13 746 755 17
		22 1018 966 19	5 1845 1799 18	22 253 276 24	14 507 461 19
		23 94 0 46	6 1808 1766 18	23 11 101 94	15 535 478 19
		24 330 229 21	7 857 850 13	24 396 443 20	16 260 259 26
		25 -150 39 30	8 1089 1014 14	25 274 261 25	17 547 577 17
		26 179 183 32	9 1319 1264 16	26 413 428 21	18 119 120 39
		27 396 369 21	10 -65 98 40		19 77 11 52
		28 560 515 20	11 707 699 14	0 7 1	20 126 196 39
			12 97 136 35	1 432 523 14	21 374 340 21
			13 1432 1399 18	2 1247 1167 15	22 435 464 20
			14 303 354 19	3 726 741 13	23 155 199 36
			15 332 315 18	4 1285 1202 16	24 95 124 52
			16 504 521 17	5 202 16 20	
			17 935 933 17	6 965 937 15	0 10 1
			18 1021 985 18	7 179 62 22	0 415 439 16
			19 456 413 19	8 1371 1483 17	1 618 589 16
			20 199 181 30	9 420 477 16	2 324 317 18
			21 307 305 24	10 706 680 15	3 265 300 20
			22 -112 84 37	11 261 255 20	4 640 720 16
			23 793 758 17	12 191 239 24	5 800 838 16
			24 225 157 27	13 733 759 16	6 270 276 21
			25 791 726 18	14 584 638 17	7 1187 1196 18
			26 169 141 34	15 605 531 17	8 111 24 38
			27 123 132 44	16 900 850 18	9 72 71 50
				17 -52 89 63	10 208 216 26
			0 5 1	18 -175 62 25	11 894 927 18
			1 1238 1370 14	19 -145 46 32	12 31 30 75
			2 1470 1513 15	20 307 306 21	13 272 258 24
			3 207 209 17	21 151 165 34	14 528 575 19
			4 1349 1417 15	22 671 689 17	15 258 318 26
			5 319 357 14	23 156 84 35	16 -105 139 38
			6 151 219 22	24 -127 45 37	17 264 279 23
			7 1067 1091 14	25 247 256 27	18 -110 28 38
			8 522 592 13	26 374 298 23	19 425 432 19
			9 80 47 36		20 131 106 38
			10 326 271 16	0 8 1	21 194 163 30
			11 909 846 15	0 948 920 14	22 -90 39 49
			12 327 203 17	1 709 689 14	23 288 308 25
			13 922 896 16	2 937 977 15	
			14 280 264 20	3 466 423 14	0 11 1
			15 -70 35 46	4 709 762 14	1 470 431 17
			16 581 548 17	5 1198 1241 16	2 147 104 30
			17 627 586 17	6 392 383 16	3 611 525 17
			18 217 195 27	7 660 761 15	4 472 441 18
			19 315 321 23	8 128 71 30	5 583 538 17
			20 -133 52 35	9 530 610 16	6 -48 54 60
			21 545 542 17	10 782 797 16	7 329 433 21
			22 534 487 18	11 543 589 16	8 -18 31 84
			23 289 305 23	12 -99 87 36	9 753 690 18
			24 87 64 50	13 213 116 25	10 242 287 25
			25 87 69 51	14 483 516 18	11 660 609 18
			26 174 140 34	15 313 360 22	12 188 131 30
			27 510 524 20	16 356 386 21	13 513 476 20
				17 132 129 39	14 536 561 17
			0 6 1	18 183 259 33	15 122 121 38
			0 265 172 15	19 460 488 18	16 69 88 54
			1 145 8 22	20 724 752 17	17 -66 135 54
			2 123 134 25	21 175 26 31	

Aquo. Carbonyl Tetrakis(pentafluorophenyl)octachloroporphyrin Ru(II)

Page 11

18	-38	31	72	6	101	166	44	27	-102	79	45	9	529	484	13	25	130	3	41	14	683	683	18
19	233	218	26	7	155	151	33	28	437	369	21	10	649	665	14	26	754	711	19	15	-131	33	33
20	392	383	21	8	217	199	27					11	237	217	19					16	52	138	65
21	643	629	19	9	380	443	20	1	2	1		12	828	923	15	1	7	1		17	118	156	38
22	277	250	26	10	403	351	20					13	425	430	16					18	284	321	22
	0	12	1	11	-77	17	53	0	823	708	8	14	126	120	32	0	958	987	11	19	611	652	17
0	124	184	36	12	95	30	49	1	408	182	9	15	1272	1326	18	1	189	220	20	20	317	323	22
1	454	494	18	13	137	155	40	2	1210	1123	12	16	327	277	19	2	147	177	23	21	166	196	33
2	370	387	20	14	-32	44	81	3	1609	1558	15	17	968	967	17	3	921	963	14	22	178	147	32
3	508	564	18					4	1686	1848	16	18	465	442	19	4	2228	2378	22	23	509	494	20
4	354	362	20	0	16	1		5	807	626	11	19	291	265	23	5	1071	1131	15	24	493	432	20
5	-48	82	64					6	198	254	17	20	-61	100	60	6	2210	2254	22				
6	646	630	18	0	345	321	21	7	137	160	23	21	290	329	25	7	759	778	14	1	10	1	
7	270	151	24	1	476	439	19	8	477	427	12	22	293	241	22	8	733	721	15	0	717	760	11
8	322	308	22	2	217	167	27	9	1784	1821	18	23	825	810	17	9	153	107	26	1	119	15	32
9	623	561	19	3	118	35	41	10	766	772	13	24	344	308	21	10	878	907	15	2	149	69	28
10	227	188	28	4	-132	27	33	11	1315	1322	16	25	532	458	19	11	75	20	43	3	896	906	16
11	216	270	25	5	-86	12	48	12	372	333	15	26	-46	174	71	12	139	169	30	4	163	95	27
12	778	810	16	6	-70	75	55	13	655	669	15	27	776	777	19	13	1029	1033	17	5	-2	26	90
13	248	162	24	7	281	210	24	14	1227	1214	17					14	632	615	17	6	336	335	19
14	428	366	18	8	-26	67	83	15	1323	1340	18	1	5	1		15	157	110	31	7	386	449	18
15	135	70	36	9	226	319	28	16	802	781	16	0	283	203	10	16	879	860	18	8	-78	97	45
16	160	165	32	10	196	186	31	17	-26	94	73	1	1460	1504	15	17	352	380	21	9	660	688	17
17	103	35	44					18	154	170	32	2	823	839	12	18	410	429	21	10	593	623	17
18	337	286	22	0	17	1		19	766	760	18	3	768	705	12	19	-110	139	42	11	453	411	19
19	390	395	21	1	280	280	25	20	254	249	25	4	1193	1265	14	20	704	698	17	12	-86	20	46
20	251	312	27	2	232	64	27	21	483	478	20	5	1797	1793	18	21	774	728	17	13	779	810	18
	0	13	1	3	305	358	24	22	636	599	20	6	110	168	28	22	333	265	21	14	56	94	62
1	282	208	23	4	201	155	30	23	153	212	34	7	588	606	13	23	151	111	35	15	-94	43	45
2	584	534	18					24	309	310	22	8	186	207	20	24	583	594	19	16	83	95	45
3	372	410	21	1	0	1		25	288	220	24	9	65	46	41	25	263	228	26	17	317	327	21
4	350	327	22	0	267	203	9	26	605	539	18	10	255	188	18	26	609	596	20	18	168	116	31
5	173	135	32	0	2489	2370	25	27	415	415	21	11	614	656	14					19	517	563	18
6	175	148	32	1	198	420	21					12	1612	1648	19	1	8	1		20	244	234	25
7	194	51	26	6	545	650	15	1	3	1		13	324	386	18	0	213	211	14	21	458	458	20
8	644	702	16	8	540	681	17	0	289	13	9	14	436	509	17	1	1150	1108	15	22	188	84	32
9	224	174	25	10	3374	3287	36	1	870	933	11	15	43	109	61	2	432	366	15	23	219	267	30
10	346	345	20	12	168	168	32	2	360	485	12	16	678	698	17	3	707	792	14				
11	297	323	22	14	717	685	21	3	1267	1261	13	17	1024	1039	18	4	614	636	14	1	11	1	
12	105	58	42	16	1638	1596	25	4	132	2	23	18	698	691	18	5	331	340	17	0	260	266	15
13	131	51	37	18	1363	1273	25	5	816	839	11	19	806	803	18	6	309	326	17	1	844	887	17
14	419	483	19	20	842	761	25	6	194	322	18	20	-169	122	27	7	730	689	15	2	243	249	22
15	257	291	24	22	938	859	26	7	1579	1459	16	21	140	163	35	8	935	970	16	3	399	428	18
16	267	226	24	24	421	336	27	8	1954	1834	19	22	691	634	17	9	237	301	21	4	636	677	17
17	244	305	26	26	409	368	29	9	-166	23	16	23	732	737	17	10	419	405	17	5	826	786	17
18	116	82	44	28	419	355	30	10	630	661	13	24	198	162	29	11	383	405	18	6	134	48	34
	0	14	1					11	1298	1356	16	25	63	199	61	12	429	513	17	7	242	244	24
0	323	435	20	1	1	1		12	742	721	14	26	90	93	52	13	-129	1	29	8	464	525	19
1	-161	43	25	0	1666	1310	13	13	1947	1911	21	27	168	60	36	14	653	681	17	9	161	108	32
2	-28	18	74	1	115	256	18	14	575	611	15					15	235	195	25	10	180	34	31
3	-12	51	88	2	679	603	9	15	277	186	20	1	6	1		16	506	490	19	11	952	1025	18
4	126	110	36	3	763	768	16	16	763	768	16	0	461	463	9	17	582	629	19	12	444	338	20
5	74	47	51	4	994	731	11	17	663	655	17	1	602	599	12	18	-25	115	85	13	586	547	18
6	393	353	19	5	868	799	10	18	-134	1	30	2	854	850	13	19	348	309	20	14	-93	67	41
7	481	512	18	6	445	230	11	19	503	492	19	3	201	124	18	20	799	829	17	15	109	111	40
8	140	27	35	7	2455	2466	22	20	-104	91	42	4	2188	2177	21	21	501	452	18	16	446	480	18
9	203	148	27	8	1164	1077	13	21	359	358	22	5	330	153	15	22	286	260	23	17	565	548	17
10	247	265	25	9	571	601	12	22	592	602	17	6	562	527	13	23	228	244	28	18	256	229	24
11	156	112	33	10	954	913	13	23	330	342	21	7	869	878	14	24	235	198	28	19	456	460	19
12	552	518	18	11	518	491	13	24	-116	70	38	8	848	886	14	25	642	602	19	20	592	593	18
13	252	263	25	12	831	825	14	25	597	568	18	9	495	534	14					21	164	98	35
14	159	104	34	13	1122	1061	15	26	178	113	33	10	543	535	15	1	9	1					
15	171	232	33	14	211	114	21	27	421	389	21	11	496	473	15	0	536	515	11	1	12	1	
16	218	209	29	15	594	594	15	28	238	155	29	12	1131	1131	16	1	1500	1485	18	0	403	429	14
	0	15	1	16	-77	13	41					13	70	79	46	2	221	122	20	1	-112	73	36
1	166	76	31	17	144	90	30	1	4	1		14	926	982	17	3	1043	1047	16	2	512	495	18
2	419	443	19	18	709	712	16	0	1160	1252	11	15	415	316	18	4	676	595	15	3	591	607	18
3	344	260	20	19	151	226	32	1	938	1165	12	16	855	877	17	5	1642	1654	19	4	138	37	35
4	397	469	19	20	368	361	20	2	2052	1986	19	17	351	298	21	6	1655	1653	19	5</			

[illegible]

[illegible]

Aquo. Carbonyl Tetrakis(pentafluorophenyl)octachloroporphyrin Ru(II)

Page 14

3 15 1	4 2 1	14 825 866 16	3 517 515 14	4 10 1	2 364 311 19
0 214 216 19	0 1465 1427 13	15 742 732 17	4 809 768 15	0 160 97 21	3 312 333 20
1 84 86 49	1 942 987 12	16 -12 94 87	5 580 459 15	1 -47 88 58	4 186 194 27
2 122 121 38	2 162 206 20	17 1001 1004 18	6 1176 1093 16	2 78 15 46	5 -76 9 47
3 -140 16 30	3 1296 1301 14	18 24 165 82	7 134 57 29	3 501 479 17	6 156 130 31
4 26 10 78	4 1452 1397 15	19 198 176 30	8 446 410 16	4 297 234 20	7 122 64 37
5 306 295 22	5 1525 1512 16	20 61 76 64	9 283 302 19	5 676 644 17	8 196 173 27
6 169 180 31	6 317 226 14	21 211 178 27	10 362 324 18	6 101 37 41	9 -65 74 54
7 75 21 53	7 774 778 13	22 -100 129 42	11 103 136 38	7 240 208 24	10 -88 92 45
8 195 211 29	8 567 585 13	23 -64 153 58	12 86 117 44	8 461 423 18	11 155 80 33
9 88 16 50	9 512 548 14	24 125 157 40	13 296 347 21	9 412 371 19	12 348 285 21
10 -75 112 53	10 316 270 16	25 348 353 22	14 596 554 18	10 137 129 36	13 176 204 31
11 319 238 23	11 600 612 14	26 83 129 55	15 154 142 33	11 684 652 18	14 547 444 18
12 139 194 39	12 -139 56 23	4 5 1	16 -59 12 59	12 117 74 42	15 123 166 41
3 16 1	13 -113 92 29	0 947 813 11	17 429 440 20	13 282 242 25	16 -90 82 48
0 301 291 16	14 18 10 75	1 682 640 13	18 -122 116 33	14 324 232 20	17 110 45 46
1 354 330 21	15 475 480 17	2 1675 1527 18	19 274 354 22	15 96 73 44	4 14 1
2 -16 47 89	16 951 959 17	3 238 248 17	20 404 447 19	16 459 489 18	0 288 246 15
3 305 288 23	17 23 132 79	4 95 34 31	21 137 216 36	17 309 263 21	1 130 158 36
4 179 237 31	18 151 170 34	5 541 490 14	22 123 126 40	18 151 114 34	2 308 308 21
5 -107 61 41	19 173 210 32	6 687 684 14	23 78 95 55	19 -82 33 49	3 161 47 31
6 209 214 29	20 194 207 31	7 677 664 14	24 359 405 22	20 -132 28 34	4 562 545 17
7 160 153 35	21 150 154 33	8 971 975 15	25 -110 64 44	21 380 406 21	5 225 77 25
8 86 45 53	22 183 190 30	9 379 385 16	4 8 1	22 156 62 37	6 332 331 21
9 338 306 23	23 -77 182 51	10 330 314 17	0 334 306 12	4 11 1	7 182 37 29
4 0 1	24 408 423 20	11 230 234 21	1 -46 71 52	0 493 411 13	8 490 453 18
0 1079 919 13	25 516 480 19	12 1239 1242 17	2 275 326 18	1 452 403 18	9 103 19 44
2 352 375 18	26 98 3 50	13 564 510 16	3 460 348 15	2 229 144 25	10 344 298 21
4 1701 1844 21	27 239 231 29	14 823 795 17	4 1072 1118 16	3 581 530 17	11 61 51 61
6 3703 3591 39	4 3 1	15 898 891 17	5 577 545 15	4 165 119 31	12 278 188 24
8 1231 1199 19	0 1566 1592 14	16 -93 20 41	6 94 5 38	5 294 327 22	13 128 175 41
10 589 467 19	1 1265 1201 14	17 -107 27 39	7 691 618 16	6 165 198 31	14 200 197 31
12 1360 1325 22	2 1500 1429 16	18 112 137 43	8 116 82 34	7 383 368 20	4 15 1
14 38 95 78	3 2037 2002 20	19 713 693 19	9 311 309 19	8 291 266 23	0 237 254 18
16 615 560 23	4 2442 2403 23	20 232 281 25	10 293 291 20	9 544 533 19	1 137 139 36
18 -100 65 54	5 1100 1019 14	21 198 251 28	11 645 641 17	10 90 113 50	2 346 346 21
20 886 876 26	6 -38 2 50	22 265 255 24	12 301 236 21	11 47 100 62	3 130 63 37
22 407 452 27	7 858 882 14	23 -105 110 41	13 135 126 36	12 -58 4 56	4 195 236 29
24 942 912 24	8 280 271 16	24 64 50 61	14 191 147 29	13 144 144 34	5 -40 15 69
26 203 168 42	9 362 370 15	25 271 215 26	15 -23 51 83	14 287 322 22	6 388 384 20
4 1 1	10 53 150 48	26 217 234 30	16 363 344 22	15 98 69 44	7 293 295 23
0 923 907 10	11 922 925 15	4 6 1	17 162 160 30	16 341 382 21	8 241 268 26
1 618 494 11	12 501 494 15	0 565 629 10	18 -178 1 23	17 -119 66 36	9 264 250 25
2 1655 1709 17	13 1266 1320 17	1 488 531 14	19 93 245 46	18 -91 131 46	10 -96 30 46
3 916 924 12	14 994 1040 16	2 635 578 13	20 -139 82 31	19 314 292 23	11 176 62 33
4 653 635 12	15 1079 1085 17	3 1301 1383 16	21 -80 1 50	20 143 155 38	4 12 1
5 3209 3069 29	16 668 649 17	4 1258 1353 16	22 462 477 19	0 158 193 24	0 114 128 31
6 2558 2577 24	17 -80 66 47	5 1136 1151 15	23 289 298 25	1 -77 95 49	1 -139 50 32
7 2005 1903 20	18 -115 89 37	6 302 309 17	24 405 423 22	2 178 67 31	2 78 61 54
8 1934 1987 19	19 643 647 19	7 607 593 14	4 9 1	3 521 525 19	3 231 239 27
9 1212 1134 15	20 -103 105 44	8 509 527 15	0 158 45 19	4 365 243 21	4 153 74 35
10 724 703 14	21 309 350 21	9 440 459 16	1 1111 1160 17	5 924 902 18	5 339 271 22
11 1178 1240 16	22 -56 195 60	10 1057 1078 16	2 415 339 17	6 232 193 27	6 136 168 39
12 43 110 54	23 -177 19 25	11 278 279 20	3 490 537 16	7 378 407 21	7 -89 60 49
13 65 73 47	24 -173 0 26	12 595 582 16	4 208 238 23	8 187 230 27	5 0 1
14 946 957 16	25 300 296 24	13 905 929 17	5 746 791 16	9 211 229 25	0 3500 3501 31
15 67 82 49	26 127 57 42	14 138 177 33	6 693 643 16	10 266 314 22	2 2766 2774 30
16 225 164 24	27 460 451 21	15 -92 46 42	7 567 627 17	11 101 119 43	4 2601 2474 29
17 295 268 22	4 4 1	16 438 442 19	8 -107 80 35	12 156 95 32	6 1898 1851 24
18 404 412 20	0 657 725 9	17 118 227 41	9 185 203 28	13 95 181 45	8 276 321 23
19 -52 91 64	1 2058 2029 20	18 714 654 19	10 -93 44 41	14 360 315 20	10 326 424 22
20 539 532 19	2 1525 1568 16	19 473 441 17	11 -90 45 42	15 355 369 21	12 731 712 20
21 452 467 21	3 1856 1812 13	20 -30 159 75	12 434 450 19	16 323 260 22	14 106 180 48
22 -130 17 33	4 970 904 13	21 277 324 23	13 243 265 26	17 -3 146 102	16 1111 1163 24
23 -140 106 32	5 1356 1452 16	22 503 470 18	14 256 300 25	18 110 93 44	18 227 58 37
24 285 231 24	6 2087 2063 21	23 204 206 29	15 166 169 34	19 245 266 27	20 292 302 35
25 66 72 60	7 590 506 14	24 439 455 20	16 131 182 35	4 13 1	22 805 828 24
26 541 503 19	8 526 599 14	25 262 333 27	17 -104 74 39	0 205 93 18	24 470 423 27
27 148 68 39	9 -101 7 30	4 7 1	18 334 302 21	1 143 91 32	26 317 292 33
	10 217 165 21	0 564 531 10	19 209 175 27		
	11 385 409 16	1 274 50 17	20 328 378 21		
	12 321 361 18	2 1225 1138 16	21 59 158 62		
	13 323 332 18		22 221 189 28		
			23 252 287 27		

15	303	307	20
16	-112	61	35
17	417	426	19
18	1123	1095	19
19	276	301	25
20	321	363	20
21	330	335	21
22	282	300	23
23	389	419	20
24	186	162	31
25	213	299	30
26	258	303	27
5 4 1			
0	373	307	10
1	300	232	15
2	1109	1020	15
3	601	635	13
4	583	627	13
5	69	170	39
6	98	70	32
7	300	140	16
8	364	402	16
9	1516	1508	18
10	295	201	18
11	160	149	27
12	289	285	19
13	547	542	16
14	197	249	26
15	540	567	17
16	561	590	18
17	309	339	22
18	90	11	19
19	676	677	19
20	432	459	18
21	-177	50	24
22	106	186	44
23	246	229	26
24	222	212	28
25	342	345	23
26	-120	84	41
5 5 1			
0	1187	1234	12
1	498	561	14
2	1147	1220	15
3	993	928	15
4	1365	1465	17
5	45	18	50
6	649	666	14
7	113	66	32
8	872	947	15
9	1094	1072	16
10	387	380	17
11	107	139	36
12	388	412	18
13	329	338	20
14	143	240	33
15	177	188	29
16	390	387	20
17	51	71	65
18	487	490	20
19	88	27	46
20	333	347	20
21	325	379	21
22	196	203	29
23	221	264	28
24	242	305	27
25	187	236	33
5 6 1			
0	-62	62	33
1	489	452	15
2	293	416	17
3	231	242	20

4	339	302	16
5	656	633	12
6	59	12	48
7	1026	976	16
8	758	712	15
9	363	341	17
10	385	368	18
11	860	862	16
12	362	316	19
13	505	487	20
14	279	254	23
15	673	696	18
16	-126	54	34
17	212	198	28
18	501	517	17
19	250	316	23
20	564	585	17
21	180	197	30
22	-93	77	45
23	199	143	30
24	377	387	22
25	-120	202	41
5 7 1			
0	-86	67	27
1	257	227	19
2	718	718	15
3	602	524	15
4	341	421	17
5	407	419	16
6	618	630	15
7	84	29	40
8	165	148	27
9	141	74	30
10	878	940	17
11	616	630	17
12	173	73	29
13	-47	29	63
14	-119	124	36
15	379	401	21
16	634	632	19
17	216	210	25
18	-89	71	44
19	-71	29	52
20	-135	59	32
21	128	176	38
22	690	694	18
23	112	36	45
24	80	178	57
5 8 1			
0	1391	1340	14
1	317	305	18
2	533	556	16
3	314	375	18
4	420	505	16
5	433	447	16
6	820	856	17
7	291	328	20
8	750	768	16
9	50	17	59
10	862	862	17
11	330	363	21
12	1084	1065	18
13	160	143	33
14	-98	111	43
15	-140	66	32
16	-112	92	36
17	-62	27	55
18	-129	25	33
19	-173	17	24
20	195	251	29
21	169	127	32
22	59	13	63
23	-21	80	89

5	9	1	
0	84	74	32
1	77	789	16
2	582	540	16
3	409	409	17
4	482	477	17
5	162	127	25
6	192	202	29
7	-22	76	77
8	59	24	56
9	756	765	18
10	831	809	17
11	587	548	18
12	207	104	28
13	-87	127	48
14	268	247	26
15	265	193	22
16	541	580	17
17	439	451	19
18	-40	5	69
19	-92	9	45
20	-134	67	33
21	368	349	21
22	93	159	48
5	10	1	
0	177	182	20
1	769	712	17
2	280	268	22
3	106	89	39
4	314	335	21
5	540	554	17
6	250	91	24
7	1390	1410	19
8	335	262	21
9	-53	146	62
10	-122	41	35
11	332	345	22
12	307	399	20
13	522	563	17
14	510	520	17
15	97	204	45
16	-132	45	32
17	-111	30	38
18	162	173	33
19	531	487	19
20	432	396	20
21	170	179	34
5	11	1	
0	-82	6	35
1	86	33	48
2	113	131	40
3	604	555	18
4	236	118	25
5	835	846	18
6	233	135	16
7	181	34	31
8	166	206	33
9	415	404	21
10	205	201	26
11	570	545	17
12	130	174	36
13	333	343	20
14	196	201	28
15	-40	99	69
16	391	338	20
17	259	278	25
18	102	1	47
19	-139	30	34
5	12	1	
0	313	264	16
1	417	466	20

2	335	339	22
3	248	284	22
4	207	132	29
5	328	57	23
6	849	851	16
7	8	237	21
8	755	771	15
9	386	279	19
10	-48	64	63
11	365	418	20
12	424	392	19
13	268	305	23
14	199	223	29
15	102	36	45
16	80	210	53
17	-108	1	42
18	467	425	20
5 13 1			
0	84	78	35
1	176	195	29
2	113	10	39
3	207	237	18
4	342	385	20
5	312	346	21
6	312	346	21
7	38	110	69
8	605	614	17
9	211	163	27
10	375	417	20
11	77	194	52
12	-107	43	40
13	182	175	31
14	188	183	31
15	180	157	32
16	471	443	20
5 14 1			
0	284	322	16
1	27	44	77
2	157	152	32
3	73	65	52
4	89	35	47
5	91	154	46
6	435	474	19
7	220	170	26
8	320	299	22
9	233	232	26
10	197	272	30
11	128	93	40
12	321	371	23
13	206	168	30
5 15 1			
0	-124	6	26
1	-63	51	57
2	186	259	30
3	371	364	20
4	302	304	23
5	211	179	28
6	246	219	26
7	148	80	36
8	231	339	27
9	210	218	29
10	238	262	27
5 16 1			
0	150	149	27
1	309	260	23
2	141	110	38
3	269	241	25
4	-128	76	36
5	243	252	27

6	0	1	
0	300	293	15
2	1444	1353	21
4	512	595	19
6	869	900	19
8	669	663	19
10	1468	1552	23
12	608	552	22
14	621	637	22
16	928	947	24
18	179	198	43
20	333	371	28
22	512	578	25
24	142	207	51
26	297	258	35

6	1	1	
0	2248	2117	19
1	358	300	14
2	2165	2003	21
3	1087	1136	15
4	407	454	14
5	728	830	13
6	16	46	68
7	606	603	14
8	-91	51	31
9	-80	149	37
10	621	650	15
11	32	35	62
12	865	821	16
13	107	234	35
14	232	177	22
15	370	315	19
16	802	782	19
17	492	520	17
18	504	468	19
19	553	599	19
20	38	165	70
21	39	69	71
22	-130	57	34
23	306	289	23
24	488	502	19
25	240	272	28
26	479	448	21

6	2	1	
0	806	843	10
1	1046	984	14
2	919	897	14
3	919	852	14
4	796	838	14
5	246	194	17
6	1316	1150	16
7	1202	1173	16
8	292	393	17
9	553	548	15
10	1062	1058	16
11	893	906	16
12	324	212	21
13	43	52	59
14	621	683	17
15	1212	1138	18
16	225	177	25
17	349	400	21
18	177	152	32
19	51	29	68
20	77	65	51
21	537	543	18
22	121	189	40
23	186	151	31
24	103	36	47
25	-87	101	51
26	373	318	23

6	3	1	
---	---	---	--

Aquo. Carbonyl Tetrakis(pentafluorophenyl)octachloroporphyrin Ru(II)

[illegible]

Aquo. Carbonyl Tetrakis(pentafluorophenyl)octachloroporphyrin Ru(II)

Page 17

0	1379	1356	14	0	-64	78	41	10	98	14	45	13	1086	1084	18	8	459	474	17	6	1310	1286	19
1	340	277	18	1	243	279	25	11	132	79	38	14	1000	972	18	9	892	870	17	7	574	542	18
2	100	87	37	2	578	575	18	12	469	435	19	15	210	93	27	10	56	54	56	8	243	131	24
3	415	374	17	3	867	888	18	13	339	358	22	16	217	256	27	11	305	318	21	9	131	89	37
4	176	238	26	4	201	150	28	14	372	352	21	17	432	441	17	12	125	15	37	10	610	632	18
5	353	392	18	5	171	33	31	15	400	398	21	18	265	308	22	13	844	852	18	11	238	195	26
6	1441	1458	18	6	189	111	29					19	490	494	17	14	282	319	23	12	543	449	19
7	980	959	17	7	320	332	22					20	404	476	19	15	255	236	25	13	322	361	20
8	137	134	32	8	862	842	18	7	13	1		21	323	332	21	16	409	425	18	14	409	427	19
9	158	215	29	9	491	455	19	0	171	159	22	22	251	209	25	17	146	255	33	15	65	165	56
10	137	71	34	10	-59	65	61	1	107	58	41	23	-99	38	45	18	243	181	24	16	485	528	18
11	164	119	31	11	753	716	16	2	749	795	17	24	372	415	22	19	699	698	17	17	312	291	22
12	394	414	20	12	38	51	69	3	333	270	21					20	509	531	18	18	641	577	18
13	106	84	43	13	-114	3	37	4	419	392	19	8	2	1		21	254	271	25	19	186	85	31
14	527	534	19	14	220	196	26	5	169	150	31					22	112	92	44	20	481	459	20
15	74	55	56	15	607	570	17	6	232	167	25	0	289	345	13	23	356	367	22	21	325	313	23
16	476	415	17	16	350	290	21	7	238	131	25	1	1376	1382	18								
17	217	263	26	17	235	240	26	8	241	196	25	2	291	277	18	8	5	1		0	394	329	12
18	1119	1085	18	18	-78	29	52	9	166	93	33	3	344	388	17	9	716	731	16	1	173	118	30
19	83	88	50	19	499	454	19	10	290	241	24	4	581	565	15	0	435	402	17	2	1012	990	18
20	272	312	24	20	544	588	19	11	8	29	98	5	1015	979	16	3	803	813	16	3	781	761	18
21	178	207	32					12	219	199	28	6	573	583	15	4	673	620	16	4	1385	1385	20
22	258	269	26	7	10	1		13	150	66	37	7	920	884	16	5	717	691	16	5	374	292	20
23	-162	4	30									8	356	361	18	6	737	723	16	6	347	335	21
				7	7	1		0	230	230	19	9	250	232	21	7	947	930	17	7	551	520	19
				0	437	410	12	1	416	411	20	10	1428	1436	19	8	759	726	17	8	857	886	18
				1	662	690	16	2	545	502	19	11	505	462	17	9	371	413	19	9	383	382	21
				2	147	85	30	3	315	279	22	12	301	254	21	10	717	672	17	10	494	459	20
				3	796	824	16	4	63	129	58	13	1126	1079	18	11	1104	1107	18	11	274	277	22
				4	974	987	17	5	447	382	20	14	691	674	18	12	604	630	18	12	492	498	17
				5	194	48	25	6	151	12	35	15	553	541	18	13	54	41	62	13	470	443	18
				6	531	524	17	7	325	298	22	16	208	120	28	14	337	329	22	14	382	425	19
				7	333	374	20	8	542	465	16	17	682	680	16	15	469	459	17	15	428	432	19
				8	195	252	26	9	339	358	19	18	381	367	17	16	-100	39	40	16	351	382	21
				9	286	270	22	10	271	289	22	19	615	617	17	17	576	598	17	17	223	248	27
				10	701	682	18	11	146	74	33	20	250	244	24	18	960	947	17	18	77	18	55
				11	230	183	26	12	208	136	27	21	427	412	19	19	541	568	18	19	443	400	20
				12	-109	8	39	13	899	905	17	22	458	481	19	20	-149	86	30	20	479	477	20
				13	-105	101	42	14	407	426	19	23	-64	166	60	21	-81	59	51				
				14	338	333	23	15	171	96	32	24	112	92	46	22	615	607	19	23	381	345	22
				15	252	246	23	16	241	276	26	0	105	105	26					8	6	1	
				16	875	859	17	17	471	449	20	1	-67	40	45	0	617	587	12	0	597	585	13
				17	249	180	24	18	154	40	36	2	-124	16	27	1	493	524	17	1	882	850	18
				18	159	176	33	19	486	500	20	3	412	437	17	2	92	15	41	2	320	287	23
				19	249	291	25					4	82	42	41	3	88	49	43	3	105	19	45
				20	563	590	18	7	11	1		5	149	187	28	4	925	938	17	4	164	22	34
				21	150	65	36	0	253	237	19	6	1158	1174	17	5	88	49	43	5	766	812	18
				22	276	299	25	1	510	498	20	7	814	812	16	6	97	147	41	6	759	756	19
								2	222	176	24	8	181	132	25	7	221	140	24	7	141	45	38
				7	8	1		3	499	480	17	9	440	401	17	8	134	21	34	8	-71	27	50
				0	283	276	15	4	123	105	36	10	93	13	42	9	1401	1424	19	9	-61	16	55
				1	991	950	17	5	293	266	21	11	843	892	17	10	959	951	18	10	-44	59	65
				2	155	41	31	6	463	470	17	12	92	59	44	11	674	689	18	11	407	416	19
				3	379	393	19	7	683	665	16	13	1065	1072	18	12	253	248	24	12	499	548	18
				4	363	330	20	8	120	62	38	14	584	594	18	13	455	464	19	13	117	95	40
				5	561	562	18	9	261	252	23	15	237	151	26	14	558	566	19	14	-87	106	46
				6	849	863	17	10	591	574	17	16	750	713	19	15	72	140	51	15	296	308	23
				7	840	841	17	11	425	451	19	17	448	444	18	16	-158	4	26	16	-97	79	44
				8	527	539	18	12	131	130	37	18	137	180	35	17	361	391	20	17	519	521	19
				9	295	299	23	13	252	270	25	19	325	321	21	18	348	316	20	18	227	229	28
				10	438	493	20	14	256	245	25	20	157	179	33	19	319	270	22	19	534	503	20
				11	201	236	29	15	475	479	19	21	125	149	39	20	248	301	25				
				12	-149	53	30	16	341	268	22	22	186	193	31	21	478	512	19	8	10	1	
				13	556	570	17	17	465	411	20	23	679	671	18	22	298	259	24	0	290	290	18
				14	293	292	21									23	449	477	21	1	277	201	25
				15	398	392	19	7	12	1		8	4	1						2	230	174	28
				16	24	126	81	0	684	703	12									3	946	928	19
				17	358	310	21	1	153	135	32	0	672	673	11	8	7	1		4	249	115	23
				18	551	530	18	2	318	264	20	1	1030	1081	16	0	1027	1027	13	5	185	122	28
				19	454	409	19	3	285	281	22	2	869	825	16	1	22	9	78	6	433	379	18
				20	293	311	24	4	337	326	20	3	504	473	16	2	64	106	54	7	687	664	16
				21	201	212	31	5	535	478	17	4	-114	74	30	3	-66	95	51	8	120	45	38
								6	219	118	25	5	86	10	41	4	194	87	27	9	820	850	17

Aquo. Carbonyl Tetrakis(pentafluorophenyl)octachloroporphyrin Ru(II)

12	363	343	20	10	273	273	31	14	434	431	20	15	239	236	24	0	116	177	29	18	182	215	41	
13	394	458	20	12	124	37	51	15	595	645	16	16	580	560	18	1	-125	47	34	20	363	406	29	
14	-166	24	26	14	316	21	32	16	582	560	17	17	94	4	47	2	288	199	22					
15	299	324	23	16	658	828	22	17	202	20	27	18	321	337	22	3	540	509	17	10	1	1		
16	174	191	33	18	-104	82	52	18	420	418	19	19	581	587	19	4	339	297	20					
17	312	270	24	20	66	118	72	20	338	320	21	20	191	209	31	5	711	741	17	0	748	720	12	
				22	491	493	27	20	194	255	29	21	154	201	49	6	251	259	24	2	150	110	32	
	8	11	1					21	244	268	26					7	142	80	41	3	96	148	43	
					9	1	1	22	186	219	32		9	7	1	8	113	260	24	4	591	608	17	
0	538	529	12		-45	142	44		9	4	1	0	379	401	14	10	916	212	27	5	64	156	54	
1	480	461	18	0	1	216	183	23	0	245	145	16	1	183	63	30	11	215	263	28	6	262	245	23
2	405	385	19	1	2009	1991	22	0	1693	1674	20	2	1260	1242	19	12	-156	23	29	7	699	737	17	
3	155	94	32	3	354	377	18	2	316	298	20	3	496	469	19	13	163	184	34	8	346	315	20	
4	245	135	24	4	216	215	23	3	-63	43	50	5	519	494	19	14	-92	93	48	9	306	286	22	
5	941	952	17	5	385	382	18	4	391	387	18	6	304	309	23	15	218	207	29	10	237	271	25	
6	374	277	19	6	182	252	26	5	1232	1228	18	7	167	148	32	16	-77	120	55	11	581	570	18	
7	690	715	17	7	1011	969	17	6	261	296	22	8	771	837	18					12	163	90	33	
8	321	277	21	8	643	641	17	7	82	65	47	9	100	39	46	9	11	1		13	308	274	20	
9	159	112	32	9	371	382	19	8	-79	100	45	10	565	604	16	0	93	138	35	14	373	298	19	
10	215	96	27	10	371	382	19	9	804	788	17	11	122	63	36	1	512	485	18	15	457	465	17	
11	612	801	17	11	147	162	33	10	961	925	18	12	83	88	47	2	427	374	19	16	598	611	18	
12	111	404	42	12	239	109	25	11	1399	1373	20	13	297	287	21	3	731	773	17	17	420	397	19	
13	271	287	24	13	1426	1427	20	12	157	51	33	14	284	256	22	4	209	116	27	18	499	488	18	
14	-130	21	35	14	1106	1133	19	13	664	677	19	15	191	216	29	5	141	137	36	19	-101	106	42	
15	169	141	34	15	300	234	20	14	103	71	40	16	92	100	48	6	335	333	21	20	232	226	27	
	8	12	1		16	224	34	24	15	516	496	17	17	206	211	29	7	361	363	20				
0	35	70	58	16	301	326	21	15	579	573	17	18	474	541	20	8	304	222	22	10	2	1		
1	317	346	21	17	-147	45	28	17	488	534	18	19	137	135	39	9	478	461	19	11	108	81	44	
2	496	428	18	18	-58	156	58	18	-74	39	51	20	497	492	20	10	197	200	29	12	96	26	51	
3	582	634	17	19	-169	28	25	19	289	330	23					13	158	81	44	13	913	900	17	
4	634	550	17	20	286	320	24	20	161	190	34	9	8	1		14	325	330	22	4	-97	12	39	
5	469	499	18	21	386	368	21	21	110	124	45	0	572	571	14					5	488	460	18	
6	189	118	29					22	444	464	21	0	542	492	19	9	12	1		6	489	455	18	
7	196	124	28		9	2	1					1	224	165	27	0	475	372	14	7	1181	1211	18	
8	247	227	24	0	837	845	12	9	5	1		2	600	590	19	0	428	414	20	8	421	438	19	
9	284	288	23	1	634	602	16	0	-135	50	21	3	408	430	20	1	154	140	34	9	284	296	23	
10	296	312	23	2	1075	1051	17	1	450	433	18	4	600	590	19	2	428	414	20	10	415	432	20	
11	132	134	39	3	445	447	17	2	112	39	38	5	356	324	22	3	216	222	27	11	655	642	18	
12	187	106	31	4	646	623	16	3	1197	1186	18	6	387	378	21	4	292	253	23	12	409	392	21	
13	20	136	89	5	550	558	16	4	519	467	18	7	453	471	17	5	550	540	18	13	663	646	16	
14	314	303	24	6	738	777	16	5	333	348	21	8	486	496	18	6	199	214	29	14	389	405	18	
	8	13	1	7	142	32	31	6	284	258	22	10	33	153	72	7	132	39	38	15	729	720	17	
0	610	652	13	8	290	342	21	7	470	436	18	11	540	541	17	8	-109	115	40	16	131	178	36	
1	121	25	40	9	56	25	57	8	486	496	18	12	-80	84	47	9	95	42	48	17	514	545	18	
2	153	148	34	10	798	789	17	9	779	784	18	13	231	260	25	10	-107	59	42	18	247	252	25	
3	203	57	28	11	1097	1068	18	10	213	92	27	14	346	361	21	11	374	420	22	19	255	273	25	
4	393	407	20	12	1219	1205	19	11	580	535	18	15	158	201	34					20	413	448	20	
5	183	234	30	13	1397	254	20	12	147	190	36	16	280	365	24	9	13	1		21	255	212	26	
6	529	511	18	14	235	71	27	13	85	22	45	17	241	244	27	0	124	177	30					
7	235	189	26	15	475	481	17	14	931	901	16	18	483	493	20	1	205	137	30	10	153	162	23	
8	184	170	31	16	756	779	16	15	847	876	16	19	265	259	26	2	428	427	20	0	1	254	234	23
9	-83	18	50	17	905	908	17	16	514	509	17					3	236	258	27	1	2	153	178	32
10	342	317	22	18	257	305	23	17	179	232	30	0	159	116	26	4	-48	21	68	2	3	282	311	22
11	199	254	31	19	-108	15	38	18	242	270	25	2	395	315	20	5	97	131	47	3	4	173	30	30
	8	14	1	20	-87	35	46	19	365	341	21	3	749	704	16	6	140	132	38	4	5	1371	1352	19
				22	-118	37	37	20	552	578	19	4	230	123	24	7	-93	11	47	6	6	668	628	18
				23	473	475	20	21	511	508	20	5	-39	49	68	8	250	274	26	7	7	454	378	19
					9	3	1					6	133	96	35					8	8	82	98	49
G	-94	53	34		0	162	194	20	0	937	910	13	7	642	641	17	9	14	1	9	129	116	38	
1	-121	0	37	0	1	89	181	41	1	87	15	46	8	384	410	19	0	344	360	23	10	465	439	19
2	569	599	18	1	2	102	163	38	2	423	429	46	9	642	596	17				11	539	575	19	
3	120	12	41	2	3	299	286	20	3	197	22	27	10	-88	69	43	10	0	1	12	116	152	37	
4	70	161	57	3	4	151	97	30	4	1264	1244	19	11	73	54	53				13	216	237	25	
5	-137	81	33	4	5	508	487	18	5	508	487	18	12	-50	64	63	0	1345	1307	19	14	116	144	38
6	135	20	39	5	6	464	405	19	6	464	405	19	13	-145	15	30	2	1776	1653	27	15	331	331	20
7	92	53	50	6	7	139	2	35	7	139	2	35	14	242	254	26	4	-111	75	47	16	157	197	32
	9	0	1	6	8	383	398	20	8	383	398	20	15	107	163	45	6	884	944	24	17	686	686	17
0	751	752	16	7	671	658	17	9	324	282	22	16	137	263	27	8	1652	1656	27	18	-134	80	32	
1	646	683	22	8	346	322	20	10	1251	1225	19	17	247	153	27	9	678	714	25	19	269	271	24	
2	1423	1478	24	9	611	594	17	11	647	646	19					10	678	714	25	20	128	101	40	
3	265	322	29	10	379	376	20	12	409	437	18	9	10	1		11	1248	1258	23	2				

[illegible]

Aquo, Carbonyl Tetrakis(pentafluorophenyl)octachloroporphyrin Ru(II)

Page 20

11 135 160 35	1 124 2 38	13 0 1	1 621 603 17	0 152 211 27	9 204 142 30
12 -68 74 53	2 878 903 17	0 200 97 28	2 195 19 29	1 499 481 20	10 363 321 22
13 232 243 25	3 119 128 39	2 68 108 72	3 743 667 17	2 137 141 40	14 5 1
14 243 321 25	4 -119 36 36	4 612 690 24	4 -86 81 47	3 266 225 26	0 308 273 17
15 -168 36 26	5 383 407 20	5 563 543 24	5 252 239 24	14 0 1	1 183 158 32
16 182 277 31	6 313 308 22	6 741 732 24	6 525 487 18	0 650 609 18	2 246 166 27
17 -149 101 31	7 -76 50 50	7 765 720 24	7 91 89 48	2 292 287 32	3 666 679 18
12 3 1	8 -135 93 32	8 741 732 24	8 293 306 23	4 588 410 25	4 367 316 22
0 368 392 14	9 -72 120 52	9 765 720 24	9 784 778 18	6 539 495 26	5 139 3 39
1 341 344 20	10 -75 76 51	10 239 194 36	10 262 223 24	8 552 523 26	6 377 355 21
2 228 234 25	11 129 112 38	11 542 574 26	11 267 243 24	10 400 249 29	7 86 125 53
3 503 558 17	12 520 552 19	13 1 1	12 116 171 42	12 395 354 30	8 521 455 19
4 235 162 24	13 -78 84 51	0 994 1003 13	13 286 304 24	14 1 1	14 6 1
5 401 398 19	14 332 383 22	1 446 479 18	13 5 1	0 259 254 18	0 829 817 13
6 827 796 17	12 7 1	2 114 135 41	0 454 449 13	1 254 237 25	1 219 61 29
7 385 397 19	0 318 329 15	3 502 537 18	1 395 392 20	2 474 487 19	2 541 497 19
8 398 402 19	1 256 173 24	4 82 128 50	2 190 43 29	3 423 366 20	3 214 73 29
9 964 989 17	2 686 621 17	5 -22 53 82	3 127 103 39	4 1173 1142 19	4 500 485 20
10 -134 93 31	3 136 46 36	6 803 840 17	4 196 98 29	5 311 284 23	5 386 410 22
11 421 433 19	4 705 675 17	7 33 50 74	5 109 123 43	6 227 129 27	6 579 576 19
12 32 134 74	5 93 49 47	8 708 673 17	6 441 396 19	7 450 420 19	14 7 1
13 81 110 50	6 395 402 20	9 222 193 26	7 411 417 20	8 511 492 19	0 290 251 18
14 114 19 42	7 181 215 30	10 191 108 29	8 190 142 30	9 347 306 22	1 384 290 22
15 580 608 18	8 113 170 42	11 112 205 42	9 170 176 32	10 797 811 18	2 1036 1036 19
16 268 309 25	9 -56 95 61	12 590 555 18	10 162 22 34	11 -64 125 60	3 261 102 27
17 -92 179 48	10 305 278 23	13 552 512 18	11 623 644 18	14 2 1	15 0 1
12 4 1	11 159 81 34	14 452 461 20	12 302 344 24	0 444 446 14	0 242 231 27
0 171 196 22	12 425 449 20	15 242 265 27	13 6 1	1 614 555 18	2 489 539 28
1 347 407 20	13 108 155 45	13 2 1	0 455 449 14	2 171 104 32	4 606 592 27
2 402 396 19	12 8 1	0 874 854 13	1 261 142 24	3 605 560 18	6 470 515 28
3 1145 1153 17	0 417 451 14	1 465 396 18	2 805 751 18	4 400 309 20	15 1 1
4 282 286 22	1 199 144 29	2 337 313 21	3 278 197 24	5 184 123 31	0 621 613 14
5 -23 121 80	2 398 442 20	3 16 72 87	4 437 438 19	6 623 594 18	1 262 277 26
6 104 127 42	3 371 355 20	4 90 123 47	5 201 110 29	7 478 415 19	2 323 228 23
7 -41 103 68	4 273 240 24	5 -137 44 31	6 10 37 95	8 149 155 36	3 629 568 19
8 -136 7 31	5 166 39 33	6 293 243 22	7 -91 116 47	9 220 196 28	4 650 597 19
9 123 211 38	6 411 397 20	7 281 80 23	8 499 458 19	10 384 365 21	5 355 368 22
10 190 242 28	7 206 149 29	8 531 472 18	9 453 429 20	11 152 114 36	6 464 422 20
11 248 312 24	8 215 258 28	9 534 513 18	10 519 503 19	14 3 1	15 2 1
12 167 152 31	9 112 196 43	10 264 256 24	11 176 95 33	0 244 241 18	0 379 422 15
13 596 635 18	10 -56 34 63	11 382 359 20	13 7 1	1 456 389 19	1 323 287 23
14 222 126 27	11 -67 1 58	12 145 70 36	0 796 798 13	2 361 345 21	2 579 572 19
15 346 379 22	12 131 108 40	13 304 240 23	1 180 75 32	3 860 825 18	3 590 581 19
16 57 141 65	12 9 1	14 189 158 31	2 250 216 26	4 407 418 20	4 175 104 34
12 5 1	0 -148 18 22	15 380 371 21	3 56 37 64	5 222 250 28	5 203 8 31
0 638 636 12	1 -71 63 55	13 3 1	4 -133 28 34	6 147 107 36	15 3 1
1 -74 53 50	2 89 86 50	0 335 295 15	5 138 74 38	7 588 530 19	0 390 351 15
2 431 409 18	3 662 634 18	1 843 804 17	6 680 676 18	8 -37 9 75	1 635 648 19
3 316 317 21	4 232 135 27	2 235 214 25	7 89 105 51	9 561 535 19	2 173 69 35
4 448 462 18	5 313 327 23	3 226 155 26	8 305 265 24	10 169 141 34	3 122 102 44
5 501 507 18	6 191 3 31	4 459 418 19	9 229 184 28	14 4 1	4 183 147 33
6 -148 43 29	7 234 145 27	5 304 351 22	10 316 286 23	0 374 437 15	15 4 1
7 289 306 22	8 403 407 21	6 129 35 38	13 8 1	1 906 855 18	0 280 270 18
8 193 260 28	9 104 87 47	7 1034 1036 18	0 280 247 18	2 175 129 32	1 327 331 24
9 -139 2 30	10 139 111 52	8 226 212 26	1 102 57 47	3 36 4 76	
10 143 54 35	12 10 1	9 247 272 25	2 386 367 21	4 319 242 23	
11 241 300 25	0 -133 55 26	10 117 105 41	3 520 507 19	5 703 700 18	
12 -132 74 33	1 171 267 34	11 399 429 20	4 567 550 19	6 241 151 27	
13 78 140 53	2 251 227 26	12 180 161 31	5 203 56 30	7 527 515 19	
14 265 289 25	3 86 186 52	13 667 632 18	6 460 441 20	8 316 232 23	
15 358 375 22	4 207 128 30	14 398 366 21	7 117 59 44		
12 6 1	5 640 665 19	13 4 1	13 9 1		
0 258 259 17	6 213 163 30	0 331 312 15			

Appendix 5

Transient Spectra of RuTFPPCl₈(CO)
at 415 nm

DATA FILE: RUO2.001

1995-2-23 9:19:52

TIME RANGE: 50 μ s

INPUT V RANGE: 0.320V

INPUT OFFSET: 0 %

EXPERIMENT: TRANSIENT ABSORPTION

FAST (200 MHz) QUASI-DIFFERENTIAL AMP

MODE: SINGLE-ENDED

SHOTS PRE CYCLE: 10

CYCLES: 5

PMT VOLTAGE: 702 V

EXCITATION WAVELENGTH: 355 nm OBSERVATION WAVELENGTH: 415 nm

SAMPLE: RuCl₃(CO)SOLVENT: CH₂Cl₂

TEMPERATURE: rt

COMMENT: under dioxygen

COMMENT:

--> FIXED PARAMETER; ! --> FIXED SIGN

$$y(t) = C0 + C1 * e^{-k1 * t} + C2 * e^{-k2 * t}$$

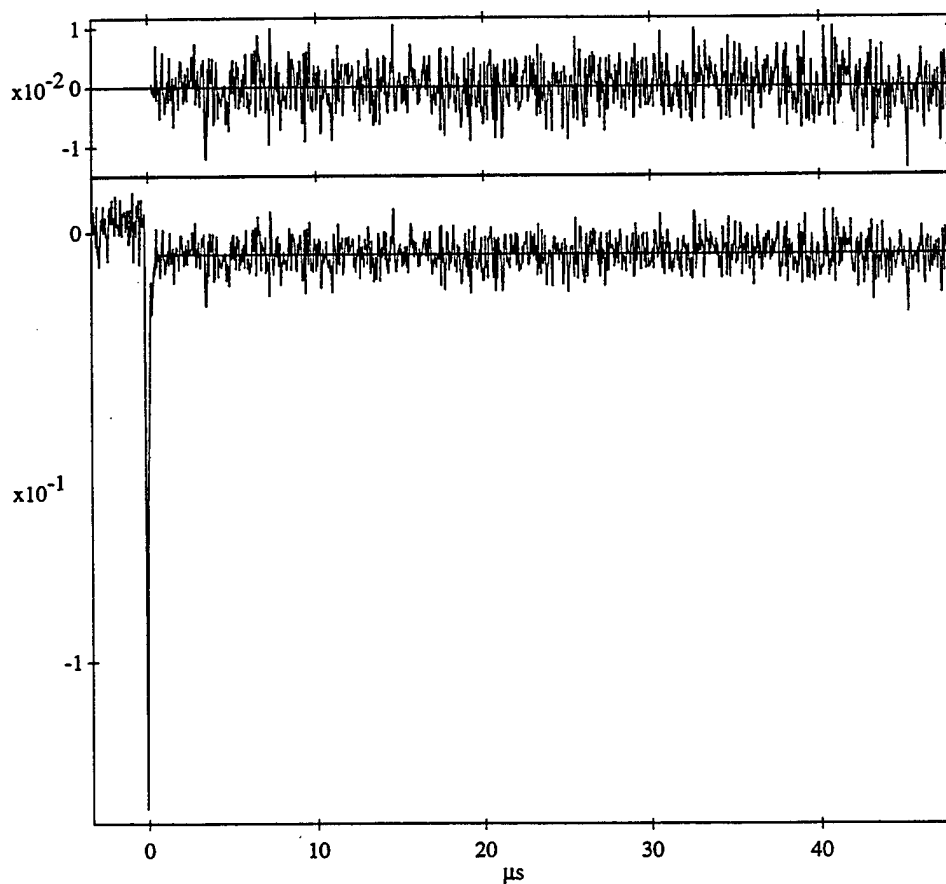
$$C0 = -5.029E-3$$

$$C1 = -1.936E-1$$

$$C2 = -6.791E-5$$

$$!k1 = 1.053E7 \text{ s}^{-1}$$

$$!k2 = 1.560E5 \text{ s}^{-1}$$



DATA FILE: RUET.002

TIME RANGE: 50 μ s

INPUT V RANGE: 0.320V

1995-2-23 9:24:35
INPUT OFFSET: 0 %

EXPERIMENT: TRANSIENT ABSORPTION

FAST (200 MHz) QUASI-DIFFERENTIAL AMP

MODE: SINGLE-ENDED

SHOTS PRE CYCLE: 10

CYCLES: 5

PMT VOLTAGE: 702 V

EXCITATION WAVELENGTH: 355 nm OBSERVATION WAVELENGTH: 415 nm

SAMPLE: RuCl₃(CO)SOLVENT: CH₂Cl₂

TEMPERATURE: rt

COMMENT: under ethylene

COMMENT:

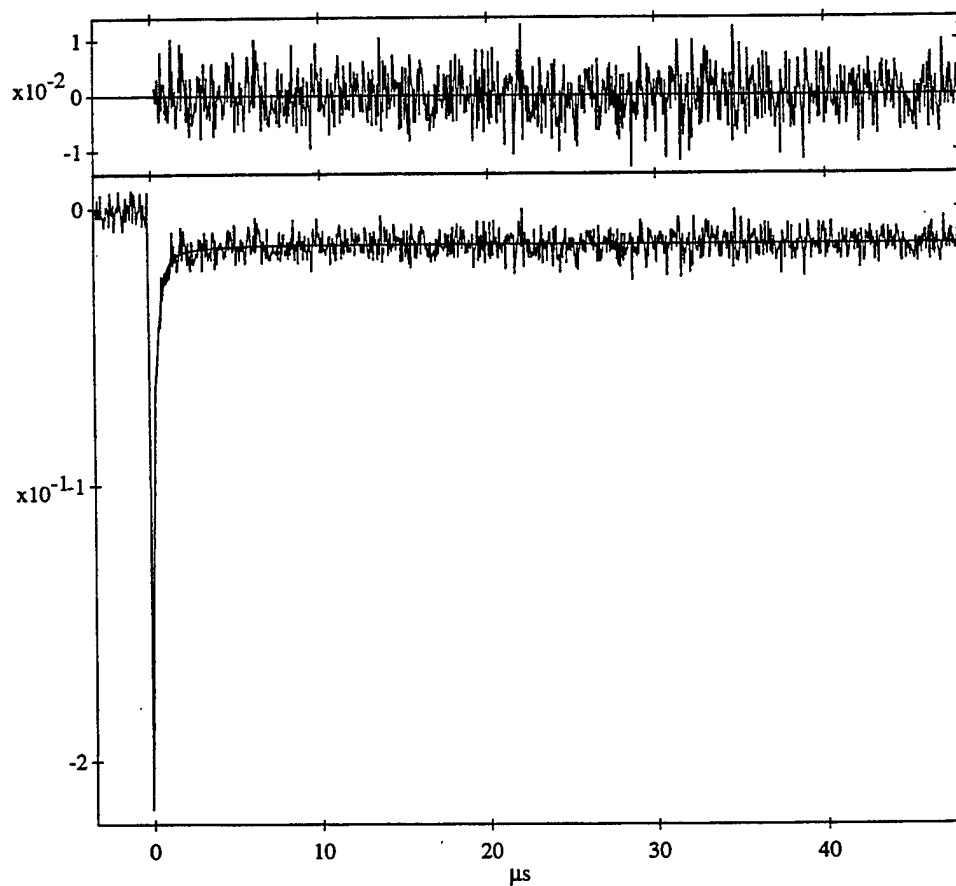
--> FIXED PARAMETER; ! --> FIXED SIGN

$$y(t) = C0 + C1 \cdot e^{-k1 \cdot t} + C2 \cdot e^{-k2 \cdot t}$$

C0 = -1.311E-2

C1 = -9.201E-2

C2 = -5.118E-3

!k1 = 2.996E6 s⁻¹!k2 = 4.197E5 s⁻¹

DATA FILE: RUAR.005

1995-2-23 9:14:31

TIME RANGE: 50 μ s

INPUT V RANGE: 0.320V

INPUT OFFSET: 0 %

EXPERIMENT: TRANSIENT ABSORPTION

FAST (200 MHz) QUASI-DIFFERENTIAL AMP

MODE: SINGLE-ENDED

SHOTS PRE CYCLE: 10

CYCLES: 5

PMT VOLTAGE: 702 V

EXCITATION WAVELENGTH: 355 nm OBSERVATION WAVELENGTH: 415 nm

SAMPLE: $\text{RuCl}_3(\text{CO})$ SOLVENT: CH_2Cl_2

TEMPERATURE: rt

COMMENT: under argon

COMMENT:

--> FIXED PARAMETER; ! --> FIXED SIGN

$$y(t) = C0 + C1 \cdot e^{-k1 \cdot t} + C2 \cdot e^{-k2 \cdot t}$$

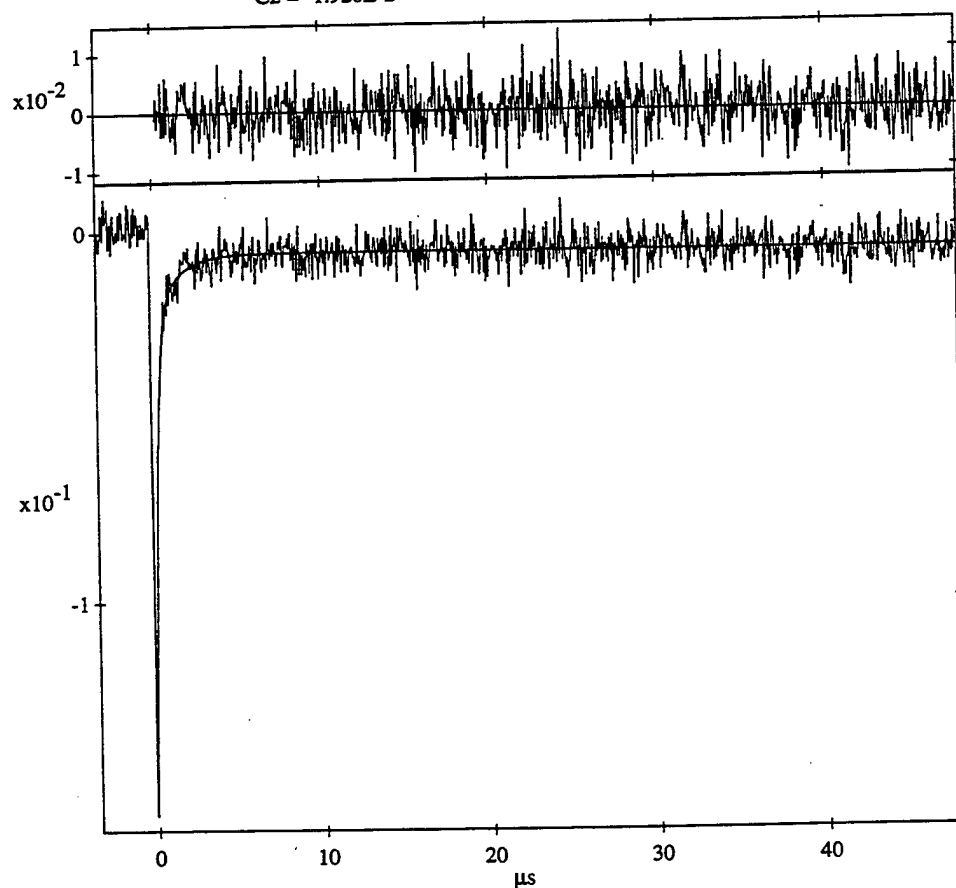
$$C0 = -5.758\text{E-}3$$

$$C1 = -1.183\text{E-}1$$

$$C2 = -1.920\text{E-}2$$

$$!k1 = 5.008\text{E}6 \text{ s}^{-1}$$

$$!k2 = 7.660\text{E}5 \text{ s}^{-1}$$



DATA FILE: RUO2.000
TIME RANGE: 5.0 μ s INPUT V RANGE: 0.320V INPUT OFFSET: 0 %
EXPERIMENT: TRANSIENT ABSORPTION
FAST (200 MHz) QUASI-DIFFERENTIAL AMP
MODE: SINGLE-ENDED

SHOTS PRE CYCLE: 10 CYCLES: 5 PMT VOLTAGE: 702 V
EXCITATION WAVELENGTH: 355 nm OBSERVATION WAVELENGTH: 415 nm
SAMPLE: RuCl₃(CO)
SOLVENT: CH₂Cl₂
TEMPERATURE: rt
COMMENT: under dioxygen
COMMENT:

--> FIXED PARAMETER; ! --> FIXED SIGN

$$y(t) = C0 + C1 * e^{-k1 * t} + C2 * e^{-k2 * t}$$

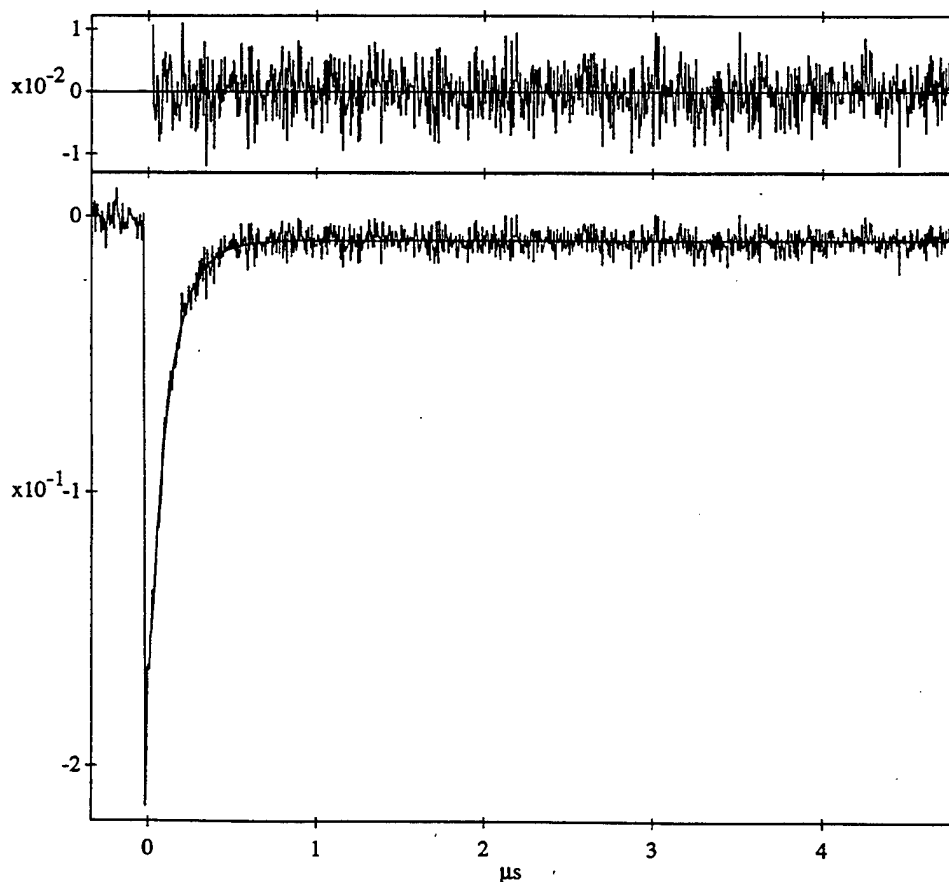
$$C0 = -8.692E-3$$

$$C1 = -6.069E-2$$

$$C2 = -1.127E-1$$

$$!k1 = 1.252E7 \text{ s}^{-1}$$

$$!k2 = 7.463E6 \text{ s}^{-1}$$



DATA FILE: RUET.001
TIME RANGE: 5.0 μ s INPUT V RANGE: 0.320V INPUT OFFSET: 0 %
EXPERIMENT: TRANSIENT ABSORPTION
FAST (200 MHz) QUASI-DIFFERENTIAL AMP
MODE: SINGLE-ENDED

SHOTS PRE CYCLE: 10 CYCLES: 5 PMT VOLTAGE: 702 V
EXCITATION WAVELENGTH: 355 nm OBSERVATION WAVELENGTH: 415 nm
SAMPLE: RuCl₃(CO)
SOLVENT: CH₂Cl₂
TEMPERATURE: rt
COMMENT: under ethylene
COMMENT:

--> FIXED PARAMETER; ! --> FIXED SIGN

$$y(t) = C_0 + C_1 e^{-k_1 t} + C_2 e^{-k_2 t}$$

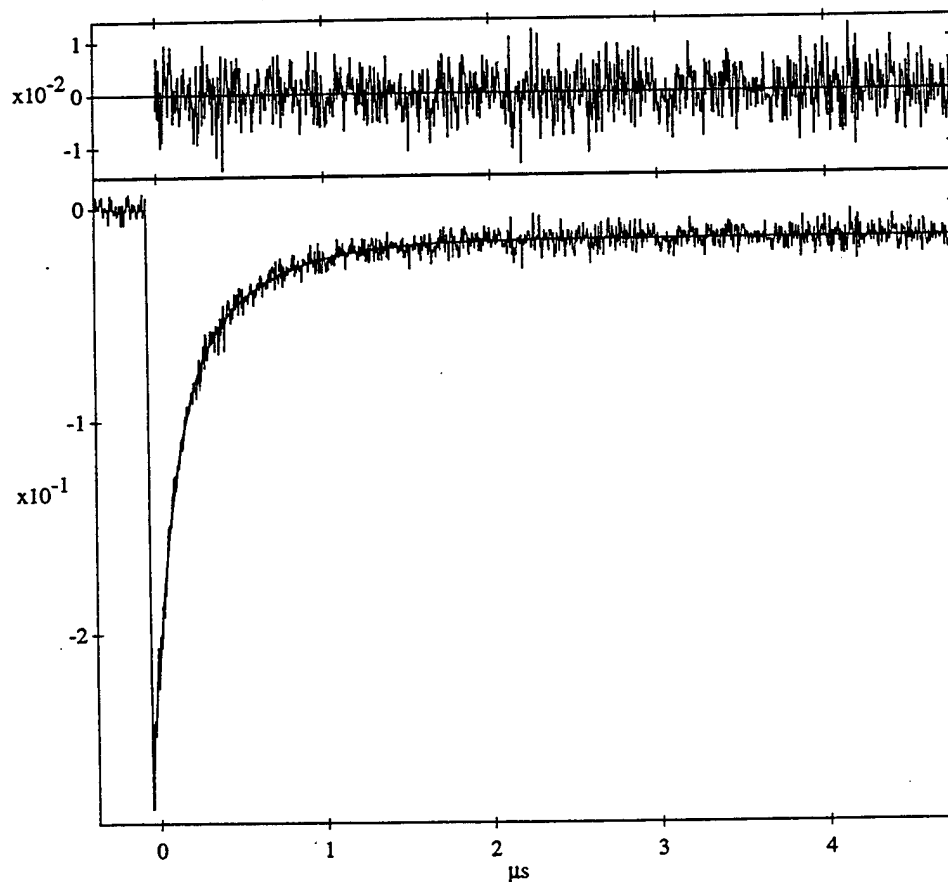
$$C_0 = -1.544E-2$$

$$C_1 = -1.144E-1$$

$$C_2 = -8.417E-2$$

$$!k_1 = 8.860E6 \text{ s}^{-1}$$

$$!k_2 = 2.281E6 \text{ s}^{-1}$$



DATA FILE: RUAR.004 1995-2-23 9:13:21
TIME RANGE: 5.0 μ s INPUT V RANGE: 0.320V INPUT OFFSET: 0 %
EXPERIMENT: TRANSIENT ABSORPTION
FAST (200 MHz) QUASI-DIFFERENTIAL AMP
MODE: SINGLE-ENDED

SHOTS PRE CYCLE: 10 CYCLES: 5 PMT VOLTAGE: 702 V
EXCITATION WAVELENGTH: 355 nm OBSERVATION WAVELENGTH: 415 nm
SAMPLE: RuCl₃(CO)
SOLVENT: CH₂Cl₂
TEMPERATURE: rt
COMMENT: under argon
COMMENT:

--> FIXED PARAMETER; ! --> FIXED SIGN

$$y(t) = C0 + C1 * e^{-k1 * t} + C2 * e^{-k2 * t}$$

$$C0 = -9.262E-3$$

$$C1 = -6.495E-2$$

$$C2 = -8.926E-2$$

$$!k1 = 7.124E6 \text{ s}^{-1}$$

$$!k2 = 2.166E6 \text{ s}^{-1}$$

